UNIVERSITE DE LIEGE

FACULTE DE MEDECINE

Evaluation of ganglion cells in ischaemic optic neuropathies

Anne-Catherine CHAPELLE

Thèse présentée en vue de l'obtention du grade de Doctorat en sciences médicales

Professeur Jean-Marie Rakic & Professeur Gordon Terence Plant

2024-2025

Evaluation of ganglion cells in ischaemic optic neuropathies

Anne-Catherine CHAPELLE

Thesis submitted to obtain the degree of Doctorate in Medical Science

Professor Jean-Marie Rakic & Professor Gordon Terence Plant

2024-2025

Acknowledgments

First and foremost, I am extremely grateful to my promotor, Professor Jean-Marie Rakic, for his encouragements to start and pursue this PhD adventure. Moreover, he was always available to share and discuss about his experiences in my research projects and in my daily practice.

I would like to also express my sincere gratitude to Doctor Gordon Plant who opened my mind and shared his in-depth knowledge during my Neuro-Ophthalmology fellowship. Thankfully, he accepted to be my co-promotor and without his guidance and advice at every stage of the research project, it would have been impossible for me to complete my study. I will always keep in mind the spelling and the history lessons!

I would like to extend my sincere thanks to my President of Jury, Professor Felix Scholtes, for his help and his kindness during the thesis process. Moreover, I would like to thank the members of my jury: Professor Dominique Dive, Professor Nathalie Collignon, Professor Matthieu Robert and Professor Julie De Zaeytijd for having agreed to read and evaluate my work.

I particularly thank all Ophthalmology department members for their support. They were a source of distraction during stressful moments, particularly during lunch. I would like to offer my special thanks to Vincent Lambert for sharing his unvaluable experience, Marilyn Vovan for finding me a quiet place to work and Caroline Di Marco for printing my drafts. I would like also to thank the strabismus team, Doctor Vincent Paris, Doctor Cecile Andris, Doctor Anne Moutschen and Zeineb Chaabouni, for their unwavering support. I also thank Doctor Bénédicte Locht and Doctor Edouard Duchateau for their belief in me and the unvaluable collaboration that we are sharing.

I would like to extend my acknowledgments to Professor Adelin Albert for teaching me rigor to analyze statistical data and Doctor Laurence Seidel for helping me with the statistical analysis. I really enjoyed this collaboration.

Finally, I would like to give a special thanks to my husband, Geoffrey, and my son, Lucas, for their love, their continuing support and their understanding when undertaking my research and writing my projects. I have a sweet thought to my father who would have been proud of me. I always remember how fortunate I was that you were in my life and I hope you will be somewhere to see my accomplishments. I also thank my mother and my brother for their endless love and trust they have given throughout my life.

Abbreviations

AION= anterior ischemic optic neuropathy

BCVA= Best Corrected Visual Acuity

BCVA= Best-Corrected Visual Acuity

CRA= Central Retinal Artery

CSF= Cerebrospinal Fluid

CSR= Central Serous Retinopathy

DNA= DeoxyriboNucleic acid

DOA= Dominant Optic Atrophy

FFA= Fundus Fluorescein Angiography

GCA= Giant Cell Arteritis

GCC= Ganglion Cell Complex (inner plexiform layer (IPL) + ganglion cell layer (GCL)

ICC= Intraclass Correlation Coefficient;

ICP= IntraCranial Pressure

IHH= Idiopathic Intracranial Hypertension

IIH= Intracranial Idiopathic Hypertension

INL= Inner Nuclear Layer

IOP= Intraocular Pressure

LGN= Lateral Geniculate Nucleus

LHON= Leber Hereditary Optic Neuropathy

mDNA= mitochondrial DeoxyriboNucleic acid

MME / MMO= Microcystic Macular Edema/Oedema

MOGAD= Myelin oligodendrocyte glycoprotein antibody-associated disease

MRI= Magnetic Retinal Imaging

MS= Multiple Sclerosis

MSON= Multiple Sclerosis Optic Neuritis

NA-AION= Non-Arteritic Anterior Ischaemic Optic Neuropathy

OCT= Optical Coherence Tomography

OD= Optic Disc

ONSAS= Optic Nerve SubArachnoid Space

OSA= Obstructive Sleep Apnoea

POHM= Peripapillary Ovoid Hyperreflective Masses

pRNFL= Peripapillary Retinal Nerve Fibre Layer

PTC= PseudoTumor Cerebri Syndrome

RAPD= Relative Afferent Pupilaary Defect

RGC= Retinal Ganglion Cell

RM= Retrograde Maculopathy

RPE= Retinal Pigmentary Epithelium

SD-OCT= Spectral Domain OCT

SPCA= Short Posterior Ciliary Artery

VF= Automated Perimetry

Table des matières

Part 1: Introduction

1. Anatomy and functional characteristics of the visual pathway

The afferent visual pathway receives, relays and processes visual information. Therefore, the visual system is one of the most organized and efficient neural system. A comprehensive understanding of visual anatomy and visual functions is essential for the accurate diagnosis of neuropathological conditions.

The aim of this chapter is to review the primary structures involved in visual physiology.

1.1. Retina

The retina plays a crucial role in transforming light energy into neural signals. Three key types of cells are important in transmitting visual information: photoreceptors, bipolar cells and ganglion cells. Other neurons, such as amacrine cells, horizontal cells and interplexiform neurons, act modulators of the signal. Müller cells, a type of glial cell, have both metabolic and structural roles, supporting retinal cells [1]. Ganglion cells are the first neurons of the optic nerve and are directly or indirectly involved in optic neuropathies. Their axons form the retinal nerve fibre layer, which exit the eye as the optic nerve.

1.1.1. Histologic classification

Under electronic microscopy, the retina consists of ten distinct layers (Figure 1). These layers include three neuronal layers (photoreceptors, bipolar cells and ganglion cells) and a layer of pigmented epithelium, with synaptic connections in between[2] .

a. ***The inner limiting membrane*** separates the retina from the vitreous body. It contains the terminations of Müller cells.

b. ***The nerve fibres layer*** consists of the axons of the ganglion cells, which converge to form the optic nerve.

c. ***The ganglion cell layer (GCL)*** axons tracts extend towards the back of the eye. In the macula, this layer is composed of 8 to 10 layers of ganglion cells, separated by the glial processes of Müller cells.

d. ***The inner plexiform layer*** contains synapses between bipolar and ganglion cells, as well as synapses between amacrine cells and ganglion cells.

e. ***The inner nuclear layer*** consists of the cell bodies of amacrine cells, Müller cells, bipolar cells and interplexiform neurons. Occasionally, ganglion cells can also be found in this layer.

f. ***The outer plexiform layer*** is where synaptic connections occur between photoreceptors and the cells of the inner nuclear layer.

g. ***The outer nuclear layer*** contains the cell bodies of the photoreceptors.

h. ***The outer limiting membrane*** is a band of zonula adherens between the photoreceptors and Müller cells, acting as a metabolic barrier.

i. ***The photoreceptors layer*** consists of the outer and inner segments of the two photoreceptors (rods and cones). Human have three types of cones that respond to specific wavelengths of light : short wavelengths cones (blue), medium wavelengths cones (green) and long wavelengths cones (red) [3]. Rods are more sensitive to light and are particularly useful in dim light. The photoreceptors convert light photons into electrical impulses in a process known as *phototransduction* [4]. The concentration of cones is 15 times higher compared to the peripheral retina whereas rods are predominantly located in the periphery[5].

j. ***The retinal pigment epithelium (RPE)*** is a single layer of cuboidal pigmented cells that provides structural and metabolic support for the photoreceptors.

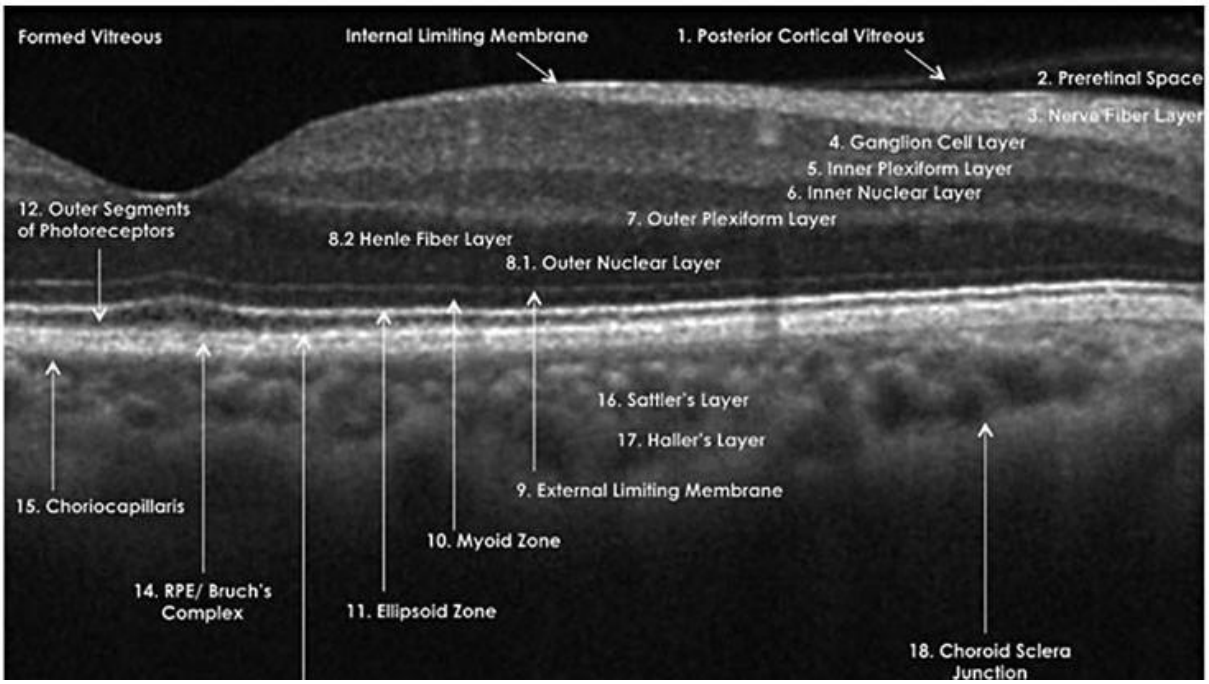

***Figure 1*: Macular SD-OCT (Heidelberg Engineering, Heidelberg, Germany) imaging.** *Section through the retina in the en-face image showing the different layers of the retina. Illustration from Liu at al (2016)* [6].

1.1.2. Function of retinal cells

The retina is typically divided into the **inner** (containing ganglion cell) and the **outer** retina (which includes photoreceptors, the RPE, and the bipolar cells). Pathologies affecting the optic nerve primarily involve the inner retina, particularly the ganglion cells, whereas the majority of retinal diseases are associated with the outer retina (Figure 2). The functions of the different retinal layers are reviewed below.

The retinal pigmented epithelium (RPE)

The RPE is derived from the ectoderm and is composed of pigmented hexagonal cells. It is tightly attached to the choroid through the Bruch's membrane. The RPE plays a crucial role in

vitamin A metabolism[7]. Moreover, it forms the blood-retinal barrier, which prevents the passage of molecules from the choroid into the retina and facilitates the active transport of molecules into and out the RPE [8]. Furthermore, the RPE is responsible for phagocytosing the outer segments of the photoreceptors [8].

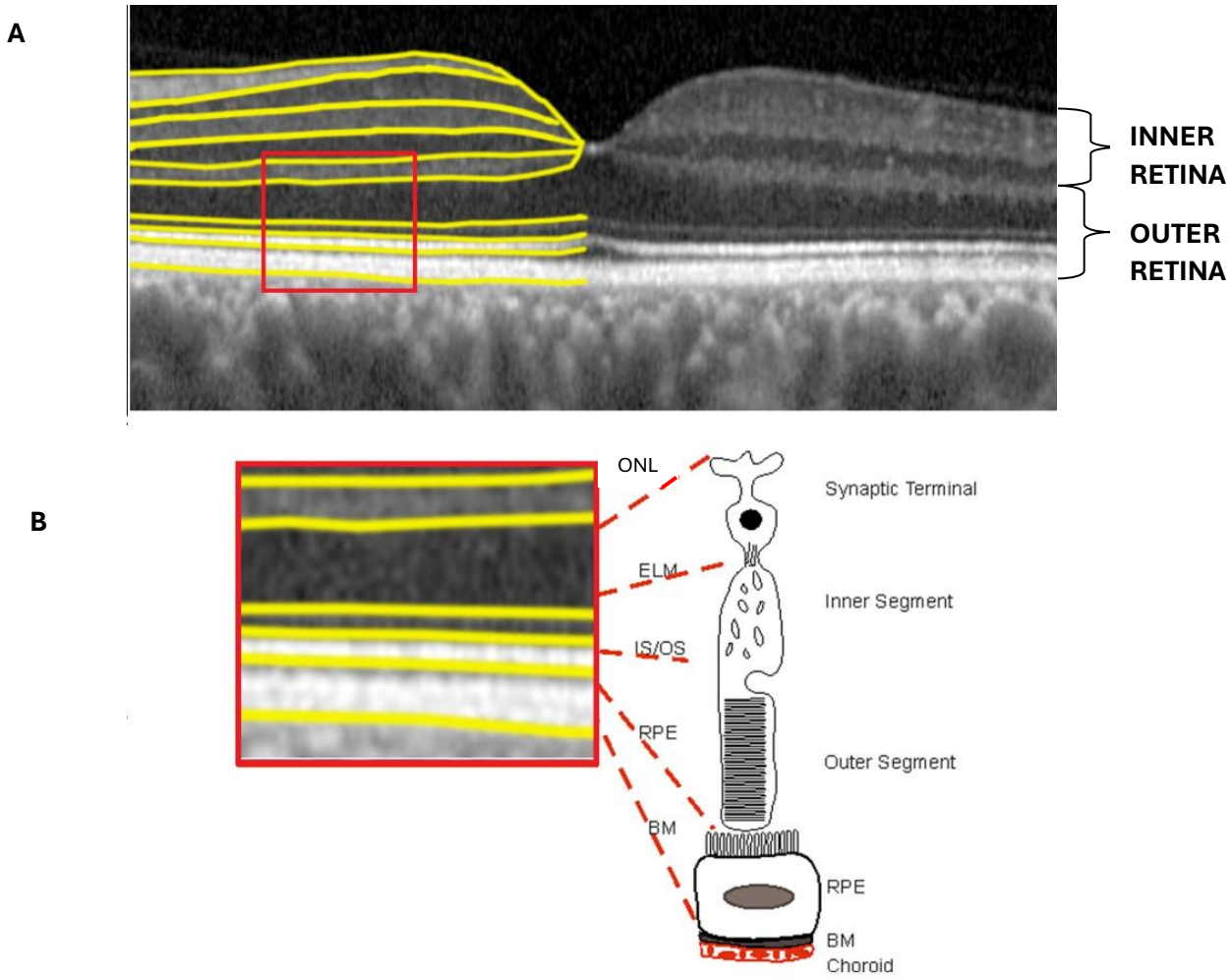

Figure 2*: A.** *Macular SD-OCT imaging illustrating the location of the inner (retinal nerve fibres layer, ganglion cells, inner plexiform layer, inner nuclear layer) and the outer retina (outer plexiform layer, outer nuclear layer, external limiting membrane, photoreceptors, retinal pigment epithelium and Bruch's membrane).* ***B. *A schematic demonstrating the correspondence between the outer retinal layers seen on OCT (red square) and the photoreceptor segment and retinal pigment epithelium. The outer nuclear layer contains the synaptic terminal of the cone and rod photoreceptors. The inner segment and outer segment (IN/OS) line is the junction between the photoreceptors outer and inner segments. The outer limited membrane is the junction between the photoreceptors inner segment and the nuclei of the photoreceptors. BM= Bruch's membrane RPE= retinal pigment epithelium. IS/OS= inner and outer segments ELM= external limiting membrane/ outer limiting membrane ONL= outer nuclear layer. Illustration from Kaye et al (2021)*[9].

The photoreceptors

Photoreceptors are divided into rods and cones. Human have three types of cones, each responding to specific wavelengths of light : *short* wavelengths cones (blue), *medium* wavelengths cones (green) and *long* wavelengths cones (red) [3]. Cones are mainly located in the macular region and are activated under bright light conditions (photopic vision) while rods are concentrated in the peripheral retina and function mainly in dim light (scotopic vision). The concentration of cones in the macula is 15 times higher than in the peripheral retina[5].

Both photoreceptors contain photopigments that absorb photons of light. These photopigments enable the conversion of light photons into electrical impulses, a phenomenon known as *phototransduction* [4]. The photopigment of rods is called rhodopsin.

Each photoreceptor consists of an outer segment, which contains the photopigments, and are connected to the inner segment by the cilium. The inner segment contains metabolite apparatus including mitochondria, the endoplasmic reticulum, and the Golgi apparatus, which are essential for producing the energy required for phototransduction. The light-induced change in membrane potential in the outer segment is transmitted through the inner segment, which ultimately alters neurotransmitter release at the synaptic terminal[10]. The cell body, containing the nucleus, lies between the outer and the inner fibres, which lead to the terminal synapse (Figure 3).

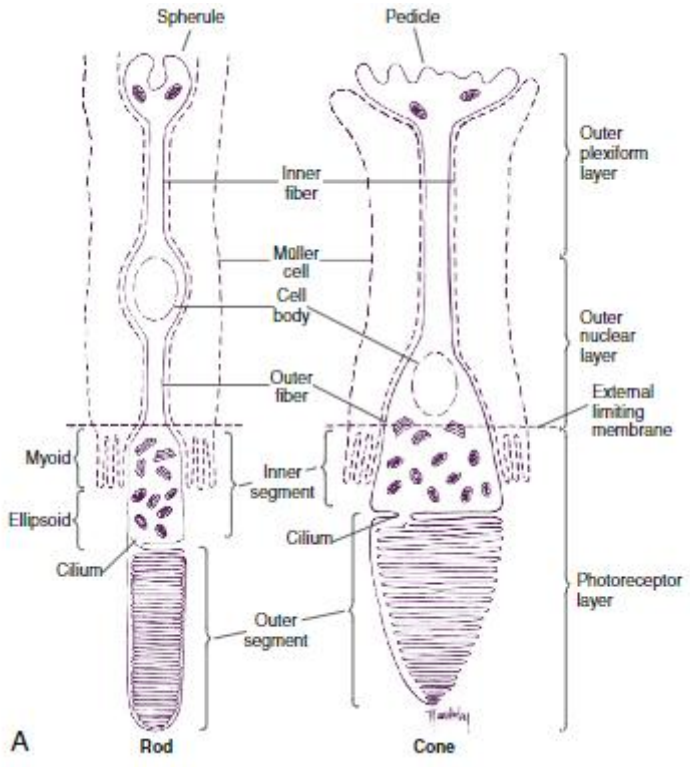

Figure 3: *Schematic diagram of human rod (right) and cone (left) photoreceptors. Illustration from Remington LA (2012)* [2]

Bipolar cells

Bipolar cells are second-order neurons in the visual pathway. They transmit visual information from photoreceptors to ganglion cells, horizontal cells and amacrine cells. Bipolar cells also receive feedback from amacrine cells [11]. They have two types of synapses: dendritic synapses, which connect with photoreceptors and horizontal cells, and axonal synapses, which connect with ganglion and amacrine cells.

Kolb et al have described eleven different types of bipolar cells including rod bipolar cells, flat bipolar cells, midget bipolar cells, diffuse cone bipolar cells, blue cone bipolar cells and giant cone bipolar cells [12]. Each bipolar cell is further subdivided into ON bipolar cells – the most

abundant- and OFF bipolar cells, depending on whether they depolarize or hyperpolarize in response to light, respectively [8].

In the fovea, each bipolar cells receives the input from one cone whereas in periphery they receive inputs from multiples photoreceptors[13]. This anatomical distinction supports the perception of detail, motion and colour vision, which is strongly supported by the macula.

Retinal ganglion cells

Retinal ganglion cells (RGC), the third-order neurons, are much more concentrated in the central retina with 6 to 7 layers and tend to be much sparser in the periphery [14]. RGC lie between the inner plexiform layer and the nuclear fibres layer. Their morphology is highly variable; they can have either small or large cell bodies [12,15]. Larger ganglion cells are typically found in the periphery, while smaller ganglion cells are located in the perifoveolar macula [16].

RGC are the final receivers and transmitters of the initial visual stimulus. Their axons follow the inner surface of the retina, converge in the optic disc, and form the optic nerve. Then, the vast majority of the axons terminate in the lateral geniculate nucleus, while about 10% project to the subthalamic area. These subthalamix axons – called the melanopsin retinal ganglion cells - are useful for the pupillary reflex and regulation of the circadian rhythm.

RGC are classified based on the layers of the lateral geniculate nucleus where they terminate: P cells in the parvocellular layers (layers 3-6) and M-type ganglion cells in the magnocellular layers (layers 1-2) [17]. P cells, accounting for 90% of the GCL, are subdivided intoas P1 cells, which receive input from two bipolar axons and in P2 cells which have a denser dendritic tree [12]. The number of P cells is higher than the M cells in the macula whereas P cells are equal to M cells in the periphery[18]. While M cells subserve general information about depth perception, motion and low spatial contrast sensitivity, P cells give information about colour vision, texture,

and high visual contrast sensitivity. The papillomacular bundle is made of small axons especially P cells[19].

The axons of the ganglion cells anterior to the lamina cribrosa are unmyelinated, resulting in slower conduction speeds and higher energy demands. This likely explains the abundance of mitochondria in this region[20]. As the axons become myelinated, the number of mitochondria decreases.

A study in mice examined the impact of aging on the number of ganglion cells and found a decrease in the ganglion cell complex (inner plexiform layer (IPL) + ganglion cell layer (GCL), GCC) by 1.3 µm in 9 months [21]. It showed that a diminution of. Similar findings have been reported in histologic studies of humans [22,23].

Horizontal cells

Horizontal cells are so named because they have a horizontal orientation in the retina. They synapse with photoreceptors, bipolar cells and other horizontal cells and play a modulatory role in the transmission of information between photoreceptors and bipolar cells [8]. Three types of horizontal cells have been described based on the number of dendrites connected to cones or rods and are designated as HI, HII and HIII [24].

Amacrine cells

Amacrine cells are interneurons that modulate the signals reaching the ganglion cells. Approximatively, 40 subtypes of amacrine cells have been described, categorized by their dendritic field diameters: narrow-field, small-field, medium-field and wide-field[25].

Müller cells

Müller cells (MC) are the most common glial cells found in the human retina [1]. Located in the outer limiting membrane[8],they have a metabolic role, synthesizing retinoic acid and recycling the photopigments. They also play a structural role, providing stability of the retinal cells and protecting them from a trauma [1].

1.2. Optic nerve

1.2.1. Retinal ganglion cell axons

Approximately 1.2 million retinal ganglion cell axons converge at the optic disc (OD) to form the optic nerve. Axons from the foveal RGC form the papillomacular bundle and enter directly into the temporal part of the OD (Figure 3). Axons from nasal RGC enter the nasal part of the disc, while axons from temporal RGCs, which correspond to the nasal visual field, form arcuate bundles on either side of the horizontal raphe and enter the superior and inferior sectors of the OD (Figure 4).

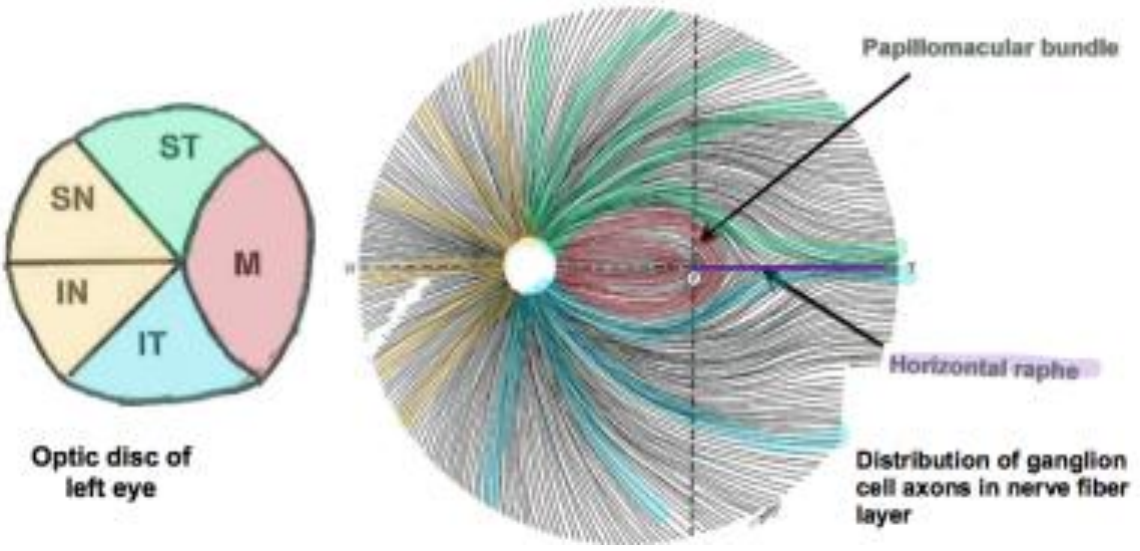

Figure 4: *Drawing illustrating the course of the retinal ganglion cells axons in nerve fibre layer in the left eye. Temporal fibres reach the optic nerve head via a superior (green) and inferior arch (blue), which stand above and below the papillomacular bundle (pink) and the macula, separated by the horizontal raphe. The fibres from the central macula have a much more direct path, via the papillomacular bundle (pink), and finally, the nasal fibres radiate directly without a horizontal raphe. Illustration from Danesh-Mayer et al, 2019* [26].

1.2.2. Clinical correlations

This specific distribution results in stereotyped patterns of visual field defects when RGC axons are injured. For instance, a *nasal step* (a localized visual field defect adjacent to the nasal horizontal meridian) occurs when temporal fibres are affected (Figure 5); whereas a *temporal wedge* (a small visual field loss located temporally to the blind spot) is seen when nasal RGC fibres are involved (Figure 6). In a nasal step defect, there is a clear respect of the horizontal meridian, unlike in temporal defects. Additionally*, arcuate scotomas* are observed in patients with damage to the temporal RGC axons (Figure 7). However, this topographic correspondence between the RGC and the optic nerve fibres becomes gradually lost once the axons enter the nerve.

This topographical arrangement of RGC axons contributes to our understanding of the retinal nerve fibres layer (RNFL) and GCC thickness across different locations. Each quadrant should be analysed independently when assessing RNFL and GCC thickness.

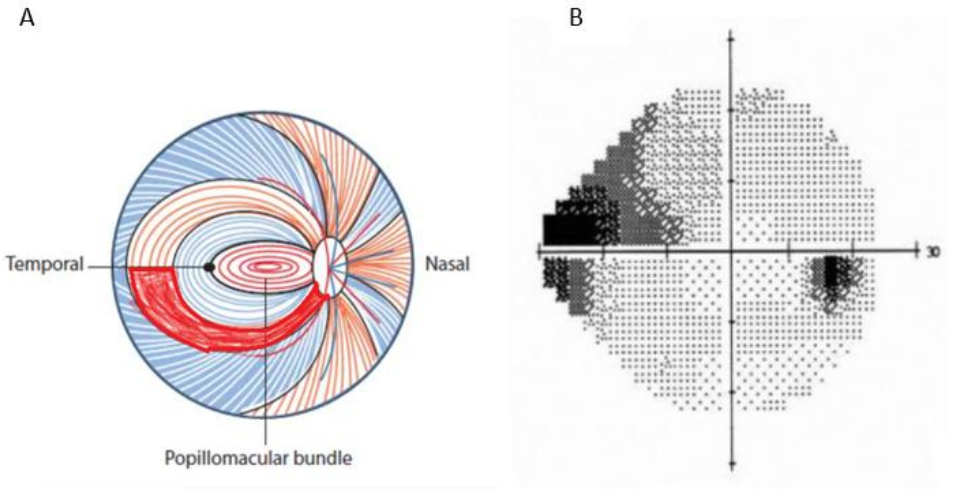

Figure 5: *Drawing illustrating the damage to inferior nerve fibres serving the inferotemporal retina (A) and the consecutive nasal step (B).*

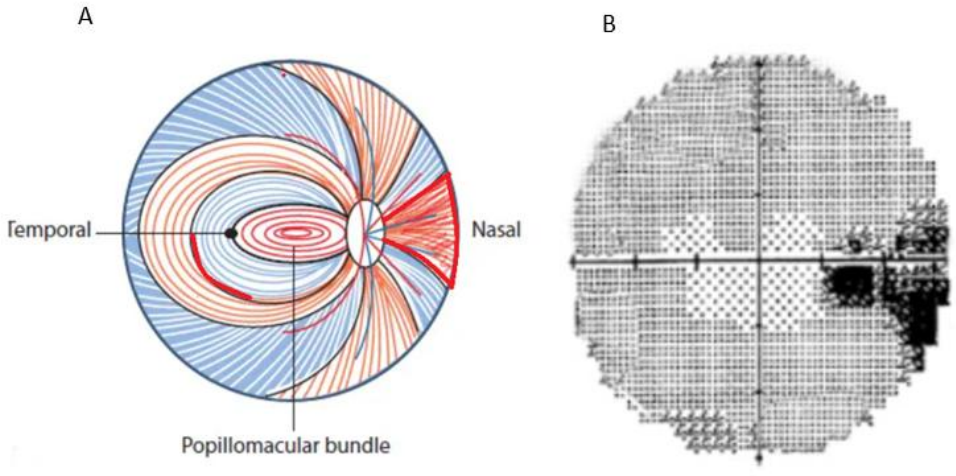

Figure 6: *Drawing illustrating the damage to nasal nerve fibres serving the nasal retina (A) and the consecutive temporal wedge (B).*

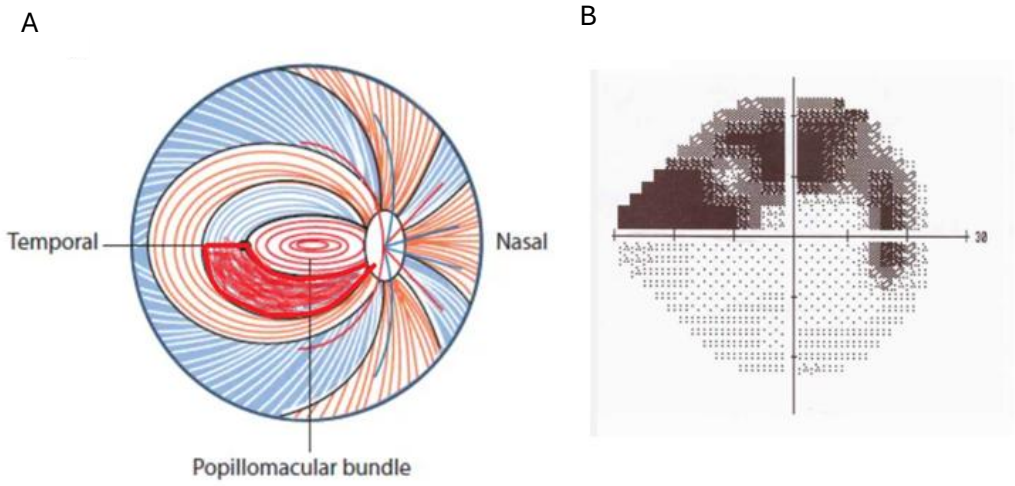

Figure 7: *Drawing illustrating an injured nerve fibre bundle containing axons from the inferonasal et inferotemporal retina (A) and the consecutive arcuate scotoma (B).*

1.2.3. The optic nerve topography

The optic nerve begins at the optic nerve head and extends to the optic chiasm. The optic nerve measures approximately 30 millimetres from the optic nerve head to the optic canal and about 55 mm from the OD to the chiasm[27]. The optic nerve is composed of RGC axons and glial cells. Main glial cells include astrocytes (which provide support and nutrition to neurons), microglial cells (which have phagocyting functions) and oligodendrocytes (which produce the myelin sheath of the optic nerve) [27]. Oligodendrocytes account for 70% of glial cells in the post laminar portion of the optic nerve.

The optic nerve is surrounded by meninges: the dura mater (outer layer), the arachnoid mater (middle layer) and the pia mater (inner layer).

The optic nerve is divided into 4 portions: intraocular (0.7 -1mm), intraorbital (25-30mm), intracanalicular (4-10mm) and intracranial (10 mm) [27] .

1.2.4. The fourth part of the optic nerve

a. The intraocular part

The OD is characterized by a central depression called the cup, through which the central ophthalmic artery and vein pass (Figure 8). A cup-disc ratio of 0.3 is typically described as the "normal" OD [28]. Due to the absence of photoreceptors in the OD region, a blind spot is observed in the visual field (Figure 9). The OD head is a complex anatomic area that provides both structural and functional support for the retinal ganglion cell axons passing through. Embryologically, the OD head represents the junction between the optic stalk and the optic vesicle. It also marks the transition between the neuroretina and the RPE (Figure 10).

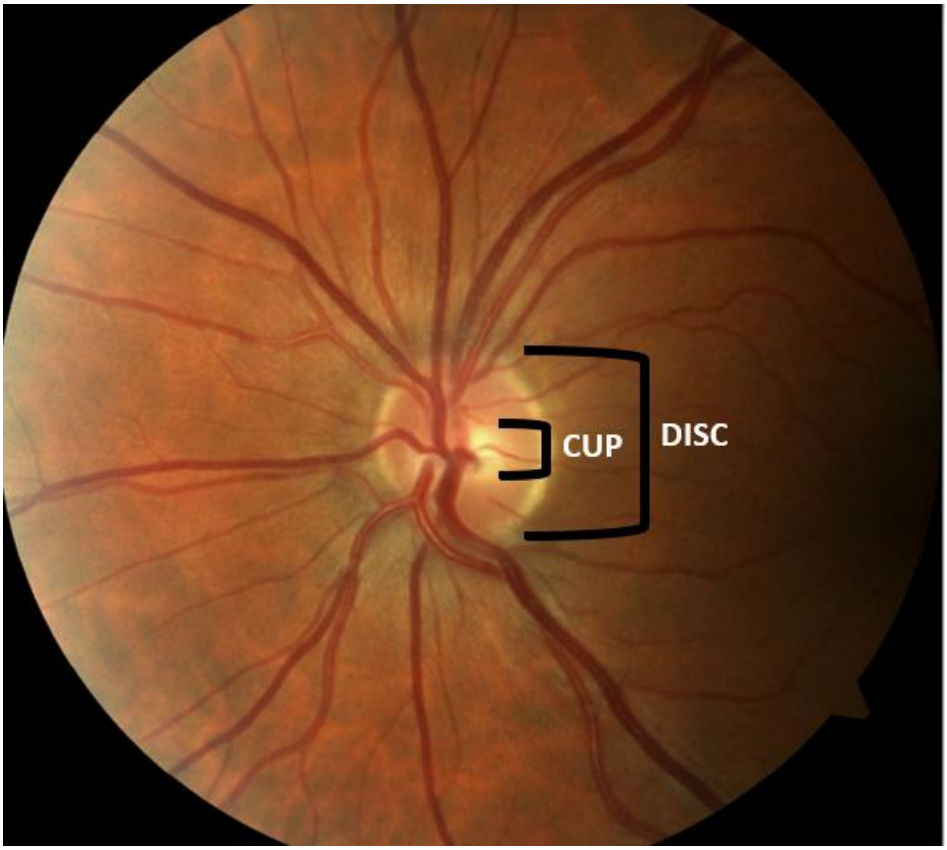

***Figure 8*: Fundus photography** *illustrating the cup-disc ratio defined as the diameter of the cup divided by the diameter of the whole nerve disc.*

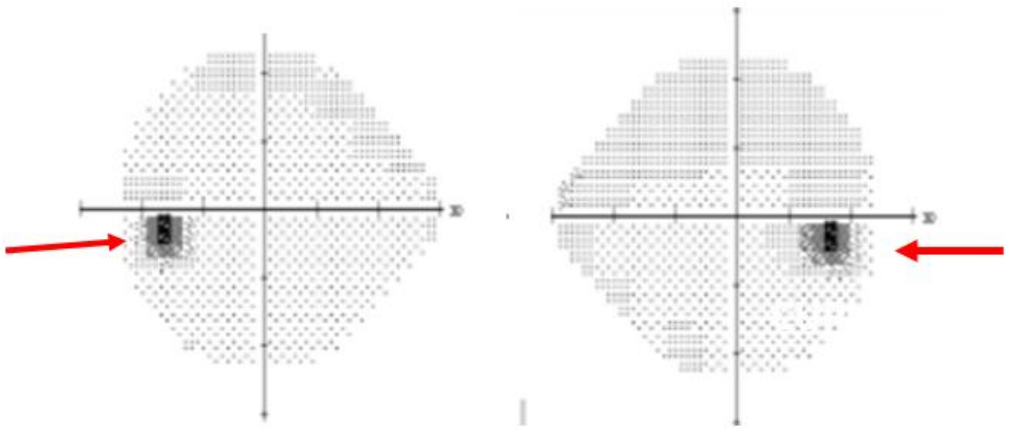

***Figure 9*: Automated Visual field** *showing the blind spot (see red arrows) corresponding to the absence of photoreceptors in the optic disc region.*

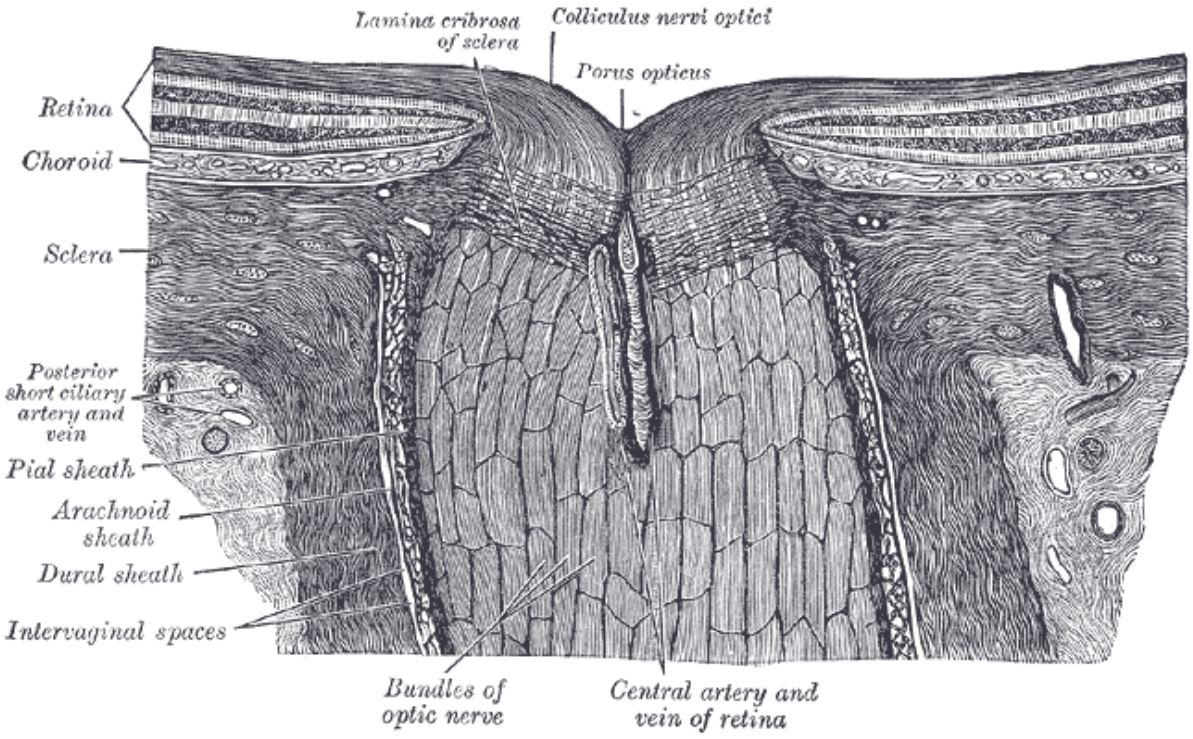

***Figure 10*:** *Drawing illustrating the cross section of the optic nerve head of the human eye. Illustration from Gray et al (1918)*[29].

b. The intraorbital part

In its orbital portion, the optic nerve is surrounded by the rectus muscles, the oblique muscles, adipose tissue and connective tissue. The optic nerve is curved and slackened, allowing free movement of the globe during ocular motility.

c. The intracanalicular part

The optic nerve passes into the brain via the optic canal, where it is surrounded by the ophthalmic artery and sympathetic nerve fibres designated for the orbit.

d. The intracranial part

The intracranial portion of the optic nerve lies within the skull and extends toward the optic chiasm This portion is located above the planum sphenoidale and the sella turcica.

1.2.5. The lamina cribrosa

The optic nerve fibres exit the eye through the lamina cribrosa. In the prelaminar region, the optic nerve fibres are unmyelinated to avoid interference with incoming light [30] whereas they are myelinated in the retrolaminar region. The prelaminar portion of the optic nerve is located above the Bruch's membrane (Figure 11).

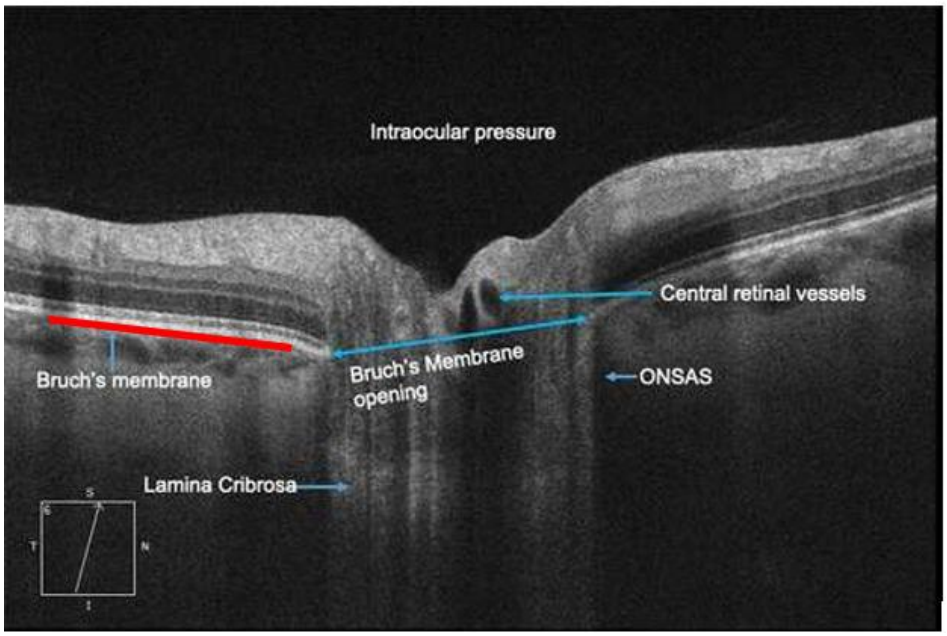

***Figure 11*: Optic nerve OCT imaging.** *Cross section through the optic nerve showing the anatomy of the prelaminar region of the optic nerve. This area is located above the Bruch's membrane (red line). Prelaminar region comprises unmyelinated optic nerve fibres and the central retinal vessels. ONSAS: Optic nerve subarachnoid space. Illustration from Kedar et al (2022)* [31]

A translaminar pressure gradient, which refers to the difference between the intracranial pressure (ICP) and the intraocular pressure (IOP) in the optic nerve sheath, may influence optic nerve conformation and contribute to axonal damage (Figure 12). This gradient seems to play a key role in the progression of glaucoma and the severity of papilledema [32].

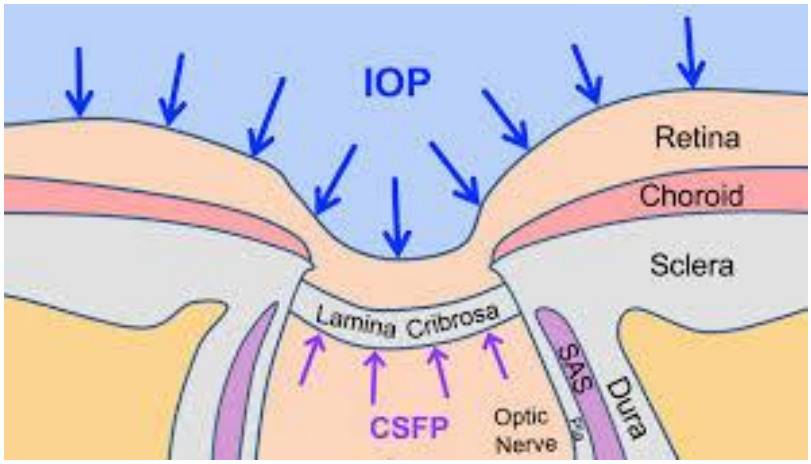

***Figure 12*:** *The translaminar pressure gradient. Graph illustrating the effects of the intraocular pressure (IOP) and the cerebrospinal fluid pressure (CSFP) on lamina cribrosa, influencing the optic nerve conformation and axonal damage. Illustration from Down JC et al, 2020* [33].

1.2.6. The vascularization of the optic nerve

The vascularization of the optic nerve is divided into two parts: the **anterior portion,** which supplies the optic nerve head and the **posterior portion**, which supplies the retrolaminar region (Figure 13).

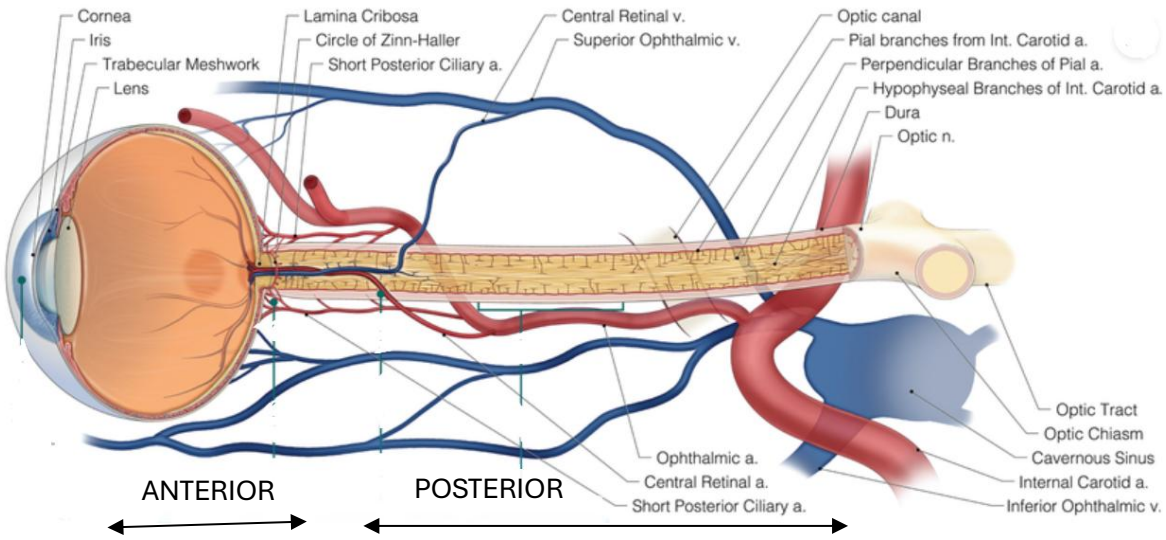

***Figure 13**: Vascularization of the optic nerve. The most anterior part of the optic nerve head (labelled "anterior") is supplied by the posterior ciliary artery and the retinal arterioles whereas the retrolaminar part of the optic nerve (labelled "posterior") is supplied by the central retinal artery, the ophthalmic artery and the pial arteries. Illustration from Mendel et al, 2017*[34].

The vascular supply of the OD remains controversial. Histopathologic studies of human eyes suggest that OD is supplied by choroidal branches and short posterior ciliary arteries (SPCA) without contributions from the central retinal artery (CRA)[35]. Others studies have observed some vascularization from the CRA and the peripapillary choroid branches[36] or exclusively from the posterior ciliary arteries [37]. More recently, Yu and al have cannulated both the CRA

and SPCA to label the microvasculature of the optic nerve and the retina, confirming that both the CRA and SPCA contribute to optic nerve vascularization[38].

Olver et al confirmed the significance of the "circle" of Haller and Zinn formed by the medial and lateral SPCA, in supplying blood to the laminar and retrolaminar regions of the optic nerve[39]. The "circle" of Haller and Zinn is identifiable in all subjects and is described as a microscopic arteriolar intrascleral anastomosis forming a horizontal ellipse which is divided into superior and inferior parts (Figure 14) [39]. However, interindividual variation is common. In some subjects, this anastomosis between the lateral and the medial SPCA may be complete or incomplete with overlapping regions[39,40]. Pial arterioles, arterial-arterial anastomoses and recurrent choroidal branches also arise from the "circle of Haller and Zinn[39]. Moreover, an extrascleral arterial anastomosis, distinct from the intrascleral 'circle' of Haller and Zinn, is formed by more distal branches of the SPCA [39].

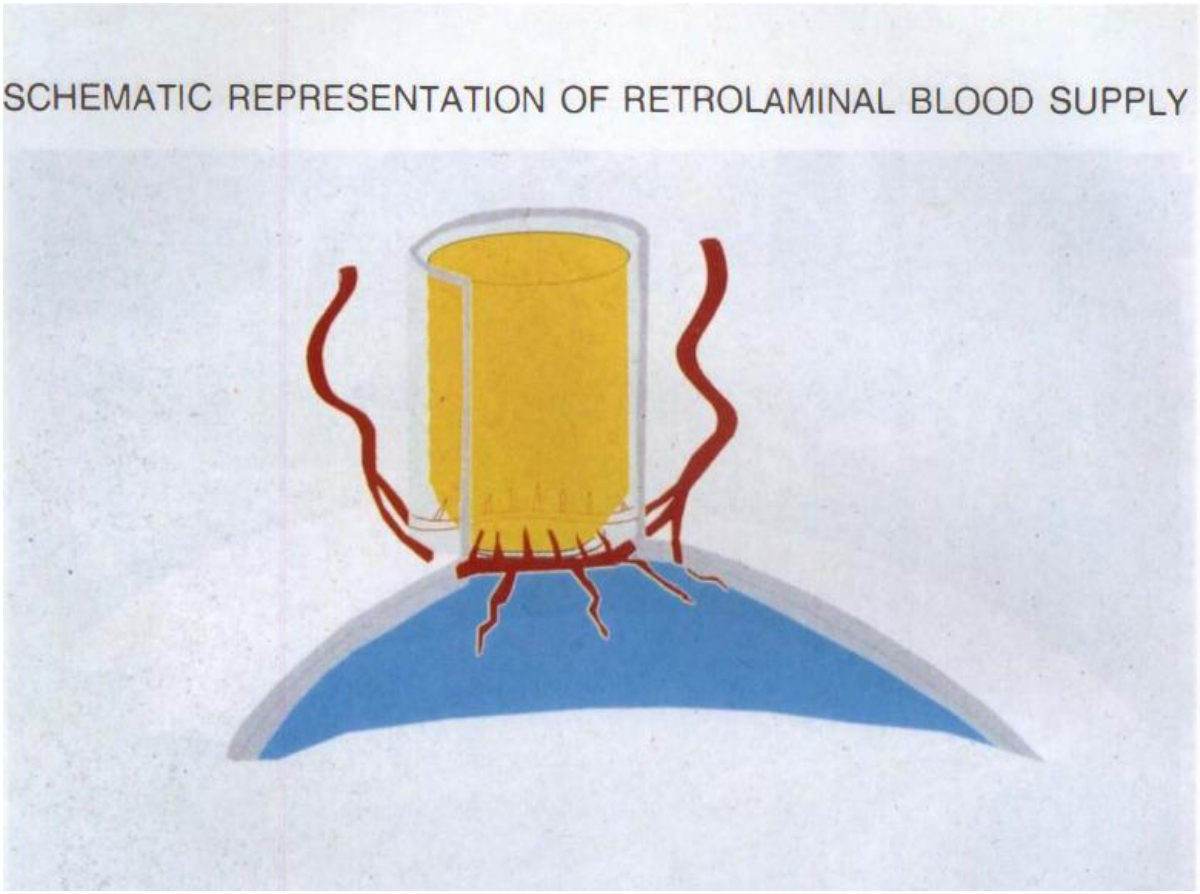

Figure 14: *Schematic representation of the "circle" of Haller and Zinn. It is an intrascleral arteriolar anastomosis derived from medial and lateral paraoptic short ciliary arteries. Illustration from Olver et al,1990* [39].

1.2.7. Optic nerve head blood flow studies

a. Fundus fluorescein angiography

Dynamic blood flow characteristics are assessed by fundus fluorescein angiography (FFA)[41] . FFA is an ophthalmic procedure in which fluorescein dye is injected into a vein (typically in the arm or the hand). As the dye passes through the retinal blood vessels, photographs are taken to analyse retinal and choroidal circulation with a fundus camera with blue and green filters. The fluorescein dye, with its low molecular weight, binds to proteins in the blood[42,43].

FFA primarily assesses the retinal vasculature. The division of the central retinal artery into four branches (nasal and temporal superior branches and nasal and temporal inferior branches) is easily observed in the photographs (Figure 15). These branches supply the inner retinal layers. The foveal avascular zone, a capillary free zone of 400 microns in the fovea, (the central part of the retina), appears hypofluorescent (dark) on the FFA (Figure 16).[44]. The outer retinal layers and the foveal avascular zone are supplied by the choroidal circulation. In approximately 20% of individuals, a cilioretinal artery is present, which supplies the papillomacular bundle.

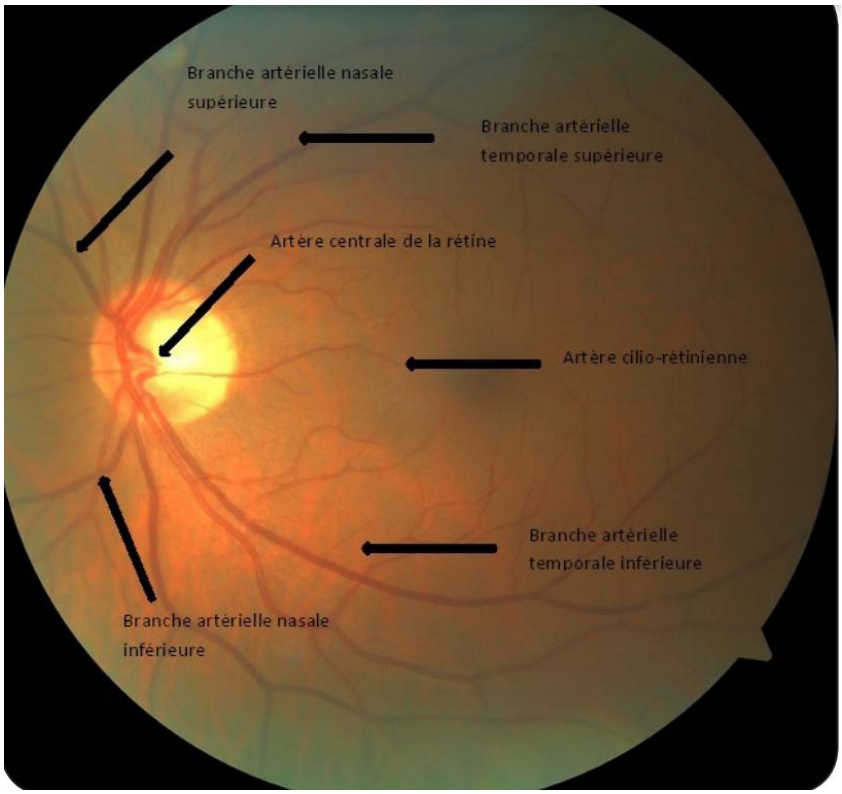

Figure 15: *Illustration of the vascularization of the retina. Illustration from Chapelle et al, 2018* [45].

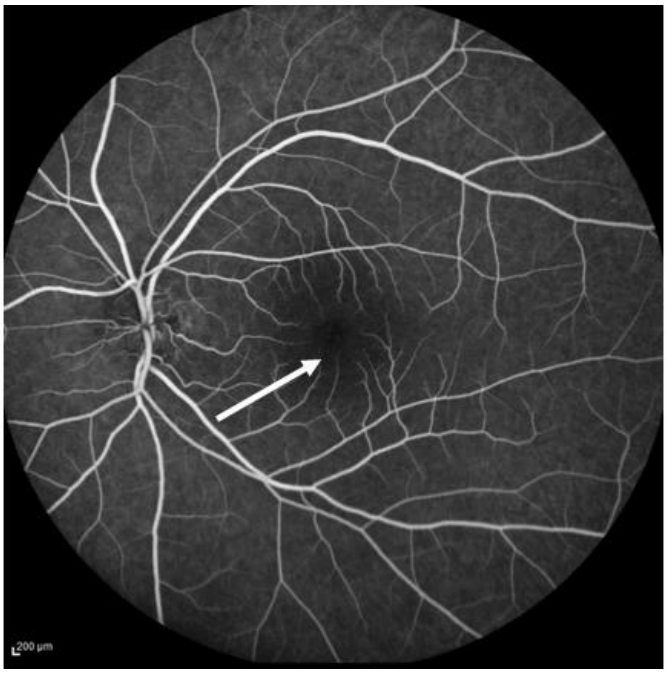

***Figure 16*: Fundus fluorescein angiography** *showing the avascular foveal zone (arrow). This zone is devoid of retinal blood vessels and is located at the centre of the retina. This is why the avascular foveal zone has a dark appearance in angiography.*

Five stages are observed in healthy patients after dye injection (Figure 17). The first is the **choroidal phase**, occurring 10 to 15 seconds after the injection, when the choroidal filling via the posterior ciliary arteries takes place. The **arterial phase** follows 1 to 2 seconds later, as the dye passes through the arteries. The third phase- the **arteriovenous phase**- happens 1 to 2 seconds after the arterial phase et corresponds to the filling of precapillary arterioles, capillaries and postcapillary venules. Afterwards, this is followed by the veinous **phase**, where the veinous filling becomes complete. Finally, in the **recirculation phase,** which occurs approximately 10 minutes after injection, dye concentration gradually decreases and staining of the optic nerve, choroid, Bruch's membrane and sclera is visible.

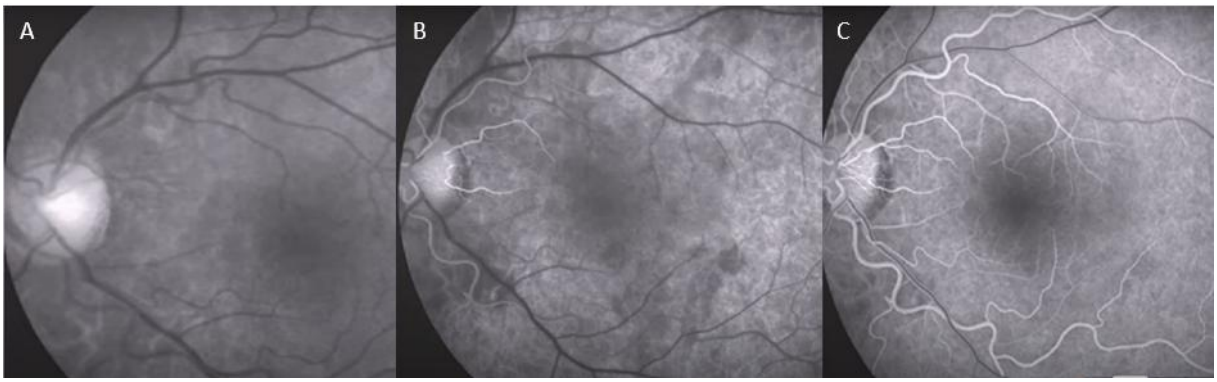

***Figure 17*: Fundus Fluorescein Angiography** *illustrating A. the choroidal phase (choroid filling via the posterior ciliary arteries) B. the arterial phase (filling of the arteries) C. the arteriovenous phase (filling of the arteries and the veins).*

b. Dynamic analysis of the optic nerve vasculature with fluorescein angiography

Assessment of the optic nerve vasculature with FFA identifies two phases corresponding to the filling of the superficial and the deep vascular networks [46,47]. During the choroidal phase, the deep plexus, which represents the microvasculature of the prelaminar/laminar region, fills while the superficial vessels begin to fill during the arterial phase[47]. The paraoptic branches of the SPCA supply the deeper network while the radiate superficial network appears to be supplied by branches of the CRA[48].

A watershed zone is observed on FFA as a delayed filling between the territories supplied by the medial and lateral posterior ciliary arteries. The optic disc is located in this area and this finding is seen in 42% of normal patients[49] (Figure 18). The impact of this watershed zone on the optic disc vasculature is still under debate.

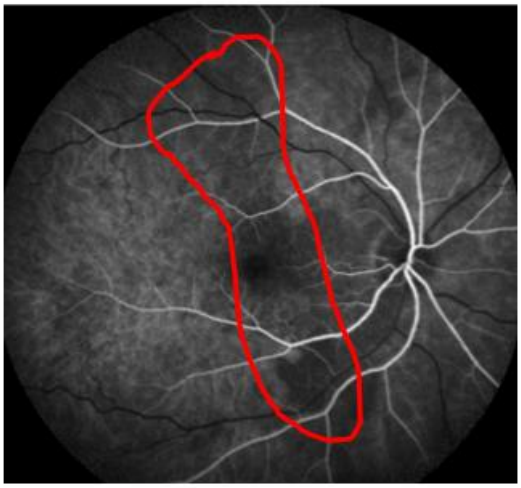

***Figure 18*: Fundus Fluoresceine angiography.** *Visualization of the watershed zone surrounded in red, revealing the demarcation line between the medial and lateral posterior ciliary artery supply.*

c. *Non-invasive study of the microvasculature of the optic nerve*

Capillaries in the peripapillary retina, the superficial part of the ON head and the retrolaminar regions form a non-fenestrated confluent network. This network varies significantly: it is irregular and complex in the prelaminar and retrolaminar region (with longitudinal and transverse capillaries) whereas the capillaries in the laminar region are mainly transverse. A polygonal network is observed through the lamina cribrosa. This microvasculature is easily studied using optical coherence tomography angiography (Figure 19). The segment at the choroidal level shows the highest capillary density [50]. These retinal peripapillary capillary networks are critical for supplying the peripapillary RNFL (pRNFL).

1

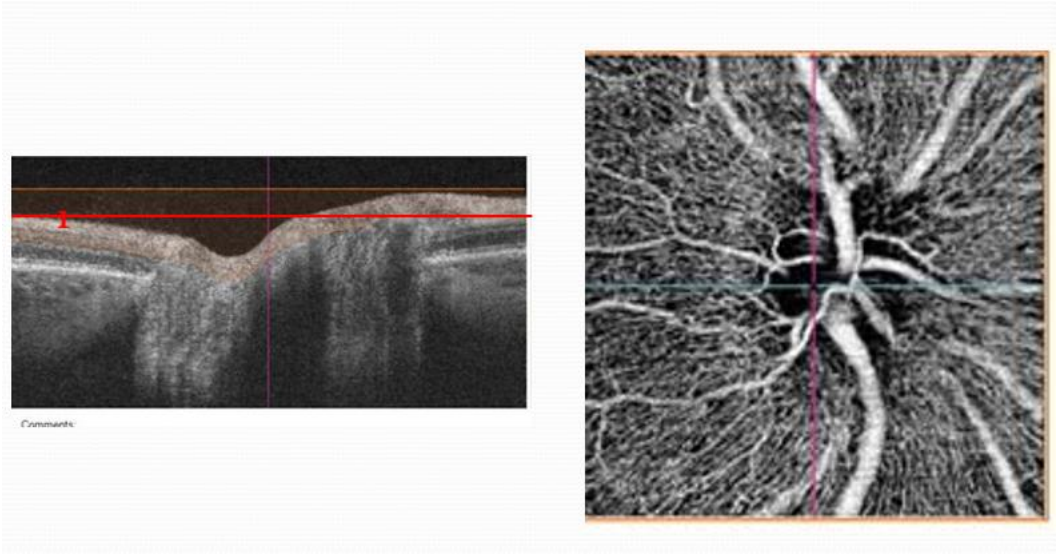

2

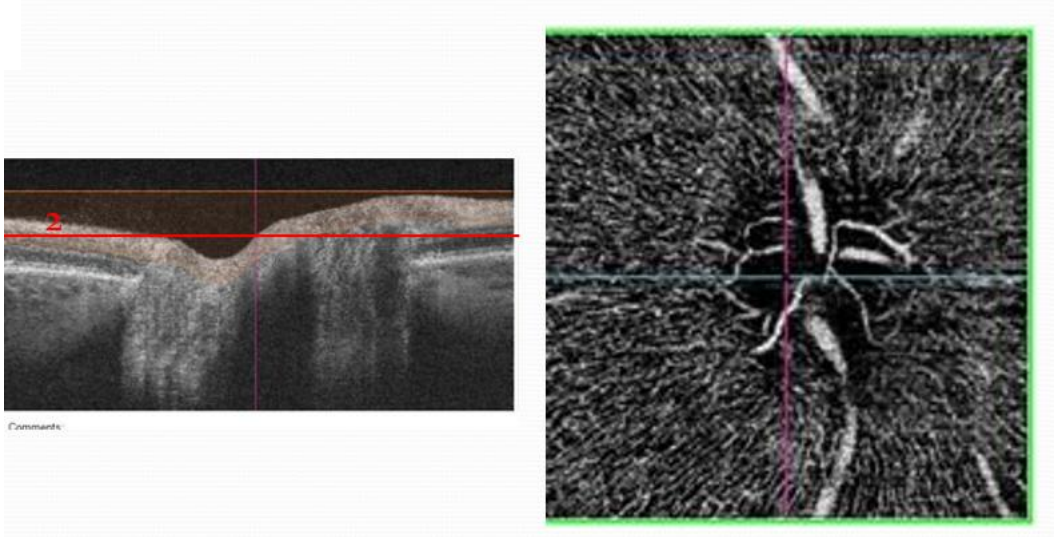

3

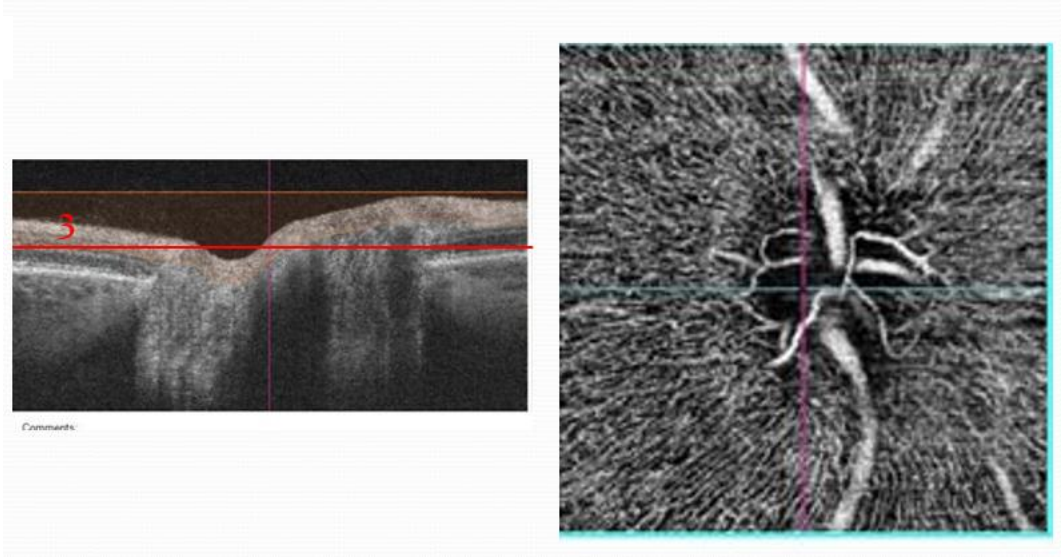

4

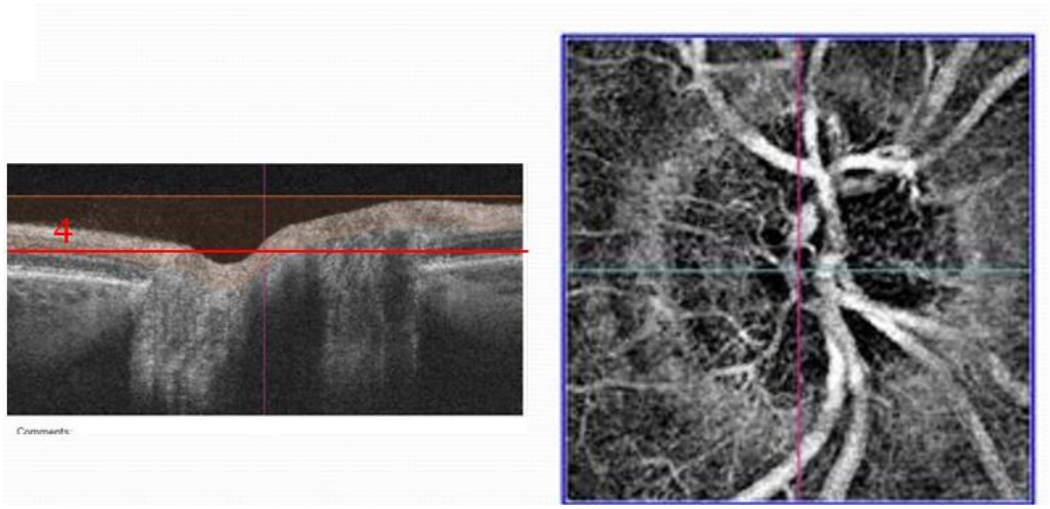

***Figure 19*: Optical Coherence Tomography Angiography.** *Vertical section through the optic nerve microvasculature (right image) at the level of the retinal nerve fibre layer (1), the superficial layer 50 µm from the internal limiting membrane (2), 70 µm from the internal limiting membrane and the whole depth (4) as indicated by the red line in the en-face image (left). This imaging study non-invasively and rapidly the microvasculature of the optic nerve disc.*

Part 2: Prerequisite

2. Non-arteritic anterior ischemic optic neuropathy: symptomatology and pathogenesis

Non-arteritic anterior ischemic optic neuropathy (NA-AION) is a common optic neuropathy affecting people over 50 years old second only to glaucoma[51]. The condition was first clearly defined as a clinical syndrome by Hayreh in 1974[52]. Patients often presented with a painless sudden loss of vision involving one eye associated with an altitudinal visual field defect [53,54] (Figure 20). The diagnosis of NA-AION is supported by the anamnesis and fundus examination, showing a swollen optic disc in the affected eye at presentation and a crowded disc in the fellow eye[51]. Sub-acute loss (progression over days or weeks) may occur[55]. The fellow eye may be involved sequentially.

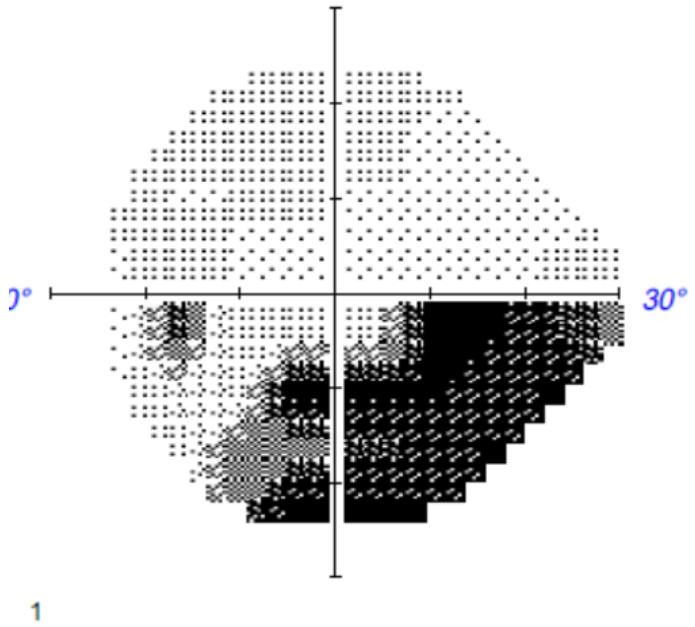

***Figure 20*: Visual field** *(Humphrey 30-2, Dublin, California) showing an inferior altitudinal defect in a patient with non-arteritic anterior ischaemic optic neuropathy in the left eye.*

Optic disc microvasculature has high implications for the understanding of ischemic anterior optic neuropathy. Indeed, in anterior ischemic optic neuropathy (AION), histopathologic studies reported infarction located in the retrolaminar part of the optic nerve head, suggesting that SPCA branches are involved in the pathogenesis (Figure 21)[56].

AION is divided into arteritic AION (A-AION, 10% of cases) and non-arteritic AION (NA-AION, 90% of cases) related to the aetiology. In fact, A-AION is due to a vasculitis of the SPCAs engendering inflammation, thrombosis and occlusion leading to infarction of the optic nerve head [57]. A-IOAN is mainly induced by giant cell arteritis (GCA) and affects the intima, causing a decreasing of the vessel lumen and then a reduction of the blood flow. It is an important diagnosis to make because it is an ocular and a vital emergency.

However, in NA-AION, histopathologic studies did not show the exact location nor the cause of the vascular compromise [56]. The disc swelling results from ischemia secondary to sectoral hypoperfusion of the pre-laminar optic nerve head due to failure of the posterior ciliary arteriolar supply. Indeed, FFA identified a sectorial delayed filling in the oedematous phase[52,56,58,59]. Collignon-Robe et al confirmed a decreased optic nerve head blood flow in patients with NA-AION compared with fellow eyes [60]. The ultimate cause of the failure of arterial supply is unknown but a major risk factor is a “crowded” optic disc (OD), which is a common variant of OD morphology (absence of a cup)[61,62]. Other likely risk factors are obstructive sleep apnoea (OSA)[63,64] and systemic hypertension[65] (although the AION associated with malignant hypertension has distinct features and can be bilateral and simultaneous [66,67]). Any risk associated with elevated intraocular pressure (IOP)[68–70]remains controversial[69,71,72].

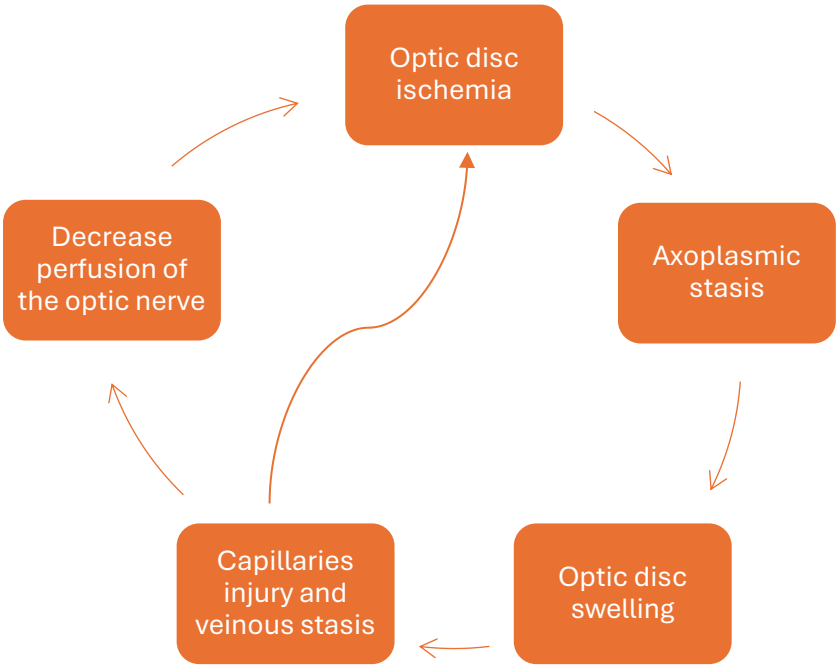

Figure 21: *Representation of the pathogenesis involved in NA-AION. Hypoperfusion of the optic nerve due to failure of the posterior artery supply induced optic disc ischaemia. A consecutive axoplasmic stasis led to intracellular axonal swelling which may further compress capillaries and produce a vicious cycle of ischemia.*

3. Optical coherence tomography

3.1. Introduction

Optical coherence tomography (OCT) has revolutionized the analysis of the optic nerve and retinal disorders. It is a non-invasive and reproductive technique generating cross-sectional images. This imaging technique allows the visualization of the different layers of the retina in vivo and have shown a good correlation with histology[73–75]. Compared to ultrasounds or MRI, OCT has substantial advantages as fast and easy acquisition without contact, high resolution (20-5µm) and rapid colocalization of retinal features. Therefore, it is not surprising that OCT has become an essential tool in ophthalmology to assess and follow optic neuropathies, maculopathies and anterior segment disorders.

3.2. Principle

OCT is based on the principle of backscattering and interferometry[76,77]. A beam of light is projected on the retina and the locations of boundaries between the layers of the retina are obtained from the time to the sensor of the reflected light. Thickness measurements of the retinal layers at the micron level are available.

OCT projects a near infrared light (820nm) which is split into two beams: one sending to the target tissue, the *sample beam*, and the other to the reference mirror at a well-known distance,

the *reference beam* (Figure 22). Then, the echo time delay of light reflected from various layers of target tissue is compared with the echo time delay of light reflected from the reference mirror.

A positive interference is produced when light reflected from target tissue and from reference mirror arrives simultaneously (only possible if the optical paths are matched to be equal in length). Interferences are associated with light intensity and are measured as an electrical signal by a photodetector, which finally produce a range time of delay for comparison (temporal coherences). Indeed, in function of the reflection of the structure, different interferences can be observed (coherent or destructively), leading to different contrast between structures (Figure 22).

Two different scans are described: the amplitude scan (A-scan) and the brightness scan (B-scan). In the A-scan, the reference mirror is scanned in depth whereas in the B scan, the sample beam is scanned laterally [77].

Over the last decades, introduction of spectral domain OCT (SD-OCT) has increased speed and image quality. In 2006, Heidelberg Engineering introduced SD-OCT combined with a scanning laser ophthalmoscope (SLO), facilitating the visualization of the fundus. Moreover, an eye tracking technology is added in this machine, which permit to follow eye movement and the realisation of scan in the same place.

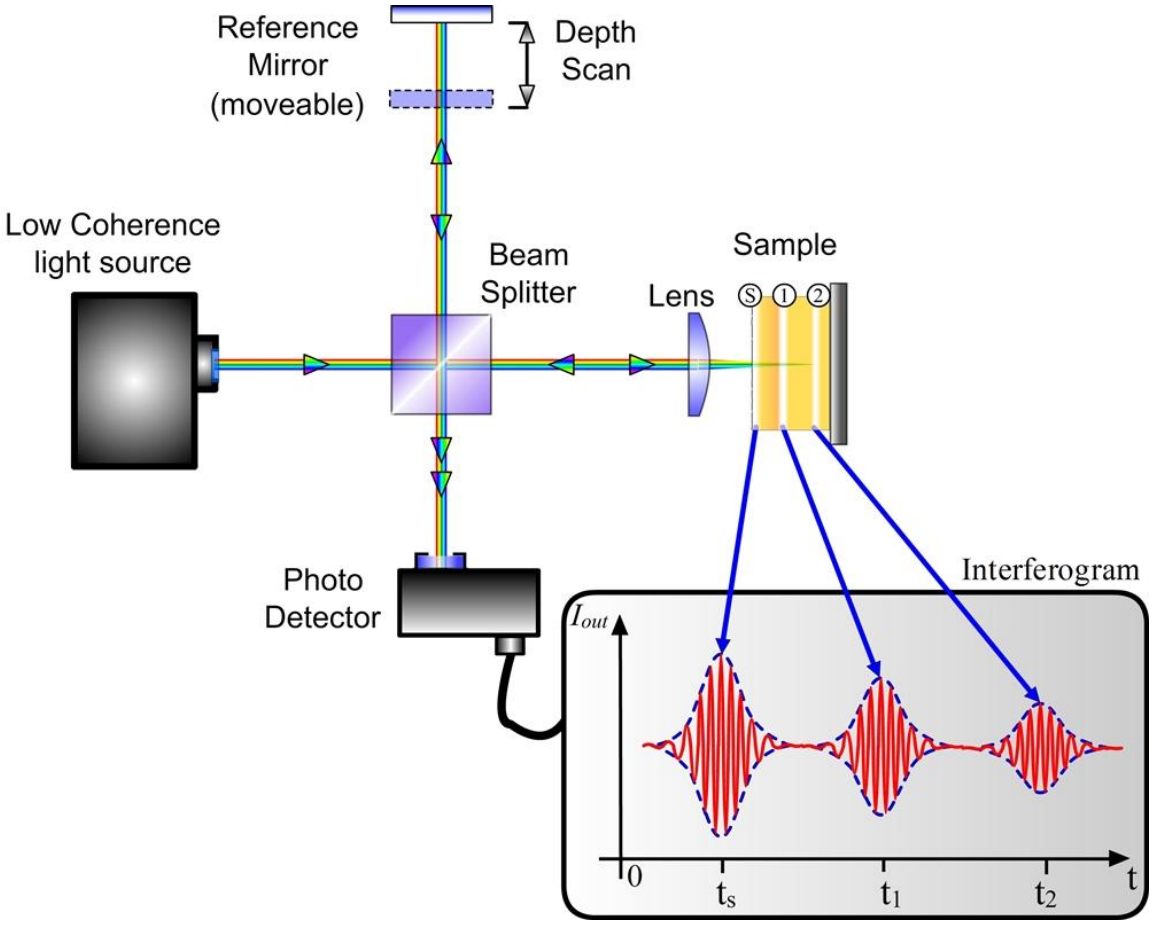

Figure 22: *Illustration of the principle of the Ocular Coherence Tomography (OCT). OCT projects a near infrared light, which is split into two beams, one being projected onto a plane mirror and the other on the eye. The two waves created are reflected. The wave sent on the mirror returning in the form of a simple echo whereas the wave sent into the eye in the form of a multitude of echoes depending on the structure crossed. These waves are compared by an interferometer which measures the coherence. Illustration from Research Centre for Non-Destructive Testing GmbH*

3.3. OCT in neuro-ophthalmology

The management of optic neuropathy is fundamental to neuro-ophthalmic practice. Following the invention of the ophthalmoscope, clinicians, for a century or more, relied upon fundus examination in the evaluation of optic neuropathy. However, the advent of optical coherence tomography has revolutionized the analysis of optic nerve and retinal disorders.

Optical coherence tomography has proven of particular value in the measurement, at the micron level, of the peripapillary retinal nerve fibre layer (Figure 23) and the ganglion cell layer (Figure 24). These measurements have proven critical in the differential diagnosis and monitoring of optic neuropathy. Specifically, thinning of the peripapillary nerve fibre layer provides evidence of axonal loss affecting any sector of the optic nerve. Thinning of the macular ganglion cell layer, on the other hand, shows a more precise correlation with visual deficits due to retrograde degeneration (axonal damage leading to a loss of the proximal axon and cell body) following optic nerve damage, although limited to central retina. Optic nerve damage induces an interruption of the axonal transport of neurotrophic support to the ganglion cells [78,79] and lead to an apoptotic cascade, starting with an accumulation of intracellular calcium [80–82].

In daily practice, optical coherence tomography is of great value in assessing the diagnosis, prognosis and response to treatment in optic neuropathy because of its reproducibility. Particular advances have been made, for example, in the assessment of optic neuritis, papilloedema and chiasmal compression which have translated to everyday practice.

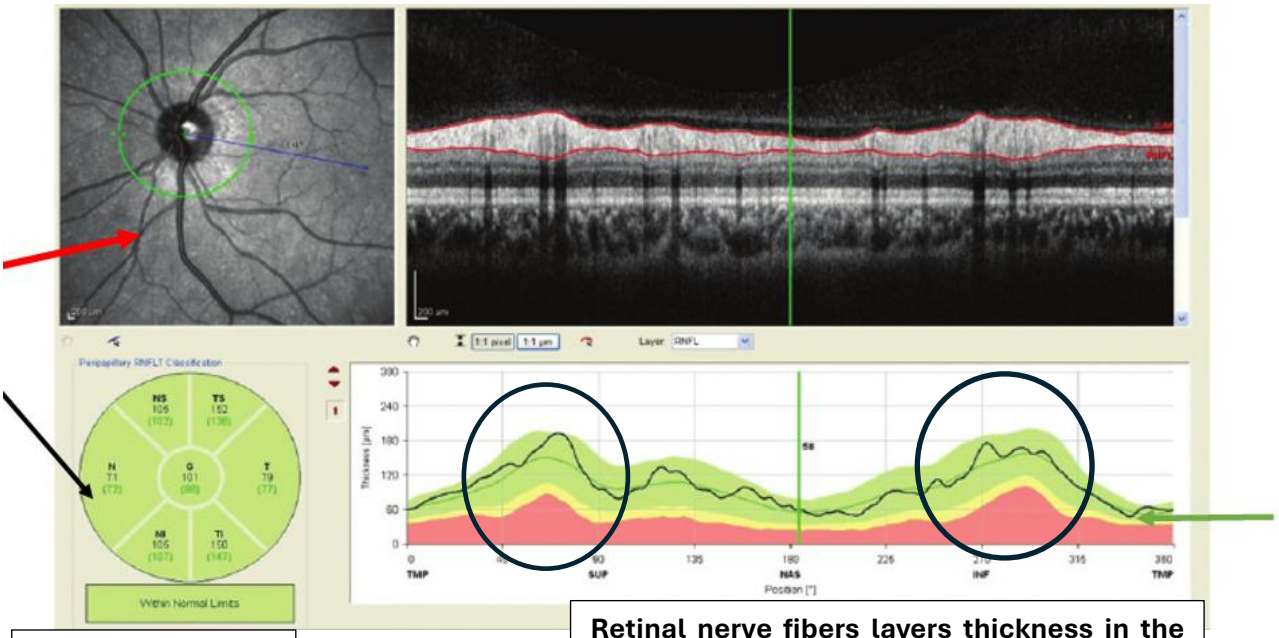

Figure 23*: Optical coherence tomography** *(Spectralis Heidelberg, Germany)* ***imaging. *Assessment of peripapillary RNFL for the left eye. The black arrow shows the RNFL quadrant average thickness matched to normative database. RNFL TSNIT graph (green arrow) displays patient's RNFL measurement along the calculation circle (red arrow), compared to a normative database. The double peaks (surrounded by blue circles) represent the superior and inferior thickness which are greater than nasal and temporal poles. It is due to the greater distribution of ganglion cell axons in retinal fibre layer in the superotemporal and inférotemporal part.*

A

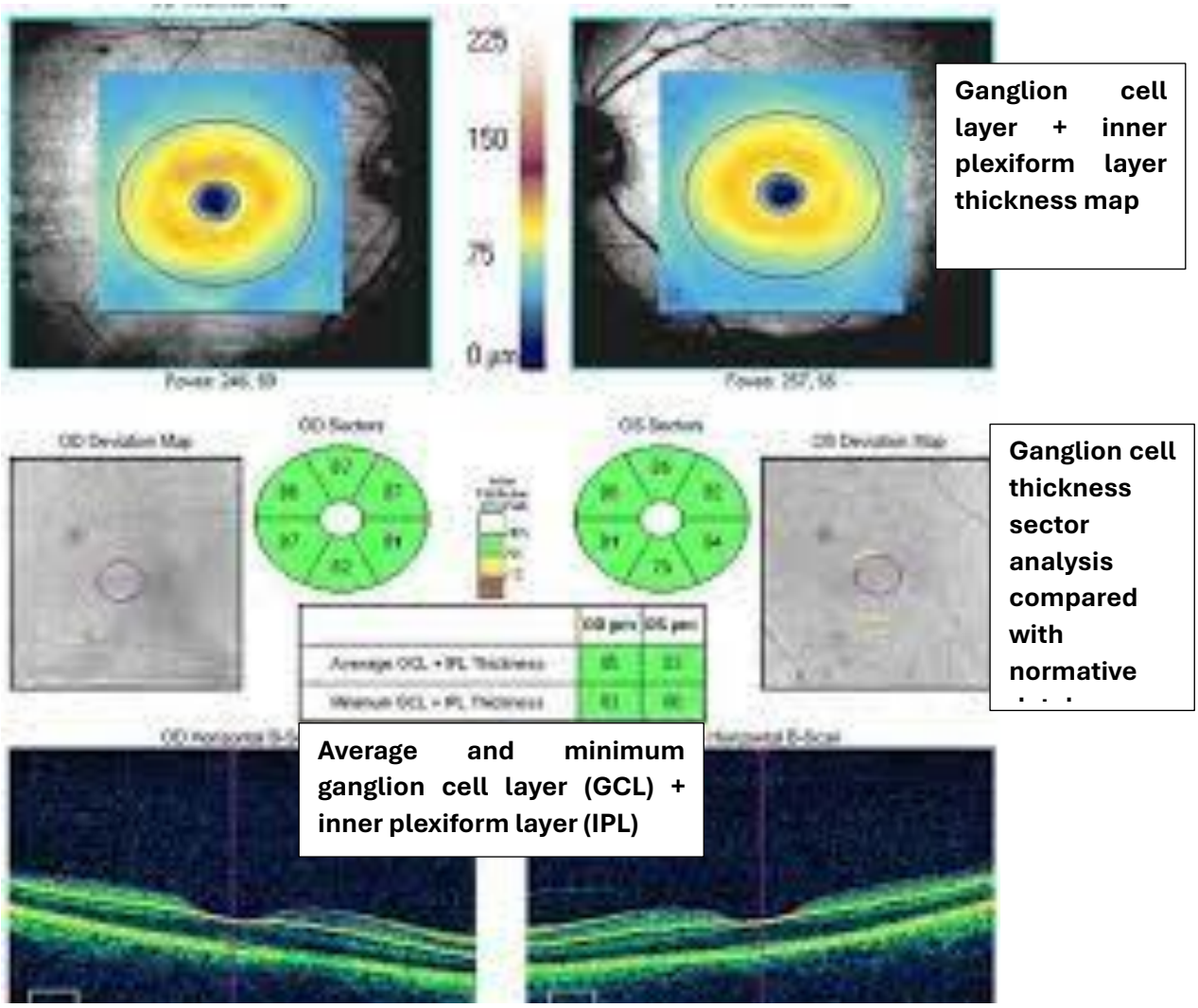

B

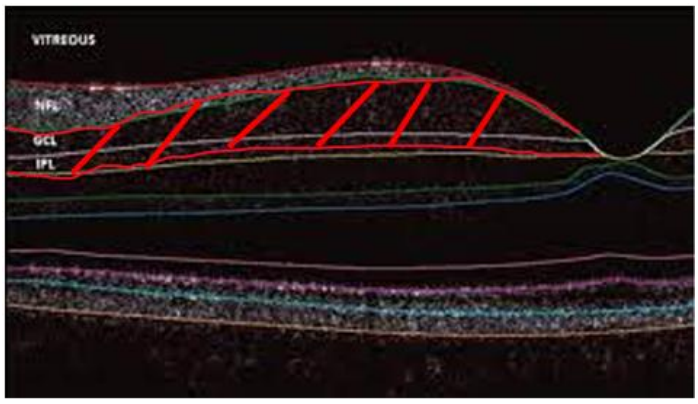

***Figure 24*: Optical coherence tomography** *(HD-OCT Cirrhus, Carl Zeiss Meditec, Dublin, California) imaging A. Assessment of Ganglion cell complex (ganglion cell layer (GCL) + inner plexiform layer (IPL) quadrant average thickness matched to normative database. B. Visualisation of the GCL and the IPL, corresponding to the ganglion cell complex represented by the red area.*

3.4. Limitations

The accuracy of our diagnosis and the analysis of the results rely on the estimation of the Ganglion Cell Complex (inner plexiform layer (IPL) + ganglion cell layer (GCL), (GCC) or RNFL thickness. A proper definition of the boundaries to avoid an overestimation or an underestimation of the RNFL and GCL thickness is warranted [74,75]. Segmentation artefact due to motion (53.3%), retinal layer misidentifications (50%) and absence of the inner segmentation line (7.8%) have a significant impact on the quality of the image [83] (Figure 25). The frequency of artefacts is greater in patients with macular pathology (dry and wet macular degeneration, pigmentary retinopathy, diabetic macular oedema and high myopia) [75,83], tilted disc, peripapillary atrophy, small cup disc ratio and optic disc swelling [84,85]. Moreover, the OCT signal strength -which can be diminished due to opacification of the macular media as in the case of corneal oedema or opacity of lens or vitreous- is an additional factor influencing the image quality and the segmentation analysis [86]. In order to avoid artefacts, developers focused on reducing the processing time, improving the volume segmentation and visualising the reconstruction of the macula in three-dimensions.

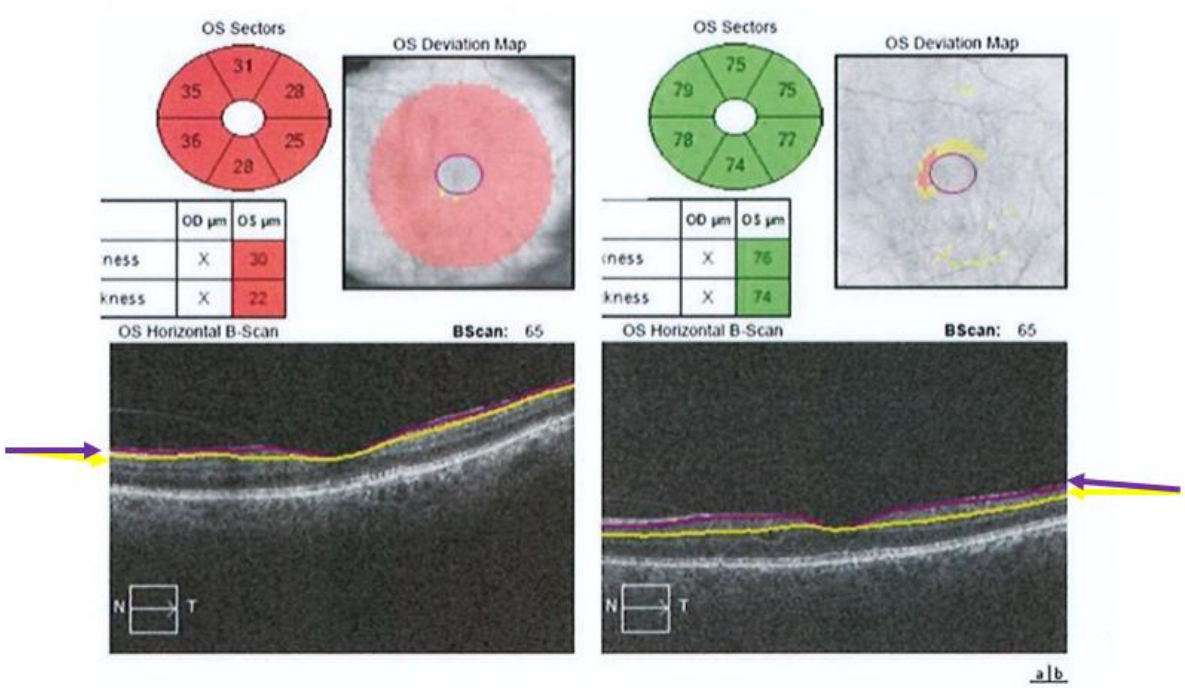

***Figure 25*: Optical coherence tomography** *(HD-OCT Cirrhus, Carl Zeiss Meditec, Dublin, California) imaging showing a retinal layer misidentification due to a vitreomacular traction (left) and a proper segmentation obtained previously in the same patient (right). The ganglion cell thickness + inner plexiform layer is measured between the purple inner boundary of the ganglion cell layer (see purple arrow) and the yellow inner boundary of the inner plexiform layer (see yellow arrow).*

Every analysis is compared to a normative reference range in function of the sex and the age. Because of the individual variation, the small size sample, or the absence of normative range, as in adolescent or children, results can be misinterpreted as outranged the reference data and considered abnormal after comparison to the normative database[87]. In fact, a good function eyes might be considered abnormal after comparison to the normative database [87]. In addition, refractive errors superior to +5.0 dioptres and inferior to -5.0 dioptres are excluded of the reference database. However, axial length influences measurements of pRNFL thickness and optic nerve head analyses. Indeed, related to a magnification effect, hyperopic eyes have a small optic nerve and an increased pRNFL whereas myopic eyes have larger disc and a decreased

pRNFL[88]. In research studies an “in house” matched control group, matched for age, gender, axial length and ethnicity, is recommended[89].

Finally, OCT cannot distinguish a functional cell from a dysfunctional cell. Indeed, in patients with no perception of light, retinal nerve fibre layer thickness is still measured at 45µm because dysfunctional cells are taken in account [90].

4. Research objectives

Optic nerve disorders often affect acutely or chronically the pRNFL and thus the RGC by direct retrograde degeneration, axonal damages leading to loss of the proximal axon. These changes significantly impact patient's visual function including visual acuity, colour vision and the visual field. Advances in OCT now allow for non-invasive, h high resolution imaging of retinal layers, facilitating the assessment of ganglion cells.

The primary objective of this work was to answer the following question: "What degree of ganglion cell loss (in terms of thickness and percentage) is required to cause permanent visual defects, leading to complete loss of function in non-arteritic anterior ischaemic optic neuropathy (NA-AION)?". To address this, longitudinal changes in GCC thickness was analysed in a cohort of patients with NA-AION, the second most common cause of optic neuropathy worldwide. The pathogenesis of NA-AION is of particular interest due to the sectorial infarction of the optic disc, which leads to apoptosis of RGCs corresponding to a persistent visual field defect.

This study assessed the percentage of ganglion cell loss at the onset of NA-AION and during follow-up. The GCC thinning was correlated with pRNFL thickness, visual acuity and visual field deficits. This analysis aimed to identify a critical threshold of ganglion cell loss necessary to preserve visual function within normal limits. Moreover, the location of GCC thinning was also determined and the qualitative loss of GCC was analysed to reveal distinct patterns useful for c an accurate differential diagnosis of miscellaneous optic neuropathies.

The secondary objective of this study was to investigate and report in detail the pattern and evolution of intra-retinal oedema and subretinal fluid accumulation in NA-AION, resulting from ischemia at the optic disc. The presence of subretinal fluid and peripapillary inner nuclear

layer oedema is likely an underestimated feature of acute NA-AION and this study aimed to clarify the pathogenesis of these findings.

Moreover, epidemiologic data on NA-AION were collected, with a focus on evaluating cardiovascular risk factors associated with the occurrence of NA-AION, as well as describing the management of patients with NA-AION.

Part 3: Assessment of retinal ganglion cells in optic neuropathies

5. Utility of ganglion cells for the evaluation of anterior visual pathway pathology

Chapelle AC, JM Rakic, GT Plant

Published as Chapelle AC, Rakic JM, Plant GT. Utility of ganglion cells for the evaluation of anterior visual pathway pathology: a review. Acta Neurol Belg. 2024.

5.1. Introduction

Optic neuropathies are a major portion of the work-load of neuro-ophthalmologists. Many are one component of a more extensive neurological disorder. For decades, neuro-ophthalmologists have utilised fundus examination (ophthalmoscopy) in the assessment of optic nerve structure. Optical coherence tomography (OCT), however, has revolutionised the analysis of both optic nerve and retinal disorders. OCT is based on the principle of backscattering and interferometry[76]. A beam of light is projected to the retina and the locations of boundaries between the retinal layers are obtained from the time to the sensor of the reflected light. Thickness measurements of the retinal layers at the micron level are available.

The RNFL is measured where it is thickest in the peripapillary region (pRNFL). The retinal ganglion cells (RGC) layer (GCL) is thickest at the macula (up to 10 cells thickness), and progressively thinner towards the periphery (down to a single cell) [14]. In practice the GCL is most commonly measured at the macula together with the inner plexiform layer (IPL) designated the Ganglion Cell Complex (GCC). RGCs are the final receivers and transmitters of the initial retinal signal. Their axons follow the inner surface of the retina and enter the optic disc to form the optic nerve.

The majority of RGCs project to the lateral geniculate nucleus (LGN) and are classified according to the LGN layer in which they terminate: P-type ganglion cells in the parvocellular layers (layers 3-6) and M-type in the magnocellular layers (layers 1-2) [17]. The P cells, accounting for 90% of the GCL, are subdivided into P1 cells, which receive input from two bipolar cell axons and in P2 cells which have a denser dendritic tree [12]. The population of P cells is greater than that of the M cells in the macula whereas in the periphery P and M cells are equal in density[18]. While M cells subserve information concerning depth perception, motion and are sensitive to lower contrasts, P cells process information related to colour vision, texture, and higher contrast. Other RGCs (a more heterogeneous population than P and M cells) project to the koniocellular (interlaminar) regions of the LGN. In many cases the function of this group is unknown. Some are involved in colour vision and others in ocular motor control.

All optic neuropathies may affect acutely or chronically the retinal nerve fibre layer (RNFL) and thus the RGC, by direct retrograde degeneration, i.e. axonal damage leading to loss of the proximal axon and cell body. Thinning of the GCC has been found to be strongly related to visual loss in optic neuropathy related to glaucoma, optic neuritis, papilloedema, intrinsic and extrinsic optic nerve tumours, ischaemic, hereditary and toxic optic neuropathy [91]. However, as with any other imaging technology, the clinician must have a clear understanding of acquisition artefacts affecting the estimation of the GCC or RNFL thickness. The relatively small normative database in sub-populations such as the young and individuals with a refractive error >+5 or <-5 dioptres influence the interpretation of the analysis is also an issue.

We will review the literature of OCT findings in miscellaneous pathologies affecting the optic nerve to illustrate the value of the findings in clinical practice.

5.2. Non-arteritic anterior ischaemic optic neuropathy (NA-AION)

NA-AION is a common optic neuropathy affecting people over 50 years old; second only to glaucoma. The diagnosis of NA-AION is supported by the anamnesis (painless sudden loss of vision involving one eye) and fundus examination (a swollen disc is observed in the affected eye at presentation).

This entity is related to a failure of arterial supply by the posterior ciliary arteries, supplying the optic nerve head. A major anatomic risk factor involved in this pathology is a crowded optic disc (absence of a cup)[62]. Emphasis in the past has been on the need to exclude an arteritic cause, hence the commonly employed negative epithet and initialism "Non-Arteritic" AION.

Classical NA-AION leads to sectoral infarction of the optic disc (OD) resulting in loss of optic nerve fibres and retinal ganglion cells (RGC) corresponding to the infarcted OD sector. A corresponding dense and persisting defect of the visual field results (Figure 26). At presentation, OCT shows an increase in pRNFL thickness followed by a progressive atrophy over a few months [92] (Figure 27). In the acute phase, a slight increase of GCL thickening may be seen due to distortion caused by peripapillary swelling and in some cases by intra- and sub-retinal fluid [93,94]. Asymmetric thinning between the superior and inferior hemi-macula is observed, resulting in an altitudinal pattern [95]. In contrast to glaucomatous optic neuropathy, an involvement of the superior, superotemporal, inferotemporal and inferonasal quadrants of the ganglion cells are most commonly affected in NA-AION [96].

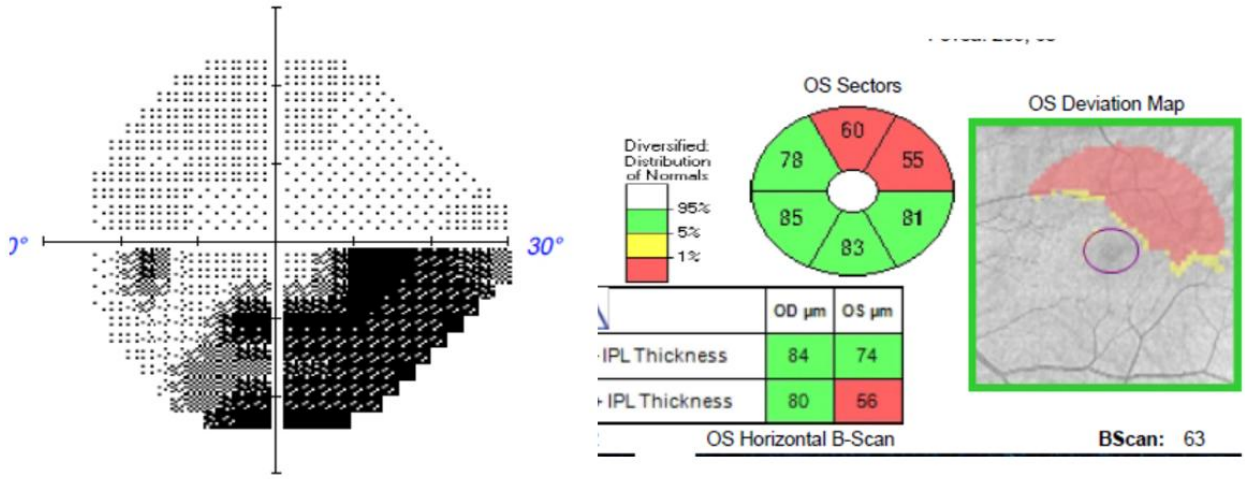

***Figure 26**: **A. Visual field (Humphrey 30-2, Dublin, California)** showing the inferior altitudinal visual defect. **B. Optical coherence tomography** (HD-OCT Cirrhus, Carl Zeiss Meditec, Dublin, California) imaging showing the corresponding superior loss of ganglion cell complex thinning. A high correlation is observed between the visual field defect and the ganglion cell thinning in a patient with a previous episode of NA-AION.*

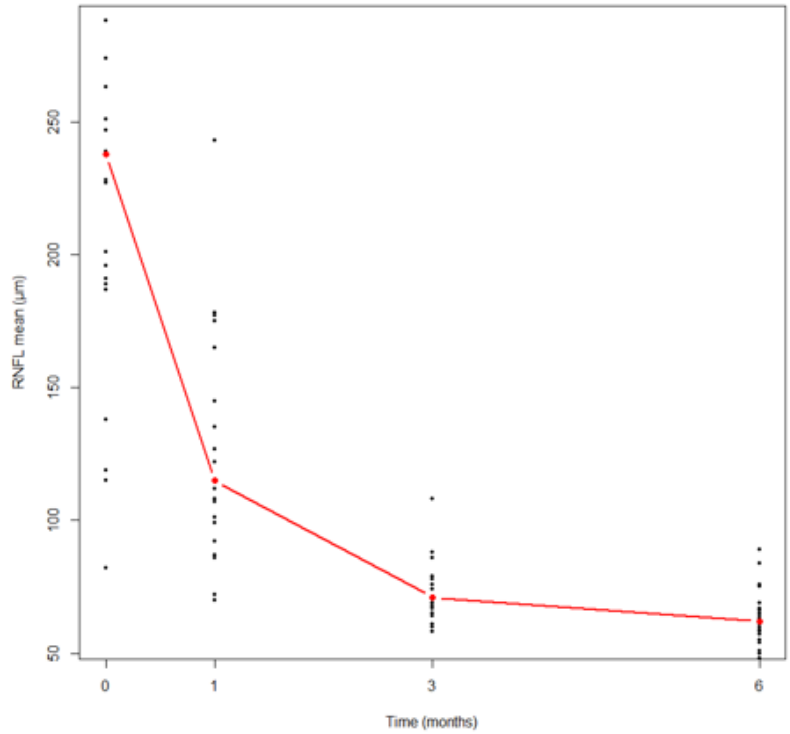

***Figure 27**: **Line graph**. Evolution of mean RNFL (µm) after an episode of NA-AION. An increase of the peripapillary RNFL thickness is observed at presentation due to optic disc swelling followed by a progressive thinning highlighting the optic disc atrophy.*

5.3. Compressive lesions of the anterior visual pathway

Compressive optic neuropathies (CON) are characterised by painless progressive loss of vision and late presentation is common. Furthermore, clinical diagnosis can be challenging, leading to further delays in treatment. Fundus examination can be normal. The optic disc may be swollen and retino-choroidal collateral vessels may be seen if the compressive lesion gives rise to venous hypertension (e.g. optic nerve sheath meningioma immediately retrobulbar) mimicking chronic papilloedema. Atrophy if present may mimic glaucoma. Compression of the visual pathway leads to loss of vision by three different mechanisms: a reversible neuronal block due to compression; and neuronal loss due to direct compression or an ischaemic mechanism. The neuronal block is reversible immediately after surgery whereas axonal loss is not. Localisation of the site of compression and identification of the causative lesion are essential to plan optimum management. While neuro-imaging is the gold standard for diagnosis, in the eye clinic OCT helps with the differential diagnosis by highlighting the location of RNFL and CGC thinning related to retrograde degeneration. OCT is valuable in the differential diagnosis of compressive lesions involving the optic nerve, chiasm and tract. Furthermore, in all cases of anterior visual pathway compression comparison of the visual loss (as seen on perimetry) with the degree of GCL loss is important in determining the prognosis for recovery following decompression.

5.3.1. Compressive lesion involving the optic nerve and chiasm

CON can be due to extrinsic compression (most commonly meningioma) or intrinsic optic nerve tumours such as glioma. However there are a variety of other causes, such as: infectious (aspergilloma [28]), inflammatory (dysthyroid optic neuropathy [97], IgG4 disease [98]) and vascular (aneurysm [99]).

There is little information about the topography of RGCs loss in optic nerve tumours. In optic nerve sheath meningioma, optic disc swelling or optic atrophy can be observed at presentation[100] depending on the course of the compressive process and the proximity of the tumour to the globe (swelling) and degree of axonal loss (atrophy). OCT will generally show diffuse pRNFL and GCC atrophy in the affected eye compared to the unaffected eye, reflecting axonal loss from chronic compression [101]. In cases diagnosed early, GCC is affected first, while RNFL thickness remains normal (Figure 28). In optic nerve glioma, the same observations are also reported compared to controls [102]. Fard MA et al found that pRNFL and GCC measurements are an important marker of the disease progression [103]. OCT is useful in the initial diagnosis (highlighting a significant asymmetric atrophy) and differential diagnosis (preservation of GCC where there is visual field loss being a hallmark of axonal conduction block in compressive pathology which is seen in neither glaucoma nor ischaemic optic neuropathy). Along with subjective visual parameters, OCT provides an objective metric for follow up of patients.

In dysthyroid eye disease, extraocular muscles and orbital fat are affected by an autoimmune inflammatory disorder. The optic nerve may be compressed at the apex of the cone of enlarged extraocular muscles. Raised intra-ocular pressure may also be a feature. Studies have shown a significant mean inferior RNFL thinning compared to controls[104].

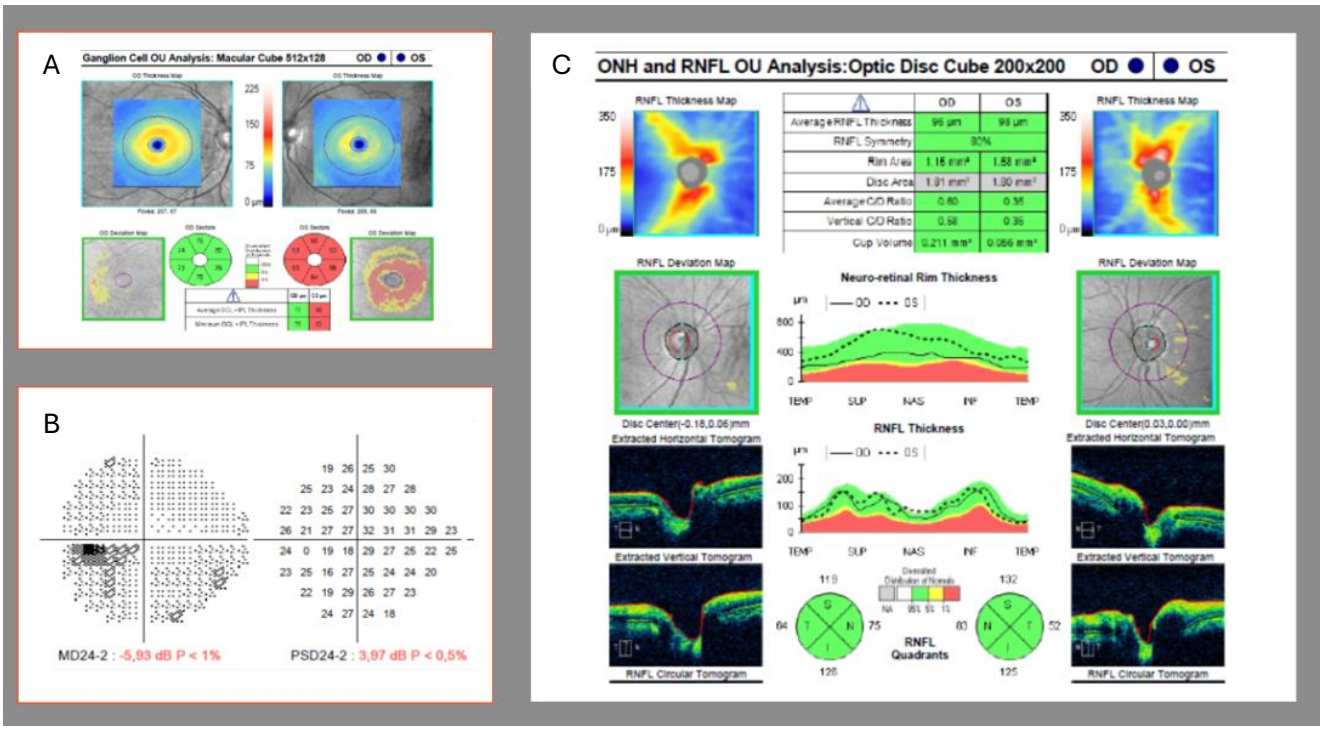

Figure 28: ***A. Optical coherence tomography*** *(HD-OCT Cirrhus, Carl Zeiss Meditec, Dublin, California) imaging showing a diffuse thinning of the ganglion cell complex on the left eye due to a retrograde degeneration.* ***B. Visual field (Humphrey 30-2, Dublin, California)*** *showing an inferior defect.* ***C. Optical coherence tomography*** *(HD-OCT Cirrhus, Carl Zeiss Meditec, Dublin, California) imaging showing a normal retinal nerve fibres layer thickness on both side despite a left optic nerve sheath meningioma. The visual field is more correlated to ganglion cell thickness complex than retinal nerve fibres layer thickness.*

5.3.2. Compressive lesion involving the chiasm

In chiasmal lesions, bilateral loss of vision is observed associated with bitemporal hemianopia as a major feature, although more anterior compression may give rise to features of unilateral optic neuropathy while a more posterior lesion may give rise to features of homonymous hemianopia due to optic tract involvement. Supra-sellar masses represent 14-18% of all brain tumours [105]. Pituitary adenoma, parasellar meningioma, craniopharyngioma and vascular abnormalities (e.g. internal carotid aneurysm for instance) are the most common causes of chiasmal compression [105]. The heteronymous nature of the visual field loss may not be noticed

by the patient, resulting in presentation with advanced disease or the deficit being detected on a routine eye test.

In the optic chiasmal syndrome, thinning of the nasal and temporal sectors of the peripapillary RNFL is seen. This has been known from ophthalmoscopic examination as band atrophy. Danesh-Meyer HV et al confirmed involvement of the nasal and temporal quadrants of the RNFL in pituitary lesions using OCT [106]. This is a result of the fact that these sectors consist entirely of nasal retinal fibres which decussate in the chiasm and are more vulnerable in chiasmal compression. There is no region of the optic disc which consists of exclusively uncrossed fibres, the arcuate bundles carrying both crossed and uncrossed fibres [107]. Studies have shown in chiasmal compression caused by a suprasellar lesion that the pattern of the GCC loss is the most sensitive parameter allowing the distinction from optic neuropathy due to glaucoma [108]. Involvement of the inferonasal and superonasal quadrant is highly suspicious of a compressive chiasmal optic neuropathy [108]. Nasal GCC is more affected because crossing fibres originating in nasal retina are involved [109]. The decrease in thickness of GCC is also well correlated to the density of the visual field defect [109] (Figure 29). GCC thickness assessment helps ophthalmologist to make an earlier diagnosis even if the RNFL OCT is still within the normal range [110]. A further refinement is to consider the naso-temporal macular GCC thickness ratio which has been compared directly in chiasmal compression and glaucoma [111].

A

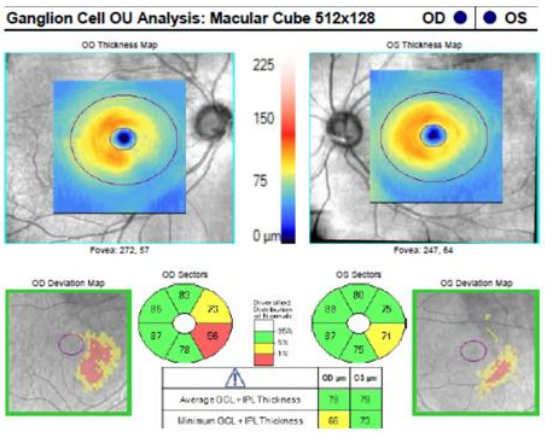

B

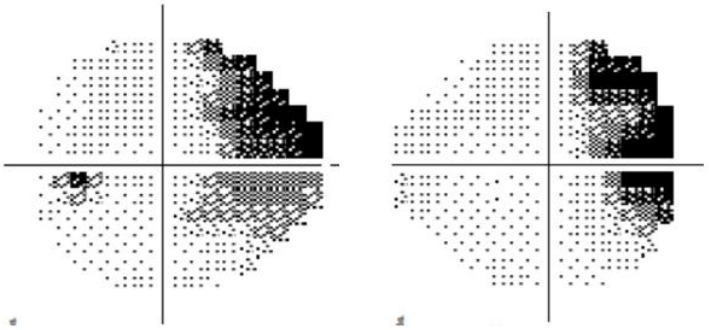

Figure 29*: A. Optical coherence tomography** *(HD-OCT Cirrhus, Carl Zeiss Meditec, Dublin, California) imaging showing the corresponding nasal ganglion cell complex on the right eye and the temporal ganglion cell complex thinning on the left eye corresponding to the visual defect.* ***B. Visual field (Humphrey 30-2, Dublin, California) *showing a right hemianopia due to a glioblastoma. This case illustrates the retrograde degeneration observed on the ganglion cell complex analysis due to compressive effect of glioblastoma on the visual pathway.*

5.3.3. OCT a marker of recovery of vision before surgery

Another special interest in compressive optic neuropathies is the possibility for the ophthalmologist, the neurologist and the neurosurgeon to predict the recovery after surgery utilising the OCT parameters. Several studies have demonstrated that prognosis for recovery is more favourable where the RNFL/GCC thicknesses are preserved, indicating conduction block rather than permanent axonal loss the recovery[106]. Moreover, in anterior optic nerve sheath meningioma, a pRNFL thickness lower than 70µm is associated with a lower probability of visual improvement after radiotherapy or decompression surgery[101].

5.4. Optic tract and post-geniculate lesions

The principal causes of optic tract lesions are infarctions (40%), tumour compression (32%) and trauma (17%) [112]. Acute MS lesions involving the optic tract are uncommon[113]. Damage to the optic tract tends to cause an incongruous homonymous hemianopia, bilateral optic atrophy and a contralateral RAPD. If retrograde degeneration of optic nerve fibres has occurred band atrophy will be seen in the contralateral eye.

In patient with cerebral lesions, OCT may be a helpful supplement to conventional perimetry. Retinal changes due to retrograde trans-synaptic neuronal degeneration are observed in animals and humans with post-geniculate lesions leading to homonymous hemianopia, initially demonstrated through studies of the peripapillary RNFL [114–116]. In later studies, thinning of the nasal hemimacula GCC in the contralateral eye and a thinning of the temporal hemimacula in the ipsilateral eye, respecting the vertical meridian have been shown [117]. These observations were noted at least 1 month after the onset [118]. If available, the OCT characteristics permits a faster and possibly more reliable diagnosis than perimetry but the changes will not be seen in the acute situation.

5.5. Idiopathic intracranial hypertension (IIH) and papilloedema

IIH is a disorder in which a pseudotumor cerebri syndrome (i.e. raised intracranial pressure (ICP) without hydrocephalus or a mass lesion; PTC) occurs in association with weight gain. It affects mainly women of childbearing age who have recently gained weight [119]. The major ophthalmic manifestation is papilloedema often presenting as transient visual obscurations. Patients may be unaware of ongoing deficit because papilloedema is another condition in which

visual field loss tends to be heteronymous with sparing of central acuity. Diplopia, most commonly due to lateral rectus paresis, may also occur. Non-ophthalmic features are headache and tinnitus. The pathogenesis of IIH still remains unclear and various hypotheses have been proposed but intracranial venous hypertension seems to be common to many causes of PTC such as dural sinus thrombosis and fistula and this may play a role in IIH also.

The pathogenesis of papilloedema is also poorly understood in this and indeed in other situations but an elevated translaminar pressure gradient (the difference between the ICP and the intraocular pressure (IOP)[32] seems to be fundamental (particularly as papilloedema is also seen with low intra-ocular pressure). There may also be a contribution from venous hypertension as the central retinal vein has a short course in the subarachnoid space and venous hypertension at the optic nerve head will invariably follow a rise in CSF pressure. Similar optic disc swelling is of course seen with central retinal vein occlusion. Whatever the underlying cause the increase in volume of the optic disc itself is due to axoplasmic stasis leading to axonal distension. There is a variable contribution from tissue oedema. These features have been more clearly delineated with the advent of OCT. In the past IIH was known as “benign” intracranial hypertension but this pathology can lead to irreversible visual loss in 25% of cases if the papilledema does not resolve [119].

In parallel with perimetry and other measures of visual function OCT is helpful in the differential diagnosis, prognosis and monitoring of papilloedema whatever the cause. Early papilloedema and anomalous, crowded optic discs can be confused leading to inappropriate management of either condition. In both situations OCT may show evidence of peripapillary axonal distension. This has been observed in pathological studies of papilloedema for some time [120] and OCT has confirmed similar findings in crowded optic discs including those harbouring drusen. Indeed in early OCT studies these were originally designated “soft drusen” but clearly shown not to be associated with visual loss, unlike true drusen [121]. More recently the

term “peripapillary ovoid hyperreflective masses” (POHM) was coined to distinguish these features from optic disc drusen which are *hypo*reflective, although a better description to match the pathology would be “peripapillary axonal distension” (PAD).

Thus, OCT can be helpful in confirming features associated with anomalous optic discs, such as lack of a cup and the presence of optic disc drusen. In papilloedema however the cup can fill in when advanced and drusen-like bodies can be seen in chronic papilloedema. Anterior displacement of the lamina cribrosa is more specific to papilloedema indicating as it does a pressure gradient indicating either raised intracranial pressure or low IOP [122].

Unfortunately, pRNFL analysis is not useful for the follow-up of these patients. A decrease of the pRNFL can be the result of either resolution of the papilloedema or the onset of atrophy and axonal loss. GCC analysis, given the ability to detect retrograde degeneration of optic nerve fibres, is the appropriate biomarker for monitoring progression of papilloedema and the risk of visual deterioration.

5.6. Inflammatory optic neuropathies

Intrinsic inflammation of the optic nerve (as opposed to contiguous inflammation such as of the optic nerve sheath), is referred to as optic neuritis. In the past (and given the prevalence of the disorder in populations of European descent) studies have been focussed principally on optic neuritis as seen in Multiple Sclerosis (MSON). The principle clinical features are an acute or subacute monocular loss of vision associated with pain on eye movement and a RAPD[123]. MSON is considered an autoimmune optic neuritis although no antibody has been described[123]. In MS optic neuritis is the presenting symptom in 25% of patients [124]. Less common in

European populations but more common in populations of Asian and African descent is autoimmune optic neuritis related to neuromyelitis optica spectrum disorder (NMOSD) and myelin oligodendrocyte glycoprotein antibody associated disease (MOGAD)[123]. Systemic disorders associated with optic neuritis include infectious, post-infectious and post-vaccination optic neuritis[123]. These latter disorders (and NMOSD) are more likely to present as bilateral simultaneous optic neuritis which is a marker of a systemic antibody response and unusual in MS. However asymptomatic involvement of the unaffected eye (as evidenced by pRNFL or GCC thinning) is an important indication of likely MS [89]. Indeed interocular asymmetry in GCL thinning is a signature of MS in a susceptible population [125,126].

The finding of a delayed Visually Evoked Potential in an asymptomatic eye has similar significance in that it is a common feature of MS (reflecting demyelination as well as axonal loss) [127].OCT has resolved an important issue, whether in MS the residual visual deficit is related primarily to demyelination or to axonal loss. It is clear that the important factor is irreversible axonal loss[89]. Demyelination is responsible for intermittent symptoms such as Uhthoff phenomenon and symptoms related to slowing of conduction in the optic nerve such as the Pulfrich effect. These symptoms may resolve as a result of remyelination[128] whereas the consequences of axonal loss are permanent, unless there is a possibility of central reorganisation[129]. A recent study has assessed a loss of 5 to 27% of GCL after optic neuritis with a full visual recovery as determined by clinical tests[130].

OCT is, therefore, a useful tool to evaluate pRNFL thinning and retrograde degeneration of the GCC. A such OCT is of particular value in monitoring any effect of treatment in reducing the permanent deficit. Moreover, the pattern of thinning shown on OCT may be helpful in differential diagnosis as pRNFL thinning is greater in the inferior and nasal sectors in MOGON than in MSON[131], where temporal thinning is observed. pRNFL thinning is greater overall in NMO than MSON, in accord with the worse visual prognosis[132]. In 2024, the optic nerve is

considered the fifth most common location affected in multiple sclerosis (MS) according to the revised McDonald criteria. Optic neuritis is a key indicator of MS.

5.7. Toxic and nutrition optic neuropathies

Optic neuropathies secondary to toxic exposure or nutritional deficiency are typically characterized by subacute, painless and bilaterally symmetrical loss of vision associated with a caeco-central visual field defect [133]. Vitamin B12 deficiency, whether dietary or associated with pernicious anaemia, is well established to cause optic neuropathy. Nutritional optic neuropathies are often found in patients who have a high carbohydrate, low protein diet as was seen in the epidemics in Tanzania and Cuba where specific micronutrient deficiencies have not been identified[134,135]. In developed economies this is more likely to be occur in patients consuming voluntarily chosen highly restrictive diets, following bariatric surgery (without adequate supplementation), or in patients who have a poor diet associated with a high alcohol consumption. There is no evidence that alcohol has a direct toxic action unlike methanol which is converted to formaldehyde by alcohol dehydrogenase.

Ethambutol, an antimycobacterial treatment, is one of the commonest causes of toxic optic neuropathy throughout the world, the precise mechanism is not understood. A possible final common path for toxic and micronutrient deficiency optic neuropathies is an effect on mitochondrial function leading to mitochondrial cytopathy, as observed in inherited optic neuropathies[136]. Mitochondrial dysfunction may explain the increased vulnerability of central vision, although a simple explanation based on fibre size cannot account for the caeco-central scotoma [137]. Indeed, this cannot be considered a universal phenomenon, in the toxic neuropathy related to vigabatrin the caeco-central projection is selectively preserved[138].

Unlike other causes of optic neuropathy considered above, the loss of ganglion cells in toxic and nutritional disorders is related to a direct cytotoxic mechanism rather than a retrograde degeneration following damage to the optic nerve fibres. Fundus imaging may be normal at presentation, and OCT may be helpful in the acute phase where thickening of the RNFL, especially the temporal sector is observed due to RNFL swelling related to the accumulation of mitochondria [139,140]. However, in the subacute and chronic stages, RNFL thinning especially in the inferotemporal part is found [141]. OCT showed GCC thinning in the inferior part of 2 mm and in the nasal part of 3 mm compared to healthy controls, supporting the fact that the papillomacular bundle (caeco-central projection) is particularly involved in this pathology [142]. One report has observed that the GCC thinning was present at the onset of symptoms and increased after 6 months[143]. GCC thinning has been shown to be significantly correlated with deficits in visual field and visual acuity[142] (Figure 30). Early treatment (restoring the deficiency or eliminating the toxic exposure) are mandatory to prevent or reduce permanent visual loss.

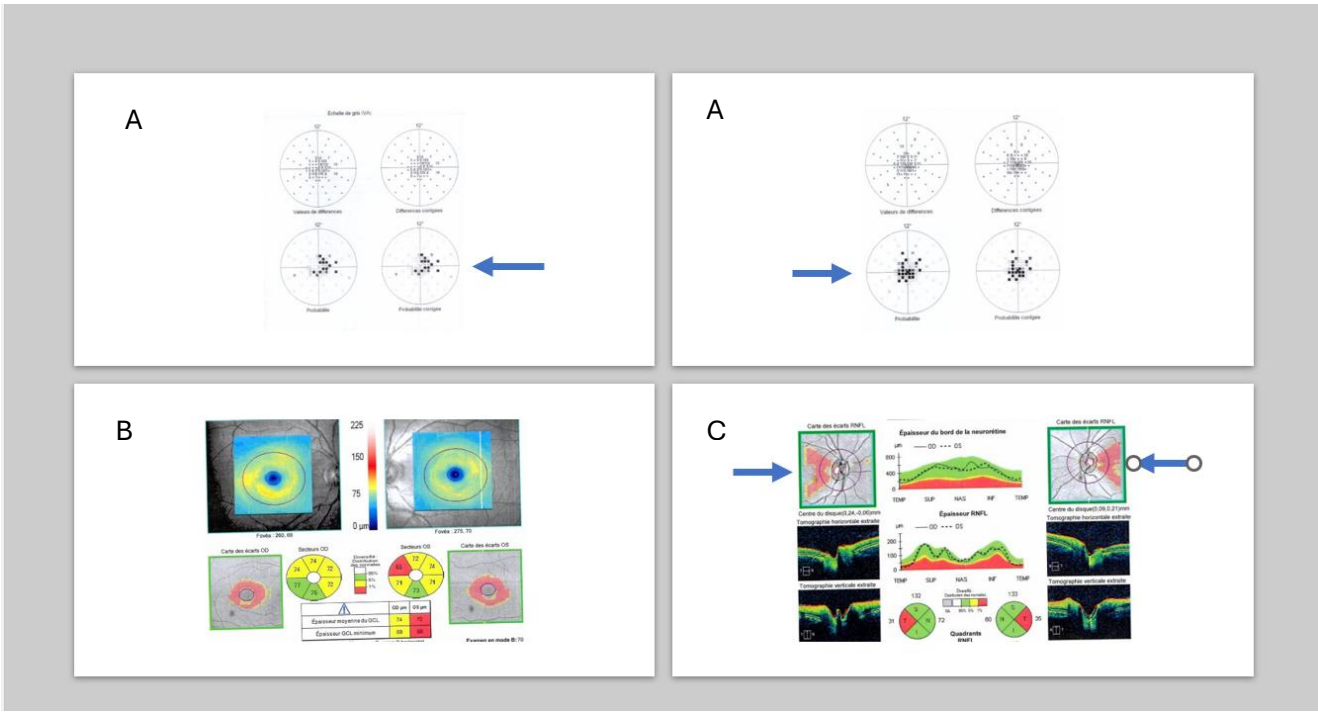

Figure 30: *Findings of a patient with toxic optic neuropathy due to Ethambutol.* ***A. Visual field (Humphrey 30-2, Dublin, California)*** *showing a central scotoma in a patient who was treated with Ethambutol (blue arrows).* ***B. Optical coherence tomography*** *(HD-OCT Cirrhus, Carl Zeiss Meditec, Dublin, California) imaging showing the corresponding thinning a the papillomacular bundle. ganglion cell complex on the right eye and the temporal ganglion cell complex thinning on the left eye corresponding to the visual defect and* ***C. Optical coherence tomography*** *(HD-OCT Cirrhus, Carl Zeiss Meditec, Dublin, California) imaging showing the typical temporal thinning.*

5.8. Inherited mitochondrial neuropathies

The principal features of inherited mitochondrial optic neuropathies are similar to the toxic and nutritional cases reviewed above: painless bilateral progressive loss of vision. Visual field is also characterised by a caeco-central scotoma caused by a loss of the papillomacular bundle. (caeco-central projection). The mutations concerned are in mitochondrial DNA (mDNA) or nuclear DNA coding for proteins expressed in mitochondria [144]. The two inherited mitochondrial neuropathies most likely to be seen in daily practice are: dominant optic atrophy (DOA) and Leber hereditary optic neuropathy (LHON).

DOA is a group of dominant inherited neuropathies which affect retinal ganglion cell functions. Commonly first symptoms appear in the first decade and are slowly progressive with preservation of peripheral vision. Many mutations are associated with DOA and the first described (and most common) being designated OPA1 [145,146].

LHON is a rare maternally inherited mitochondrial disease caused by three most common mDNA mutations (m.11778 G>A, m.3460G>A m.11484T>C) [147]. It mainly affects men between the second and third decades [148]. At onset, a subacute loss of vision is observed in both eyes simultaneously or sequentially within weeks or months.

In acute LHON, authors have observed thickening of the RNFL in the acute stage followed by atrophy in chronic LHON [149,150]. However, GCC thinning was found in the early acute phase and worsened gradually (mean GCC thickness 24 weeks or more after the symptoms: 50.8µm) [151]. In DOA patients, OCT studies showed a decrease in mean RNFL thickness compared to controls and the temporal sector was particularly affected with a thickness loss of 59% [152]. Moreover, RNFL was thinner in DOA than in chronic LHON [149]. Compared to controls, the temporal and superior sectors of RNFL were more affected in DOA [153]. GCC analysis showed a diffuse thickness decrease in all quadrants in these two pathologies and could be an early

marker of the disease [149]. In DAO associated with the OPA1 mutation a more significant involvement of the inferior, inferonasal and superonasal sector of GCC was observed [153].

5.9. Conclusions

OCT is a useful tool providing quantitative measures of pRNFL and GCC thickness in optic neuropathy, which are directly correlated with visual function. GCC analysis can identify early change related to atrophy and assist in the diagnosis and differential diagnosis of optic neuropathy. Because of its reproducibility, these measurements are crucial to monitor the disease progression and have recently become a standard for the longitudinal assessment of ocular diseases. Moreover, recognition of the OCT pattern is crucial to differentiate optic neuropathies. Indeed, GCL atrophy involving superior or inferior hemi-macula is an argument for NA-AION, whereas GCL atrophy respecting the vertical meridian indicate an optic tract lesion. Therefore, the GCC analysis could be considered as a key marker to identify the type of optic neuropathy, to facilitate the follow-up and to assess the odds of recovery after an episode or after a surgery decompression for instance.

However, in order to diminish some segmentation artefact and improving the images quality, developers should focus on reducing the processing time, improving the volume segmentation, and visualising the reconstruction of the macula in three-dimensions. Moreover, the future normative database should take into account the axial length and a more comprehensive age range.

Part 4: Pattern and evolution of retinal fluid in non-arteritic anterior ischemic optic neuropathy

6. The Occurrence of Intra- and Sub-Retinal Fluid in Anterior Ischemic Optic Neuropathy: Pathogenesis, Prognosis and Treatment

Chapelle AC, JM Rakic, GT Plant

Published as Chapelle AC, Rakic JM, Plant GT. The Occurrence of Intra- and Sub-Retinal Fluid in Anterior Ischemic Optic Neuropathy: Pathogenesis, Prognosis and Treatment. Ophthalmology 2023.

6.1. Introduction

After glaucoma, non-arteritic anterior ischaemic optic neuropathy (NA-AION) is the most common optic neuropathy affecting people over 50 years of age after glaucoma [51]. The condition was first clearly defined as a clinical syndrome by Hayreh in 1974 [52] and by Boghen and Glaser in 1975 [154]. Patients present with painless unilateral acute loss of vision associated, by definition, with a swollen optic disc [51]. Sub-acute loss (progression over days or weeks) may occur[55,155]. The fellow eye may be involved sequentially. The disc swelling results from ischaemia secondary to sectoral hypoperfusion of the pre-laminar optic nerve head due to failure of the posterior ciliary arteriolar supply. The ultimate cause of the failure of arterial supply is unknown but a major risk factor is a "crowded" optic disc (OD), a common variant of OD morphology with absence of a cup[61,62,156]. Other likely risk factors are obstructive sleep apnoea (OSA)[63,64] and systemic hypertension[65] (although the AION associated with malignant

hypertension has distinct features and can be bilateral and simultaneous [66,67]). Any risk associated with elevated intraocular pressure (IOP)[68–70]remains controversial[69,71,72]. Classical NA-AION leads to sectoral infarction of the OD resulting in loss of optic nerve fibres and retinal ganglion cells (RGC) corresponding to the infarcted OD sector. A corresponding dense and persisting defect of the visual field results.

Many important questions regarding the disorder remain unanswered. The relationship to cerebrovascular disease in general is uncertain: for example, thromboembolism very rarely results in this clinical picture; and the role of conventional preventive measures for vascular disease is unknown. Emphasis in the past has been on the need to exclude an arteritic cause, hence the commonly employed negative epithet "non-arteritic" anterior ischaemic optic neuropathy. Cases of acute visual loss are increasingly referred to stroke management units and a consensus needs to be reached regarding management. A degree of spontaneous recovery of vision [55] and the variable nature of the visual deficit (depending as it does on the optic nerve sectors affected) has bedevilled work on therapeutic intervention.

Another important pathological feature in the acute setting is the finding of sub-retinal fluid [92,157].The use of corticosteroids in order to decrease the capillary leakage presumed to underly the formation of fluid has been proposed to decrease optic disc swelling and potentially improve visual outcome[158]. In the reported study a higher probability of visual improvement was found in patients treated with oral prednisone 80 mg daily from presentation. However, Rebolleda et al have found no change with this intervention[159]. Others have proposed the use of intravenous or oral prednisone specifically in patients with subretinal fluid[160,161].

Optical coherence tomography (OCT) has revolutionised the analysis of optic nerve and retinal disorders. OCT is based on the principle of backscattering and interferometry[76,77]. A beam of light is projected on the retina and the locations of boundaries between the layers of the retina

are obtained from the time to the sensor of the reflected light. Thickness measurements of the retinal layers at the micron level are available.

OCT can therefore be employed to demonstrate pathological changes in thickness of the retinal layers and also certain changes in their intrinsic architecture, in particular the presence of fluid. In studies of NAION, OCT, confirming clinical observation of optic disc swelling, shows an increased peripapillary retinal nerve fibre layer (pRNFL) thickness followed by progressive thinning over a few months as atrophy ensues[92].

The aim of the study reported here has been to assess incidence and severity of subretinal fluid at presentation utilising the precision of OCT measurement. We wished to investigate the influence on visual outcome and to further elucidate the pathogenesis. We also wish to highlight the frequency of this finding as its presence acutely or the subsequent "macular star" (pattern of "hard" exudates around the macula) may lead to a misdiagnosis of neuroretinitis (personal observations of the authors).

6.2. Material and Methods

This retrospective observational study aimed to assess the evolution of patients with NA-AION following changes in both visual function and fundus imaging. The diagnosis of NA-AION was made based on the clinical history and the findings in funduscopic examination. Patients presented with unilateral painless loss of vision, there were no systemic signs or symptoms of giant cell arteritis and inflammatory biomarkers (erythrocyte sedimentation rate or C reactive protein) were within the respective reference range.

We reviewed the records of 34 patients (45 affected eyes and 23 healthy fellow eyes) who presented as NA-AION between 2014 and 2021 in the Ophthalmology Department of the University Hospital of Liège, Belgium. Two patients (3 affected eyes and 1 healthy fellow eye) with NA-AION associated with optic nerve drusen were excluded from the study. Seven patients had a subsequent episode of NA-AION in the fellow eye (Supplementary figure 1A et 1B) and 4 patients had had a previous episode of NA-AION in the fellow eye at presentation (Figure 31). Risk factors such as OSA, high blood pressure, diabetes, obesity and crowded disc were recorded for each patient based on the history. Prior medication including antihypertensive treatment before the episode was also noted. Following the diagnosis of NA-AION, blood pressure measurement and a polysomnography study were carried out routinely for all patients. Where blood pressure was found to be elevated at presentation, 24-hour ambulatory blood pressure monitoring was performed, whether or not there was a history of treated hypertension.

The following ophthalmic examinations were carried out: visual field (VF, Humphrey 30-2, Dublin, California); best corrected visual acuity (BCVA, Snellen scale); and optical coherence tomography (HD-OCT Cirrhus, Carl Zeiss Meditec, Dublin, California). The latter was performed at baseline and after 1, 3 and 6 months. Peripapillary retinal nerve fibre layer (pRNFL) and the GCC (inner plexiform layer + ganglion cell layer) layer thickness were evaluated at each visit whereas fundus fluorescein angiography (FFA) was done only at baseline. Twenty-seven (64,3%) affected eyes underwent a FFA at presentation.

Thirty-one eyes had an examination within a median of 5 days of symptom onset (range: 1 to 30 days). For those in whom subretinal fluid associated with the swollen disc was identified on standard OCT a macular OCT (Spectralis Heidelberg,Germany) was performed. The maximal subfoveal fluid and parafoveal fluid height was measured manually by one of the authors and also by 2 technicians and 1 ophthalmologist, who were blinded to the aim of the project. The maximal height was defined as the maximal distance between the retinal pigment epithelium

(RPE) and the photoreceptor layer on the OCT images within the foveal area (in the case of subfoveal fluid) and the peripapillary region (peripapillary fluid). The maximal parafoveal fluid was defined as the maximum vertical distance between the outer plexiform layer and ellipsoid zone in the peripapillary region on the macula OCT images. Interobserver reproducibility was evaluated by the intraclass correlation coefficient (ICC).

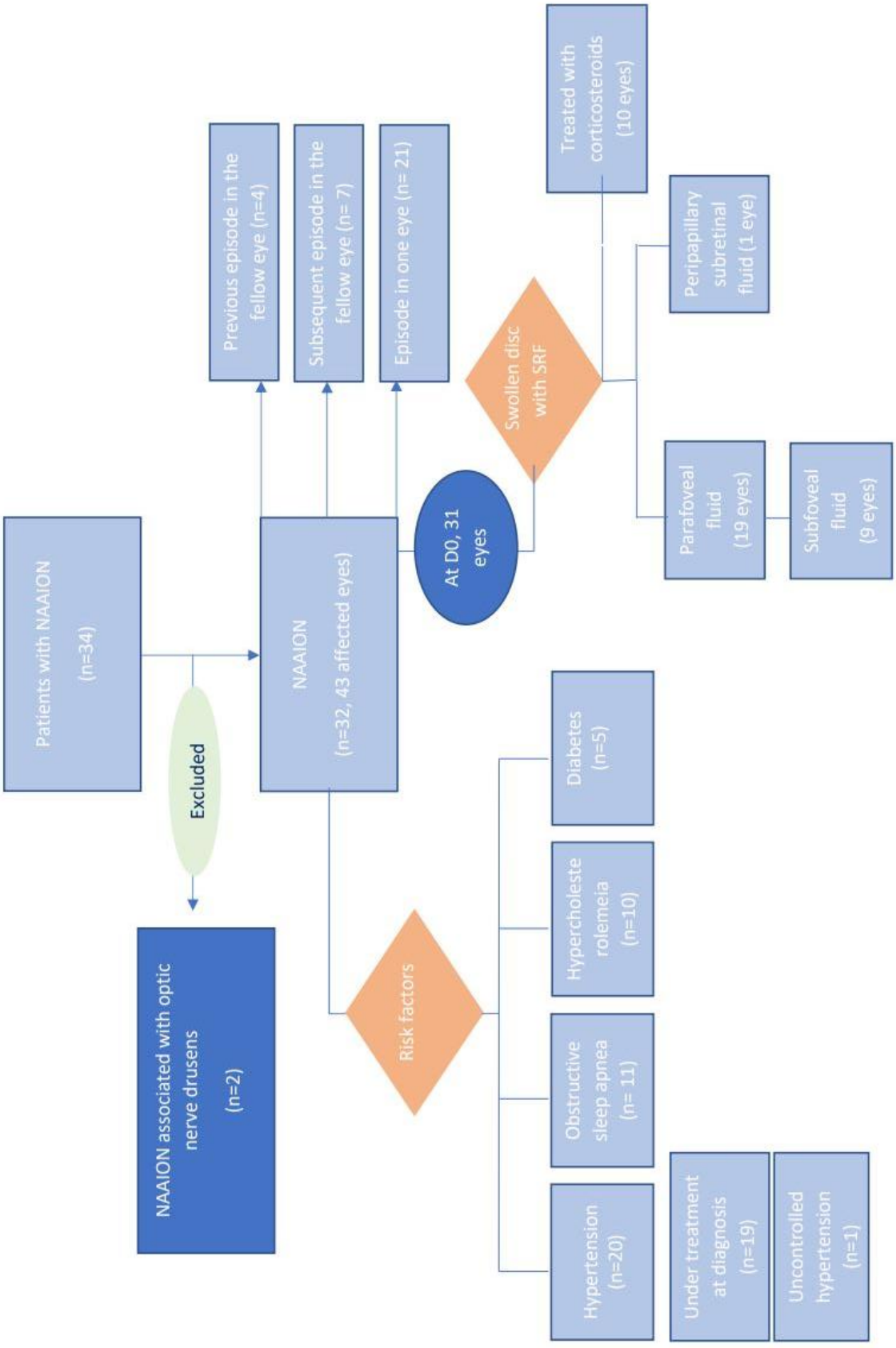

Figure 31: *Flow chart of patients in the cohort study.*

P values were calculated between the different groups using paired Student test and Wilcoxon signed-rank test for the continuous variables and McNemar test was performed for qualitative variables. Analysis of correlations between continuous data sets employed Pearson correlation coefficient rank correlation coefficient and the relationship between a continuous variable and a qualitative variable is performed with the ANOVA-1 test. A spaghetti plot test was performed to evaluate evolution of vision with time. Regarding the comparative analyses, patients with both eyes involved at presentation were excluded and we selected the better documented eye in the patients with bilateral sequential episodes.

A post-hoc analysis was performed to analyse the impact of corticosteroids on visual recovery in patients with subretinal fluid. When reviewing the charts, decision to treat was based on the clinician assessment and the severity of the swollen disc. Patients were also routinely treated if there had been a previous episode in the fellow eye. Within the sub-group found to have subretinal fluid (n=21), the cases (n=10) treated and not treated (n=11) with corticosteroids were compared with respect to age, sex, initial visual acuity, intraocular pressure, identified risk factors, pRNFL and GCC thickness, visual field and refractive error.

A favourable opinion of the ethics committee at the University of Liège for the study had been received. The study adhered to the tenets of the declaration of Helsinki.

6.3. Results

6.3.1. Summary of findings

A total of 32 patients were included in the analysis, with a mean age of 60 years (SD: ±12.5; range: 22-88 years, median: 60.5). 65.6% were male (Figure1). At presentation, mean (±SD) pRNFL thickness in patients with NA-AION was 227.1 (±70.1) and 92.3 µm (±8.5) in the fellow eyes ($p<0.05$). Four patients (12.5%) had a prior history of NA-AION in the fellow eye and were included in the study. At 6 months, a significant decrease was observed in the affected eyes (62.4 (±10.0) µm). GCL thickness at presentation and at 6 months in the NA-AION eyes were 67.2 ± 18.7 and 61.1 ±9.4 µm, respectively, a non-significant difference. When compared to the fellow eyes (80.9±6.5 µm), we observed a significant reduction of the GCC thickness corresponding to a mean loss of 24.8% (median: 27.6; range: 2.5-42.6%; $p<0.0001$) at 6 months. A slight increase of the GCC thickness was observed between baseline and 1 month, likely related to segmentation artefacts induced by the swollen disc and the presence of subretinal fluid. In fact, after excluding segmentation artefacts relating to subretinal fluid, the mean GCC at presentation was 72.8±8.5 (n=11). Moreover, a correlation ($r=0.727$, $p<0.005$) was observed between Δfovea thickness and Δmean GCC thickness. Finally, an inferior altitudinal defect, either complete or sectoral, was observed in the majority of patients (24 eyes, 75%).

6.3.2. Retinal fluid associated with NA-AION

Macular OCT performed at presentation showed retinal fluid in 21 eyes (46.7%). In this study, retinal fluid was divided into three categories regarding the localisation of the fluid: peripapillary subretinal fluid (n=1), i.e. subretinal fluid localised in the peripapillary region; sub-foveal fluid (n=9), i.e. subretinal fluid localised in the foveal region; and parafoveal fluid

(n=19), i.e. fluid localised between the ellipsoid zone and the outer plexiform layer in the parafoveal region. In the majority of patients both sub-foveal fluid and parafoveal fluid were found (9/21). One patient had only sub-foveal fluid in the context of NA-AION with severe systemic hypertension. The maximal sub-foveal fluid and parafoveal fluid height ranged from 66 µm to 204 µm (mean ± SD: 136.8 ± 71.8 µm; median: 148µm, ICC (95% confidence interval) between the 4 observers 0.90 (0.85-0.98)) and from 59µm to 310µm (mean ± SD: 162.8 ± 68.9 µm; median: 165µm; ICC (95% confidence interval) between the 4 observers 0.70 (0.60-0.84)), respectively. The maximal height of peripapillary subretinal fluid was 100 µm. OCT showed thickening of the GCL and pRNFL layers and microcystic oedema in the inner nuclear layer (INL), similar to what has been termed microcystic macular oedema(MMO)[162] although unlike that finding was associated with fluid infiltration of the outer nuclear layer (ONL) (Figure 32) and was a transient phenomenon.

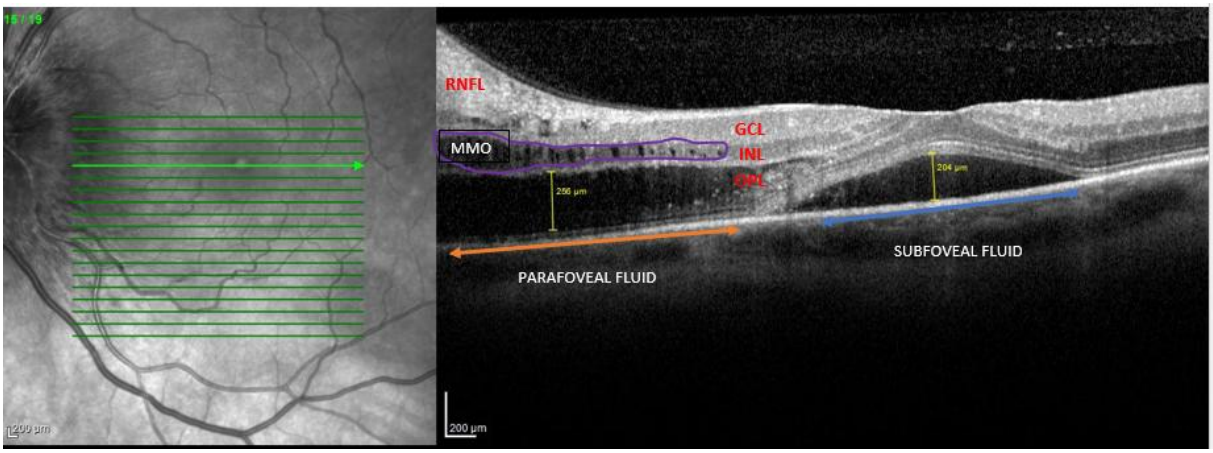

***Figure 32*: Macular SD-OCT (Heidelberg Engineering, Heidelberg, Germany) imaging** *Vertical section through the retina (right image) as indicated by the green arrow in the en face image (left). Thickening of the GCL and RNFL layer, microcystic oedema (MMO) in the inner nuclear layer (INL) and fluid infiltration of the outer nuclear layer (ONL) visible in the macular region in moderate disc swelling (Cohort case in the subfoveal group). Arrows labelling subfoveal (blue) and parafoveal fluid (orange) and outline (purple) labelling MMO. Measurements of fluid height are shown (see text).*

Macular thickness map analysis showed that extensive OD swelling involving the superior and inferior temporal sectors of the optic nerve head is associated with subretinal fluid. A "V" pattern (Figure 33) is seen in patients with sub- foveal fluid with diffuse OD swelling. Patients with either superior or inferior swelling of the OD, but not both, were found to have subretinal fluid. Moreover, parafoveal subretinal fluid was associated with an "O" pattern (Figure 42). Patients showing the "V" pattern were found to have more marked traction on the retina, as can be observed on the three-dimension representation (Figure 34). Although the traction may contribute to the presence of subretinal fluid it seems that the quantity of fluid generated is also an important factor. Indeed, parafoveal (intraretinal) fluid localised less than 1 mm from the fovea is strongly associated with the presence of subfoveal fluid ($p=0.0021$) compared to fluid localised within 1 and 2 mm or within 2 and 3 mm from the fovea. One explanation might be that a greater fluid transudation led to traction on the retina and consequent overwhelming of reabsorption of fluid. However, it is important to note that subfoveal fluid tended to resolve before peripapillary fluid. Indeed, in some cases subfoveal fluid may have been missed because it is already resolved. Fluorescein angiography (which was performed in 90% of patients with subretinal fluid (19/21 eyes) did not show any leakage in the macular region, excluding the presence of choroidal neovascularisation or other factors local to the fovea.

At long-term follow-up, four patients were found to have MMO (also known as retrograde maculopathy because of its association with ganglion cell loss)[163]. These cases are described in detail elsewhere [164,165] .

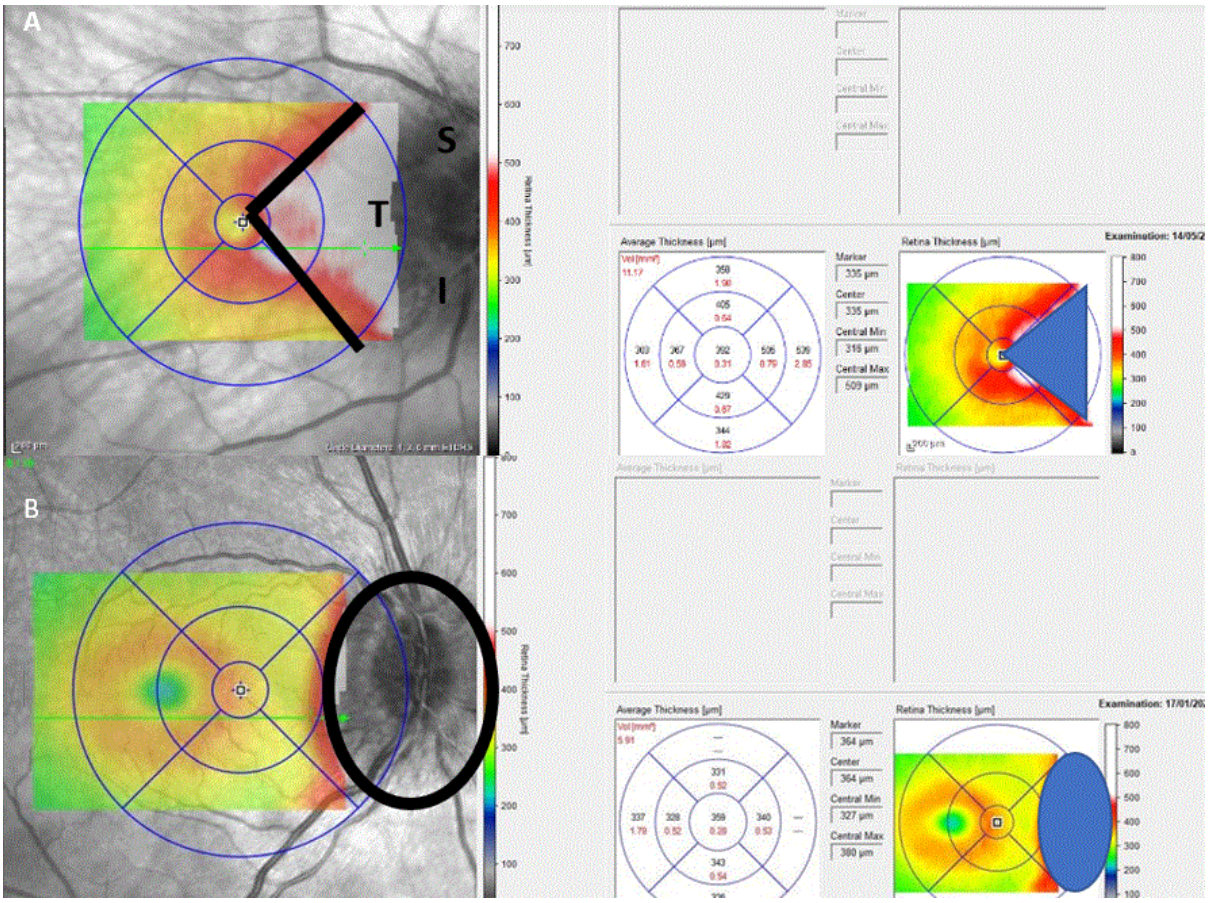

***Figure 33*: Retinal thickness map in the HRA/Spectralis viewing module (Heidelberg Engineering, Heidelberg, Germany). (A)** *An example of subfoveal fluid (blue triangle) observed in a patient with a" V"(black line) pattern of swelling localised to the inferior (I) and superior (S) temporal (T) sectors of the optic nerve.* **(B)** *An example of parafoveal subretinal fluid limited (filled blue oval, right image) to the peripapillary region associated with an "O" pattern (black outline, left image) of optic disc swelling.*

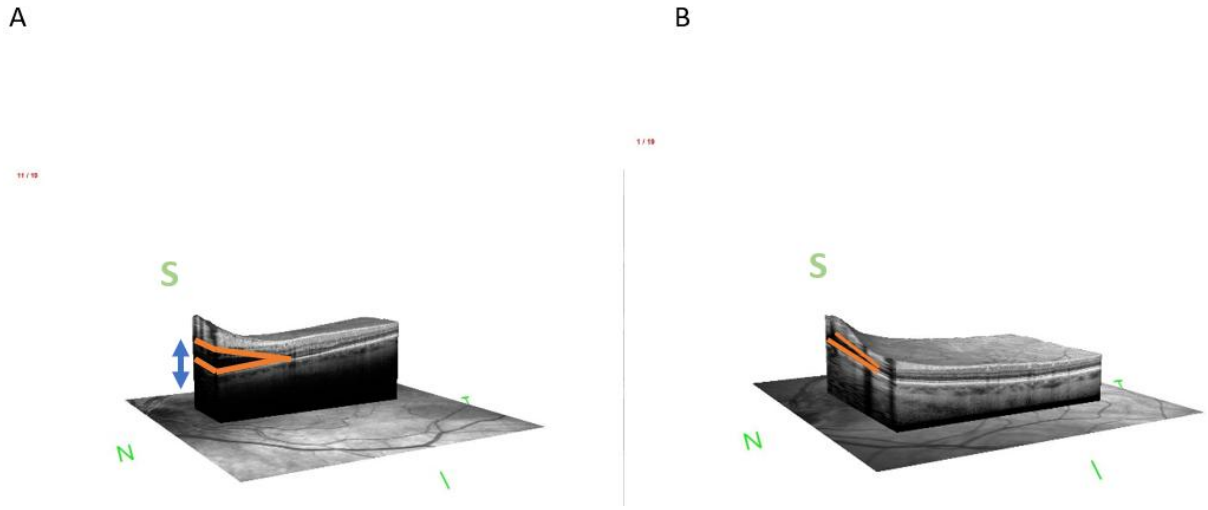

Figure 34: ***Three-dimensional images in the HRA/Spectralis viewing module (Heidelberg Engineering, Heidelberg, Germany).*** *(**A**) Vitreoretinal traction associated with extensive swelling pushes inward the retinal nerve fibre layer (labelled by the orange outline) (Cohort case). (**B**) Moderate vitreoretinal traction in patient with optic disc swelling limited to the superior (S) sector (labelled by the orange line) (Cohort case).*

6.3.3. Evolution of visual acuity in patient with NA-AION associated with retinal fluid

Overall, visual acuity and foveal thresholds were stable after an NA-AION episode with time (p=0.94 and p=0.36) (Figure 35). An upward trend was observed between presentation and one month after the episode in patients with sub-foveal fluid, which may have been related to fluid resorption. However, this trend was also seen in the subgroup without subretinal fluid, suggesting that the upward trend could be due to a neuro-adaptive phenomenon (Figure 36). Regarding visual acuity, no significant difference was seen between eyes with or without subretinal fluid (p=0.91) nor between the different subtypes of retinal fluid (p=0.42) (Figure 45). There was a correlation neither between visual acuity nor between foveal threshold and the thickness of subretinal fluid at presentation and at 6 months. Moreover, subjective refraction remained the same at presentation and after resorption of fluid in the subfoveal group (0.53±1.3 and 0.48±1.2).

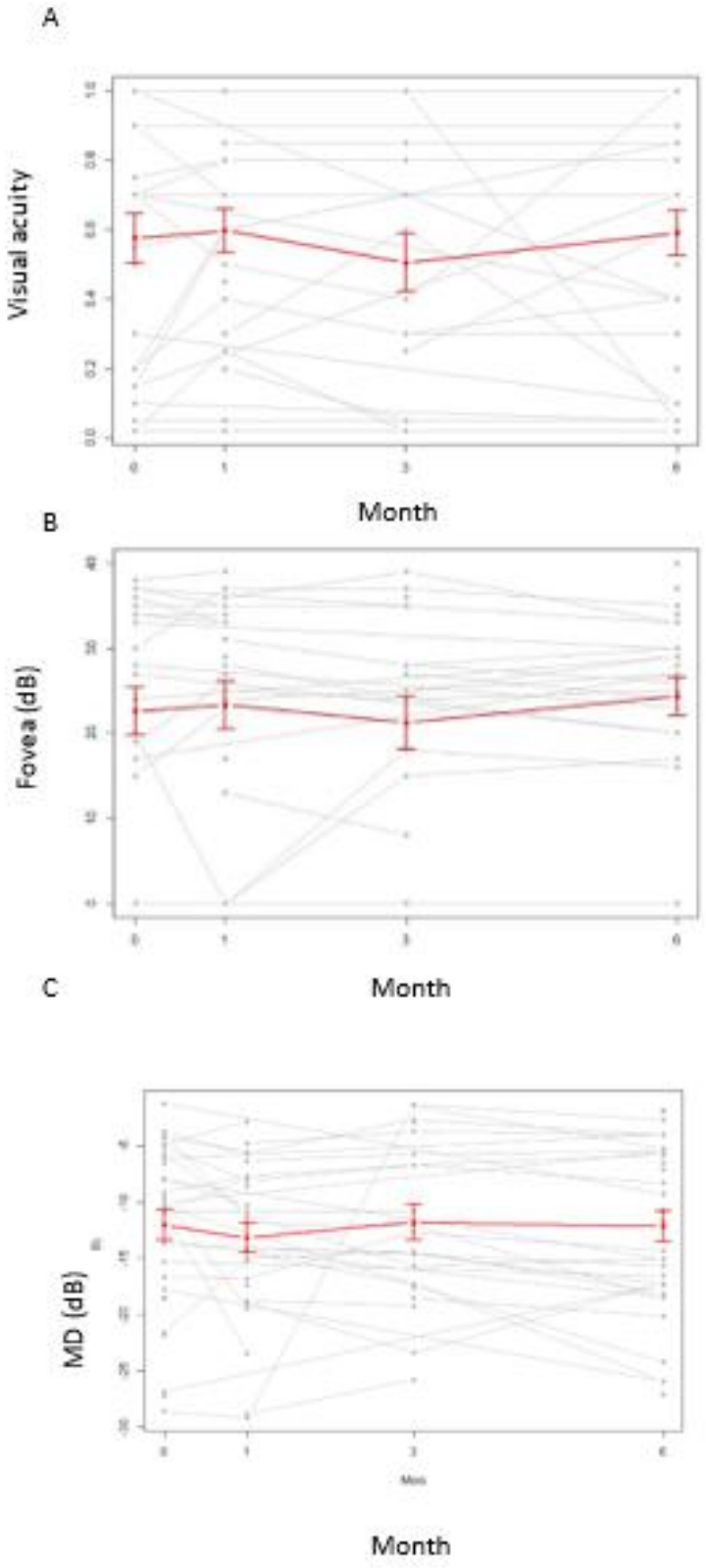

***Figure 35*: Spaghetti plot graph.** *(**A**) Evolution of mean visual acuity (Snellen scale) over 6 months. (**B**) Evolution of mean foveal threshold (dB) over 6 months. (**C**) Evolution of MD (dB) over 6 months. Overall these measures remain stable from acute presentation to 6 month follow up.*

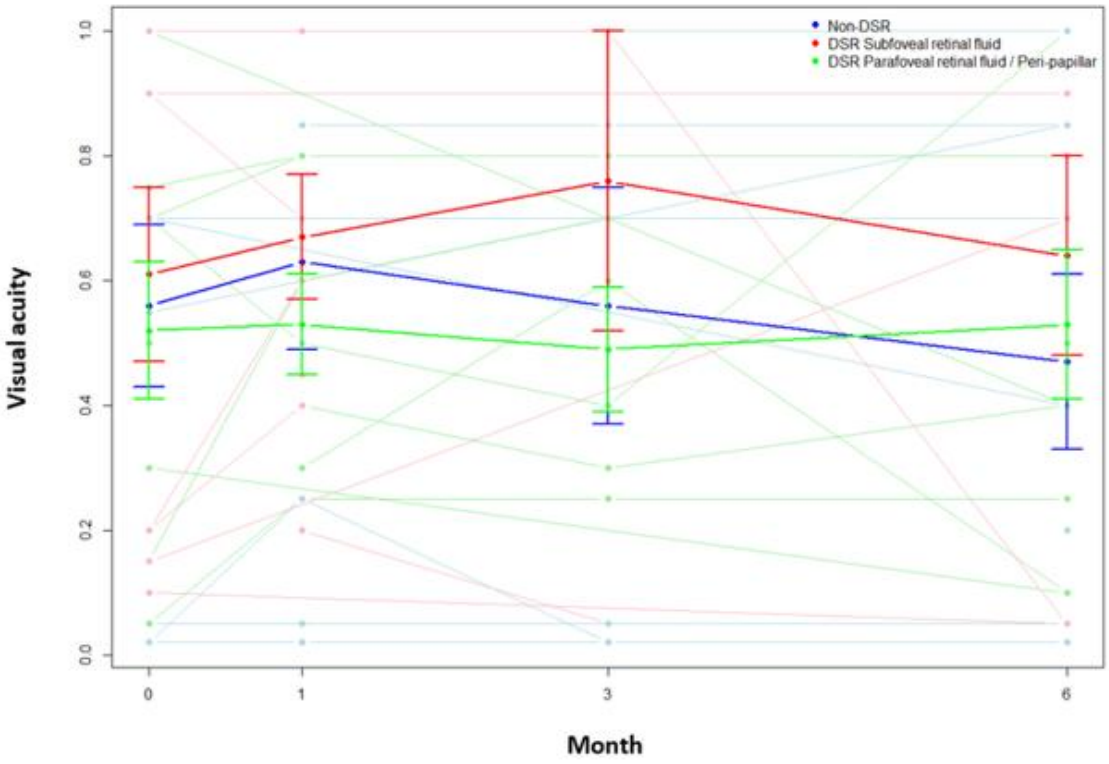

***Figure 36*: Spaghetti plot graph.** *(A) Comparison of mean visual acuity over 6 months in patients with subretinal fluid and those who do not have retinal fluid (subgroup without subretinal fluid: blue line, subgroup with subfoveal fluid: red line, subgroup with parafoveal or peripapillary fluid: green line). Overall, visual acuity was roughly stable after an NA-AION episode with time. A slight non-significant improvement between presentation and 3 months was observed in the subfoveal fluid group.*

6.3.4. Effect of corticosteroid therapy on visual prognosis

Among eyes with a swollen disc associated with retinal fluid, 10 were treated with Methylprednisolone 64 mg tapered down over one months and 11 eyes were not treated. Although there was no randomisation, characteristics of both groups were similar for age (55.7 ±13.1 in MP group and 61.5 ± 7.8.; p= 0.44) , gender (90% of male in MP group and 72.7% in control group; p=0.31), degree of disc swelling at presentation (pRNFL: 242.6µm in the MP group and 231.8µm in the control group; p=0.7), initial mean deviation (MD) (-12.37 in the

MP group and -10.69 in the control group, p=0.61), refractive error (0.35±1.1 in the MP group and 0.75±1.5 dioptres in the control group, p=0.51), IOP (MP group: 17.9 ±3. 3.8 mmHg, control group: 16.18±3.4; p=0.28) and risk factors (arterial hypertension: 60% in MP group and 72.7% in control group, p=0.54; OSA: 50% in MP group and 45.5% in control group, p=0.83; hypercholesterolemia: 30% in MP group and 54.5% in control group, p=0.26; diabetes: 20% in MP group and 18.2% in control group, p=0.92) (Supplementary figure 2). We did not observe any difference in visual function at 6 months (visual acuity, p=0.13; fovea threshold p=0.59; MD p=0.66) between these two subgroups (Supplementary figure 2). Hayreh postulated that corticosteroids speed up the subretinal fluid resorption but in our study, all patients except one did not show any subretinal fluid after the first month[158]. In order to answer more precisely this question, measurements during the first 15 days should have been performed.

6.3.5. Risk factors associated with NA-AION

Finally, hypertension was noted in 62.5% (n=20) and OSA in 34.4% (n=11) of patients in the entire cohort. Among patient with hypertension, 95% (n=19) were under antihypertensive treatment before the attack. Only one patient in the entire cohort had uncontrolled hypertension confirmed by 24-hour blood pressure monitoring, this patient did have subretinal fluid. The hypertension rate in our study is not consistent with the previous studies which showed a lower rate, ranged between 34 to 57%[62,166–168]. A possible consideration is that it may be the hypotensive treatment (resulting in nocturnal hypotension) that is a risk factor for NA-AION rather than hypertension (as has been suggested by Hayreh[167,169–171]). Five patients (15,6%) of the entire cohort had diabetes but none of these patients presented subfoveal fluid associated with the OD swelling.

6.4. Discussion

6.4.1. The influence of retinal fluid on visual outcome

In NA-AION, it is hypothesised that hypoperfusion of the optic nerve induces axoplasmic flow stasis and leading to axonal swelling and further vascular compromise[172]. This leads to a viscious cycle inducing an ischaemic cascade including leakage of the peripapillary vessels [172]. The fluid extravasates through the retina and accumulates in the retina due to hyperosmolarity[173]. In a study including 76 patients with NA-AION, subretinal fluid was observed in 50% of patients but was sub-foveal in only 10% of cases[157]. Our study demonstrates a higher rate of NA-AION with sub-foveal fluid. This discrepancy is likely to be due to the first examination of the patients being undertaken with a median of 5 days after the onset of the symptoms whereas patients in the cited study were examined up to 4 weeks after onset. Moreover, in our case series, macular OCT was carried out when some subretinal fluid was suspected on the standard OCT. Some cases with mild degree of fluid in NA-AION might be missed and thus be underestimated in clinical practice. As a clinician, it is important to know that NA-AION is often associated with retinal fluid (subretinal or parafoveal fluid) to avoid misdiagnosis with neuroretinitis, which is common in ophthalmology. The question also arises as to whether the presence of absence of subretinal fluid influences outcome and hence, potentially, management.

Although a significant deterioration of visual acuity is often observed in IIH patients diagnosed with sub-foveal and parafoveal fluid due to papilloedema[174,175] and in patients with CRVO and SRD[176], we did not observe any effect of the presence of retinal fluid on visual acuity, MD and

foveal threshold at 6 months. In subretinal fluid observed in NA-AION, we postulated that a complete recovery is mostly observed because of the absence of dysfunction of the photoreceptors or RPE which is generating the fluid for example in acute CSR[177]. However, authors have found that the subretinal fluid height was negatively correlated with foveal retinal sensitivity and the foveal retinal defect even though visual acuity was roughly preserved in CSR[178]. In our study, there was no correlation between the presence or absence of subretinal fluid and the foveal retinal threshold. We assume that the fluid was insufficient to decrease contrast sensitivity. Some authors have suggested treatment with corticosteroids to accelerate recovery, perhaps by avoiding permanent macular damage [160]. In theory corticosteroids intake given promptly after the onset would decrease the subretinal fluid and optic disc swelling was proposed by Hayreh[179]. In our cohort, we found no significant difference in visual outcome between patients with retinal fluid (subfoveal or parafoveal fluid) who were treated with steroids and those who were not at 1, 3 and 6 months (Figure 37).

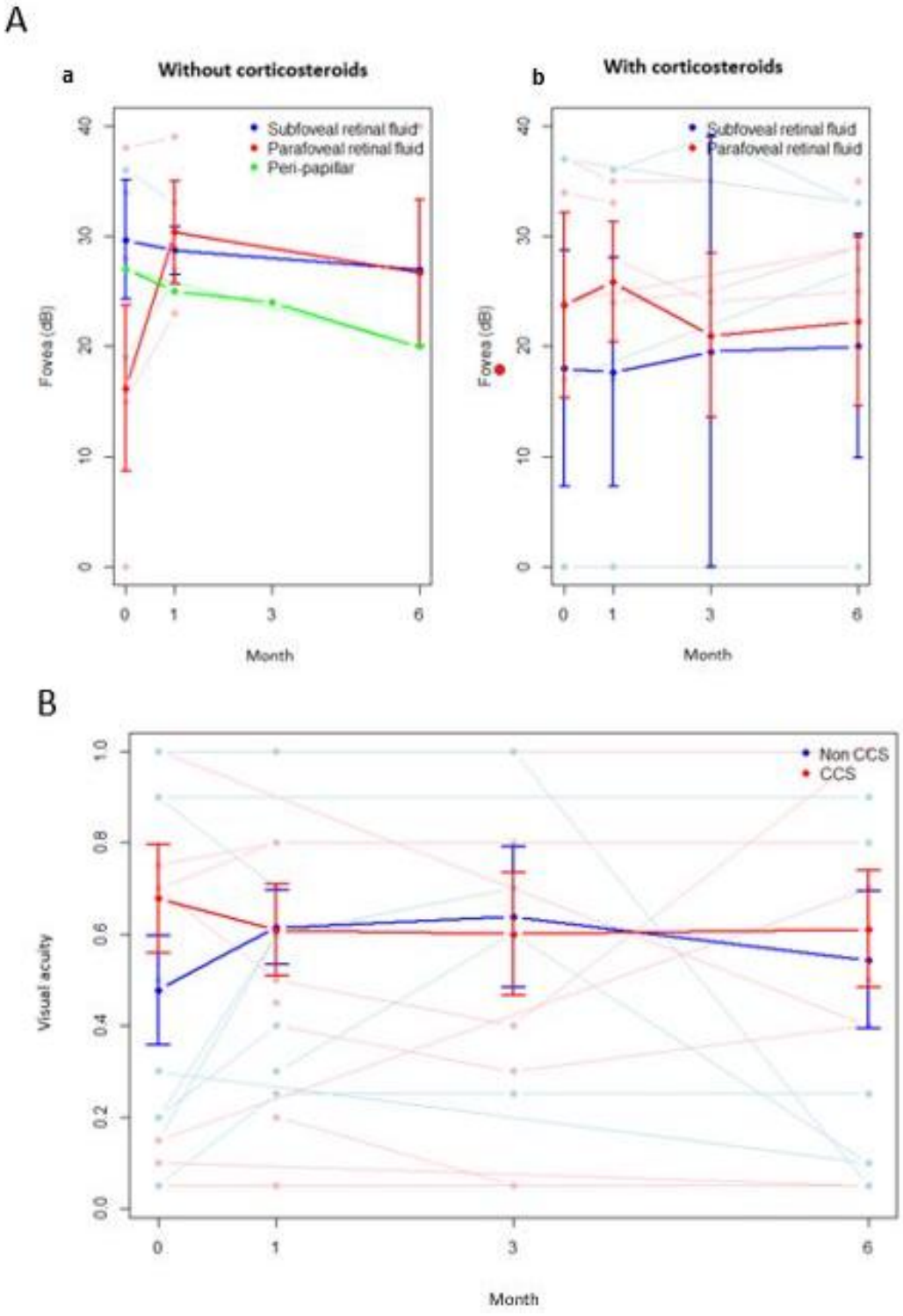

<u>Figure 37</u>: Spaghetti plot graph. *(**A**) Comparison of mean foveal threshold (dB) over 6 months in patients with subretinal fluid treated **(a)** and untreated with corticosteroids **(b)** (subgroup without subfoveal fluid: blue line, subgroup with parafoveal fluid: red line, subgroup with peripapillary fluid: green line). (**B**) Comparison of mean visual acuity (Snellen scale) over 6 months in patients with subretinal fluid treated and not treated with corticosteroids (subgroup with subretinal fluid treated with corticosteroids: blue line, subgroup with subretinal fluid not treated with steroids: red line). No difference in visual function at 6 months (visual acuity and fovea threshold) was observed between subretinal fluid patients treated and untreated with corticosteroids.*

To conclude, we have addressed the following: "Does sub-foveal fluid affect our management in NA-AION?". One issue is that erroneous measurements using ganglion cell OCT analysis may occur in patients with subretinal fluid. Secondly, Hedges and Hoye postulated that a correlation was found between visual acuity deficit and subretinal fluid[22,65]. However, no statistical analysis was carried out and the groups studied were small in number. Our findings confirm an upward trend in visual acuity recovery in the subgroup of patients with sub-foveal fluid. The detection of subretinal fluid in the acute assessment of NA-AION may influence prognosis. However, corticosteroid intake at presentation did not affect visual recovery in our cohort. Presence of subretinal fluid should not be an argument to treat patient as the visual prognosis remained unchanged.

6.4.2. Pathogenesis of intra- and subretinal fluid in NA-AION compared to other disorders

Following the advent of OCT, subretinal fluid is detected more easily in clinical practice[180]. Clinicians refer to "serous retinal detachment" (SRD) when the source of subretinal fluid is the retinal vessels, choroidal vessels or both as in central serous retinopathy (CRS), central retinal venous occlusion (CRVO) or in Vogt-Koyanagi-Harada (VKH) syndrome, for example [181] . However, subretinal fluid can also be seen in other pathological processes associated with a swollen disc (NA-AION, Myelin Oligodendrocyte glycoprotein (MOG) optic neuritis, papilloedema due to raised intracranial pressure, neuroretinitis and papillitis). Subretinal fluid is observed between the retinal pigment epithelium (RPE) and the neurosensory retina in the subretinal space, the remnant of the embryonic optic vesicle[182]. The subretinal region concerned is composed of the interphotoreceptor matrix which surrounds the photoreceptors and their

outer segments[183,184] this constitutes a *potential* space, where fluid can accumulate in certain conditions.

In those optic disc disorders where subretinal and parafoveal fluid occur either a transudate, an exudate or a combination of the two can occur, as already confirmed by histopathologic studies in papilloedema [185]. A transudate results from the alteration of mechanical factors influencing the formation or resorption of fluid[186,187] whereas an exudate occurs in the presence of diseases engendering inflammation (e.g. malignancy, tuberculosis, systemic lupus erythematosus)[186]. For example, in pleural effusion pneumonologists have distinguished exudate from transudate in pleural effusion by the former having a protein concentration above 3,0 g/100ml[188] and a cholesterol greater than 40mg/Dl[189].

In the case of subretinal fluid associated with NA-AION, a transudate is likely because there is no evidence of inflammation and so-called "hard" exudates are not commonly seen. The "macular star" results from the deposition of lipoproteins in the outer plexiform layer taking up the radiating pattern of fibres in Henle's layer[190]. Although such exudates located only in the nasal hemifovea and hence a hemi star can occasionally occur in NA-AION because of the presence of fluid (personal observation) none were observed in the present cohort. A macular star or hemi-star ("fan") has been described in neuroretinitis, papilloedema due to severe or longstanding intracranial hypertension[191] and MOG optic neuropathies[192]. In these cases, exudates form from a proteinaceous fluid, composed of serum proteins and lipids, resulting from a breakdown of the blood retinal barrier[193]. The lipid component tracks in the outer plexiform layer and the liquid component accumulates in the subretinal space because liquid can percolate through the external limiting membrane[173,194]. In our series, no exudate on OCT or through indirect ophthalmoscopy were observed, which is in favour of transudation. In addition, veinous hypertension caused by the swollen disc is likely to induce transudation. Indeed, authors have hypothesised that optic disc swelling in general lead to compression of

the superficial retinal veins or an increase in retrolaminar retinal veinous pressure induced by an augmentation of the optic nerve tissue volume[195,196]. This hypothesis provides an explanation for the absence of spontaneous veinous pulsation in patients with optic disc swelling, regardless of the cause[195–198]. In chronic papilloedema, such as in IIH, no exudates are observed except in longstanding and severe intracranial hypertension [191].

It has been suggested that the propagation of fluid within the retina is caused by vitreoretinal traction secondary to the optic nerve swelling in NA-

AION and in other aetiology [92,199]. Indeed, extensive swelling pushes forward the retinal nerve fibre layer thus potentially allowing fluid to more easily progress along the potential space. Our results showed that patients who had subretinal fluids tend to have more extensive oedema in the temporal disc sector. In these cases, a "V" pattern was observed on the thickness map and subfoveal fluid was always noticed, which is in favour of the presence of vitreoretinal traction from the OD. However, we consider the volume of transudate to be the more likely determining factor, which is also likely to be related to the magnitude of optic disc swelling.

Similarities with subretinal fluid in macular pathologies, as CSR, VKH and CRVO, suggest a similar underlying mechanism. Many hypotheses have been proposed as an inability of draining vascular system or an impairment of the RPE which cannot pump the excess fluid[176,200]. In NA-AION, however, the volume of fluid emanating from the optic nerve head is likely to exceed the pump capacities of the RPE, leading to the accumulation of retinal fluid[160].

Finally, over the past five years, there has been increasing recognition of a paravascular transport system in the retina and around the optic nerve similar to the glymphatic system existing in the brain[201–203]. Moreover, this glymphatic system could communicate with the vascular system and could be involved in the viscious cycle observed in ischaemia of the optic nerve. Indeed, Müller cells and the superficial and deep vascular plexus under normal condition

can reabsorb fluid[203,204] but after hypoperfusion and large extravasation of liquid from capillaries and veins as observed in NA-AION, Müller cells are saturated. Therefore, it explains why we observe with the OCT a thickening of the inner nuclear layer, quite similar to what has been observed in microcystic macula oedema[162], although not involving the macula. The fact that Müller cells density decreased with eccentricity might explain why we do not observe this image within the fovea[205]. Moreover, our study showed that parafoveal fluid localised less than 1 mm from the fovea is strongly associated with subretinal fluid. We propose that it is the volume of fluid generated acutely by the ischaemic process at the optic nerve head that overwhelms the glymphatic system.

6.4.3. Limitations

The main limitation of our study is that we do not have the OCT of patients at the onset of symptoms, which may give further insight into the pathogenesis and prevalence of subretinal fluid in patients with NA-AION. Furthermore, follow-up studies during the first fifteen days may better permit evaluation of the time course of fluid resorption allow us to estimate the delay for the resorption of fluid. A randomized and blinded prospective study would be required to evaluate definitively the efficacy of steroids in NA-AION associated with subretinal fluid.

Part 5: Ganglion cell thinning and microcystic macular oedema

7. Non-arteritic anterior ischemic optic neuropathy: ganglion cell thinning correlated with cystic change in the inner nuclear layer due to microcystic oedema and retrograde maculopathy

Chapelle AC, JM Rakic , GT Plant

Published as Chapelle AC, Rakic JM, Plant, Gordon. Non-arteritic anterior ischemic optic neuropathy: cystic change in the inner nuclear layer due to edema and to retrograde maculopathy. Ophthalmology Science. 2022.

7.1. Introduction

MMO was first described in the context of optical coherence tomography (OCT) findings in Multiple Sclerosis by Gelfand *et al.* [162]. The abnormality was more likely to be seen in patients who had had a previous episode of optic neuritis and in cases with more marked thinning of the retinal nerve fibre and ganglion cell layers. INL cell loss and thinning had previously been reported in a histopathological study of the retina in MS, also correlated with the severity of axonal loss, without mention of the presence of cystic change [206]. The microcysts are located in the INL and show a perifoveal distribution [162,207]. MMO is associated with severe optic atrophy found in: optic neuritis [162,208]; neuromyelitis optica [209,210]; hereditary optic neuropathies [211,212]; toxic and nutritional deficiency neuropathy [213,214]; glaucomatous neuropathy[215,216], compressive optic neuropathy[163]; and infiltrative optic neuropathy such as glioma [217,218]. Abegg has

suggested the term “retrograde maculopathy” (RM) for INL cystic change in this context [217,219]. However, similar changes have also been described in *retinal* pathology for example in: epiretinal membrane [220]; age related macular degeneration; diabetic retinopathy; and central serous retinopathy[221]. Indeed, the earliest use of the term MMO known to the authors (albeit in Romanian as “edemul macular microchistic”) was published in a description of an “isolated case” of suspected microcystic macular dystrophy in 1988 [222].

We consider the following case series concerning three patients with NA-AION to be of particular interest in this context. These patients showed early acute *transient* microcystic change in the INL associated with disc swelling in parallel with other evidence of retinal oedema. Longstanding, perhaps permanent, MMO was developed subsequently. The pathophysiological basis for these two manifestations of INL cystic change following NA-AION will be discussed.

7.2. Material and Methods

A retrospective observational case series was carried out at the University Hospital of Liège, Belgium. 23 patients were referred complaining of sudden painless monocular loss of vision to our Neuro-ophthalmology department or to the Emergency Department (9 cases). Recruitment took place between 2014 and 2021. The diagnosis of NA-AION was based on the anamnesis (painless sudden loss of vision involving one eye) and fundus examination. The latter showed a swollen disc in the affected eye and, in the fellow eye, either a crowded disc (typical of the “disc at risk” associated with NA-AION, [61,62,156]) or sectoral atrophy indicating a previous episode of NA-AION. Spontaneous resolution of the optic disc swelling was noted within 8 weeks and the outcome was sectorial infarction. Giant cell arteritis was excluded by appropriate

investigations including inflammatory biomarkers, temporal ultrasound, positron emission tomography, and temporal artery biopsy in cases of uncertainty. The clinical features were not compatible with a diagnosis of optic neuritis. Two patients were excluded because optic nerve head drusen were identified on OCT (see Figure 31 in Chapter 6). Patients were white European, representing the typical local population of the clinic, except one who was Turkish. The mean age of the subjects was 60±12.5 years (range: 22-88 years, median: 60.5) and 65.6% were male. A favourable opinion of the ethics committee at the University of Liège for the study had been received.

The patients were all followed at baseline and at 1-, 3- and 6-months post episode. Fundus fluorescein angiography (FFA) and a macular spectral domain OCT (Heidelberg Engineering, Heidelberg, Germany) were performed in 27 patients at baseline: 6-line radial scans and/or 25-line raster scans centred on the fovea were obtained. Subsequently, patients were seen annually. Clinical examination included best-corrected visual acuity (BCVA, Snellen scale), slit-lamp examination and fundus biomicroscopy. At follow-up, patients underwent automated perimetry (VF, Humphrey 24-2, Dublin, California), with appropriate refractive correction and OCT (HD-OCT Cirrhus, Carl Zeiss Meditec, Dublin, California), for which manual correction of segmentation was not possible. Thickness of the peripapillary retinal nerve fibre layer (pRNFL) and of the Ganglion Cell Complex (Inner plexiform layer + ganglion cell layer, GCC) were evaluated at each visit along with *en face* OCT B-scan. Studies demonstrating poor image quality, not allowing adequate visualisation of all retinal layers, were excluded. Scans were analysed for the presence of intraretinal fluid and subretinal fluid by 3 skilled observers who were masked as to the aim of the study. For the 3 patients described in this series, INL thickness was also evaluated initially and at the latest follow-up visit. For INL thickness assessment, adequate segmentation was assessed and adjusted manually in one case with macular spectral domain OCT.

Grading of the acute optic disc swelling was carried out as a function of the mean RNFL thickness and the numbers of quadrant sectors involved (temporal, superior, inferior, nasal). For example, optic disc swelling showing pRNFL thickening in at least one sector to be less than 120 µm was considered moderate. In the three cases described below, the swelling of the disc was considered severe because all sectors were involved (pRNFL thickness of all sectors greater than 120µm) and the mean pRNFL thickness was high (mean (±SD): 257.7 ± 81 µm, range: 189-347µm).

7.3. Results

7.3.1. Summary of findings

In the cohort of 34 patients (45 affected eyes and 23 healthy fellow eyes), we identified a transient microcystic change in the INL associated with optic disc swelling in 19 eyes at presentation. In these cases, the vacuoles were localised to the INL and were associated with transudation of intra- and sub-retinal fluid originating from the optic disc (see Figure 38 for one example). The microcystic change in these cases was transient and had resolved in all cases at 1 month (Figure 38). In cases with moderate optic disc swelling assessed in the global cohort, cystic changes were visible only in the peripapillary region (e.g., Figure 38). Four patients, who had shown this transient change subsequently developed MMO which remained fixed during the period of observation (range: 12-34 months). The other cases (n=30) did not show MMO during the follow-up period.

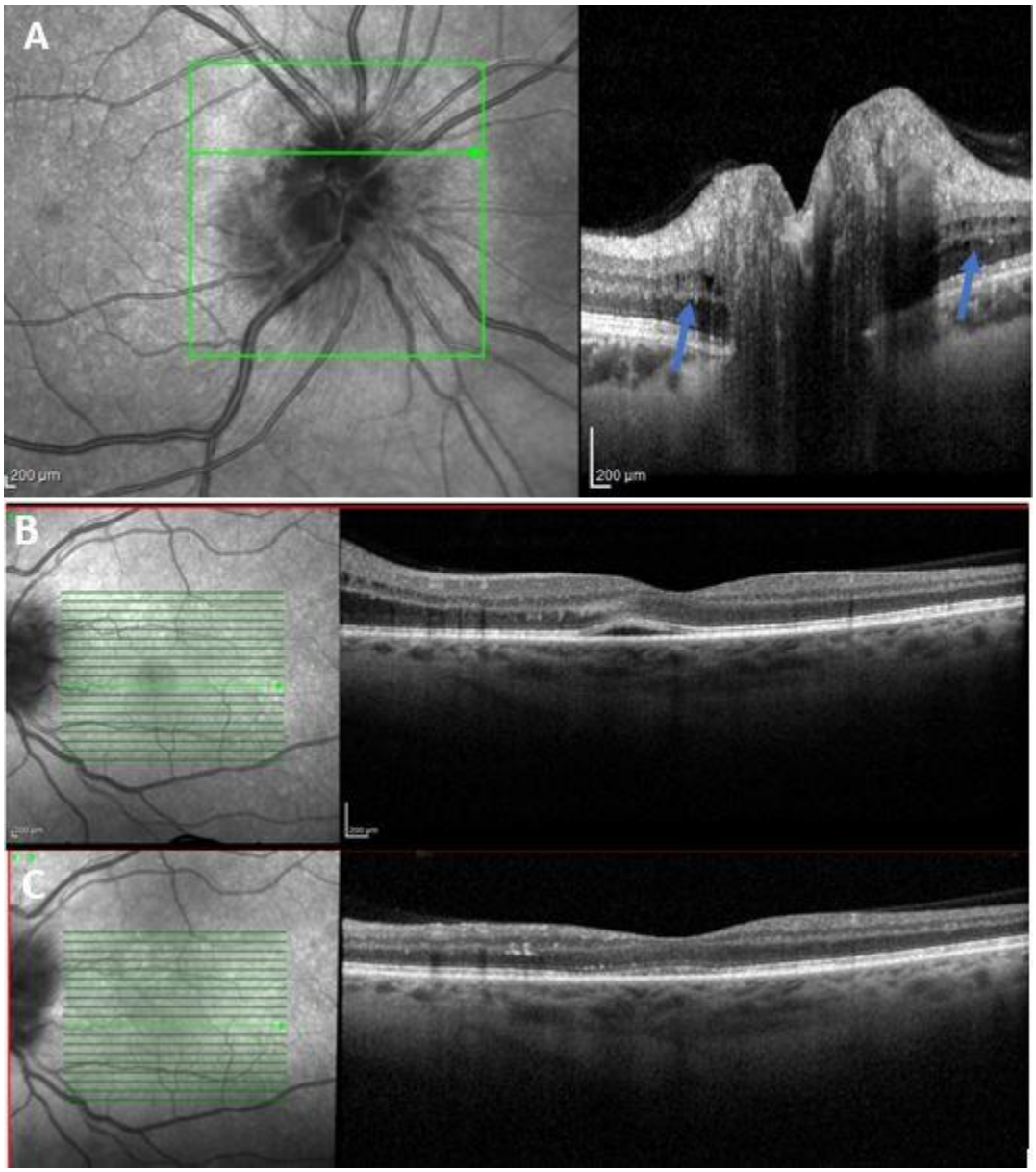

Figure 38*: SD-OCT** *(Heidelberg Engineering, Heidelberg, Germany) imaging. Illustration of retinal fluid associated with non-arteritic anterior ischaemic optic neuropathy.* ***A*. Inner nuclear layer microcystic change visible in the peripapillary region in moderate swelling of the disc (Cohort case; blue arrows)* ***B.*** *Transudation of fluid through the retina at presentation due to optic disc swelling and (****C****)23 days later in one case selected from the 19 out 34 cases showing disc change without subsequent retrograde maculopathy (Cohort case)*

At baseline, mean INL thickness in these three cases was 48.9 ± 17.03 µm in the affected eyes compared to 45.3 ± 1.7µm in the unaffected eyes (p=0.77). INL thickening was greatest in case 2 associated with the greatest microcystic change (mean INL thickness: 68.4 and maximal INL

thickness 137µm). At the final follow-up visit (range: 2 to 3 years post episode), no significant INL thinning was observed between the affected and unaffected eyes (40.7 ± 5.3 µm and 39.4 ± 2.0 µm, respectively). However, we observed an upward trend in affected eyes possibly related to the continuing presence of microcystic change. Significant GCC thinning was observed at 6 months in all patients compared to the unaffected eye in the superior hemi-maculae (mean loss of GCC thickness: -28.2 ± 5.2 µm (-33.3%, range: -22.3 -30.3 µm) and in the inferior hemi-maculae (mean loss of GCC thickness: -30.7 ± 5.6 µm (-31.0%, range: -24.3 -34.8 µm) (Figure 39). We observe a significant GCC thinning in both hemi-maculae in patients with MMO compared to the entire cohort, where greater involvement of the superior hemi-macula is shown (mean superior hemi-macula thinning: -23.01 ± 9.33, -27.9%, range: 1 to 40.7µm, mean inferior hemi-macula thinning: -19.14 ± 12.1µm, -28.51%, range: 5 to -39µm; Figure 2). In two patients with similar lesion of GCC, only one had also MMO (Figure 33). She had a better fovea threshold (25dB), suggesting a better residual function than the other (mean ±SD: 16±2.6). Finally, in these three patients we observed significant thinning of the RNFL at 6 months (mean pRNFL: 57.7 ± 2.5µm; temporal RNFL: 48.7± 1.5; nasal pRNFL: 56 ± 6.2; inferior pRNFL: 62 ± 2.6µm and superior pRNFL: 63.7±3.5). Mean pRNFL was especially thin compared to the overall cohort (mean pRNFL: 62.3 ± 9.7 µm; median: 61µm; temporal pRNFL: 51.7± 15.5 µm; median: 49.5µm, nasal pRNFL: 60.1 ± 11.8 µm; median: 49.5µm; inferior pRNFL: 74.9±24.4µm; median: 66µm and superior pRNFL: 62.78 ± 13 µm; median: 62µm).

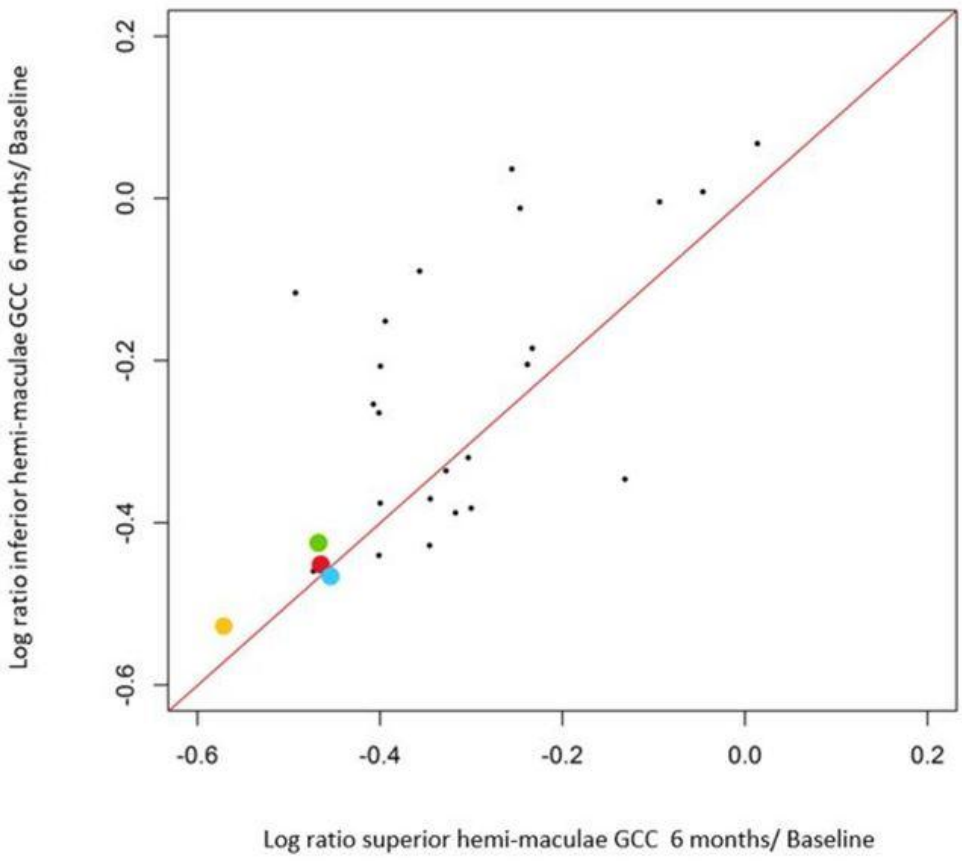

Figure 39: *Log ratio of GCC thickness in the superior (x axis) and inferior (y axis) hemi-maculae between 6 months and baseline. Patients with MMO had significant thinning of both the superior and inferior hemi-maculae (case 1: blue dot, case 2: green dot, case 3: red point). One additional patient of the cohort who had significant thinning of both the superior and inferior hemi-maculae at 6 months had also significant MMO observed (yellow dot). The red line represents the 45-degree line where Δ inferior hemi-macula and Δ superior hemi-macula are equal. See Supplementary figures 3A and 3B for data related to this figure.*

7.3.2. Case Histories

CASE 1

A 42- year-old gentleman was referred because of sudden painless loss of vision in his right eye which developed 4 days previously. At presentation, the best corrected visual acuity (BCVA) was 1/20 in the right eye and 10/10 in the left eye. Fundoscopy showed an optic disc swelling

and haemorrhages in the right eye. In the left eye, a crowded disc was noted. A diffuse visual field defect with central involvement was observed in the affected eye (Figure 40). OCT showed a significant thickening of mean pRNFL (363µm) and a normal thickness of GCC (85µm). Peripapillary microcystic oedema in the INL was also observed on the macular OCT. FFA showed a superior hypoperfusion of the optic disc and a late leakage around it. No choroidal filling defect was observed.

Full blood count and inflammatory biomarkers (ESR or CRP) were within normal limits. However, hypercholesterolemia (LDL 121 mg/dL, reference range <100mg/dL) was noted. Severe obstructive sleep apnoea (OSA) was diagnosed following polysomnography and pre-existing hypertension was shown to have been inadequately treated. Magnetic resonance imaging (MRI) with and without gadolinium enhancement of the brain demonstrated evidence of small vessel disease. A diagnosis of NA-AION was made.

At follow-up visits, OCT showed a diffuse thinning of the GCC (55 µm at 3 and 6 months) and a significant thinning of mean pRNFL (64µm at 3 months and 55 µm at 6 months). Microcysts were observed in the INL in a perifoveal circular distribution. The cysts appeared similar to those seen at presentation apart from the location (Figure 35). The microcysts were first seen four months post episode in the superior hemi-macula, corresponding to the greater involvement of the inferior visual field. At 6 months cystic change in the inferior and central regions of the macula was observed and persisted unchanged at the most recent assessment (36 months; Figure 41).

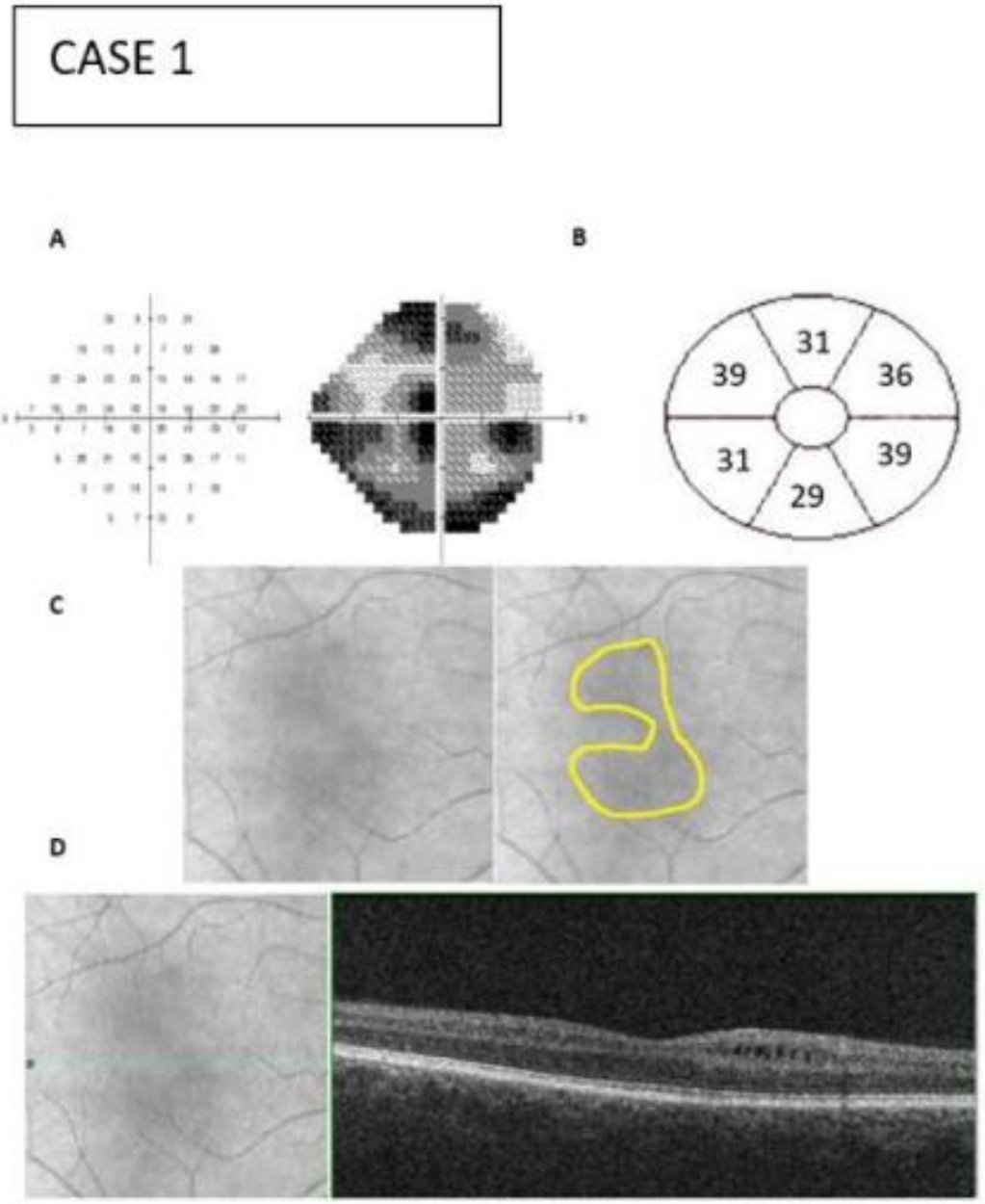

***Figure 40*: CASE 1.** *(**A**) Visual field showing central involvement (**B**) illustration of Δ GCL thickness (**C**) Cirrhus HD-OCT fundoscopic images showing a hypointense circular distribution of the inner nuclear layer cystic change (**D**) En face Cirrhus OCT showing microcystic macular change (Case 1).*

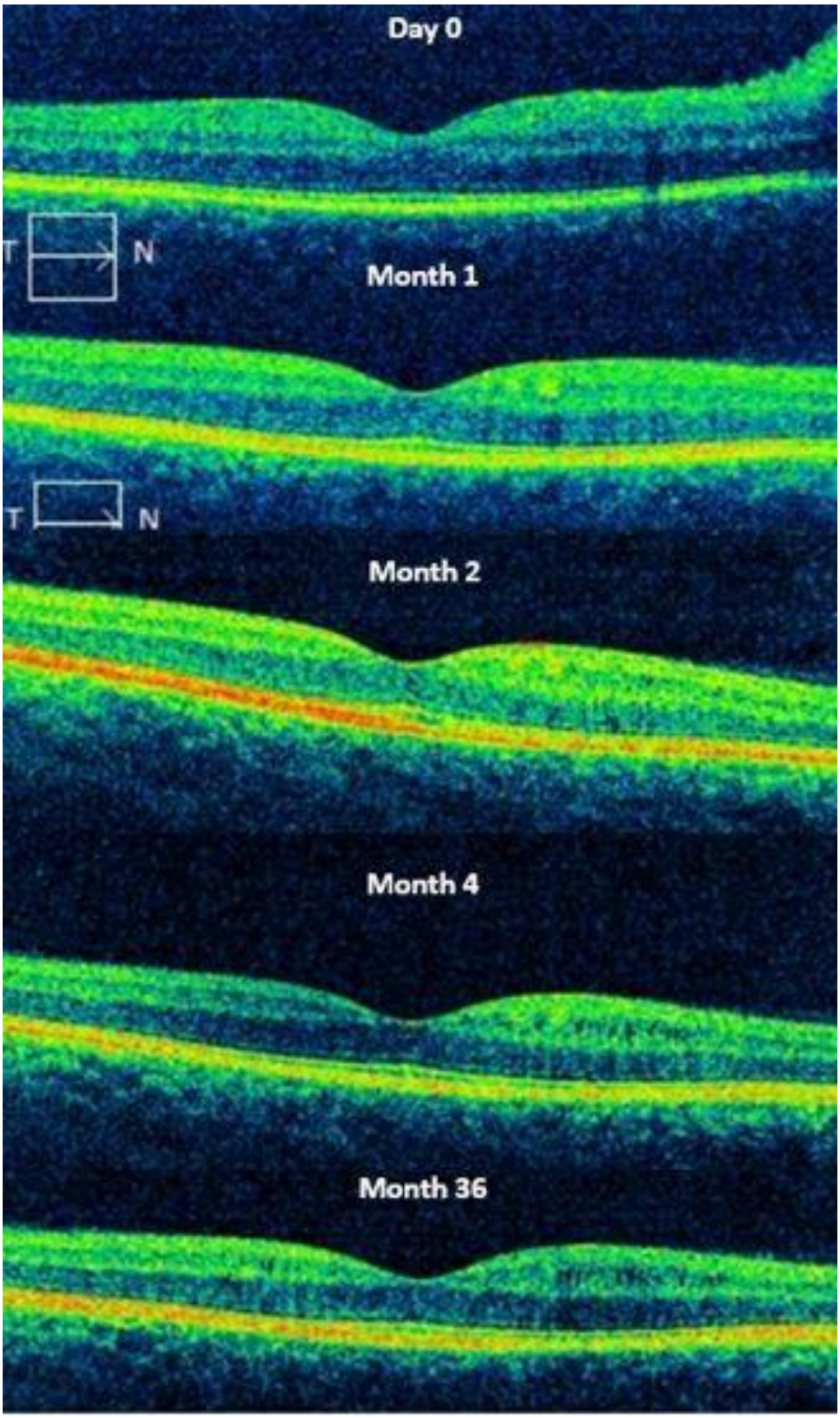

Figure 41: *Evolution of the microcysts in the inner nuclear layer which persist over time (Case 1) with SD-OCT B-scans (HD-OCT Cirrhus, Carl Zeiss Meditec, Dublin, California).*

CASE 2

A 67- year-old man was seen for the first time in 2019 complaining of sudden loss of vision associated with a superior visual field defect in his left eye (Figure 42). He had a past history of treated hypertension and had had a pacemaker implanted. He was borderline overweight (body mass index: 24.3). Polysomnography was within normal limits.

At presentation, BCVA was 10/10 in the right eye and 1.5/10 in the left eye. Examination showed left optic disc swelling. Perimetry revealed a superior visual field defect with a nasal step and central involvement. Early phases of FFA showed a superior sectoral delayed filling of the optic disc, confirming the diagnosis of NA-AION [52]. Late leakage at the macula was not observed excluding local vasculopathy. Macular OCT showed sub-foveal fluid and microcysts in the INL which resolved within one month as did the pRNFL thickening. GCC analyses were difficult to interpret because of segmentation failure (mean GCC: 70µm) and pRNFL was thickened (mean pRNFL: 189µm)

Ophthalmic and Neurologic examination were otherwise normal. Full blood count, blood chemistry and inflammatory biomarkers were within the respective reference ranges. MRI with and without gadolinium enhancement of the brain and orbits was normal.

Six months post episode, pRNFL was reduced at 58µm and GCC was thinned (mean GCC: 68µm). At one year follow-up, MMO was observed limited to the inferior hemi-macula (Figure 5) matching the area of greater GCC loss.

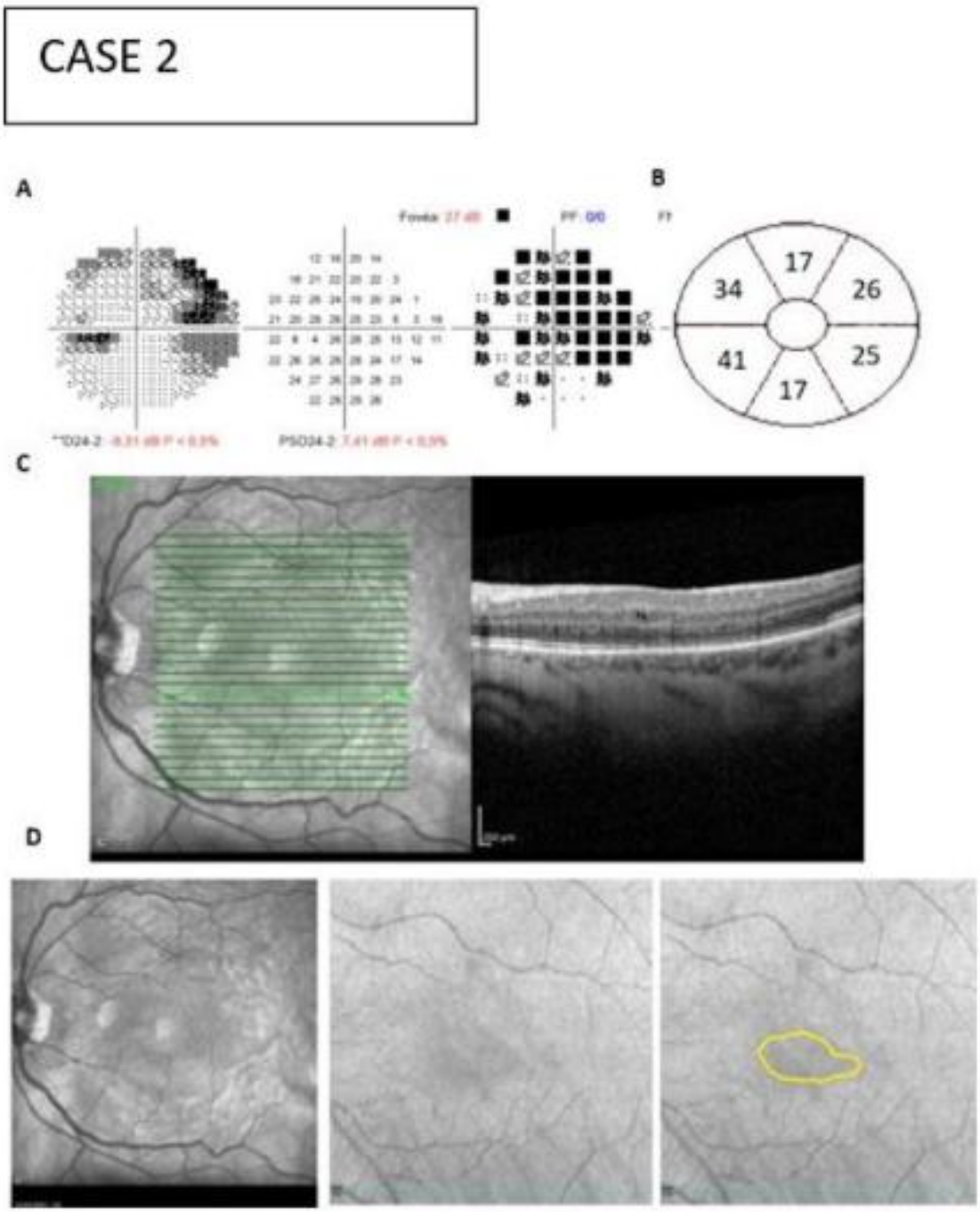

***Figure 42*: CASE 2.** *(**A**) Visual field showing a superior altitudinal defect (**B**) illustration of corresponding ΔGCL (µm) thinning between the affected eye at 6 months and the unaffected eye (**C**) En face HRA OCT (Heidelberg Engineering, Heidelberg, Germany) showing microcystic macular change located in the inferior hemi-macula (**D**) HRA infrared imaging and Cirrhus HD-OCT funduscopic imaging showing an inferior hypointense distribution of the vacuoles.*

CASE 3

A 52- year-old truck driver presented with blurred vision in his left eye. He suffered previously from an episode of NA-AION in the fellow eye. BCVA was 1/20 in the right eye and 8/10 in the left eye. A swollen optic disc in the affected eye and diffuse pallor in the fellow eye were observed. Visual field showed an inferior altitudinal defect (Figure 6). Mean pRNFL and GCC were 237µm and 67µm, respectively. Macular OCT scans revealed traction of the retina induced by the disc swelling associated with fluid between the retinal pigmentary epithelium and the outer nuclear layer together with cystic change in the INL. FFA was not carried out at presentation.

Hypercholesterolemia (total cholesterol: 220 mg/dL, reference range <190mg/dL; LDL 143mg/dL, reference range <100mg/dL) and a slightly elevated glycosylated haemoglobin (43mmol/mol, reference range: 20-42 mmol/mol) were noted although his full blood count and inflammatory biomarkers (erythrocyte sedimentation rate or C reactive protein) were within the reference ranges. Polysomnography was performed because of a history of snoring and mild OSA was diagnosed. Magnetic resonance imaging (MRI) with and without gadolinium enhancement of the brain was within normal limits.

Thinning of the GCC was observed (55 µm and 52µm at 3 and 6 months respectively) and the pRNFL (79µm at 3 months and 60 µm at 6 months). Microcysts were observed in the superior hemi-maculae 6 months post episode and were persistent at the latest follow-up (24 months post episode; Figure 43).

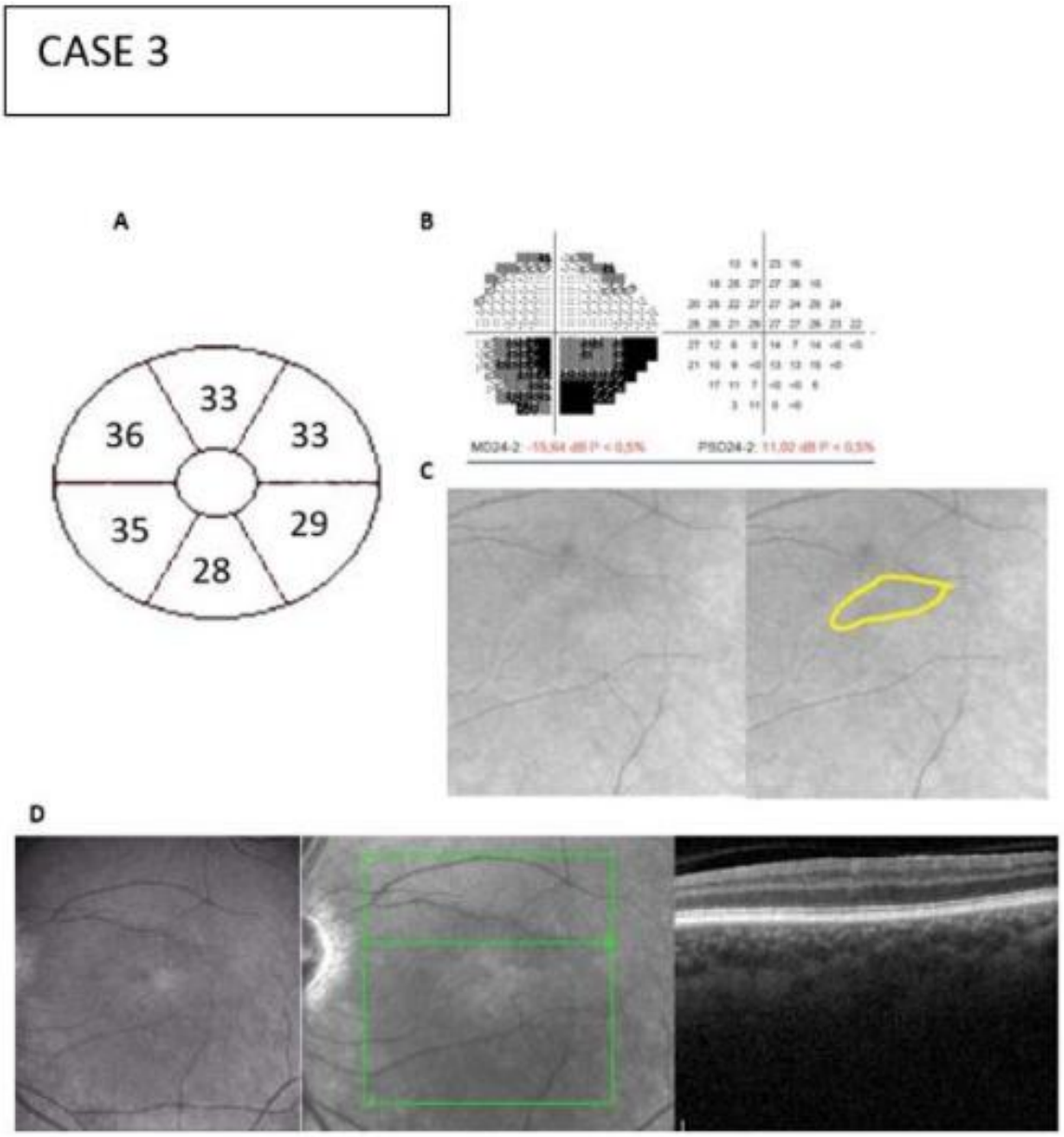

***Figure 43*: CASE 3.** *(**A**) Illustration of corresponding ΔGCL (μm) thinning between the eye before the event and 6 months post episode (**B**) Visual field showing a superior altitudinal defect (**C**) HD-OCT fundoscopy images showing hypointense lesion corresponding to location of microcyst (**D**) HRA en-face OCT (Heidelberg Engineering, Heidelberg, Germany) showing inner nuclear layer microcysts in the inferior hemi macula. This cystic change develops over time, is longstanding, possibly permanent and corresponds with the GCC thinning and visual field loss. For each patient, the distribution of cystic change was confirmed by inspection of the horizontal scans.*

7.4. Discussion

A degenerative change in the INL following ganglion cell loss was first reported in 1963 [223] in post-mortem studies of primates following chiasmal transection; and shown a few years later in post-mortem studies of human cases of optic neuropathy [224]. In the primate study, the cystic degeneration was distributed in an annular perifoveal distribution from around 500μm outwith the foveal margin extending over a further 1 mm, where the ratio of Müller cells to cone bipolar cells is low (1:4 rising to 1:1 at 3 mm eccentricity) although Müller cell to total bipolar cell ratio remains more constant [205]. Histological examination in the primate study showed debris and tissue in the larger cysts [223] -confirming that is not oedema- and some authors have suggested that degeneration of the Müller cells plays a key role because the MMO is localized in the poorly perivascularized rim [162,204,225] .Müller cells are glial cells which provide metabolic and structural support to retinal neurons [226]. The microcystic appearance observed in the INL may correlate with the vertical orientation of Müller cells [227].

Following the use of OCT, it has become possible to identify acute and chronic cystic change in the INL in daily practice and the clinical spectrum of appearances designated MMO has widened in recent years [221]. Indeed, it has been described not only in retinal pathology but also in patient with severe optic neuropathy with no known associated retinal pathology and this aetiological diversity has led to some confusion among clinicians. There is no consensus regarding the pathogenesis of MMO, some authors have suggested that it may be related to transsynaptic degeneration of bipolar cells [217,224] others to Müller cell dysfunction [203,204]. In some cases it may be a genuine manifestation of interstitial oedema perhaps secondary to Müller cell dysfunction.

Initially the three patients described above had transient reversible microcystic change affecting the INL. We propose that this is related to transudation of fluid from the ischaemic optic nerve head sectors extending within and under the retina. This finding recovered spontaneously after one month. These microcystic changes were observed in the peripapillary region and were associated with fluid localised between the ellipsoid zone and the outer plexiform layer in the parafoveal region (Figure 44). Because we are describing this microcystic change in the peripapillary region, and as it is likely to be genuine interstitial oedema a better term could be "microcystic peripapillary oedema" within the INL although it can extend into the macula (Figure 44). Subsequently, these three patients developed the now "classical" MMO in the perifoveal region, which we have shown may be very long-standing perhaps, permanent.

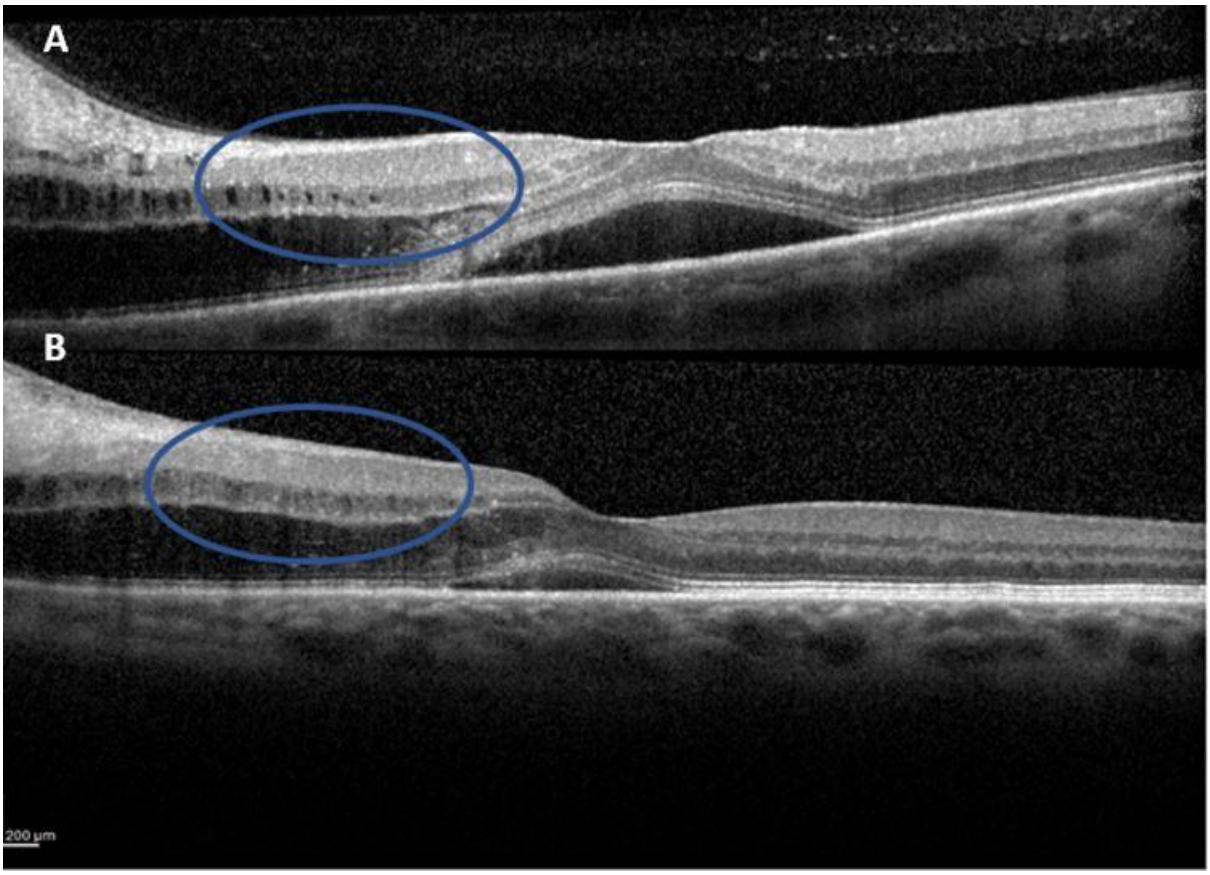

***Figure 44*: SD-OCT** *(Heidelberg Engineering, Heidelberg, Germany) imaging illustrating microcystic change in the inner nuclear layer in patients with acute non-arteritic anterior ischaemic optic neuropathy. Extension of microcystic change in the INL close to the fovea in one case from the cohort (Cohort case) (**A**) and in Case 3 (**B**). These changes correspond to the degree of optic disc swelling and are reversible with resolution of the retinal oedema.*

Acute microcytic change associated with disc swelling is probably caused by a disruption of the blood-retinal barrier as proposed by Gelfand [209], leading to the overwhelming of Müller cell function. Over the past five years, various authors have described the presence of a paravascular transport system in the retina and around the optic nerve similar to the glymphatic system existing in the brain [201–203]. In a human post-mortem study assessing cross-section of the optic nerve, Wostyn et al found an accumulation of India Ink in paravascular spaces around the central retina vein and artery, which could correspond to an optic nerve glymphatic system [202]. It has also been suggested that a hyporeflective area around the vessel walls observed on OCT provide

evidence for such a system [201]. In NA-AION, the glymphatic system could be compromised along with the venous drainage by some common mechanisms observed in ischaemia of the optic nerve. Müller cells and the superficial and deep vascular plexuses under normal conditions have a role in the reabsorption of fluid [203,204] but following arterial hypoperfusion and extensive extravasation of fluid from capillaries and veins Müller cells and other mechanisms of tissue homeostasis are saturated. This explains why we observe the OCT microcysts in the INL, similar to what has been observed in MMO [162], although the retinal distribution differed. Another factor may be that the transudate forming subretinal fluid might induce traction on the Müller footplates explaining the cystic appearance observed [211,218]. Once the disc swelling had resolved, we observe a complete resolution of the cystic change.

In contrast MMO appeared a few months post episode – after 4 months in the first case - and persisted over time (at least 36 months). Burgraff et al have described that MMO was transient in 84% of their series but most of the cases were AMD and ERM traction, where the pathogenesis may be quite different. In our cases, we observed the persistence of MMO, indicating a likely permanent change as also observed by Abegg et al [217]. Therefore, retinal ganglion cell (RGC) loss inducing vitreoretinal traction on the Müller cells is a less likely pathogenesis than a metabolic change related to retrograde transsynaptic degeneration [212,219]; either dysfunction of the Müller cells [207] or empty space induced by Müller cell degeneration now fluid filled [163]. Indeed, the stationary nature of the cysts over a long follow-up period (3 years), suggesting a fixed change very unlikely to be interstitial oedema (Figure 4).

In NA-AION, patients present with an altitudinal defect corresponding to the loss of ganglion cells induced by hypoperfusion (infarction) of one or more optic disc sectors. We observed a strong relation between the location of MMO and the thinning of ganglion cells, corresponding to the visual field defect. Indeed, MMO seems to respect the horizontal meridian in case 2 and 3, suggesting a causative effect of retrograde degeneration. Moreover, greater RNFL and GCC

thinning are observed in these patients compared to the entire cohort (Figure 33). Contrary to the conclusions of Lee DH et al [220], in NA-AION, a poorer overall visual outcome is not necessary to observe MMO but rather it is a significant localised loss of RGCs is key. MMO was indeed observed by us in two patients who had poor vision (Case 1 and Case 2) but also in a patient with good overall vision because central vision was spared (Case 3). The question arises as to the impact of the INL change on visual function. Clearly, it signifies greater RGC loss but whether any additional impairment of function occurs is unknown. To investigate this question in NA-AION would require detailed visual function analysis and possibly electroretinography concentrating on the macula, comparing cases with comparable visual field loss with and without MMO.

7.5. Conclusions

In conclusion, our study indicates two causes of MMO in the same patients suffering from NA-AION, one reversible and the other likely permanent. Müller cell dysfunction seems to play a key role in this finding and offer a potential explanation for both conditions. This finding highlights the distinction between genuine oedema related to transudation of fluid (here associated with optic disc swelling) and the phenomenon observed in RM related to the degree of RNFL loss. We consider that MMO might be considered a misnomer if there is no tissue oedema and, until the exact pathology is identified, would recommend the use of the term "retrograde maculopathy" [163,219]. The distribution of the change corresponded in our cases to both the more significant visual field loss and the greater GCC thinning. It appeared after a time interval of some weeks and may persist for many months or years. These are not the characteristics that would be expected if tissue oedema were the underlying mechanism giving

rise to the INL cystic change. NA-AION is also a useful model because of the localised retinal change corresponding to localised axonal loss, as has also been found in the nasal hemi-macula in chiasmal compression [228].

Part 6 : Conclusions and Perspectives

8. Conclusions and perspectives

With the advance of OCT in Neuro-Ophthalmology, we are able to investigate easily and accurately the thickness of the GCL, layer connected directly with the brain. The structure and the organization of the retina are unique and the use of OCT is a great opportunity to detect the short-term and long-term change after an episode of optic neuropathy.

Throughout this work, we have chosen to focus on NA-AION because it is a common cause of presentation in the ophthalmologic department. Indeed, the incidence of NA-AION in patients aged over 50 years old is 10.2 per 100 000 individuals[229]. Moreover, pathogenesis (the hypoperfusion involving one or more ON head sectors) in NA-AION is particularly interesting because it induces a permanent loss of visual function (permanent visual field defect) corresponding to the loss of ganglion cells. This aspect was crucial to permit the assessment of an inferior GCC thickness threshold and the use of ganglion cells OCT as a potential marker of recovery.

Moreover, we have identified a specific sub-population of patients with NA-AION: NA-AION patients associated with fluid. Therefore, we investigated the visual impact in patients with and without fluid and the pathogenesis of fluid in these patients during the study.

8.1. Assessment of ganglion cell complex thickness

In neuro-ophthalmology, pRNFL and GCC thickness obtained by OCT are objective measures whereas visual field testing is subjective. Moreover, visual field may not reflect early or mild axonal damage. Compared to RNFL analyses, the GCC assessment provide an earlier window

to monitor NA-AION sequelae because it is less impacted by the optic disc swelling. Indeed, the GCC measurement is more reliable in our cohort and is approximately stable after 3 months although the RNFL loss is more progressive and becomes stable about 6 months after the episode. Moreover, the visual field was more strongly correlated to GCC thickness than to RNFL thickness.

NA-AION is also a useful model because of the localised retinal change corresponding to localised axonal loss, as has also been found in the nasal hemi-macula in chiasmal compression[109]. Indeed, GCC thinning in NA-AION often respects the horizontal meridian whereas a chiasmal compression respects the vertical meridian. Identification of GCC thinning pattern on OCT is a useful method for early detection of visual pathway injury but also to diagnose adequately the aetiology of an optic neuropathy.

The principal aim of this work was to determine an inferior ganglion cell thickness threshold at which point a permanent visual field defect become detectable on examination. This critical threshold is reached when the remaining axons and ganglion cells are not able to compensate for the loss. In other words, GCC parameters could be a predictor of the degree of long-term visual field or visual acuity recovery. In order to achieve this purpose, we reviewed 45 eyes with NA-AION and 23 healthy follow eyes (34 patients). We considered NA-AION as a unique model because the axonal loss corresponds to the visual defect. This loss is usually found in the superior or the inferior hemi-macula corresponding to the inferior or superior altitudinal visual field defect (Figure 45). In our study, the *main objective* was to examine the GCC thickness in the superior and inferior hemi-macula. This variable was assessed at baseline and at 6 months after the episode.

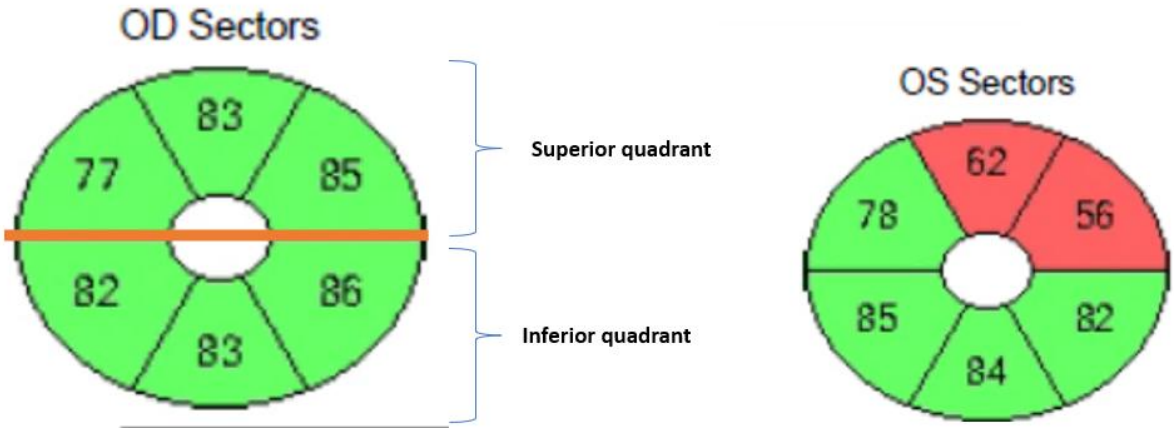

***Figure 45*: Ganglion cell complex thickness analysis obtained by optical coherence tomography** *(HD-OCT Cirrhus, Carl Zeiss Meditec, Dublin, California). Ganglion cell complex sectors analysis illustrating the superior hemi-macula ganglion cell complex quadrant average thinning after a NA-AION episode in the left eye (right image) compared to the unaffected right eye (left image). In this case, a loss of 25.30% and 34.00% is observed in the superior and the superotemporal sectors 6 months after an episode of NA-AION, respectively. OD: right eye OS: left eye*

In our cohort, we observed a significant GCC thinning of 33.3% (-28.2 ± 5.2 µm) in the superior hemi-macula and 31.0% (-30.7 ± 5.6 µm) in the inferior hemi-macula at 6 months after the episode compared to the unaffected eye. We also calculate the relative GCC thickness change between baseline and 6 months using log GCC thickness at baseline/GCC thickness at 6 months(Δ) (Figure 46). On the logarithmic scale, we mostly observe a thinning of the superior and inferior hemi-macula as confirmed by the negative Δ (Δ=log ratio inferior/ superior hemi-macula GCC 6months/GCC baseline).

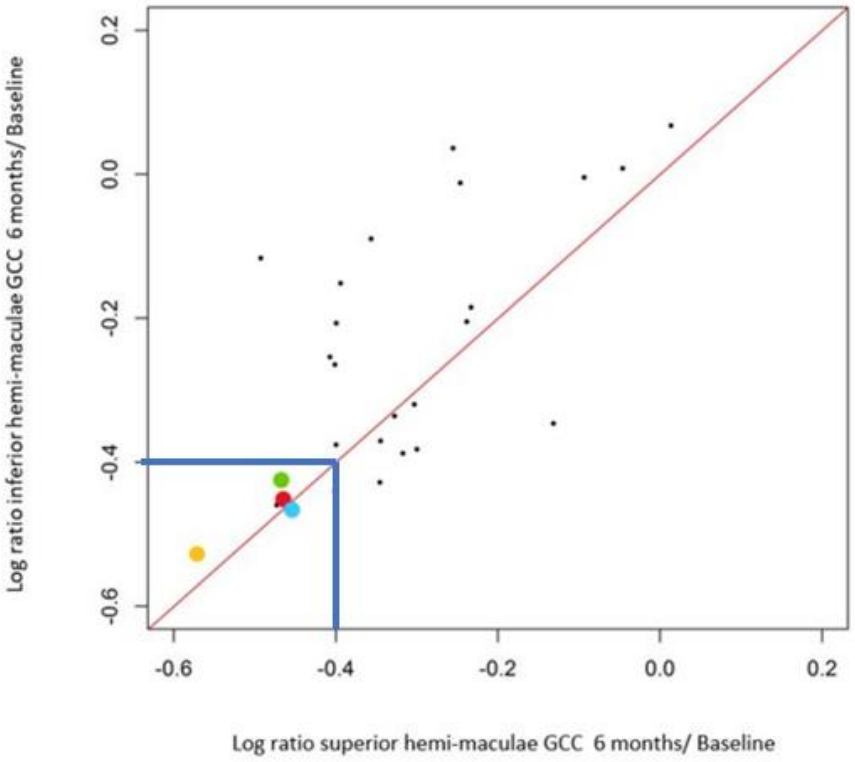

Figure 46: *Log ratio of GCC thickness in the superior (x axis) and inferior (y axis) hemi-maculae between 6 months and baseline. Overall, superior and inferior hemi-macula thickness decrease in all patients as shown by the negative Δ. Patients with MMO had significant thinning of both the superior and inferior hemi-maculae (case 1: blue dot, case 2: green dot, case 3: red point). One additional patient of the cohort who had significant thinning of both the superior and inferior hemi-maculae at 6 months had also significant MMO observed (yellow dot). In these patients, a reduction of at least 33% (Δ ≤-0,4, labelling by the blue square) is observed in the superior and inferior hemi-macula compared to baseline. The red line represents the 45-degree line where Δ inferior hemi-macula and Δ superior hemi-macula are equal.*

However, in order to confirm this figures, we add another marker that can reveal a definite loss of function: the retrograde maculopathy (RM). Overall, we observed a RM only in 4 patients at the long-term follow-up. As mentioned, this process is related to a retrograde transsynaptic degeneration of the Müller cells. This finding has been found in patients who presented simultaneously a significant GCC thinning in the superior (thickness reduction of 27.9%, -23.01 ± 9.33µm) and the inferior hemi-macula (thickness reduction of 28.51%, -19.14 ± 12.1 µm), indicating a greater RNFL loss. Figure 46 shows that the 4 patients with MMO (yellow, green,

red and blue dots) are well separated from the other patients. They are distinguished by a major superior and inferior hemi-macula GCC thinning with a $\Delta \leq -0{,}40$ (corresponding to a reduction equal or greater than 33,33% between baseline and presentation, as illustrated on the figure by the blue lines).

The location of the microcysts in patients with RM was correlated with the visual field defect (respecting the horizontal meridian) and the greater loss of GCC. Surprisingly, RM was not reported in the literature in patients with NA-AION because it was probably overlooked by clinicians. A recent and detailed review written by Gaudric et al discussed about non-vasogenic cystoid maculopathies and optic nerve diseases but did not mentioned non-arteritic anterior ischaemic optic neuropathy as a potential cause[230]. However, this change has a particularly clinical significance and should be systematically looked for.

In summary, a loss of 33% of GCC thickness in the superior and inferior hemi-macula is necessary to observe a RM, indicating a complete loss of function by retrograde negative feedback. This finding will add another reliable information that could be used to follow-up and investigate possible complications in patients with chronic optic neuropathies (IIH or compressive optic neuropathies, for example) but also to estimate the visual prognosis in preoperative patients with compressive optic neuropathy (pituitary adenoma or meningioma).

However, we should keep in mind that OCT provides only a thickness measurement of the GCC layer and does not precise the functional status of the RGC. It would be interesting to compare the OCT analyses with the electrophysiology – pattern and multifocal ERG- to assess the correlation between structure and function in patients with the same visual field loss with and without MMO. Furthermore, it is not impossible that some adaptive phenomenon can compensate the loss of RGC by an increase in the ganglion cell receptive field.

Moreover, the presence of MMO may be associated with greater ischemic involvement. Further studies are needed to correlate the location and significance of the watershed zone in these cases with FFA.

8.2. An epidemiologic study in NA-AION patients

8.2.1. Retinal fluid and NA-AION

Although NA-AION is common in neuro-ophthalmology, this retrospective study has demonstrated new and significant findings concerning the OCT analyses in patients with NA-AION. We had the chance to examine the patients at the onset of symptoms and we highlighted the effects of optic disc swelling induced by ischemia on the retina, leading to a microcystic change in the INL and retinal fluid. This phenomenon recovers spontaneously after 1 month and is often missed by ophthalmologist in patients examined 4 weeks or more after the onset of symptoms.

We firstly try to elucidate the pathogenesis of retinal fluid in these cases by comparing with other retinal disorders. Initially, various macular anomalies were considered as “macular oedema” in the nineteenth century. Then, Gass and Norton described in patients with vasogenic macular oedema a leakage of dye during fundus fluorescein angiography (FFA)[231]. Nowadays, this feature has been a key finding for the diagnosis of macular oedema due to vascular and inflammatory disease. We had the chance to have in our cohort 27 patients (63.4%) who had a FFA at presentation. Among patients with subretinal fluid, 90% had this angiographic study. This exam showed a leakage around the disc but no leakage in the macular region, excluding

the presence of choroidal neovascularization and others factors local to the fovea. FFA confirmed that the fluid due to ischemia was generated by the peripapillary vessels.

We hypothesized that this fluid was a transudate. Indeed, the sudden high volume of fluid due to the ischemic cascade extravasated through the retina and overwhelmed the compensating factors of retinal fluid resorption as the draining vascular system, the pump capacities of the RPE or the glymphatic system. The development of a macular star is also evidence of intraretinal fluid which has been reported in MOG-ON. It may be evidence for an inflammatory exudate rather than an ischaemic transudate as in NA-AION, since no hard exudates were found in our cohort. In the future, it would also be useful to confirm if the presence of subretinal fluid and peripapillary inner nuclear layer oedema are distinguishing features of acute NA-AION.

Moreover, at acute phase, microcystic change in the INL - hyporeflective cavities- were observed in the peripapillary region. Interestingly, this microcystic change are strictly limited to the INL. INL comprises the cell bodies of amacrine, bipolar and horizontal cells as well as Müller cells bodies. Müller cells are intrinsically involved in the reabsorption of fluid that percolates through the retina. Because of the high quantity of fluid, these cells are overwhelmed -secondary Müller cells dysfunction- leading to a swollen of these cells. Moreover, Müller cells processes stabilized mechanically the retina. In case of vitreomacular traction due to optic disc swelling, the dissociation between different Müller cells can create cystoid space. The role of Müller cells is probably essential in the pathogenesis of this finding.

Finally, it is the first time that the pathological change in the retina due to optic disc swelling were described. In our clinical practice, it is not so rare to observe retinal fluid associated with optic disc swelling and the primum movens should be identified to diagnose and treat adequately the patient. We should systematically address this question: “Is the retinal fluid related to the optic nerve or the retina itself? “. In case of fluid associated with optic disc swelling, structural changes mainly in the *peripapillary* retina will be observed: microcystic

change in the INL and fluid infiltration in the outer nuclear layer. Traction caused by the optic disc swelling may contribute to the presence of subretinal fluid but it seems also that the fluid amount generated is also an important factor. Indeed, parafoveal fluid is often observed in association with subretinal fluid in patients with optic disc swelling (p=0.0021). OCT scanning of the peripapillary region especially in patients with severe loss of vision out of the proportion to the retinal finding should be done systematically. In addition, FFA should be realised in patients with retinal fluid of unknown origin to identify a dye leakage. Understanding the pathogenesis of retinal fluid associated with optic disc swelling will help us to better interpret OCT findings and will help us in the differential diagnosis between a retinal disorder or retinal fluid associated with an optic nerve disorder. Indeed, this finding illustrates what is often observed in "neuroretinitis" or other causes of neuropathies associated with optic disc swelling and permit to understand easily the high risk of misdiagnosis because of the similar underlying mechanism. Identifying the origin of fluid in the retina is crucial to treat adequately these patients. In fact, in case of blood retinal barrier breakdown, anti-angiogenic agents will be efficient whereas these drugs will have no effects on patients with retinal fluid associated with optic nerve disorders.

8.2.2. Outcome and management of NA-AION

This thesis was also the opportunity to investigate retrospectively the visual outcome in patients with NA-AION associated or not with retinal fluid. First of all, our results confirmed that inferior altitudinal defect was observed in the majority of the patients (75%). Even if this finding is commonly reported in the literature, no explanation was found. One hypothesis could be that an anatomic factor makes the superior ciliary posterior artery more vulnerable to ischemia because of their location in the optic disc. Indeed, Hayreh et al identified more superior branch

retinal artery occlusion (BRAO) (42%, 11% of superior BRAO and 31% of superior temporal BRAO)[232]. Another thought could be that the superior part of the OD might be more susceptible to ischemia in patient with crowded disc (a small cup-disc ratio). Indeed, we can easily imagine that less blood arrives in the superior artery -in case of hypoperfusion- due to the gravity effect. Causes of superior artery involvement should be investigated in the future and maybe could help us to avoid episodes of NA-AION in patients at risk.

Moreover, it is mentioned in the literature that some cases of NA-AION recover slightly few weeks after the attack[157]. Therefore, we hypothesized that this vision recovery was due to the resorption of fluid. However, our results showed that subretinal fluid associated with NA-AION do not influence the visual outcome. Indeed, there was no significant difference concerning the visual acuity in patients with and without retinal fluids (p=0.91). An upward trend is observed concerning the visual acuity between the onset and 1 month in patients with NA-AION and could be due to cerebral compensatory mechanisms permitting a better utilization of the remained visual field. Although OD swelling can induce a hyperopic shift, the upward trend was not related to a change of the subjective refraction.

In neuro-ophthalmology, questions concerning the utility of corticosteroids in NA-AION raises each time we face a patient with this condition. In our study, although there was no randomization, we did not observe any differences concerning the visual prognosis in patients treated and non-treated with corticosteroids. However, a question remains unanswered: “Do the corticosteroid fasten the subretinal fluid resorption?”. In order to address this question, measurements of fluids should be evaluated within the first few days after the onset of symptoms.

Finally, an important point is the possibility to avoid bilateralisation of NA-AION by treating cardiovascular risk factors. OSA should be systematically screened in these patients. Indeed, OSA was found in 34.4% (n=11) of patients with NA-AION. When analysing our results,

treated systematic hypertension is highly associated with NA-AION (62.5%, n=20). At first, we tried to identify if this association was caused by a potential side effect of the medication. However, multiple drugs were taken by the patients: angiotensin blockers (n=4), beta-blockers (n=3), angiotensin-converting enzyme inhibitors (n=4), calcium channel blockers (n=2), and diverse associations (n=7). A majority of patients was treated with at least 2 antihypertensive drugs which can induce a greater drop of blood pressure. Thus, clinicians should be aware that hypotension can be as involved as hypertension in these patients. Indeed, ocular blood flow to the ON head is directly affected by the ocular perfusion pressure[233–235]. The ocular pressure perfusion is defined as the difference between blood pressure and IOP. Hypertension and hypotensive drugs impair the autoregulation mechanism leading to a reduction of the ocular blood flow due to a decrease of perfusion pressure. Thus, we can easily imagine that autoregulatory mechanisms can maintain the blood supply to the ON head to a certain extent before observing an abnormal perfusion and the subsequent ischemia of the ON head, playing a major role in the pathogenesis of NA-AION. Moreover, it is important to remember that hypertension is a major cardiovascular risk factor that can contribute to the pathogenesis of atherosclerosis, ultimately leading to optic nerve hypoperfusion.

8.3. Microcystic macular oedema: a misnomer?

Following the use of OCT, we have been able to detect tinny change in the different layer of human retina in few seconds. MMO was described initially by Gelfand et al in patients with MS who had had a severe episode of optic neuritis with a marked RNFL thinning [162]. This microcysts are located in the INL and show a perifoveal distribution[162,209].

However, in clinical practice, it is sometimes very challenging to interpretate adequately these findings and the literature review regarding MMO illustrates quite well the confusion found among clinicians. In fact, an apparent same finding- microcystic macular oedema- may be related to distinct pathogenesis. A recent review focused on the "non-vasogenic cystoid maculopathies" seems to confirm this thought but did not mention acute NA-AION as a possible cause of INL cystic change[230].

We described three patients with NA-AION who had ***transient*** microcystic macular oedema and ***persistent*** microcystic macular oedema. We suggested that these findings were related to transudation of fluid due to optic disc swelling in the acute phase of NA-AION and retrograde transsynaptic degeneration of bipolar cells[217,224] or Müller cells dysfunction [203,204] in the chronic phase of NA-AION.

Although in both entities the microcysts are located in the INL, some characteristics drastically differ. The microcysts are transient in fluid transudation and are related to a genuine oedema whereas they are permanent in retrograde degeneration due to Müller cell apoptosis secondary to retrograde degeneration.

In summary, it illustrates how a same finding on OCT, consequence of the anatomical structure of the INL, can have two distinct pathogenesis and the impact on conclusion in some trial mixing the two entities. In order to avoiding misunderstanding in the future, we should use two different terms: retrograde maculopathy in retrograde transsynaptic degeneration due to optic neuropathies and microcystic macular oedema in genuine oedema related to transudation of fluid. Therefore, the term MMO is misleading in cases of retrograde maculopathy which is unrelated to tissue edema.

8.4. Clinical relevance and perspectives

As demonstrated by the outcomes of the thesis, OCT have become a useful biomarker in optic neuropathies and neurological diseases. OCT is a non-invasive device providing reproductive measurements of the retinal layers and is considered as harmless and comfortable by the patients. Physicians obtain in few seconds real-time images, helping in the understanding of the patients complains. The GCC thickness assessment provide an additional reliable information that should be used in the ophthalmology, neurology and neurosurgical department.

The retina is considered as an extension of the central nervous system [236]. Indeed, RGC share some similarities with central nervous system neurons and optic nerve fibres. Moreover, embryonically, the eye developed from diencephalon of central nervous system [236]. Recently, OCT have given *insights into the prognosis of neurological diseases*. In Parkinson's disease (PD), a diffuse thinning of the GCC was observed in PD patients compared to controls and was correlated with reduced volume of some brain structures as the thalamus and the putamen, explaining the cognitive impairment [237]. GCC thickness was inversely correlated with disease duration and severity. Similar findings have been found in mild cognitive impairment and Alzheimer's disease [238]. A decreased macular and RNFL (superior and inferior quadrants) thickness was observed in patients with Alzheimer's disease even in patients with normal visual acuity, visual field and colour vision, highlighting the degenerative process [239]. Therefore, the OCT has the advantage of permitting an early recognition of some conditions in pauci symptomatic patients and in atypical manifestations of a neurological disease.

Moreover, GCC thickness analysis adds an important clinical value for the *assessment of the clinical activity* of a disease as in multiple sclerosis. OCT can confirm and reveal a previous

episode of optic neuritis. In fact, a loss of 5 to 27% of GCL after optic neuritis with a full visual recovery as determined by clinical tests is observed in a recent study[130]. Long-term evaluation of patients with MS can also identify some specific pattern as progressive visual failure. This subtype of optic neuropathy dominantly affects males and is a bilateral disease associated with primary progressive multiple sclerosis[240]. Thus, OCT is a high-value tool for the longitudinal follow-up in chronic conditions as in inflammatory diseases (MOGAD, NMOSD and MS, for example) or IIH. Thinning of the RNFL and GCC is observed in MS patients, even in those without a history of optic neuritis.

OCT can also be considered as a *marker of recovery of vision* before surgery with the OCT parameters. Indeed, we could demonstrate if a permanent axonal loss is present related to the retrograde degeneration. A thinning of the GCC superior to 33,33% will indicate a permanent visual defect in patient with optic nerve sheath meningioma for example by extrapolation of the results of the thesis (see section 8.1. Assessment of ganglion cell thickness).

In addition, OCT is a *potential screening tool* which represent a protective effect due to subsequent treatment started. In ophthalmology, it is also well known that we can detect glaucoma optic neuropathy in a preclinic stage because of a GCC thinning even if the visual field and the visual acuity are still normal. They give us the possibility to treat the patients earlier and a 50% reduction of glaucoma-related blindness is observed in screened patients [241].

Finally, it seems obvious that continuing advances will appear in the future concerning OCT technology. Next-generation OCT will achieve a sub-micrometre level of precision and we will be able to detect new pathologies. Vascularization study of the optic nerve will probably help us to better understand the pathogenesis of the NA-AION by identifying some embolism or reduced flow in posterior ciliary arteries. However, manufacturers should work on the diminution of acquisition and analysis artefacts by reducing the processing time and increasing the volume segmentation. Moreover, in order to have a better comparison with the normative

database, they should increase the population with patients with very high and short axial length. Extreme age population and all ethnicities should also be more represented.

Artificial intelligence (AI) combined with OCT is likely to play a major role in Ophthalmology in a few years [242,243]. This new technology will help to detect some change undetectable to the ophthalmologist eye in identifying optic nerve abnormalities [244], aid in the diagnosis of neurodegenerative diseases [245] and make the difference between arteritic and non-arteritic AION. Moreover, artificial intelligence will help us to predict the risk of a disease. For example, we will be able to predict the cardiovascular risk factors based on the retinal fundus photographs[246] or estimate accurately the biological age using retinal images [247].

Currently, ophthalmologists and neurologists do not have any drugs to treat NA-AION. However, we could prevent the occurrence of NA-AION through preventive measures (control of the cardiovascular risk factors, for example). AI would play a major role in the future to establish the prediction of occurrence of NA-AION in global population or in a subpopulation treated with antihypertensive drugs, for instance. First of all, we could identify some unknown factors involving in the pathogenesis of NA-AION as some anatomical features using some big data set. We could integrate the anatomical factors – presence of a crowded disc and the OCT parameters - and their medical history (severity of nocturnal apnoea, level of high blood pressure, diabetes, drugs taken). Therefore, we could assess the risk for each patient and categorize them in low, medium or high risk of NA-AION. This comprehensive integration of diverse risks factors could lead to preventive management, and we could identify personalized treatment options (instauration of systemic antihypertensive drugs or decrease the intraocular pressure) in order to avoid an NA-AION episode. We could also be capable to observe the influence of a treatment by pretesting the patient without putting the actual patient through damaging drugs. AI could bring in the future a customised and a systemic approach to prevent the occurrence of NA-AION.

Although this technology has already been used to detect diabetic retinopathy by endocrinologists for years, we are at the very beginning of the millions of possibilities that this technology can offer. We should keep in mind that it is essential to obtain a strong training dataset to have accurate outcomes. A huge challenge is waiting for us because we will need to learn how to use it and how to keep our holistic mind to treat the best as we can our patients.

Finally, collaboration with neuroradiologists is essential. We have already highlighted the importance of evaluating brain MRI for microvascular disease. Another important area for future development involves assessing focal brain MRI atrophy in the primary and secondary visual cortex in cases of retinal atrophy, with or without visual acuity impairment.

9. Supplementary figures

Variable	N	Mean	SD	SE	Min	Q1	Median	Q3	Max
Mean RNFL (µm)	6	96.50	5.36	2.19	91.0	91.0	96.50	99.0	105.0
Superior RNFL (µm)	6	122.33	11.55	4.72	111.0	112.0	119.00	136.0	137.0
Temporal RNFL (µm)	6	61.83	11.16	4.56	52.0	55.0	56.00	74.0	78.0
Nasal RNFL (µm)	6	76.67	10.23	4.18	66.0	68.0	74.00	87.0	91.0
Inferior RNFL (µm)	6	124.67	21.39	8.73	102.0	103.0	124.00	142.0	153.0
Mean GCC (µm)	5	81.20	2.95	1.32	76.0	82.0	82.00	83.0	83.0
Minimal GCC (µm)	5	80.00	4.69	2.10	72.0	80.0	82.00	82.0	84.0
Superior GCC (µm)	5	77.80	4.49	2.01	72.0	74.0	80.00	81.0	82.0
Supero-temporal GCC (µm)	5	80.20	4.15	1.85	75.0	78.0	80.00	82.0	86.0
Superonasal GCC (µm)	5	83.20	3.03	1.36	80.0	82.0	82.00	84.0	88.0
Inferior GCC (µm)	5	79.00	4.58	2.05	71.0	80.0	80.00	82.0	82.0
Inferotemporal GCC (µm)	5	83.20	2.17	0.97	80.0	82.0	84.00	85.0	85.0
Inferonasal GCC (µm)	5	83.00	3.54	1.58	77.0	83.0	84.00	85.0	86.0
Visual acuity	6	1.00	0.00	0.00	1.0	1.0	1.00	1.0	1.0

Supplementary figure 1 A: *Descriptive analysis of the characteristics of eyes prior to an episode of NA-AION in patients with bilateral NA-AION. N= number, RNFL= Retinal Nerve Fibre Layer, GCC= Ganglion Cell Complex*

N° Patient	**RNFL baseline (µm)**	**RNFL 6 months after NA-AION (µm)**	**GCC baseline (µm)**	**GCC 6 months after NA-AION (µm)**
101	99	60	82	52
102	91	64	83	68
105	105	62	82	55
106	95	66	72	34
107	107	60	90	69

Supplementary figure 1B*: Retinal nerve fibre layer (RNFL) and ganglion cell complex (GCC) thickness before and 6 months after the episode of NA-AION in 5 patients with bilateral involvement.*

		No CCS		CCS		
Variable	Categories	N	Number (%)	N	Number (%)	p-value
Sexe		11		10		0.31
	H		8 (72.7)		9 (90.0)	
	F		3 (27.3)		1 (10.0)	
Arterial Hypertension		11		10		0.54
	Non		3 (27.3)		4 (40.0)	
	Oui		8 (72.7)		6 (60.0)	
Sleep apnea		11		10		0.83
	Non		6 (54.5)		5 (50.0)	
	Oui		5 (45.5)		5 (50.0)	
Hypercholesterolemia		11		10		0.26
	Non		5 (45.5)		7 (70.0)	
	Oui		6 (54.5)		3 (30.0)	
Diabetes		11		10		0.92
	No		9 (81.8)		8 (80.0)	
	Yes		2 (18.2)		2 (20.0)	
Heart attack		11		10		NA
	Non		11 (100.0		10 (100.0	
Anti-hypertensive drug intake		11		10		0.86
	Non		4 (36.4)		4 (40.0)	
	Oui		7 (63.6)		6 (60.0)	
High blood pressure newly diagnosed		7		6		0.34
	Non		6 (85.7)		6 (100.0	
	Oui		1 (14.3)		0 (0.0)	

Variable	N	Nmiss	Mean	SD	Min	Q1	Median	Q3	Max	p-value
Age 1er Onset (years)										
No CCS	11	0	57.75	13.167	41.64	51.68	55.46	63.22	88.13	0.44
CCS	10	0	61.50	7.775	51.19	55.87	61.13	69.25	70.50	

Supplementary figure 2*: Comparative table illustrating the characteristics of the patient group with retinal fluid treated (CCS) and not treated (No CCS) with steroids. The following parameters were compared: sex, age, and cardiovascular risk factors.*

N° Paire	GCC Hemi-Sup Baseline	GCC Hemi-Sup 6 months	Difference (%)
1	90.0000	60.3333	-32.9630
2	.	59.6667	.
3	78.6667	52.6667	-33.0508
4	87.6667	55.6667	-36.5019
5	.	51.0000	.
6	78.3333	71.3333	-8.9362
7	.	.	.
8	70.6667	55.6667	-21.2264
9	.	77.6667	.
10	.	60.6667	.
11	83.3333	60.6667	-27.2000
12	81.6667	51.6667	-36.7347
13	.	53.0000	.
14	82.3333	64.3333	-21.8623
16	74.3333	.	.
17	85.3333	63.0000	-26.1719
18	78.3333	68.6667	-12.3404
19	73.3333	46.3333	-36.8182
20	81.3333	50.6667	-37.7049
21	.	59.0000	.
22	77.6667	55.0000	-29.1845
23	73.3333	51.3333	-30.0000
24	77.3333	48.6667	-37.0690
25	85.6667	52.3333	-38.9105
26	74.0000	.	.
101	81.3333	51.0000	-37.2951
102	.	66.0000	.
103	76.3333	55.0000	-27.9476
104	82.3333	.	.
105	78.6667	55.6667	-29.2373
106	.	60.0000	.

Supplementary figure 3A: *Ganglion cell complex (GCC) thickness in the superior hemi-maculae (Hemi-Sup) between 6 months and baseline. The highlighted coloured lines correspond to the coloured dots on the graph.*

N° Paire	GCC Hemi-Inf Baseline	GCC Hemi-Inf 6 months	Difference (%)
1	88.3333	60.6667	-31.3208
2	.	69.3333	.
3	83.3333	53.6667	-35.6000
4	88.6667	55.6667	-37.2180
5	.	49.6667	.
6	79.3333	79.0000	-0.4202
7	.	.	.
8	66.6667	54.3333	-18.5000
9	.	79.0000	.
10	.	65.3333	.
11	83.0000	56.3333	-32.1285
12	83.0000	52.3333	-36.9478
13	.	56.0000	.
14	84.0000	83.0000	-1.1905
16	71.3333	.	.
17	89.0000	64.6667	-27.3408
18	76.3333	54.0000	-29.2576
19	77.0000	49.0000	-36.3636
20	82.3333	52.0000	-36.8421
21	.	69.6667	.
22	78.6667	54.3333	-30.9322
23	74.0000	67.6667	-8.5586
24	78.0000	49.6667	-36.3248
25	85.0000	75.6667	-10.9804
26	73.6667	.	.
101	82.3333	53.6667	-34.8178
102	.	69.0000	.
103	76.0000	54.3333	-28.5088
104	84.0000	.	.
105	83.3333	54.3333	-34.8000
106	.	74.0000	. .

Supplementary figure 3B: *Ganglion cell complex (GCC) thickness in the inferior hemi-maculae (Hemi-Inf) between 6 months and baseline. The highlighted coloured lines correspond to the coloured dots on the graph.*

10. References

1. Güngör Kobat S. Importance of Müller Cells. *Beyoglu Eye J*. Published online 2020. doi:10.14744/bej.2020.28290

2. Remington LA. Visual System. In: *Clinical Anatomy and Physiology of the Visual System*. Elsevier; 2012:1-9. doi:10.1016/B978-1-4377-1926-0.10001-3

3. Kolb H, Fernandez E, Nelson R, eds. *Webvision: The Organization of the Retina and Visual System*. University of Utah Health Sciences Center; 1995. Accessed September 20, 2023. http://www.ncbi.nlm.nih.gov/books/NBK11530/

4. Salesse C. Physiologie du signal visuel rétinien : de la phototransduction jusqu'au cycle visuel. *Journal Français d'Ophtalmologie*. 2017;40(3):239-250. doi:10.1016/j.jfo.2016.12.006

5. Hirsch J, Curcio CA. The spatial resolution capacity of human foveal retina. *Vision Research*. 1989;29(9):1095-1101. doi:10.1016/0042-6989(89)90058-8

6. Liu G, Liu X, Li H, Du Q, Wang F. Optical Coherence Tomographic Analysis of Retina in Retinitis Pigmentosa Patients. *Ophthalmic Res*. 2016;56(3):111-122. doi:10.1159/000445063

7. Wald G. Vitamin A in the Retina. *Nature*. 1933;132(3330):316-317. doi:10.1038/132316a0

8. Mahabadi N, Al Khalili Y. Neuroanatomy, Retina. In: *StatPearls*. StatPearls Publishing; 2023. Accessed September 20, 2023. http://www.ncbi.nlm.nih.gov/books/NBK545310/

9. Kaye RA, Patasova K, Patel PJ, Hysi P, Lotery AJ, UK Biobank Eye and Vision Consortium. Macular thickness varies with age-related macular degeneration genetic risk variants in the UK Biobank cohort. *Sci Rep*. 2021;11(1):23255. doi:10.1038/s41598-021-02631-2

10. Cote RH. Photoreceptor Phosphodiesterase (PDE6): A G-Protein-Activated PDE Regulating Visual Excitation in Rod and Cone Photoreceptor Cells. In: *Cyclic Nucleotide Phosphodiesterases in Health and Disease*. CRC Press; 2007.

11. Ayoub GS, Matthews G. Substance P modulates calcium current in retinal bipolar neurons. *Vis Neurosci*. 1992;8(6):539-544. doi:10.1017/S0952523800005630

12. Kolb H, Linberg KA, Fisher SK. Neurons of the human retina: A Golgi study. *J Comp Neurol*. 1992;318(2):147-187. doi:10.1002/cne.903180204

13. Prasad S, Galetta SL. Anatomy and physiology of the afferent visual system. In: *Handbook of Clinical Neurology*. Vol 102. Elsevier; 2011:3-19. doi:10.1016/B978-0-444-52903-9.00007-8

14. Polyak SL. The Retina. In: *The Retina*. University of Chicago; 1941.

15. Wall M. Examination of the Ten Degrees of Visual field Surrounding Fixation. In: Wall M, Sadun AA, eds. *New Methods of Sensory Visual Testing*. Springer New York; 1989:94-111. doi:10.1007/978-1-4613-8835-7_6

16. Shapley R, Hugh Perry V. Cat and monkey retinal ganglion cells and their visual functional roles. *Trends in Neurosciences*. 1986;9:229-235. doi:10.1016/0166-2236(86)90064-0

17. Hubel D, Livingstone M. Segregation of form, color, and stereopsis in primate area 18. *J Neurosci*. 1987;7(11):3378-3415. doi:10.1523/JNEUROSCI.07-11-03378.1987

18. Glaser JS, Sadun AA. Anatomy of the visual sensory system. In: *Neuro-Ophthalmology*. Glaser JS. J.B. Lippincott Co; 1990:61-82.

19. Sadun AA, Win PH, Ross-Cisneros FN, Walker SO, Carelli V. Leber's hereditary optic neuropathy differentially affects smaller axons in the optic nerve. *Trans Am Ophthalmol Soc*. 2000;98:223-232; discussion 232-235.

20. Wang L, Dong J, Cull G, Fortune B, Cioffi GA. Varicosities of Intraretinal Ganglion Cell Axons in Human and Nonhuman Primates. *Invest Ophthalmol Vis Sci*. 2003;44(1):2. doi:10.1167/iovs.02-0333

21. Shariati MA, Park JH, Liao YJ. Optical Coherence Tomography Study of Retinal Changes in Normal Aging and After Ischemia. *Invest Ophthalmol Vis Sci*. 2015;56(5):2790. doi:10.1167/iovs.14-15145

22. Bowd C, Zangwill LM, Blumenthal EZ, et al. Imaging of the optic disc and retinal nerve fiber layer: the effects of age, optic disc area, refractive error, and gender. *J Opt Soc Am A*. 2002;19(1):197. doi:10.1364/JOSAA.19.000197

23. Budenz DL, Anderson DR, Varma R, et al. Determinants of Normal Retinal Nerve Fiber Layer Thickness Measured by Stratus OCT. *Ophthalmology*. 2007;114(6):1046-1052. doi:10.1016/j.ophtha.2006.08.046

24. Kolb H, Fernandez E, Schouten J, Ahnelt P, Linberg KA, Fisher SK. Are there three types of horizontal cell in the human retina? *J Comp Neurol*. 1994;343(3):370-386. doi:10.1002/cne.903430304

25. Kolb H. Roles of Amacrine Cells. In: Kolb H, Fernandez E, Nelson R, eds. *Webvision: The Organization of the Retina and Visual System*. University of Utah Health Sciences Center; 1995. Accessed September 21, 2023. http://www.ncbi.nlm.nih.gov/books/NBK11539/

26. Danesh-Meyer HV, Yoon JJ, Lawlor M, Savino PJ. Visual loss and recovery in chiasmal compression. *Prog Retin Eye Res*. 2019;73:100765. doi:10.1016/j.preteyeres.2019.06.001

27. Optic Nerve. In: *Basic and Clinical Science Course, Section 05: Neuro-Ophtahlmology*. Debra J Shetlar. American Academy of Ophthalmology; 2015:47-48.

28. Jonas JB, Schmidt AM, Müller-Bergh JA, Schlötzer-Schrehardt UM, Naumann GO. Human optic nerve fiber count and optic disc size. *Invest Ophthalmol Vis Sci*. 1992;33(6):2012-2018.

29. Gray, Henry. *Anatomy of the Human Body, by Henry Gray. 20th Ed., Thoroughly Rev. and Re-Edited by Warren H. Lewis.* Lea & Febiger; 1918.

30. Smith AM, Czyz CN. Neuroanatomy, Cranial Nerve 2 (Optic). In: *StatPearls*. StatPearls Publishing; 2023. Accessed September 21, 2023. http://www.ncbi.nlm.nih.gov/books/NBK507907/

31. Kedar S, Tong J, Bader J, et al. Effects of Acute Intracranial Pressure Changes on Optic Nerve Head Morphology in Humans and Pig Model. *Current Eye Research*. 2022;47(2):304-311. doi:10.1080/02713683.2021.1952604

32. Morgan WH, Yu DY, Balaratnasingam C. The Role of Cerebrospinal Fluid Pressure in Glaucoma Pathophysiology: The Dark Side of the Optic Disc. *Journal of Glaucoma*. 2008;17(5):408-413. doi:10.1097/IJG.0b013e31815c5f7c

33. Downs JC. Neural coupling of intracranial pressure and aqueous humour outflow facility: A potential new therapeutic target for intraocular pressure management. *The Journal of Physiology*. 2020;598(8):1429-1430. doi:10.1113/JP279355

34. Mendel E, Stoicea N, Rao R, et al. Revisiting Postoperative Vision Loss following Non-Ocular Surgery: A Short Review of Etiology and Legal Considerations. *Front Surg*. 2017;4:34. doi:10.3389/fsurg.2017.00034

35. Henkind P, Levitzky M. Angioarchitecture of the Optic Nerve. *American Journal of Ophthalmology*. 1969;68(6):979-986. doi:10.1016/0002-9394(69)93437-0

36. Hayreh SS. Blood supply of the optic nerve head and its role in optic atrophy, glaucoma, and oedema of the optic disc. *British Journal of Ophthalmology*. 1969;53(11):721-748. doi:10.1136/bjo.53.11.721

37. Anderson DR, Braverman S. Reevaluation of the Optic Disk Vasculature. *American Journal of Ophthalmology*. 1976;82(2):165-174. doi:10.1016/0002-9394(76)90414-1

38. Yu PK, McAllister IL, Morgan WH, Cringle SJ, Yu DY. Inter-Relationship of Arterial Supply to Human Retina, Choroid, and Optic Nerve Head Using Micro Perfusion and Labeling. *Invest Ophthalmol Vis Sci*. 2017;58(9):3565-3574. doi:10.1167/iovs.17-22191

39. Olver JM, Spalton DJ, McCartney AC. Microvascular study of the retrolaminar optic nerve in man: the possible significance in anterior ischaemic optic neuropathy. *Eye (Lond)*. 1990;4 (Pt 1):7-24. doi:10.1038/eye.1990.3

40. Onda E, Cioffi GA, Bacon DR, Van Buskirk EM. Microvasculature of the Human Optic Nerve. *American Journal of Ophthalmology*. 1995;120(1):92-102. doi:10.1016/S0002-9394(14)73763-8

41. Marmor MF, Ravin JG. Fluorescein angiography: insight and serendipity a half century ago. *Arch Ophthalmol*. 2011;129(7):943-948. doi:10.1001/archophthalmol.2011.160

42. Xu R, Teich W, Frenzel F, et al. Optical Characterization of Sodium Fluorescein In Vitro and Ex Vivo. *Front Oncol*. 2021;11:654300. doi:10.3389/fonc.2021.654300

43. O'goshi K ichiro, Serup J. Safety of sodium fluorescein for in vivo study of skin. *Skin Res Technol*. 2006;12(3):155-161. doi:10.1111/j.0909-752X.2006.00147.x

44. Ruia S, Tripathy K. Fluorescein Angiography. In: *StatPearls*. StatPearls Publishing; 2023. Accessed November 28, 2023. http://www.ncbi.nlm.nih.gov/books/NBK576378/

45. Chapelle AC, Rakic JM. [Ocular vascular pathologies : keep an eye open!]. *Rev Med Liege*. 2018;73(5-6):351-358.

46. Hill DW. Some clinical applications of fluorescense retinal photography. *Trans Ophthalmol Soc U K (1962)*. 1966;86:125-138.

47. O'Day D, Crock G, Galbraith JEK, Parel JM, Wigley A. FLUORESCEIN ANGIOGRAPHY OF NORMAL AND ATROPHIC OPTIC DISCS. *The Lancet*. 1967;290(7509):224-226. doi:10.1016/S0140-6736(67)92295-7

48. Ernest JT, Archer D. Fluorescein angiography of the optic disk. *Am J Ophthalmol*. 1973;75(6):973-978. doi:10.1016/0002-9394(73)91084-2

49. Arnold AC, Hepler RS. Fluorescein Angiography in Acute Nonarteritic Anterior Ischemic Optic Neuropathy. *American Journal of Ophthalmology*. 1994;117(2):222-230. doi:10.1016/S0002-9394(14)73080-6

50. Lim CW, Cheng J, Tay ELT, et al. Optical coherence tomography angiography of the macula and optic nerve head: microvascular density and test-retest repeatability in normal subjects. *BMC Ophthalmology*. 2018;18(1):315. doi:10.1186/s12886-018-0976-y

51. Miller NR, Arnold AC. Current concepts in the diagnosis, pathogenesis and management of nonarteritic anterior ischaemic optic neuropathy. *Eye*. 2015;29(1):65-79. doi:10.1038/eye.2014.144

52. Hayreh SS. Anterior ischaemic optic neuropathy. II. Fundus on ophthalmoscopy and fluorescein angiography. *Br J Ophthalmol*. 1974;58(12):964-980. doi:10.1136/bjo.58.12.964

53. Levin LA, Rizzo JF, Lessell S. Neural network differentiation of optic neuritis and anterior ischaemic optic neuropathy. *Br J Ophthalmol*. 1996;80(9):835-839. doi:10.1136/bjo.80.9.835

54. Scherer RW, Feldon SE, Levin L, et al. Visual Fields at Follow-up in the Ischemic Optic Neuropathy Decompression Trial. *Ophthalmology*. 2008;115(10):1809-1817. doi:10.1016/j.ophtha.2008.03.020

55. Dickersin K. Optic Nerve Decompression Surgery for Nonarteritic Anterior Ischemic Optic Neuropathy (NAION) Is Not Effective and May Be Harmful. *JAMA*. 1995;273(8):625. doi:10.1001/jama.1995.03520320035038

56. Arnold A. Vascular supply of the optic nerve head: implications for optic disc ischaemia. *Br J Ophthalmol*. 2023;107(5):595-599. doi:10.1136/bjo-2022-322254

57. Henkind P, Charles NC, Pearson J. Histopathology of Ischemic Optic Neuropathy. *American Journal of Ophthalmology*. 1970;69(1):78-90. doi:10.1016/0002-9394(70)91859-3

58. Eagling EM, Sanders MD, Miller SJ. Ischaemic papillopathy. Clinical and fluorescein aniographic review of forty cases. *British Journal of Ophthalmology*. 1974;58(12):990-1008. doi:10.1136/bjo.58.12.990

59. Arnold AC, Costa RMS, Dumitrascu OM. The spectrum of optic disc ischemia in patients younger than 50 years (an Amercian Ophthalmological Society thesis). *Trans Am Ophthalmol Soc*. 2013;111:93-118.

60. Collignon-Robe NJ, Feke GT, Rizzo JF. Optic nerve head circulation in nonarteritic anterior ischemic optic neuropathy and optic neuritis. *Ophthalmology*. 2004;111(9):1663-1672. doi:10.1016/j.ophtha.2004.05.020

61. Beck RW, Servais GE, Hayreh SS. Anterior ischemic optic neuropathy. IX. Cup-to-disc ratio and its role in pathogenesis. *Ophthalmology*. 1987;94(11):1503-1508.

62. Arnold AC. Pathogenesis of nonarteritic anterior ischemic optic neuropathy. *J Neuroophthalmol*. 2003;23(2):157-163. doi:10.1097/00041327-200306000-00012

63. Mojon DS. Association Between Sleep Apnea Syndrome and Nonarteritic Anterior Ischemic Optic Neuropathy. *Arch Ophthalmol*. 2002;120(5):601. doi:10.1001/archopht.120.5.601

64. Palombi K, Renard E, Levy P, et al. Non-arteritic anterior ischaemic optic neuropathy is nearly systematically associated with obstructive sleep apnoea. *British Journal of Ophthalmology*. 2006;90(7):879-882. doi:10.1136/bjo.2005.087452

65. Hayreh SS. Systemic arterial blood pressure and the eye. *Eye*. 1996;10(1):5-28. doi:10.1038/eye.1996.3

66. Hayreh SS, Servais GE, Virdi PS. Fundus Lesions in Malignant Hypertension. *Ophthalmology*. 1986;93(1):74-87. doi:10.1016/S0161-6420(86)33773-4

67. Hammond S, Wells JR, Marcus DM, Prisant LM. Ophthalmoscopic Findings in Malignant Hypertension. *The Journal of Clinical Hypertension*. 2006;8(3):221-223. doi:10.1111/j.1524-6175.2005.04147.x

68. Katz B, Weinreb RN, Wheeler DT, Klauber MR. Anterior ischaemic optic neuropathy and intraocular pressure. *British Journal of Ophthalmology*. 1990;74(2):99-102. doi:10.1136/bjo.74.2.99

69. Lacharme T, Almanjoumi A, Aptel F, et al. Twenty-four-hour rhythm of ocular perfusion pressure in non-arteritic anterior ischaemic optic neuropathy. *Acta Ophthalmol*. 2014;92(5):e346-e352. doi:10.1111/aos.12352

70. Yang JM, Park SW, Ji YS, Kim J, Yoo C, Heo H. Postural effects on intraocular pressure and ocular perfusion pressure in patients with non-arteritic anterior ischemic optic neuropathy. *BMC Ophthalmol*. 2017;17(1):47. doi:10.1186/s12886-017-0441-3

71. James CB, Smith SE. The effect of posture on the intraocular pressure and pulsatile ocular blood flow in patients with non-arteritic anterior ischaemic optic neuropathy. *Eye*. 1991;5(3):309-314. doi:10.1038/eye.1991.49

72. Kalenak JW. Nonarteritic Anterior Ischemic Optic Neuropathy and Intraocular Pressure. *Arch Ophthalmol*. 1991;109(5):660. doi:10.1001/archopht.1991.01080050074032

73. Toth CA, Narayan DG, Boppart SA, et al. A comparison of retinal morphology viewed by optical coherence tomography and by light microscopy. *Arch Ophthalmol*. 1997;115(11):1425-1428. doi:10.1001/archopht.1997.01100160595012

74. Ho J, Sull AC, Vuong LN, et al. Assessment of Artifacts and Reproducibility across Spectral and Time Domain Optical Coherence Tomography Devices. *Ophthalmology*. 2009;116(10):1960-1970. doi:10.1016/j.ophtha.2009.03.034

75. Alshareef RA, Goud A, Mikhail M, et al. Segmentation errors in macular ganglion cell analysis as determined by optical coherence tomography in eyes with macular pathology. *Int J Retin Vitr*. 2017;3(1):25. doi:10.1186/s40942-017-0078-7

76. Fujimoto JG, Pitris C, Boppart SA, Brezinski ME. Optical Coherence Tomography: An Emerging Technology for Biomedical Imaging and Optical Biopsy. *Neoplasia*. 2000;2(1-2):9-25. doi:10.1038/sj.neo.7900071

77. Aumann S, Donner S, Fischer J, Müller F. Optical Coherence Tomography (OCT): Principle and Technical Realization. In: Bille JF, ed. *High Resolution Imaging in Microscopy and Ophthalmology*. Springer International Publishing; 2019:59-85. doi:10.1007/978-3-030-16638-0_3

78. Almasieh M, Lieven CJ, Levin LA, Di Polo A. A Cell-Permeable Phosphine-Borane Complex Delays Retinal Ganglion Cell Death After Axonal Injury Through Activation of The Pro-Survival extracellular signal-regulated kinases 1/2 Pathway. *J Neurochem*. 2011;118(6):1075-1086. doi:10.1111/j.1471-4159.2011.07382.x

79. Takihara Y, Inatani M, Hayashi H, et al. Dynamic Imaging of Axonal Transport in Living Retinal Ganglion Cells In Vitro. *Invest Ophthalmol Vis Sci*. 2011;52(6):3039-3045. doi:10.1167/iovs.10-6435

80. Ghaffarieh A, Levin LA. Optic nerve disease and axon pathophysiology. *Int Rev Neurobiol*. 2012;105:1-17. doi:10.1016/B978-0-12-398309-1.00002-0

81. Berkelaar M, Clarke D, Wang Y, Bray G, Aguayo A. Axotomy results in delayed death and apoptosis of retinal ganglion cells in adult rats. *J Neurosci*. 1994;14(7):4368-4374. doi:10.1523/JNEUROSCI.14-07-04368.1994

82. Saatman KE, Abai B, Grosvenor A, Vorwerk CK, Smith DH, Meaney DF. Traumatic Axonal Injury Results in Biphasic Calpain Activation and Retrograde Transport Impairment in Mice. *J Cereb Blood Flow Metab*. 2003;23(1):34-42. doi:10.1097/01.WCB.0000035040.10031.B0

83. Alshareef RA, Dumpala S, Rapole S, et al. Prevalence and Distribution of Segmentation Errors in Macular Ganglion Cell Analysis of Healthy Eyes Using Cirrus HD-OCT. Khanna H, ed. *PLoS ONE*. 2016;11(5):e0155319. doi:10.1371/journal.pone.0155319

84. Menke MN, Feke GT, Trempe CL. OCT Measurements in Patients with Optic Disc Edema. *Invest Ophthalmol Vis Sci*. 2005;46(10):3807. doi:10.1167/iovs.05-0352

85. Bayer A, Akman A. Artifacts and Anatomic Variations in Optical Coherence Tomography. *tjo*. 2020;50(2):99-106. doi:10.4274/tjo.galenos.2019.78000

86. Cheung CYL, Leung CKS, Lin D, Pang CP, Lam DSC. Relationship between Retinal Nerve Fiber Layer Measurement and Signal Strength in Optical Coherence Tomography. *Ophthalmology*. 2008;115(8):1347-1351.e2. doi:10.1016/j.ophtha.2007.11.027

87. Ghadiali Q, Hood DC, Lee C, et al. An Analysis of Normal Variations in Retinal Nerve Fiber Layer Thickness Profiles Measured With Optical Coherence Tomography. *Journal of Glaucoma*. 2008;17(5):333-340. doi:10.1097/IJG.0b013e3181650f8b

88. Savini G, Barboni P, Parisi V, Carbonelli M. The influence of axial length on retinal nerve fibre layer thickness and optic-disc size measurements by spectral-domain OCT. *Br J Ophthalmol*. 2012;96(1):57-61. doi:10.1136/bjo.2010.196782

89. Trip SA, Schlottmann PG, Jones SJ, et al. Retinal nerve fiber layer axonal loss and visual dysfunction in optic neuritis. *Ann Neurol*. 2005;58(3):383-391. doi:10.1002/ana.20575

90. Chai SJ, Foroozan R. Decreased retinal nerve fibre layer thickness detected by optical coherence tomography in patients with ethambutol-induced optic neuropathy. *British Journal of Ophthalmology*. 2007;91(7):895-897. doi:10.1136/bjo.2006.113118

91. Chen JJ, Kardon RH. Avoiding Clinical Misinterpretation and Artifacts of Optical Coherence Tomography Analysis of the Optic Nerve, Retinal Nerve Fiber Layer, and Ganglion Cell Layer. *Journal of Neuro-Ophthalmology*. 2016;36(4):417-438. doi:10.1097/WNO.0000000000000422

92. Savini G. Detection and Quantification of Retinal Nerve Fiber Layer Thickness in Optic Disc Edema Using Stratus OCT. *Arch Ophthalmol*. 2006;124(8):1111. doi:10.1001/archopht.124.8.1111

93. Hedges TR. Subretinal Fluid From Anterior Ischemic Optic Neuropathy Demonstrated by Optical Coherence Tomography. *Arch Ophthalmol*. 2008;126(6):812. doi:10.1001/archopht.126.6.812

94. Chapelle AC, Rakic JM, Plant GT. The Occurrence of Intra- and Sub-Retinal Fluid in Anterior Ischemic Optic Neuropathy: Pathogenesis, Prognosis and Treatment. *Ophthalmology*. Published online July 2023:S0161642023004955. doi:10.1016/j.ophtha.2023.07.015

95. MacIntosh PW. Acute changes in ganglion cell layer thickness in ischemic optic neuropathy compared to optic neuritis using optical coherence tomography. *Int J Ophthalmol*. 2020;13(1):120-123. doi:10.18240/ijo.2020.01.17

96. Lee YH, Kim KN, Heo DW, Kang TS, Lee SB, Kim C sik. Difference in patterns of retinal ganglion cell damage between primary open-angle glaucoma and non-arteritic anterior ischaemic optic neuropathy. Lewin AS, ed. *PLoS ONE*. 2017;12(10):e0187093. doi:10.1371/journal.pone.0187093

97. Saeed P, Tavakoli Rad S, Bisschop PHLT. Dysthyroid Optic Neuropathy. *Ophthalmic Plastic & Reconstructive Surgery*. 2018;34(4S):S60-S67. doi:10.1097/IOP.0000000000001146

98. Aryasit O, Tiraset N, Preechawai P, Kayasut K, Sanghan N, Sittivarakul W. IgG4-related disease in patients with idiopathic orbital inflammation. *BMC Ophthalmol*. 2021;21(1):356. doi:10.1186/s12886-021-02115-x

99. Peiris JB, Ross Russell RW. Giant aneurysms of the carotid system presenting as visual field defect. *Journal of Neurology, Neurosurgery & Psychiatry*. 1980;43(12):1053-1064. doi:10.1136/jnnp.43.12.1053

100. Imes RK. Evolution of Optociliary Veins in Optic Nerve Sheath Meningioma: Evolution. *Arch Ophthalmol*. 1985;103(1):59. doi:10.1001/archopht.1985.01050010063020

101. Loo JL, Tian J, Miller NR, Subramanian PS. Use of optical coherence tomography in predicting post-treatment visual outcome in anterior visual pathway meningiomas. *Br J Ophthalmol*. 2013;97(11):1455-1458. doi:10.1136/bjophthalmol-2013-303449

102. Chang L, El-Dairi MA, Frempong TA, et al. Optical coherence tomography in the evaluation of neurofibromatosis type-1 subjects with optic pathway gliomas. *Journal of American Association for Pediatric Ophthalmology and Strabismus*. 2010;14(6):511-517. doi:10.1016/j.jaapos.2010.08.014

103. Fard MA, Fakhree S, Eshraghi B. Correlation of optical coherence tomography parameters with clinical and radiological progression in patients with symptomatic optic pathway gliomas. *Graefes Arch Clin Exp Ophthalmol*. 2013;251(10):2429-2436. doi:10.1007/s00417-013-2394-4

104. Sayın O, Yeter V, Arıtürk N. Optic Disc, Macula, and Retinal Nerve Fiber Layer Measurements Obtained by OCT in Thyroid-Associated Ophthalmopathy. *Journal of Ophthalmology*. 2016;2016:1-7. doi:10.1155/2016/9452687

105. Al-Dahmani K, Mohammad S, Imran F, et al. Sellar Masses: An Epidemiological Study. *Can J Neurol Sci*. 2016;43(2):291-297. doi:10.1017/cjn.2015.301

106. Danesh-Meyer HV, Yap J, Frampton C, Savino PJ. Differentiation of Compressive from Glaucomatous Optic Neuropathy with Spectral-Domain Optical Coherence Tomography. *Ophthalmology*. 2014;121(8):1516-1523. doi:10.1016/j.ophtha.2014.02.020

107. Moura FC, Medeiros FA, Monteiro MLR. Evaluation of Macular Thickness Measurements for Detection of Band Atrophy of the Optic Nerve Using Optical Coherence Tomography. *Ophthalmology*. 2007;114(1):175-181. doi:10.1016/j.ophtha.2006.06.045

108. Lee EJ, Yang HK, Kim TW, Hwang JM, Kim YH, Kim CY. Comparison of the Pattern of Retinal Ganglion Cell Damage Between Patients With Compressive and Glaucomatous Optic Neuropathies. *Invest Ophthalmol Vis Sci*. 2015;56(12):7012. doi:10.1167/iovs.15-17909

109. Monteiro MLR, Hokazono K, Fernandes DB, et al. Evaluation of Inner Retinal Layers in Eyes With Temporal Hemianopic Visual Loss From Chiasmal Compression Using Optical Coherence Tomography. *Invest Ophthalmol Vis Sci*. 2014;55(5):3328. doi:10.1167/iovs.14-14118

110. Micieli JA, Newman NJ, Biousse V. The role of optical coherence tomography in the evaluation of compressive optic neuropathies. *Current Opinion in Neurology*. 2019;32(1):115-123. doi:10.1097/WCO.0000000000000636

111. Kleerekooper I, Wagner SK, Trip SA, et al. Differentiating glaucoma from chiasmal compression using optical coherence tomography: the macular naso-temporal ratio. *Br J Ophthalmol*. Published online June 28, 2023:bjo-2023-323529. doi:10.1136/bjo-2023-323529

112. Zhang X, Kedar S, Lynn MJ, Newman NJ, Biousse V. Homonymous hemianopias: Clinical-anatomic correlations in 904 cases. *Neurology*. 2006;66(6):906-910. doi:10.1212/01.wnl.0000203913.12088.93

113. Plant GT, Kermode AG, Turano G, et al. Symptomatic retrochiasmal lesions in multiple sclerosis: clinical features, visual evoked potentials, and magnetic resonance imaging. *Neurology*. 1992;42(1):68-76. doi:10.1212/wnl.42.1.68

114. Hendrickson A, Warner CE, Possin D, Huang J, Kwan WC, Bourne JA. Retrograde transneuronal degeneration in the retina and lateral geniculate nucleus of the V1-lesioned marmoset monkey. *Brain Struct Funct*. 2015;220(1):351-360. doi:10.1007/s00429-013-0659-7

115. Cowey A, Stoerig P. Blindsight in monkeys. *Nature*. 1995;373(6511):247-249. doi:10.1038/373247a0

116. Jindahra P, Petrie A, Plant GT. Retrograde trans-synaptic retinal ganglion cell loss identified by optical coherence tomography. *Brain*. 2009;132(3):628-634. doi:10.1093/brain/awp001

117. Kanamori A, Nakamura M, Yamada Y, Negi A. Spectral-domain optical coherence tomography detects optic atrophy due to optic tract syndrome. *Graefes Arch Clin Exp Ophthalmol*. 2013;251(2):591-595. doi:10.1007/s00417-012-2096-3

118. Keller J, Sánchez-Dalmau BF, Villoslada P. Lesions in the Posterior Visual Pathway Promote Trans-Synaptic Degeneration of Retinal Ganglion Cells. Aktas O, ed. *PLoS ONE*. 2014;9(5):e97444. doi:10.1371/journal.pone.0097444

119. Fraser C, Plant GT. The syndrome of pseudotumour cerebri and idiopathic intracranial hypertension. *Current Opinion in Neurology*. 2011;24(1):12-17. doi:10.1097/WCO.0b013e328341f94a

120. Cogan DG, Kuwabara T. Papilledema. *Experimental Eye Research*. 1977;25:419-433. doi:10.1016/S0014-4835(77)80039-0

121. Traber GL, Weber KP, Sabah M, Keane PA, Plant GT. Enhanced Depth Imaging Optical Coherence Tomography of Optic Nerve Head Drusen. *Ophthalmology*. 2017;124(1):66-73. doi:10.1016/j.ophtha.2016.09.022

122. Villarruel JM, Li XQ, Bach-Holm D, Hamann S. Anterior Lamina Cribrosa Surface Position in Idiopathic Intracranial Hypertension and Glaucoma. *European Journal of Ophthalmology*. 2017;27(1):55-61. doi:10.5301/ejo.5000806

123. Petzold A, Fraser CL, Abegg M, et al. Diagnosis and classification of optic neuritis. *The Lancet Neurology*. 2022;21(12):1120-1134. doi:10.1016/S1474-4422(22)00200-9

124. McDonald WI, Barnes D. The ocular manifestations of multiple sclerosis. 1. Abnormalities of the afferent visual system. *Journal of Neurology, Neurosurgery & Psychiatry*. 1992;55(9):747-752. doi:10.1136/jnnp.55.9.747

125. Coric D, Balk LJ, Uitdehaag BMJ, Petzold A. Diagnostic accuracy of optical coherence tomography inter-eye percentage difference for optic neuritis in multiple sclerosis. *Eur J Neurol*. 2017;24(12):1479-1484. doi:10.1111/ene.13443

126. Petzold A, Chua SYL, Khawaja AP, et al. Retinal asymmetry in multiple sclerosis. *Brain*. 2021;144(1):224-235. doi:10.1093/brain/awaa361

127. Kupersmith MJ, Nelson JI, Seiple WH, Carr RE, Weiss PA. The 20/20 eye in multiple sclerosis. *Neurology*. 1983;33(8):1015-1015. doi:10.1212/WNL.33.8.1015

128. Brusa A, Jones SJ, Plant GT. Long-term remyelination after optic neuritis. *Brain*. 2001;124(3):468-479. doi:10.1093/brain/124.3.468

129. Werring DJ. Recovery from optic neuritis is associated with a change in the distribution of cerebral response to visual stimulation: a functional magnetic resonance imaging study. *Journal of Neurology, Neurosurgery & Psychiatry*. 2000;68(4):441-449. doi:10.1136/jnnp.68.4.441

130. Sherif M, Bergin C, Borruat FX. Normal Visual Recovery after Optic Neuritis Despite Significant Loss of Retinal Ganglion Cells in Patients with Multiple Sclerosis. *Klin Monatsbl Augenheilkd*. 2019;236(04):425-428. doi:10.1055/a-0853-1721

131. Park KA, Kim J, Oh SY. Analysis of spectral domain optical coherence tomography measurements in optic neuritis: differences in neuromyelitis optica, multiple sclerosis, isolated optic neuritis and normal healthy controls. *Acta Ophthalmologica*. 2014;92(1):e57-e65. doi:10.1111/aos.12215

132. Schneider E, Zimmermann H, Oberwahrenbrock T, et al. Optical Coherence Tomography Reveals Distinct Patterns of Retinal Damage in Neuromyelitis Optica and Multiple Sclerosis. Linker RA, ed. *PLoS ONE*. 2013;8(6):e66151. doi:10.1371/journal.pone.0066151

133. Kerrison J. Optic neuropathies caused by toxins and adverse drug reactions. *Ophthalmology Clinics of North America*. 2004;17(3):481-488. doi:10.1016/j.ohc.2004.05.005

134. Plant GT, Mtanda AT, Arden GB, Johnson GJ. An epidemic of optic neuropathy in Tanzania: Characterization of the visual disorder and associated peripheral neuropathy. *Journal of the Neurological Sciences*. 1997;145(2):127-140. doi:10.1016/S0022-510X(96)00162-1

135. Thomas PK, Plant GT, Baxter P, Bates C, Santiago Luis R. An epidemic of optic neuropathy and painful sensory neuropathy in Cuba: Clinical aspects. *J Neurol*. 1995;242(10):629-638. doi:10.1007/BF00866912

136. Korkiamäki P, Kervinen M, Karjalainen K, Majamaa K, Uusimaa J, Remes AM. Prevalence of the primary LHON mutations in Northern Finland associated with bilateral optic atrophy and tobacco-alcohol amblyopia. *Acta Ophthalmol*. 2013;91(7):630-634. doi:10.1111/j.1755-3768.2012.02506.x

137. Plant GT, Perry VH. The anatomical basis of the caecocentral scotoma: new observations and a review. *Brain*. 1990;113(5):1441-1457. doi:10.1093/brain/113.5.1441

138. Clayton LM, Devile M, Punte T, et al. Patterns of Peripapillary Retinal Nerve Fiber Layer Thinning in Vigabatrin-Exposed Individuals. *Ophthalmology*. 2012;119(10):2152-2160. doi:10.1016/j.ophtha.2012.05.009

139. Moura F, Monteiro M. Evaluation of retinal nerve fiber layer thickness measurements using optical coherence tomography in patients with tobacco-alcohol-induced toxic optic neuropathy. *Indian J Ophthalmol*. 2010;58(2):143. doi:10.4103/0301-4738.60087

140. Barboni P, Carbonelli M, Savini G, et al. Natural History of Leber's Hereditary Optic Neuropathy: Longitudinal Analysis of the Retinal Nerve Fiber Layer by Optical Coherence Tomography. *Ophthalmology*. 2010;117(3):623-627. doi:10.1016/j.ophtha.2009.07.026

141. Wang MY, Sadun AA. Drug-Related Mitochondrial Optic Neuropathies. *Journal of Neuro-Ophthalmology*. 2013;33(2):172-178. doi:10.1097/WNO.0b013e3182901969

142. Vieira LMC, Silva NFA, Dias Dos Santos AM, et al. Retinal Ganglion Cell Layer Analysis by Optical Coherence Tomography in Toxic and Nutritional Optic Neuropathy. *Journal of Neuro-Ophthalmology*. 2015;35(3):242-245. doi:10.1097/WNO.0000000000000229

143. Han J, Byun MK, Lee J, Han SY, Lee JB, Han SH. Longitudinal analysis of retinal nerve fiber layer and ganglion cell–inner plexiform layer thickness in ethambutol-induced optic neuropathy. *Graefes Arch Clin Exp Ophthalmol*. 2015;253(12):2293-2299. doi:10.1007/s00417-015-3150-8

144. Delettre C, Lenaers G, Pelloquin L, Belenguer P, Hamel CP. OPA1 (Kjer Type) Dominant Optic Atrophy: A Novel Mitochondrial Disease. *Molecular Genetics and Metabolism*. 2002;75(2):97-107. doi:10.1006/mgme.2001.3278

145. Delettre C, Lenaers G, Griffoin JM, et al. Nuclear gene OPA1, encoding a mitochondrial dynamin-related protein, is mutated in dominant optic atrophy. *Nat Genet*. 2000;26(2):207-210. doi:10.1038/79936

146. Alexander C, Votruba M, Pesch UEA, et al. OPA1, encoding a dynamin-related GTPase, is mutated in autosomal dominant optic atrophy linked to chromosome 3q28. *Nat Genet*. 2000;26(2):211-215. doi:10.1038/79944

147. Wallace DC, Singh G, Lott MT, et al. Mitochondrial DNA Mutation Associated with Leber's Hereditary Optic Neuropathy. *Science*. 1988;242(4884):1427-1430. doi:10.1126/science.3201231

148. Spruijt L, Kolbach DN, De Coo RF, et al. Influence of Mutation Type on Clinical Expression of Leber Hereditary Optic Neuropathy. *American Journal of Ophthalmology*. 2006;141(4):676-676.e8. doi:10.1016/j.ajo.2005.11.007

149. Asanad S, Tian JJ, Frousiakis S, et al. Optical Coherence Tomography of the Retinal Ganglion Cell Complex in Leber's Hereditary Optic Neuropathy and Dominant Optic Atrophy. *Current Eye Research*. 2019;44(6):638-644. doi:10.1080/02713683.2019.1567792

150. Savini G, Barboni P, Valentino M, et al. Retinal nerve fiber layer evaluation by optical coherence tomography in unaffected carriers with Leber's hereditary optic neuropathy mutations. *Ophthalmology*. 2005;112(1):127-131. doi:10.1016/j.ophtha.2004.09.033

151. Hedges TR, Gobuty M, Manfready RA, Erlich-Malona N, Monaco C, Mendoza-Santiesteban CE. The Optical Coherence Tomographic Profile of Leber Hereditary Optic Neuropathy. *Neuro-Ophthalmology*. 2016;40(3):107-112. doi:10.3109/01658107.2016.1173709

152. Yu-Wai-Man P, Bailie M, Atawan A, Chinnery PF, Griffiths PG. Pattern of retinal ganglion cell loss in dominant optic atrophy due to OPA1 mutations. *Eye*. 2011;25(5):596-602. doi:10.1038/eye.2011.2

153. Barboni P, Savini G, Cascavilla ML, et al. Early Macular Retinal Ganglion Cell Loss in Dominant Optic Atrophy: Genotype-Phenotype Correlation. *American Journal of Ophthalmology*. 2014;158(3):628-636.e3. doi:10.1016/j.ajo.2014.05.034

154. Boghen DR, Glaser JS. Ischaemic optic neuropathy: the clinical profile and natural history. *Brain*. 1975;98(4):689-708. doi:10.1093/brain/98.4.689

155. Hayreh SS, Podhajsky PA, Zimmerman B. Nonarteritic Anterior Ischemic Optic Neuropathy: Time of Onset of Visual Loss. *American Journal of Ophthalmology*. 1997;124(5):641-647. doi:10.1016/S0002-9394(14)70902-X

156. Buono LM, Foroozan R, Sergott RC, Savino PJ. Nonarteritic anterior ischemic optic neuropathy. *Curr Opin Ophthalmol*. 2002;13(6):357-361. doi:10.1097/00055735-200212000-00003

157. Hedges TR. Subretinal Fluid From Anterior Ischemic Optic Neuropathy Demonstrated by Optical Coherence Tomography. *Arch Ophthalmol*. 2008;126(6):812. doi:10.1001/archopht.126.6.812

158. Hayreh SS. Treatment of non-arteritic anterior ischemic optic neuropathy with high-dose systemic corticosteroid therapy. *Graefes Arch Clin Exp Ophthalmol*. 2013;251(3):1029-1030. doi:10.1007/s00417-012-2062-0

159. Rebolleda G, Pérez-López M, Casas-LLera P, Contreras I, Muñoz-Negrete FJ. Visual and anatomical outcomes of non-arteritic anterior ischemic optic neuropathy with high-dose systemic corticosteroids. *Graefes Arch Clin Exp Ophthalmol*. 2013;251(1):255-260. doi:10.1007/s00417-012-1995-7

160. Demirel S, Batıoğlu F, Oguz YG, Özmert E. Macular Involvement and Response to Steroid Therapy Demonstrated by Optical Coherence Tomography in Non-arteritic Anterior Ischaemic Optic Neuropathy. *Neuro-Ophthalmology*. 2013;37(4):161-164. doi:10.3109/01658107.2013.809365

161. Takayama K, Kaneko H, Kachi S, Ra E, Ito Y, Terasaki H. High-dose intravenous pulse steroid therapy for optic disc swelling and subretinal fluid in non-arteritic anterior ischemic optic neuropathy. Published online February 2017. doi:10.18999/nagjms.79.1.103

162. Gelfand JM, Nolan R, Schwartz DM, Graves J, Green AJ. Microcystic macular oedema in multiple sclerosis is associated with disease severity. *Brain*. 2012;135(Pt 6):1786-1793. doi:10.1093/brain/aws098

163. Abegg M, Dysli M, Wolf S, Kowal J, Dufour P, Zinkernagel M. Microcystic macular edema: retrograde maculopathy caused by optic neuropathy. *Ophthalmology*. 2014;121(1):142-149. doi:10.1016/j.ophtha.2013.08.045

164. 15th EUNOS Congress. *Neuro-Ophthalmology*. 2022;46(sup1):50. doi:10.1080/01658107.2022.2064188

165. Chapelle AC, Rakic JM, Plant, Gordon. Non-arteritic anterior ischemic optic neuropathy: cystic change in the inner nuclear layer due to edema and to retrograde maculopathy. *Ophthalmology Science*. 2022.

166. Kim DH, Shin GR, Choi YJ. Risk Factors for Non-arteritic Anterior Ischaemic Optic Neuropathy in a Korean Population. *Neuro-Ophthalmology*. 2017;41(2):68-75. doi:10.1080/01658107.2016.1267771

167. Jacobson DM. Nonarteritic Anterior Ischemic Optic Neuropathy: A Case-Control Study of Potential Risk Factors. *Arch Ophthalmol*. 1997;115(11):1403. doi:10.1001/archopht.1997.01100160573008

168. Salomon O. Analysis of prothrombotic and vascular risk factors in patients with nonarteritic anterior ischemic optic neuropathy. *Ophthalmology*. 1999;106(4):739-742. doi:10.1016/S0161-6420(99)90159-8

169. Hayreh S, Podhajsky P, Zimmerman MB. Role of Nocturnal Arterial Hypotension in Optic Nerve Head Ischemic Disorders. *Ophthalmologica*. 1999;213(2):76-96. doi:10.1159/000027399

170. Hayreh SS. Role of nocturnal arterial hypotension in the development of ocular manifestations of systemic arterial hypertension: *Current Opinion in Opthalmology*. 1999;10(6):474-482. doi:10.1097/00055735-199912000-00017

171. Landau K. 24-Hour Blood Pressure Monitoring in Patients With Anterior Ischemic Optic Neuropathy. *Arch Ophthalmol*. 1996;114(5):570. doi:10.1001/archopht.1996.01100130562012

172. Hayreh SS. Ischemic optic neuropathy. *Progress in Retinal and Eye Research*. 2009;28(1):34-62. doi:10.1016/j.preteyeres.2008.11.002

173. Marmor MF. Mechanisms of fluid accumulation in retinal edema. *Documenta Ophthalmologica*. 1999;97(3/4):239-249. doi:10.1023/A:1002192829817

174. Hoye VJ. Optical Coherence Tomography Demonstrates Subretinal Macular Edema From Papilledema. *Arch Ophthalmol*. 2001;119(9):1287. doi:10.1001/archopht.119.9.1287

175. Schirmer CM, Hedges TR. Mechanisms of visual loss in papilledema. *FOC*. 2007;23(5):E5. doi:10.3171/FOC-07/11/E5

176. Ozdemir H, Karacorlu M, Karacorlu S. SEROUS MACULAR DETACHMENT IN CENTRAL RETINAL VEIN OCCLUSION: *Retina*. 2005;25(5):561-563. doi:10.1097/00006982-200507000-00003

177. Pizzimenti JJ, Daniel KP. Central Serous Chorioretinopathy After Epidural Steroid Injection. *Pharmacotherapy*. 2005;25(8):1141-1146. doi:10.1592/phco.2005.25.8.1141

178. Dinc UA, Yenerel M, Tatlipinar S, Gorgun E, Alimgil L. Correlation of Retinal Sensitivity and Retinal Thickness in Central Serous Chorioretinopathy. *Ophthalmologica*. 2010;224(1):2-9. doi:10.1159/000233229

179. Hayreh SS, Zimmerman MB. Non-arteritic anterior ischemic optic neuropathy: role of systemic corticosteroid therapy. *Graefes Arch Clin Exp Ophthalmol*. 2008;246(7):1029-1046. doi:10.1007/s00417-008-0805-8

180. Kang Li, Xiaodong Wu, Chen DZ, Sonka M. Optimal Surface Segmentation in Volumetric Images-A Graph-Theoretic Approach. *IEEE Trans Pattern Anal Mach Intell*. 2006;28(1):119-134. doi:10.1109/TPAMI.2006.19

181. Ghazi NG, Green WR. Pathology and pathogenesis of retinal detachment. *Eye*. 2002;16(4):411-421. doi:10.1038/sj.eye.6700197

182. Amer R, Nalcı H, Yalçındağ N. Exudative retinal detachment. *Survey of Ophthalmology*. 2017;62(6):723-769. doi:10.1016/j.survophthal.2017.05.001

183. Messner A, Werkmeister RM, Seidel G, Stegmann H, Schmetterer L, Aranha dos Santos V. Light-induced changes of the subretinal space of the temporal retina observed via optical coherence tomography. *Sci Rep*. 2019;9(1):13632. doi:10.1038/s41598-019-50057-8

184. Ishikawa M, Sawada Y, Yoshitomi T. Structure and function of the interphotoreceptor matrix surrounding retinal photoreceptor cells. *Experimental Eye Research*. 2015;133:3-18. doi:10.1016/j.exer.2015.02.017

185. Reese AB. Peri-Papillary Detachment of the Retina Accompanying Papilledema. *Trans Am Ophthalmol Soc*. 1930;28:341-351.

186. Light RW. Pleural Effusions: The Diagnostic Separation of Transudates and Exudates. *Ann Intern Med*. 1972;77(4):507. doi:10.7326/0003-4819-77-4-507

187. Agostoni A, Marasini B. Orosomucoid Contents of Pleural and Peritoneal Effusions of Various Etiologies. *Am J Clin Pathol*. 1977;67(2):146-148. doi:10.1093/ajcp/67.2.146

188. Carr DT, Power MH. Clinical Value of Measurements of Concentration of Protein in Pleural Fluid. *N Engl J Med*. 1958;259(19):926-927. doi:10.1056/NEJM195811062591909

189. Hamm H, Brohan U, Bohmer R, Missmahl HP. Cholesterol in Pleural Effusions. *Chest*. 1987;92(2):296-302. doi:10.1378/chest.92.2.296

190. El-Dairi M. Neuroretinitis. In: *Handbook of Pediatric Retinal OCT and the Eye-Brain Connection*. Elsevier; 2020:308-309. doi:10.1016/B978-0-323-60984-5.00068-8

191. Morris AT, Sanders MD. Macular changes resulting from papilloedema. *British Journal of Ophthalmology*. 1980;64(3):211-216. doi:10.1136/bjo.64.3.211

192. Moura FC, Sato DK, Rimkus CM, et al. Anti-MOG (Myelin Oligodendrocyte Glycoprotein)–Positive Severe Optic Neuritis with Optic Disc Ischaemia and Macular Star. *Neuro-Ophthalmology*. 2015;39(6):285-288. doi:10.3109/01658107.2015.1084332

193. Otani T, Kishi S. Tomographic findings of foveal hard exudates in diabetic macular edema. *American Journal of Ophthalmology*. 2001;131(1):50-54. doi:10.1016/S0002-9394(00)00661-9

194. Kitamei H, Kitaichi N, Namba K, et al. Clinical features of intraocular inflammation in Hokkaido, Japan. *Acta Ophthalmologica*. 2009;87(4):424-428. doi:10.1111/j.1755-3768.2008.01282.x

195. McCulley TJ, Lam BL, Feuer WJ. Nonarteritic anterior ischemic optic neuropathy and surgery of the anterior segment: temporal relationship analysis. *American Journal of Ophthalmology*. 2003;136(6):1171-1172. doi:10.1016/S0002-9394(03)00676-7

196. Jacks AS. Spontaneous retinal venous pulsation: aetiology and significance. *Journal of Neurology, Neurosurgery & Psychiatry*. 2003;74(1):7-9. doi:10.1136/jnnp.74.1.7

197. Levine DN. Spontaneous Pulsation of the Retinal Veins. *Microvascular Research*. 1998;56(3):154-165. doi:10.1006/mvre.1998.2098

198. D'Antona L, McHugh JA, Ricciardi F, et al. Association of Intracranial Pressure and Spontaneous Retinal Venous Pulsation. *JAMA Neurol*. 2019;76(12):1502. doi:10.1001/jamaneurol.2019.2935

199. Tawse KL, Hedges TR, Gobuty M, Mendoza-Santiesteban C. Optical coherence tomography shows retinal abnormalities associated with optic nerve disease. *Br J Ophthalmol*. 2014;98(Suppl 2):ii30-ii33. doi:10.1136/bjophthalmol-2013-304301

200. Hirami Y, Tsujikawa A, Sasahara M, et al. Alterations of retinal pigment epithelium in central serous chorioretinopathy. *Clin Exp Ophthalmol*. 2007;35(3):225-230. doi:10.1111/j.1442-9071.2006.01447.x

201. Denniston AK, Keane PA, Aojula A, Sinclair AJ, Mollan SP. The Ocular Glymphatic System and Idiopathic Intracranial Hypertension: Author Response to "Hypodense Holes and the Ocular Glymphatic System." *Invest Ophthalmol Vis Sci*. 2017;58(2):1134-1136. doi:10.1167/iovs.17-21479

202. Wostyn P, De Groot V, Van Dam D, Audenaert K, De Deyn PP, Killer HE. The Glymphatic System: A New Player in Ocular Diseases? *Investigative Ophthalmology & Visual Science*. 2016;57(13):5426-5427. doi:10.1167/iovs.16-20262

203. Petzold A. Retinal glymphatic system: an explanation for transient retinal layer volume changes? *Brain*. 2016;139(11):2816-2819. doi:10.1093/brain/aww239

204. Balk LJ, Killestein J, Polman CH, Uitdehaag BMJ, Petzold A. Microcystic macular oedema confirmed, but not specific for multiple sclerosis. *Brain*. 2012;135(Pt 12):e226; author reply e227. doi:10.1093/brain/aws216

205. Masri RA, Weltzien F, Purushothuman S, Lee SCS, Martin PR, Grünert U. Composition of the Inner Nuclear Layer in Human Retina. *Invest Ophthalmol Vis Sci*. 2021;62(9):22. doi:10.1167/iovs.62.9.22

206. Green AJ, McQuaid S, Hauser SL, Allen IV, Lyness R. Ocular pathology in multiple sclerosis: retinal atrophy and inflammation irrespective of disease duration. *Brain*. 2010;133(Pt 6):1591-1601. doi:10.1093/brain/awq080

207. Dysli M, Rückert R, Munk MR. Differentiation of Underlying Pathologies of Macular Edema Using Spectral Domain Optical Coherence Tomography (SD-OCT). *Ocul Immunol Inflamm*. 2019;27(3):474-483. doi:10.1080/09273948.2019.1603313

208. Kaufhold F, Zimmermann H, Schneider E, et al. Optic neuritis is associated with inner nuclear layer thickening and microcystic macular edema independently of multiple sclerosis. *PLoS One*. 2013;8(8):e71145. doi:10.1371/journal.pone.0071145

209. Gelfand JM, Cree BA, Nolan R, Arnow S, Green AJ. Microcystic inner nuclear layer abnormalities and neuromyelitis optica. *JAMA Neurol*. 2013;70(5):629-633. doi:10.1001/jamaneurol.2013.1832

210. Sotirchos ES, Saidha S, Byraiah G, et al. In vivo identification of morphologic retinal abnormalities in neuromyelitis optica. *Neurology*. 2013;80(15):1406-1414. doi:10.1212/WNL.0b013e31828c2f7a

211. Barboni P, Carelli V, Savini G, Carbonelli M, La Morgia C, Sadun AA. Microcystic macular degeneration from optic neuropathy: not inflammatory, not trans-synaptic degeneration. *Brain*. 2013;136(Pt 7):e239. doi:10.1093/brain/awt014

212. Lujan BJ, Horton JC. Microcysts in the inner nuclear layer from optic atrophy are caused by retrograde trans-synaptic degeneration combined with vitreous traction on the retinal surface. *Brain*. 2013;136(Pt 11):e260. doi:10.1093/brain/awt154

213. Kisimbi J, Shalchi Z, Mahroo OA, et al. Macular spectral domain optical coherence tomography findings in Tanzanian endemic optic neuropathy. *Brain*. 2013;136(Pt 11):3418-3426. doi:10.1093/brain/awt221

214. Haldar S, Mukherjee R, Elston J. Microcystic macular edema in a case of tobacco-alcohol optic neuropathy. *Can J Ophthalmol*. 2017;52(1):e19-e22. doi:10.1016/j.jcjo.2016.07.014

215. Murata N, Togano T, Miyamoto D, Ochiai S, Fukuchi T. Clinical evaluation of microcystic macular edema in patients with glaucoma. *Eye (Lond)*. 2016;30(11):1502-1508. doi:10.1038/eye.2016.190

216. Brazerol J, Iliev ME, Höhn R, Fränkl S, Grabe H, Abegg M. Retrograde Maculopathy in Patients With Glaucoma. *J Glaucoma*. 2017;26(5):423-429. doi:10.1097/IJG.0000000000000633

217. Abegg M, Zinkernagel M, Wolf S. Microcystic macular degeneration from optic neuropathy. *Brain*. 2012;135(Pt 12):e225. doi:10.1093/brain/aws215

218. Bhatti MT, Mansukhani SA, Chen JJ. Microcystic Macular Edema in Optic Nerve Glioma. *Ophthalmology*. 2020;127(7):930. doi:10.1016/j.ophtha.2020.03.017

219. Mahroo OA, Shalchi Z, Williamson TH, Plant GT. Re: Bhatti et al.: Microcystic macular edema in optic nerve glioma (Ophthalmology. 2020;127:930). *Ophthalmology*. 2021;128(1):e9. doi:10.1016/j.ophtha.2020.07.053

220. Lee DH, Park SE, Lee CS. Microcystic macular edema and cystoid macular edema before and after epiretinal membrane surgery. *Retina*. 2021;41(8):1652-1659. doi:10.1097/IAE.0000000000003087

221. Burggraaff MC, Trieu J, de Vries-Knoppert WAEJ, Balk L, Petzold A. The clinical spectrum of microcystic macular edema. *Invest Ophthalmol Vis Sci*. 2014;55(2):952-961. doi:10.1167/iovs.13-12912

222. Munteanu G, Sărăcăceanu L. [Idiopathic microcystic macular edema]. *Rev Chir Oncol Radiol O R L Oftalmol Stomatol Ser Oftalmol*. 1988;32(2):131-135.

223. Van Buren JM. Trans-synaptic retrograde degeneration in the visual system of primates. *Journal of Neurology, Neurosurgery & Psychiatry*. 1963;26(5):402-409. doi:10.1136/jnnp.26.5.402

224. Gills JP, Wadsworth JA. Degeneration of the inner nuclear layer of the retina following lesions of the optic nerve. *Trans Am Ophthalmol Soc*. 1966;64:66-88.

225. Bringmann A, Reichenbach A, Wiedemann P. Pathomechanisms of Cystoid Macular Edema. *Ophthalmic Res*. 2004;36(5):241-249. doi:10.1159/000081203

226. Bringmann A, Pannicke T, Grosche J, et al. Müller cells in the healthy and diseased retina. *Prog Retin Eye Res*. 2006;25(4):397-424. doi:10.1016/j.preteyeres.2006.05.003

227. Matet A, Savastano MC, Rispoli M, et al. En face optical coherence tomography of foveal microstructure in full-thickness macular hole: a model to study perifoveal Müller cells. *Am J Ophthalmol*. 2015;159(6):1142-1151.e3. doi:10.1016/j.ajo.2015.02.013

228. Monteiro MLR, Sousa RM, Araújo RB, et al. Diagnostic ability of confocal near-infrared reflectance fundus imaging to detect retrograde microcystic maculopathy from chiasm compression. A comparative study with OCT findings. *PLoS One*. 2021;16(6):e0253323. doi:10.1371/journal.pone.0253323

229. Foster R, Crum O, Lesser E, Hodge DO, Bhatti M, Chen J. Reexamining the incidence of nonarteritic anterior ischemic optic neuropathy. *Invest Ophthalmol Vis Sci*. 2019;60(9):2268-2268.

230. Gaudric A, Audo I, Vignal C, et al. Non-vasogenic cystoid maculopathies. *Progress in Retinal and Eye Research*. 2022;91:101092. doi:10.1016/j.preteyeres.2022.101092

231. Gass JD, Norton EW. Cystoid macular edema and papilledema following cataract extraction. A fluorescein fundoscopic and angiographic study. *Arch Ophthalmol*. 1966;76(5):646-661. doi:10.1001/archopht.1966.03850010648005

232. Hayreh SS, Podhajsky PA, Zimmerman MB. Branch Retinal Artery Occlusion. *Ophthalmology*. 2009;116(6):1188-1194.e4. doi:10.1016/j.ophtha.2009.01.015

233. Hayreh SS. Blood flow in the optic nerve head and factors that may influence it. *Prog Retin Eye Res*. 2001;20(5):595-624. doi:10.1016/s1350-9462(01)00005-2

234. Werne A, Harris A, Moore D, BenZion I, Siesky B. The circadian variations in systemic blood pressure, ocular perfusion pressure, and ocular blood flow: risk factors for glaucoma? *Surv Ophthalmol*. 2008;53(6):559-567. doi:10.1016/j.survophthal.2008.08.021

235. Harris A, Werne A, Cantor LB. Vascular abnormalities in glaucoma: from population-based studies to the clinic? *Am J Ophthalmol*. 2008;145(4):595-597. doi:10.1016/j.ajo.2007.12.019

236. London A, Benhar I, Schwartz M. The retina as a window to the brain—from eye research to CNS disorders. *Nat Rev Neurol*. 2013;9(1):44-53. doi:10.1038/nrneurol.2012.227

237. Sung MS, Choi SM, Kim J, et al. Inner retinal thinning as a biomarker for cognitive impairment in de novo Parkinson's disease. *Sci Rep*. 2019;9(1):11832. doi:10.1038/s41598-019-48388-7

238. Kesler A, Vakhapova V, Korczyn AD, Naftaliev E, Neudorfer M. Retinal thickness in patients with mild cognitive impairment and Alzheimer's disease. *Clin Neurol Neurosurg*. 2011;113(7):523-526. doi:10.1016/j.clineuro.2011.02.014

239. Hinton DR, Sadun AA, Blanks JC, Miller CA. Optic-nerve degeneration in Alzheimer's disease. *N Engl J Med*. 1986;315(8):485-487. doi:10.1056/NEJM198608213150804

240. Kleerekooper I, Traber GL, Dell'Arti L, et al. Early Visual Failure in Multiple Sclerosis due to a Primary Progressive Bilateral Optic Neuropathy.

241. Aspberg J, Heijl A, Bengtsson B. Screening for Open-Angle Glaucoma and Its Effect on Blindness. *American Journal of Ophthalmology*. 2021;228:106-116. doi:10.1016/j.ajo.2021.03.030

242. Kapoor R, Whigham BT, Al-Aswad LA. Artificial Intelligence and Optical Coherence Tomography Imaging. *The Asia-Pacific Journal of Ophthalmology*. 2019;8(2):187. doi:10.22608/APO.201904

243. Li Z, Wang L, Wu X, et al. Artificial intelligence in ophthalmology: The path to the real-world clinic. *Cell Rep Med*. 2023;4(7):101095. doi:10.1016/j.xcrm.2023.101095

244. Vasseneix C, Nusinovici S, Xu X, et al. Deep Learning System Outperforms Clinicians in Identifying Optic Disc Abnormalities. *Journal of Neuro-Ophthalmology*. 2023;43(2):159-167. doi:10.1097/WNO.0000000000001800

245. Cheung CY, Ran AR, Wang S, et al. A deep learning model for detection of Alzheimer's disease based on retinal photographs: a retrospective, multicentre case-control study. *The Lancet Digital Health*. 2022;4(11):e806-e815. doi:10.1016/S2589-7500(22)00169-8

246. Poplin R, Varadarajan AV, Blumer K, et al. Prediction of cardiovascular risk factors from retinal fundus photographs via deep learning. *Nat Biomed Eng*. 2018;2(3):158-164. doi:10.1038/s41551-018-0195-0

247. Wang J, Gao Y, Wang F, et al. Accurate estimation of biological age and its application in disease prediction using a multimodal image Transformer system. *Proc Natl Acad Sci U S A*. 2024;121(3):e2308812120. doi:10.1073/pnas.2308812120

11. ANNEXES

Chapelle AC, Rakic JM, Plant GT. Utility of ganglion cells for the evaluation of anterior visual pathway pathology: a review. Acta Neurol Belg. 2024.

REVIEW ARTICLE

Utility of ganglion cells for the evaluation of anterior visual pathway pathology: a review

Anne-Catherine Chapelle[1] · Jean-Marie Rakic[1] · Gordon Terence Plant[2]

Received: 29 November 2023 / Accepted: 1 March 2024 / Published online: 27 March 2024

Abstract
The management of optic neuropathy is fundamental to neuro-ophthalmic practice. Following the invention of the ophthalmoscope, clinicians, for a century or more, relied upon fundus examination in the evaluation of optic neuropathy. However, the advent of optical coherence tomography, based on the principle of backscattering of light and interferometry, has revolutionized the analysis of optic nerve and retinal disorders. Optical coherence tomography has proven of particular value in the measurement, at the micron level, of the peripapillary retinal nerve fibre layer and the ganglion cell layer. These measurements have proven critical in the differential diagnosis and monitoring of optic neuropathy. Specifically, thinning of the peripapillary nerve fibre layer provides evidence of axonal loss affecting any sector of the optic nerve. Thinning of the macular ganglion cell layer, on the other hand, shows a more precise correlation with visual deficits due to retrograde degeneration following optic nerve damage, although limited to central retina. In daily practise, optical coherence tomography is of great value in assessing the diagnosis, prognosis and response to treatment in optic neuropathy. Particular advances have been made, for example, in the assessment of optic neuritis, papilloedema and chiasmal compression which have translated to everyday practice. As with any other imaging technology the clinician must have a clear understanding of acquisition artefacts. A further issue is the relatively limited normative database in sub-populations such as the young and individuals with a refractive error > +5 or < −5 dioptres.

Keywords Optical coherence tomography · Neuro-ophthalmology · Ganglion cells layer · Retinal nerve fibres layer · Optical neuropathy

Abbreviations

AION	Anterior ischemic optic neuropathy
CON	Compressive optic neuropath
GCC	Ganglion cell complex (inner plexiform layer (IPL) + ganglion cell layer (GCL)
ICP	Intracranial pressure
IHH	Idiopathic intracranial hypertension
INL	Inner nuclear layer
IOP	Intraocular pressure
MMO	Microcystic macular oedema
NAAION	Non-Arteritic anterior ischaemic optic neuropathy
OCT	Optical coherence tomography
OD	Optic disc
pRNFL	Peripapillary retinal nerve fibre layer
RGC	Retinal ganglion cell
VF	Automated perimetry

Anne Catherine Chapelle and Gordon T. Plant contributed equally to this work.

✉ Anne-Catherine Chapelle
ac.chapelle@chuliege.be

[1] Department of Ophthalmology, Central University Hospital of Liège, University of Liège, Avenue de L'hôpital, 4000 Liège, Belgium

[2] Department of Neurodegeneration and Rehabilitation, Faculty of Brain Sciences, UCL Institute of Neurology, University College London, London WC1N 3BG, UK

Introduction

Optic neuropathies are a major portion of the work-load of neuro-ophthalmologists. Many are one component of a more extensive neurological disorder. For decades, neuro-ophthalmologists have utilised fundus examination (ophthalmoscopy) in the assessment of optic nerve structure. Optical coherence tomography (OCT), however, has revolutionised the analysis of both optic nerve and retinal disorders. OCT is based on the principle of backscattering

and interferometry [1]. A beam of light is projected to the retina and the locations of boundaries between the retinal layers are obtained from the time to the sensor of the reflected light. Thickness measurements of the retinal layers at the micron level are available.

The RNFL is measured where it is thickest in the peripapillary region (pRNFL). The retinal ganglion cells (RGC) layer (GCL) is thickest at the macula (up to 10 cells thickness), and progressively thinner towards the periphery (down to a single cell) [2]. In practice the GCL is most commonly measured at the macula together with the inner plexiform layer (IPL) designated the ganglion cell complex (GCC). RCGs are the final receivers and transmitters of the initial retinal signal. Their axons follow the inner surface of the retina and enter the optic disc to form the optic nerve.

The majority of RGCs project to the lateral geniculate nucleus (LGN) and are classified according to the LGN layer in which they terminate: P-type ganglion cells in the parvocellular layers (layers 3–6) and M-type in the magnocellular layers (layers 1–2) [3]. The P cells, accounting for 90% of the GCL, are subdivided into P1 cells, which receive input from two bipolar cell axons and in P2 cells which have a denser dendritic tree [4]. The population of P cells is greater than that of the M cells in the macula whereas in the periphery P and M cells are equal in density [5]. While M cells subserve information concerning depth perception, motion and are sensitive to lower contrasts, P cells process information related to colour vision, texture, and higher contrast. Other RGCs (a more heterogeneous population than P and M cells) project to the koniocellular (interlaminar) regions of the LGN. In many cases the function of this group is unknown. Some are involved in colour vision and others in ocular motor control.

All optic neuropathies may affect acutely or chronically the retinal nerve fibre layer (RNFL) and thus the RGC, by direct retrograde degeneration, i.e. axonal damage leading to loss of the proximal axon and cell body. Thinning of the GCC has been found to be strongly related to visual loss in optic neuropathy related to glaucoma, optic neuritis, papilloedema, intrinsic and extrinsic optic nerve tumours, ischaemic, hereditary and toxic optic neuropathy [6]. However, as with any other imaging technology, the clinician must have a clear understanding of acquisition artefacts affecting the estimation of the GCC or RNFL thickness. The relatively small normative database in sub-populations such as the young and individuals with a refractive error $> +5$ or < -5 dioptres influence the interpretation of the analysis is also an issue.

We will review the literature of OCT findings in miscellaneous pathologies affecting the optic nerve to illustrate the value of the findings in clinical practice.

Non-arteritic anterior ischaemic optic neuropathy (NAAION)

NAAION is a common optic neuropathy affecting people over 50 years old; second only to glaucoma. The diagnosis of NAAION is supported by the anamnesis (painless sudden loss of vision involving one eye) and fundus examination (a swollen disc is observed in the affected eye at presentation).

This entity is related to a failure of arterial supply by the posterior ciliary arteries, supplying the optic nerve head. A major anatomic risk factor involved in this pathology is a crowded optic disc (absence of a cup) [7]. Emphasis in the past has been on the need to exclude an arteritic cause, hence the commonly employed negative epithet and initialism "Non-Arteritic" AION.

Classical NAAION leads to sectoral infarction of the optic disc (OD) resulting in loss of optic nerve fibres and retinal ganglion cells (RGC) corresponding to the infarcted OD sector. A corresponding dense and persisting defect of the visual field results (Fig. 1). At presentation, OCT shows an increase in pRNFL thickness followed by a progressive atrophy over a few months [8] (Fig. 2). In the acute phase, a slight increase of GCL thickening may be seen due to distortion caused by peripapillary swelling and in some cases by intra- and sub-retinal fluid [9, 10]. Asymmetric thinning between the superior and inferior hemi-macula is observed, resulting in an altitudinal pattern [11]. In contrast to glaucomatous optic neuropathy, an involvement of the superior, superotemporal, inferotemporal and inferonasal quadrants of the ganglion cells are most commonly affected in NAAION [12].

Compressive lesions of the anterior visual pathway

Compressive optic neuropathies (CON) are characterised by painless progressive loss of vision and late presentation is common. Furthermore, clinical diagnosis can be challenging, leading to further delays in treatment. Fundus examination can be normal. The optic disc may be swollen and retino-choroidal collateral vessels may be seen if there compressive lesion gives rise to venous hypertension (e.g. optic nerve sheath meningioma immediately retrobulbar) mimicking chronic papilloedema. Atrophy if present may mimic glaucoma. Compression of the visual pathway leads to loss of vision by three different mechanisms: a reversible neuronal block due to compression; and neuronal loss due to direct compression or an ischaemic mechanism. The neuronal block is reversible immediately after surgery whereas axonal loss is not. Localisation of the site of compression and identification of the causative

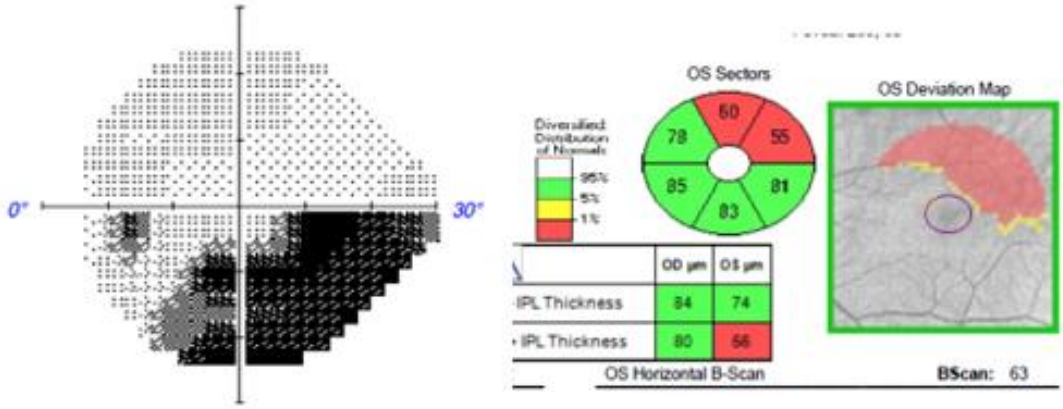

Fig. 1 **A** Visual field (Humphrey 30–2, Dublin, California) showing an inferior altitudinal defect. **B** Optical coherence tomography (HD-OCT Cirrhus, Carl Zeiss Meditec, Dublin, California) imaging showing the superior loss of ganglion cell complex thinning corresponding to the visual defect

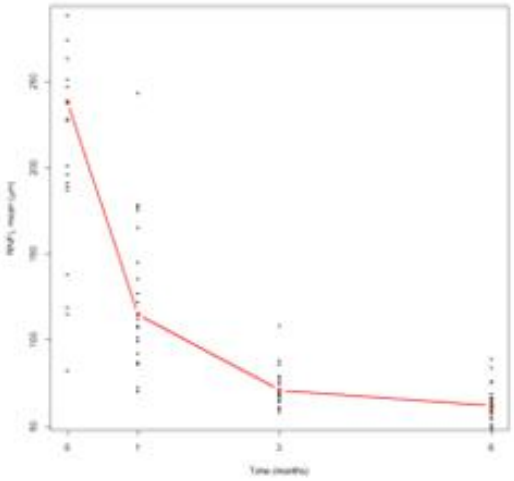

Fig. 2 Line graph. Evolution of mean RNFL (µm) after an episode of AION

lesion are essential to plan optimum management. While neuro-imaging is the gold standard for diagnosis, in the eye clinic OCT helps with the differential diagnosis by highlighting the location of RNFL and CGC thinning related to retrograde degeneration. OCT is valuable in the differential diagnosis of compressive lesions involving the optic nerve, chiasm and tract. Furthermore, in all cases of anterior visual pathway compression comparison of the visual loss (as seen on perimetry) with the degree of GCL loss is important in determining the prognosis for recovery following decompression.

Compressive lesion involving the optic nerve and chiasm

CON can be due to extrinsic compression (most commonly meningioma) or intrinsic optic nerve tumours such as glioma. However there are a variety of other causes, such as: infectious (aspergilloma [13]), inflammatory (dysthyroid optic neuropathy [14], IgG4 disease [15]) and vascular (aneurysm [16]).

There is little information about the topography of RGCs loss in optic nerve tumours. In optic nerve sheath meningioma, optic disc swelling or optic atrophy can be observed at presentation [17] depending on the course of the compressive process and the proximity of the tumour to the globe (swelling) and degree of axonal loss (atrophy). OCT will generally show diffuse pRNFL and GCC atrophy in the affected eye compared to the unaffected eye, reflecting axonal loss from chronic compression [18] (Fig. 3). In optic nerve glioma, the same observations are also reported compared to controls [19]. Fard MA et al. found that pRNFL and GCC measurements are an important marker of the disease progression [20]. OCT is useful in the initial diagnosis (highlighting a significant asymmetric atrophy) and differential diagnosis (preservation of GCC where there is visual field loss being a hallmark of axonal conduction block in compressive pathology which is seen in neither glaucoma nor ischaemic optic neuropathy). Along with subjective visual parameters, OCT provides an objective metric for follow up of patients.

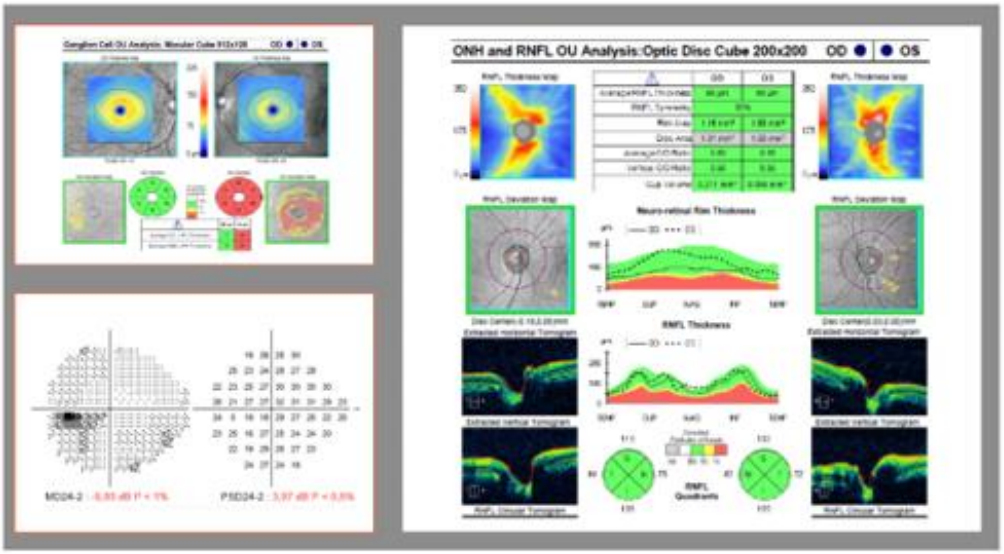

Fig. 3 **A** Optical coherence tomography (HD-OCT Cirrhus, Carl Zeiss Meditec, Dublin, California) imaging showing a diffuse thinning of the ganglion cell complex on the left eye due to a retrograde degeneration. **B** Visual field (Humphrey 30–2, Dublin, California) showing an inferior defect. **C** Optical coherence tomography (HD-OCT Cirrhus, Carl Zeiss Meditec, Dublin, California) imaging showing a normal RNFL thickness on both side despite a left optic nerve sheath meningioma

In dysthyroid eye disease, extraocular muscles and orbital fat are affected by an autoimmune inflammatory disorder. The optic nerve may be compressed at the apex of the cone of enlarged extraocular muscles. Raised intra-ocular pressure may also be a feature. Studies have shown a significant mean inferior RNFL thinning compared to controls [21].

Compressive lesion involving the chiasm

In chiasmal lesions, bilateral loss of vision is observed associated with bitemporal hemianopia as a major feature, although more anterior compression may give rise to features of unilateral optic neuropathy while a more posterior lesion may give rise to features of homonymous hemianopia due to optic tract involvement. Supra-sellar masses represent 14–18% of all brain tumours [22]. Pituitary adenoma, parasellar meningioma, craniopharyngioma and vascular abnormalities (e.g. internal carotid aneurysm for instance) are the most common causes of chiasmal compression [22]. The heteronymous nature of the visual field loss may not be noticed by the patient, resulting in presentation with advanced disease or the deficit being detected on a routine eye test.

In the optic chiasmal syndrome, thinning of the nasal and temporal sectors of the peripapillary RNFL is seen. This has been known from ophthalmoscopic examination as band atrophy. Danesh-Meyer HV et al. confirmed involvement of the nasal and temporal quadrants of the RNFL in pituitary lesions using OCT [23]. This is a result of the fact that these sectors consist entirely of nasal retinal fibres which decussate in the chiasm and are more vulnerable in chiasmal compression. There is no region of the optic disc which consists of exclusively uncrossed fibres, the arcuate bundles carrying both crossed and uncrossed fibres [24]. Studies have shown in chiasmal compression caused by a suprasellar lesion that the pattern of the GCC loss is the most sensitive parameter allowing the distinction from optic neuropathy due to glaucoma [25]. Involvement of the inferonasal and superonasal quadrant is highly suspicious of a compressive chiasmal optic neuropathy [25]. Nasal GCC is more affected because crossing fibres originating in nasal retina are involved [26]. The decrease in thickness of GCC is also well correlated to the density of the visual field defect [26]. GCC thickness assessment helps ophthalmologist to make an earlier diagnosis even if the RNFL OCT is still within the normal range [27]. A further refinement is to consider the naso-temporal macular GCC thickness ratio which has been compared directly in chiasmal compression and glaucoma [28].

OCT a marker of recovery of vision before surgery

Another special interest in compressive optic neuropathies is the possibility for the ophthalmologist, the neurologist and the neurosurgeon to predict the recovery after surgery utilising the OCT parameters. Several studies have demonstrated that prognosis for recovery is more favourable where the RNFL/GCC thicknesses are preserved, indicating conduction block rather than permanent axonal loss the recovery [23]. Moreover, in anterior optic nerve sheath meningioma, a pRNFL thickness lower than 70 µm is associated with a lower probability of visual improvement after radiotherapy or decompression surgery [18].

Optic tract and post-geniculate lesions

The principal causes of optic tract lesions are infarctions (40%), tumour compression (32%) and trauma (17%) [29]. Acute MS lesions involving the optic tract are uncommon [30]. Damage to the optic tract tends to cause an incongruous homonymous hemianopia, bilateral optic atrophy and a contralateral RAPD. If retrograde degeneration of optic nerve fibres has occurred band atrophy will be seen in the contralateral eye.

In patient with cerebral lesions, OCT may be a helpful supplement to conventional perimetry. Retinal changes due to retrograde trans-synaptic neuronal degeneration are observed in animals and humans with post-geniculate lesions leading to homonymous hemianopia, initially demonstrated through studies of the peripapillary RNFL [31–33]. In later studies, thinning of the nasal hemimacula GCC in the contralateral eye and a thinning of the temporal hemimacula in the ipsilateral eye, respecting the vertical meridian have been shown [34] (Fig. 4). These observations were noted at least 1 month after the onset [35]. If available, the OCT characteristics permits a faster and possibly more reliable diagnosis than perimetry but the changes will not be seen in the acute situation.

Idiopathic intracranial hypertension (IIH) and papilloedema

IIH is a disorder in which a pseudotumor cerebri syndrome (i.e. raised intracranial pressure(ICP) without hydrocephalus or a mass lesion; PTC) occurs in association with weight gain. It affects mainly women of childbearing age who have recently gained weight [36]. The major ophthalmic manifestation is papilloedema often presenting as transient visual obscurations. Patients may be unaware of ongoing deficit because papilloedema is another condition in which visual field loss tends to be heteronymous with sparing of central acuity. Diplopia, most commonly due to lateral rectus paresis, may also occur. Non-ophthalmic features are headache and tinnitus. The pathogenesis of IIH still remains unclear and various hypotheses have been proposed but intracranial venous hypertension seems to be common to many causes of PTC such as dural sinus thrombosis and fistula and this may play a role in IIH also.

The pathogenesis of papilloedema is also poorly understood in this and indeed in other situations but an elevated translaminar pressure gradient (the difference between the ICP and the intraocular pressure (IOP) [37] seems to be fundamental (particularly as papilloedema is also seen with low intra-ocular pressure). There may also be a contribution from venous hypertension as the central retinal vein has a short course in the subarachnoid space and venous hypertension at the optic nerve head will invariably follow a rise in CSF pressure. Similar optic disc swelling is of course seen

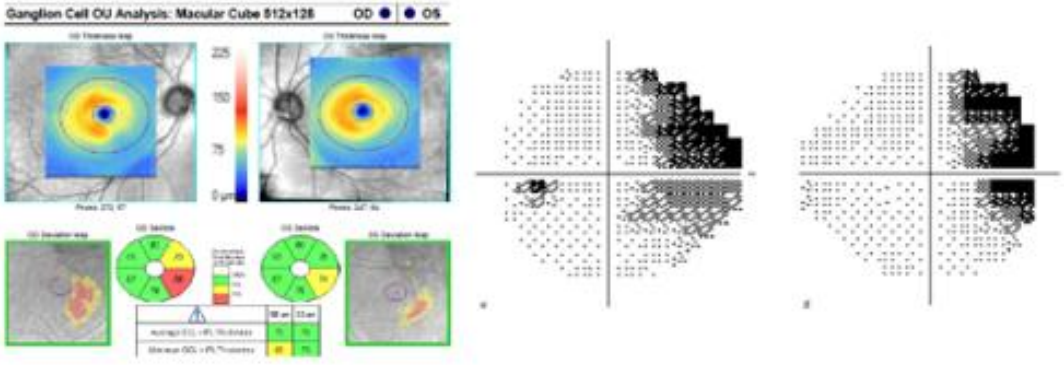

Fig. 4 **A** Visual field (Humphrey 30–2, Dublin, California) showing a right hemianopia due to a glioblastoma. **B** Optical coherence tomography (HD-OCT Cirrhus, Carl Zeiss Meditec, Dublin, California) imaging showing the corresponding nasal ganglion cell complex on the right eye and the temporal ganglion cell complex thinning on the left eye corresponding to the visual defect

with central retinal vein occlusion. Whatever the underlying cause the increase in volume of the optic disc itself is due to axoplasmic stasis leading to axonal distension. There is a variable contribution from tissue oedema. These features have been more clearly delineated with the advent of OCT. In the past IIH was known as "benign" intracranial hypertension but this pathology can lead to irreversible visual loss in 25% of cases if the papilledema does not resolve [36].

In parallel with perimetry and other measures of visual function OCT is helpful in the differential diagnosis, prognosis and monitoring of papilloedema whatever the cause. Early papilloedema and anomalous, crowded optic discs can be confused leading to inappropriate management of either condition. In both situations OCT may show evidence of peripapillary axonal distension. This has been observed in pathological studies of papilloedema for some time [38] and OCT has confirmed similar findings in crowded optic discs including those harbouring drusen. Indeed in early OCT studies these were originally designated "soft drusen" but clearly shown not to be associated with visual loss, unlike true drusen [39]. More recently the term "peripapillary ovoid hyperreflective masses" (POHM) was coined to distinguish these features from optic disc drusen which are *hypo*reflective, although a better description to match the pathology would be "peripapillary axonal distension" (PAD).

Thus, OCT can be helpful in confirming features associated with anomalous optic discs, such as lack of a cup and the presence of optic disc drusen. In papilloedema however the cup can fill in when advanced and drusen-like bodies can be seen in chronic papilloedema. Anterior displacement of the lamina cribrosa is more specific to papilloedema indicating as it does a pressure gradient indicating either raised intracranial pressure or low IOP [40].

Unfortunately, pRNFL analysis is not useful for the follow-up of these patients. A decrease of the pRNFL can be the result of either resolution of the papilloedema or the onset of atrophy and axonal loss. GCC analysis, given the ability to detect retrograde degeneration of optic nerve fibres, is the appropriate biomarker for monitoring progression of papilloedema and the risk of visual deterioration.

Inflammatory optic neuropathies

Intrinsic inflammation of the optic nerve (as opposed to contiguous inflammation such as of the optic nerve sheath), is referred to as optic neuritis. In the past (and given the prevalence of the disorder in populations of European descent) studies have been focussed principally on optic neuritis as seen in Multiple Sclerosis (MSON). The principle clinical features are an acute or subacute monocular loss of vision associated with pain on eye movement and a RAPD [41]. MSON is considered an autoimmune optic neuritis although no antibody has been described [41]. In MS optic neuritis is the presenting symptom in 25% of patients [42]. Less common in European populations but more common in populations of Asian and African descent is autoimmune optic neuritis related to neuromyelitis optica spectrum disorder (NMOSD) and myelin oligodendrocyte glycoprotein antibody associated disease (MOGAD) [41]. Systemic disorders associated with optic neuritis include infectious, post-infectious and post-vaccination optic neuritis [41]. These latter disorders (and NMOSD) are more likely to present as bilateral simultaneous optic neuritis which is a marker of a systemic antibody response and unusual in MS. However asymptomatic involvement of the unaffected eye (as evidenced by pRNFL or GCC thinning) is an important indication of likely MS [43]. Indeed interocular asymmetry in GCL thinning is a signature of MS in a susceptible population [44, 45].

The finding of a delayed Visually Evoked Potential in an asymptomatic eye has similar significance in that it is a common feature of MS (reflecting demyelination as well as axonal loss) [46].OCT has resolved an important issue, whether in MS the residual visual deficit is related primarily to demyelination or to axonal loss. It is clear that the important factor is irreversible axonal loss [43]. Demyelination is responsible for intermittent symptoms such as Uhthoff phenomenon and symptoms related to slowing of conduction in the optic nerve such as the Pulfrich effect. These symptoms may resolve as a result of remyelination [47] whereas the consequences of axonal loss are permanent, unless there is a possibility of central reorganisation [48]. A recent study has assessed a loss of 5 to 27% of GCL after optic neuritis with a full visual recovery as determined by clinical tests [49].

OCT is, therefore, a useful tool to evaluate pRNFL thinning and retrograde degeneration of the GCC. A such OCT is of particular value in monitoring any effect of treatment in reducing the permanent deficit. Moreover, the pattern of thinning shown on OCT may be helpful in differential diagnosis as pRNFL thinning is greater in the inferior and nasal sectors in MOGON than in MSON [50], where temporal thinning is observed. pRNFL thinning is greater overall in NMO than MSON, in accord with the worse visual prognosis [51].

Toxic and nutrition optic neuropathies

Optic neuropathies secondary to toxic exposure or nutritional deficiency are typically characterized by subacute, painless and bilaterally symmetrical loss of vision associated with a caeco-central visual field defect [52]. Vitamin B12 deficiency, whether dietary or associated with pernicious anaemia, is well established to cause optic neuropathy. Nutritional optic neuropathies are often found in patients who have a high carbohydrate, low protein diet as was seen in the epidemics in Tanzania and Cuba where specific

micronutrient deficiencies have not been identified [53, 54]. In developed economies this is more likely to be occur in patients consuming voluntarily chosen highly restrictive diets, following bariatric surgery (without adequate supplementation), or in patients who have a poor diet associated with a high alcohol consumption. There is no evidence that alcohol has a direct toxic action unlike methanol which is converted to formaldehyde by alcohol dehydrogenase.

Ethambutol, an antimycobacterial treatment, is one of the commonest causes of toxic optic neuropathy throughout the world, the precise mechanism is not understood. A possible final common path for toxic and micronutrient deficiency optic neuropathies is an effect on mitochondrial function leading to mitochondrial cytopathy, as observed in inherited optic neuropathies [55]. Mitochondrial dysfunction may explain the increased vulnerability of central vision, although a simple explanation based on fibre size cannot account for the caeco-central scotoma [56]. Indeed, this cannot be considered a universal phenomenon, in the toxic neuropathy related to vigabatrin the caeco-central projection is selectively preserved [57].

Unlike other causes of optic neuropathy considered above, the loss of ganglion cells in toxic and nutritional disorders is related to a direct cytotoxic mechanism rather than a retrograde degeneration following damage to the optic nerve fibres. Fundus imaging may be normal at presentation, and OCT may be helpful in the acute phase where thickening of the RNFL, especially the temporal sector is observed due to RNFL swelling related to the accumulation of mitochondria [58, 59]. However, in the subacute and chronic stages, RNFL thinning especially in the inferotemporal part is found [60]. OCT showed GCC thinning in the inferior part of 2 mm and in the nasal part of 3 mm compared to healthy controls, supporting the fact that the papillomacular bundle (caeco-central projection) is particularly involved in this pathology [61]. One report has observed that the GCC thinning was present at the onset of symptoms and increased after 6 months [62]. GCC thinning has been shown to be significantly correlated with deficits in visual field and visual acuity [61] (Fig. 5). Early treatment (restoring the deficiency or eliminating the toxic exposure) are mandatory to prevent or reduce permanent visual loss.

Inherited mitochondrial neuropathies

The principal features of inherited mitochondrial optic neuropathies are similar to the toxic and nutritional cases reviewed above: painless bilateral progressive loss of vision. Visual field is also characterised by a caeco-central scotoma caused by a loss of the papillomacular bundle. (caeco-central

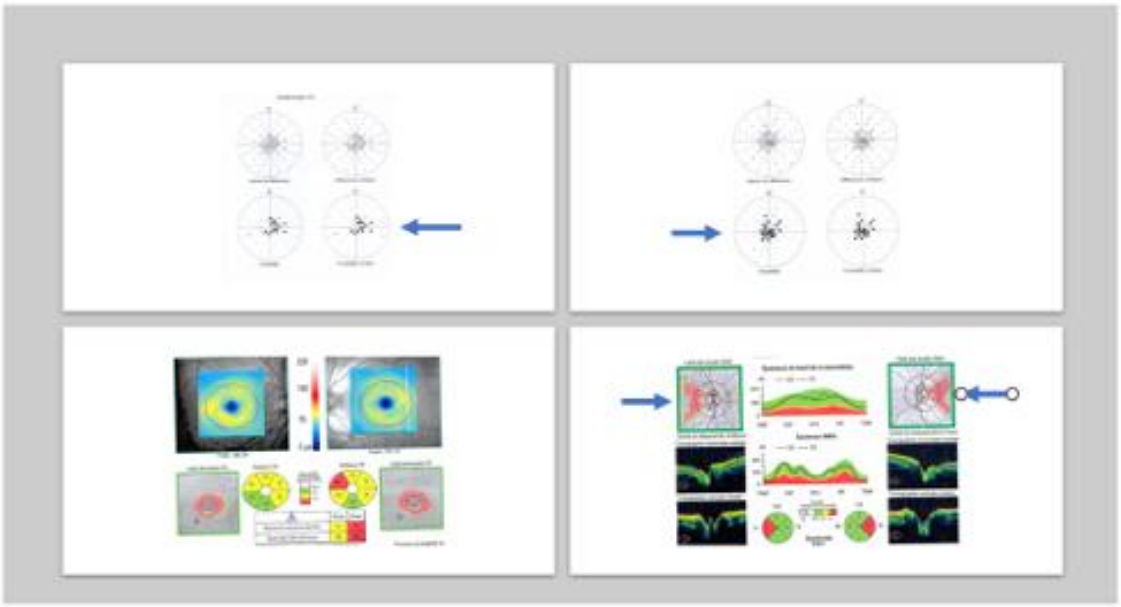

Fig. 5 **A** Visual field (Humphrey 30–2, Dublin, California) showing a central scotoma in a patient who was treated with Ethambutol. **B** Optical coherence tomography (HD-OCT Cirrhus, Carl Zeiss Meditec, Dublin, California) imaging showing the corresponding thinning a the papillomacular bundle. Ganglion cell complex on the right eye and the temporal ganglion cell complex thinning on the left eye corresponding to the visual defect and **C** Optical coherence tomography (HD-OCT Cirrhus, Carl Zeiss Meditec, Dublin, California) imaging showing the typical temporal thinning

projection). The mutations concerned are in mitochondrial DNA (mDNA) or nuclear DNA coding for proteins expressed in mitochondria [63]. The two inherited mitochondrial neuropathies most likely to be seen in daily practice are: dominant optic atrophy (DOA) and Leber hereditary optic neuropathy (LHON).

DOA is a group of dominant inherited neuropathies which affect retinal ganglion cell functions. Commonly first symptoms appear in the first decade and are slowly progressive with preservation of peripheral vision. Many mutations are associated with DOA and the first described (and most common) being designated OPA1 [64, 65].

LHON is a rare maternally inherited mitochondrial disease caused by three most common mDNA mutations (m.11778 G > A, m.3460G > A m.11484 T > C) [66]. It mainly affects men between the second and third decades [67]. At onset, a subacute loss of vision is observed in both eyes simultaneously or sequentially within weeks or months.

In acute LHON, authors have observed thickening of the RNFL in the acute stage followed by atrophy in chronic LHON [68, 69]. However, GCC thinning was found in the early acute phase and worsened gradually (mean GCC thickness 24 weeks or more after the symptoms: 50.8 µm) [70]. In DOA patients, OCT studies showed a decrease in mean RNFL thickness compared to controls and the temporal sector was particularly affected with a thickness loss of 59% [71]. Moreover, RNFL was thinner in DOA than in chronic LHON [68]. Compared to controls, the temporal and superior sectors of RNFL were more affected in DOA [72]. GCC analysis showed a diffuse thickness decrease in all quadrants in these two pathologies and could be an early marker of the disease [68]. In DAO associated with the OPA1 mutation a more significant involvement of the inferior, inferonasal and superonasal sector of GCC was observed [72].

Limitations of the OCT

The accuracy of our diagnosis and the analysis of the results rely on the estimation of the GCC or RNFL thickness. A proper definition of the boundaries to avoid an overestimation or an underestimation of the RNFL and GCL thickness is warranted. Segmentation artefact due to motion (53.3%), retinal layer misidentifications (50%) and absence of the inner segmentation line (7.8%) have a significant impact on the quality of the image. [73] The frequency of artefacts is greater in patients with macular pathology (dry and wet macular degeneration, pigmentary retinopathy, diabetic macular oedema and high myopia) [73, 74], tilted disc, peripapillary atrophy, small cup disc ratio and optic disc swelling [75, 76]. Moreover, the OCT signal strength -which can be diminished due to opacification of the macular media as in the case of corneal oedema or opacity of lens or vitreous- is an additional factor influencing the image quality and the segmentation analysis [77].

Every analysis is compared to a normative reference range in function of the sex and the age. Because of the individual variation, the small size sample, or the absence of normative range, as in adolescent or children, results can be misinterpreted as outranged the reference data and considered abnormal after comparison to the normative database [78]. In addition, refractive errors superior to + 5.0 dioptres and inferior to −5.0 dioptres are excluded of the reference database. In research studies an "in house" matched control group, matched for age, gender, axial length and ethnicity, is recommended [43].

Finally, OCT cannot distinguish a functional cell from a dysfunctional cell. Indeed, in patients with no perception of light, retinal nerve fibre layer thickness is still measured at 45 µm because dysfunctional cells are taken in account [79].

Conclusion

OCT is a useful tool providing quantitative measures of pRNFL and GCC thickness in optic neuropathy, which are directly correlated with visual function. GCC analysis can identify early change related to atrophy and assist in the diagnosis and differential diagnosis of optic neuropathy. Because of its reproducibility, these measurements are crucial to monitor the disease progression and have recently become a standard for the longitudinal assessment of ocular diseases. Moreover, recognition of the OCT pattern is crucial to differentiate optic neuropathies. Indeed, GCL atrophy involving superior or inferior hemi-macula is an argument for NA-AION, whereas GCL atrophy respecting the vertical meridian indicate an optic tract lesion. Therefore, the GCC analysis could be considered as a key marker to identify the type of optic neuropathy, to facilitate the follow-up and to assess the odds of recovery after an episode or after a surgery decompression for instance.

However, in order to diminish some segmentation artefact and improving the images quality, developers should focus on reducing the processing time, improving the volume segmentation, and visualising the reconstruction of the macula in three-dimensions. Moreover, the future normative database should take into account the axial length and a more comprehensive age range.

Funding No funding was received towards this work.

Declarations

Conflict of interest The authors report no competing interests.

References

1. Fujimoto JG, Pitris C, Boppart SA, Brezinski ME (2000) Optical coherence tomography: an emerging technology for biomedical imaging and optical biopsy. Neoplasia 2:9–25. https://doi.org/10.1038/sj.neo.7900071
2. Polyak SL (1941)The retina: the anatomy and the histology of the retina in man, ape, and monkey, including the consideration of visual functions, the history of physiological optics, and the histological laboratory technique. University of Chicago Press, Chicago, pp 402–404
3. Hubel D, Livingstone M (1987) Segregation of form, color, and stereopsis in primate area 18. J Neurosci 7:3378–3415. https://doi.org/10.1523/JNEUROSCI.07-11-03378.1987
4. Kolb H, Linberg KA, Fisher SK (1992) Neurons of the human retina:a Golgi study. J Comp Neurol 318:147–187. https://doi.org/10.1002/cne.903180204
5. Glaser JS, Sadun AA (1990) Anatomy of the visual sensory system. In: Glaser JS (ed) Neuro-Ophthalmology. J.B Lippincott Co, Philadelphia, pp 61–82
6. Chen JJ, Kardon RH (2016) Avoiding clinical misinterpretation and artifacts of optical coherence tomography analysis of the optic nerve, retinal nerve fiber layer, and ganglion cell layer. J Neuroophthalmol 36:417–438. https://doi.org/10.1097/WNO.0000000000000422
7. Arnold AC (2003) Pathogenesis of nonarteritic anterior ischemic optic neuropathy. J Neuroophthalmol 23:157–163. https://doi.org/10.1097/00041327-200306000-00012
8. Savini G (2006) Detection and quantification of retinal nerve fiber layer thickness in optic disc edema using stratus OCT. Arch Ophthalmol 124:1111. https://doi.org/10.1001/archopht.124.8.1111
9. Hedges TR (2008) Subretinal fluid from anterior ischemic optic neuropathy demonstrated by optical coherence tomography. Arch Ophthalmol 126:812. https://doi.org/10.1001/archopht.126.6.812
10. Chapelle AC, Rakic JM, Plant GT (2023) The occurrence of intra- and sub-retinal fluid in anterior ischemic optic neuropathy: pathogenesis prognosis and treatment. Ophthalmology. https://doi.org/10.1016/j.ophtha.2023.07.015
11. MacIntosh PW (2020) Acute changes in ganglion cell layer thickness in ischemic optic neuropathy compared to optic neuritis using optical coherence tomography. Int J Ophthalmol 13:120–123. https://doi.org/10.18240/ijo.2020.01.17
12. Lee YH, Kim KN, Heo DW et al (2017) Difference in patterns of retinal ganglion cell damage between primary open-angle glaucoma and non-arteritic anterior ischaemic optic neuropathy. PLoS ONE 12:e0187093. https://doi.org/10.1371/journal.pone.0187093
13. Jonas JB, Schmidt AM, Müller-Bergh JA et al (1992) Human optic nerve fiber count and optic disc size. Invest Ophthalmol Vis Sci 33:2012–2018
14. Saeed P, Tavakoli Rad S, Bisschop PHLT (2018) Dysthyroid optic neuropathy. Ophthalmic Plast Reconstr Surg 34:S60–S67. https://doi.org/10.1097/IOP.0000000000001146
15. Aryasit O, Tiraset N, Preechawai P et al (2021) IgG4-related disease in patients with idiopathic orbital inflammation. BMC Ophthalmol 21:356. https://doi.org/10.1186/s12886-021-02115-x
16. Peiris JB, Ross Russell RW (1980) Giant aneurysms of the carotid system presenting as visual field defect. J Neurol Neurosurg Psychiatry 43:1053–1064. https://doi.org/10.1136/jnnp.43.12.1053
17. Imes RK (1985) Evolution of optociliary veins in optic nerve sheath meningioma: evolution. Arch Ophthalmol 103:59. https://doi.org/10.1001/archopht.1985.01050010063020
18. Loo J-L, Tian J, Miller NR, Subramanian PS (2013) Use of optical coherence tomography in predicting post-treatment visual outcome in anterior visual pathway meningiomas. Br J Ophthalmol 97:1455–1458. https://doi.org/10.1136/bjophthalmol-2013-303449
19. Chang L, El-Dairi MA, Frempong TA et al (2010) Optical coherence tomography in the evaluation of neurofibromatosis type-1 subjects with optic pathway gliomas. J Am Assoc Pediatr Ophthalmol Strabismus 14:511–517. https://doi.org/10.1016/j.jaapos.2010.08.014
20. Fard MA, Fakhree S, Eshraghi B (2013) Correlation of optical coherence tomography parameters with clinical and radiological progression in patients with symptomatic optic pathway gliomas. Graefes Arch Clin Exp Ophthalmol 251:2429–2436. https://doi.org/10.1007/s00417-013-2394-4
21. Sayın O, Yeter V, Arıtürk N (2016) Optic disc, macula, and retinal nerve fiber layer measurements obtained by OCT in thyroid-associated ophthalmopathy. J Ophthalmol 2016:1–7. https://doi.org/10.1155/2016/9452687
22. Al-Dahmani K, Mohammad S, Imran F et al (2016) Sellar masses: an epidemiological study. Can J Neurol Sci 43:291–297. https://doi.org/10.1017/cjn.2015.301
23. Danesh-Meyer HV, Yap J, Frampton C, Savino PJ (2014) Differentiation of compressive from glaucomatous optic neuropathy with spectral-domain optical coherence tomography. Ophthalmology 121:1516–1523. https://doi.org/10.1016/j.ophtha.2014.02.020
24. Moura FC, Medeiros FA, Monteiro MLR (2007) Evaluation of macular thickness measurements for detection of band atrophy of the optic nerve using optical coherence tomography. Ophthalmology 114:175–181. https://doi.org/10.1016/j.ophtha.2006.06.045
25. Lee EJ, Yang HK, Kim T-W et al (2015) Comparison of the pattern of retinal ganglion cell damage between patients with compressive and glaucomatous optic neuropathies. Invest Ophthalmol Vis Sci 56:7012. https://doi.org/10.1167/iovs.15-17909
26. Monteiro MLR, Hokazono K, Fernandes DB et al (2014) Evaluation of inner retinal layers in eyes with temporal hemianopic visual loss from chiasmal compression using optical coherence tomography. Invest Ophthalmol Vis Sci 55:3328. https://doi.org/10.1167/iovs.14-14118
27. Micieli JA, Newman NJ, Biousse V (2019) The role of optical coherence tomography in the evaluation of compressive optic neuropathies. Curr Opin Neurol 32:115–123. https://doi.org/10.1097/WCO.0000000000000636
28. Kleerekooper I, Wagner SK, Trip SA et al (2023) Differentiating glaucoma from chiasmal compression using optical coherence tomography: the macular naso-temporal ratio. Br J Ophthalmol. https://doi.org/10.1136/bjo-2023-323529
29. Zhang X, Kedar S, Lynn MJ et al (2006) Homonymous hemianopias: Clinical-anatomic correlations in 904 cases. Neurology 66:906–910. https://doi.org/10.1212/01.wnl.0000203913.12088.93
30. Plant GT, Kermode AG, Turano G et al (1992) Symptomatic retrochiasmal lesions in multiple sclerosis: clinical features, visual evoked potentials, and magnetic resonance imaging. Neurology 42:68–76. https://doi.org/10.1212/wnl.42.1.68
31. Hendrickson A, Warner CE, Possin D et al (2015) Retrograde transneuronal degeneration in the retina and lateral geniculate nucleus of the V1-lesioned marmoset monkey. Brain Struct Funct 220:351–360. https://doi.org/10.1007/s00429-013-0659-7
32. Cowey A, Stoerig P (1995) Blindsight in monkeys. Nature 373:247–249. https://doi.org/10.1038/373247a0
33. Jindahra P, Petrie A, Plant GT (2009) Retrograde trans-synaptic retinal ganglion cell loss identified by optical coherence tomography. Brain 132:628–634. https://doi.org/10.1093/brain/awp001
34. Kanamori A, Nakamura M, Yamada Y, Negi A (2013) Spectral-domain optical coherence tomography detects optic atrophy due to optic tract syndrome. Graefes Arch Clin Exp Ophthalmol 251:591–595. https://doi.org/10.1007/s00417-012-2096-3

35. Keller J, Sánchez-Dalmau BF, Villoslada P (2014) Lesions in the posterior visual pathway promote trans-synaptic degeneration of retinal ganglion cells. PLoS ONE 9:e97444. https://doi.org/10.1371/journal.pone.0097444
36. Fraser C, Plant GT (2011) The syndrome of pseudotumour cerebri and idiopathic intracranial hypertension. Curr Opin Neurol 24:12–17. https://doi.org/10.1097/WCO.0b013e328341f94a
37. Morgan WH, Yu DY, Balaratnasingam C (2008) The role of cerebrospinal fluid pressure in glaucoma pathophysiology: the dark side of the optic disc. J Glaucoma 17:408–413. https://doi.org/10.1097/IJG.0b013e31815c5f7c
38. Cogan DG, Kuwabara T (1977) Papilledema. Exp Eye Res 25:419–433. https://doi.org/10.1016/S0014-4835(77)80039-0
39. Traber GL, Weber KP, Sabah M et al (2017) Enhanced depth imaging optical coherence tomography of optic nerve head drusen. Ophthalmology 124:66–73. https://doi.org/10.1016/j.ophtha.2016.09.022
40. Villarruel JM, Li XQ, Bach-Holm D, Hamann S (2017) anterior lamina cribrosa surface position in idiopathic intracranial hypertension and glaucoma. Eur J Ophthalmol 27:55–61. https://doi.org/10.5301/ejo.5000806
41. Petzold A, Fraser CL, Abegg M et al (2022) Diagnosis and classification of optic neuritis. The Lancet Neurology 21:1120–1134. https://doi.org/10.1016/S1474-4422(22)00200-9
42. McDonald WI, Barnes D (1992) The ocular manifestations of multiple sclerosis. 1. abnormalities of the afferent visual system. J Neurol Neurosurg Psychiatry 55:747–752. https://doi.org/10.1136/jnnp.55.9.747
43. Trip SA, Schlottmann PG, Jones SJ et al (2005) Retinal nerve fiber layer axonal loss and visual dysfunction in optic neuritis. Ann Neurol 58:383–391. https://doi.org/10.1002/ana.20575
44. Coric D, Balk LJ, Uitdehaag BMJ, Petzold A (2017) Diagnostic accuracy of optical coherence tomography inter-eye percentage difference for optic neuritis in multiple sclerosis. Eur J Neurol 24:1479–1484. https://doi.org/10.1111/ene.13443
45. Petzold A, Chua SYL, Khawaja AP et al (2021) Retinal asymmetry in multiple sclerosis. Brain 144:224–235. https://doi.org/10.1093/brain/awaa361
46. Kupersmith MJ, Nelson JI, Seiple WH et al (1983) The 20/20 eye in multiple sclerosis. Neurology 33:1015–1015. https://doi.org/10.1212/WNL.33.8.1015
47. Brusa A, Jones SJ, Plant GT (2001) Long-term remyelination after optic neuritis. Brain 124:468–479. https://doi.org/10.1093/brain/124.3.468
48. Werring DJ (2000) Recovery from optic neuritis is associated with a change in the distribution of cerebral response to visual stimulation: a functional magnetic resonance imaging study. J Neurol Neurosurg Psychiatry 68:441–449. https://doi.org/10.1136/jnnp.68.4.441
49. Sherif M, Bergin C, Borruat F-X (2019) Normal visual recovery after optic neuritis despite significant loss of retinal ganglion cells in patients with multiple sclerosis. Klin Monatsbl Augenheilkd 236:425–428. https://doi.org/10.1055/a-0853-1721
50. Park K-A, Kim J, Oh SY (2014) Analysis of spectral domain optical coherence tomography measurements in optic neuritis: differences in neuromyelitis optica, multiple sclerosis, isolated optic neuritis and normal healthy controls. Acta Ophthalmol 92:e57–e65. https://doi.org/10.1111/aos.12215
51. Schneider E, Zimmermann H, Oberwahrenbrock T et al (2013) Optical coherence tomography reveals distinct patterns of retinal damage in neuromyelitis optica and multiple sclerosis. PLoS ONE 8:e66151. https://doi.org/10.1371/journal.pone.0066151
52. Kerrison J (2004) Optic neuropathies caused by toxins and adverse drug reactions. Ophthalmol Clin North Am 17:481–488. https://doi.org/10.1016/j.ohc.2004.05.005
53. Plant GT, Mtanda AT, Arden GB, Johnson GJ (1997) An epidemic of optic neuropathy in Tanzania: characterization of the visual disorder and associated peripheral neuropathy. J Neurol Sci 145:127–140. https://doi.org/10.1016/S0022-510X(96)00162-1
54. Thomas PK, Plant GT, Baxter P et al (1995) An epidemic of optic neuropathy and painful sensory neuropathy in cuba: clinical aspects. J Neurol 242:629–638. https://doi.org/10.1007/BF00866912
55. Korkiamäki P, Kervinen M, Karjalainen K et al (2013) Prevalence of the primary LHON mutations in Northern Finland associated with bilateral optic atrophy and tobacco-alcohol amblyopia. Acta Ophthalmol 91:630–634. https://doi.org/10.1111/j.1755-3768.2012.02506.x
56. Plant GT, Perry VH (1990) The anatomical basis of the caeco-central scotoma: new observations and a review. Brain 113:1441–1457. https://doi.org/10.1093/brain/113.5.1441
57. Clayton LM, Devile M, Punte T et al (2012) Patterns of peripapillary retinal nerve fiber layer thinning in vigabatrin-exposed individuals. Ophthalmology 119:2152–2160. https://doi.org/10.1016/j.ophtha.2012.05.009
58. Moura F, Monteiro M (2010) Evaluation of retinal nerve fiber layer thickness measurements using optical coherence tomography in patients with tobacco-alcohol-induced toxic optic neuropathy. Indian J Ophthalmol 58:143. https://doi.org/10.4103/0301-4738.60087
59. Barboni P, Carbonelli M, Savini G et al (2010) Natural history of Leber's hereditary optic neuropathy: longitudinal analysis of the retinal nerve fiber layer by optical coherence tomography. Ophthalmology 117:623–627. https://doi.org/10.1016/j.ophtha.2009.07.026
60. Wang MY, Sadun AA (2013) Drug-related mitochondrial optic neuropathies. J Neuroophthalmol 33:172–178. https://doi.org/10.1097/WNO.0b013e3182901969
61. Vieira LMC, Silva NFA, Dias Dos Santos AM et al (2015) Retinal ganglion cell layer analysis by optical coherence tomography in toxic and nutritional optic neuropathy. J Neuroophthalmol 35:242–245. https://doi.org/10.1097/WNO.0000000000000229
62. Han J, Byun MK, Lee J et al (2015) Longitudinal analysis of retinal nerve fiber layer and ganglion cell–inner plexiform layer thickness in ethambutol-induced optic neuropathy. Graefes Arch Clin Exp Ophthalmol 253:2293–2299. https://doi.org/10.1007/s00417-015-3150-8
63. Delettre C, Lenaers G, Pelloquin L et al (2002) OPA1 (Kjer Type) dominant optic atrophy: a novel mitochondrial disease. Mol Genet Metab 75:97–107. https://doi.org/10.1006/mgme.2001.3278
64. Delettre C, Lenaers G, Griffoin J-M et al (2000) Nuclear gene OPA1, encoding a mitochondrial dynamin-related protein, is mutated in dominant optic atrophy. Nat Genet 26:207–210. https://doi.org/10.1038/79936
65. Alexander C, Votruba M, Pesch UEA et al (2000) OPA1, encoding a dynamin-related GTPase, is mutated in autosomal dominant optic atrophy linked to chromosome 3q28. Nat Genet 26:211–215. https://doi.org/10.1038/79944
66. Wallace DC, Singh G, Lott MT et al (1988) Mitochondrial DNA Mutation Associated with Leber's hereditary optic neuropathy. Science 242:1427–1430. https://doi.org/10.1126/science.3201231
67. Spruijt L, Kolbach DN, De Coo RF et al (2006) Influence of mutation type on clinical expression of Leber hereditary optic neuropathy. Am J Ophthalmol 141:676-676.e8. https://doi.org/10.1016/j.ajo.2005.11.007
68. Asanad S, Tian JJ, Frousiakis S et al (2019) Optical coherence tomography of the retinal ganglion cell complex in Leber's hereditary optic neuropathy and dominant optic atrophy. Curr Eye Res 44:638–644. https://doi.org/10.1080/02713683.2019.1567792
69. Savini G, Barboni P, Valentino M et al (2005) Retinal nerve fiber layer evaluation by optical coherence tomography in unaffected

Chapelle AC, Rakic JM, Plant, Gordon. Non-arteritic anterior ischemic optic neuropathy: cystic change in the inner nuclear layer due to edema and to retrograde maculopathy. Ophthalmology Science. 2022.

AMERICAN ACADEMY OF OPHTHALMOLOGY®

Nonarteritic Anterior Ischemic Optic Neuropathy

Cystic Change in the Inner Nuclear Layer Caused by Edema and Retrograde Maculopathy

Anne-Catherine Chapelle, MD,[1] Jean-Marie Rakic, MD, PhD,[1] Gordon T. Plant, MD, FRCOphth[2]

Purpose: Microcystic macular edema (MME), also known as retrograde maculopathy (RM), is associated with severe optic atrophy because of a range of causes. However, similar changes have also been described in primary *retinal* pathology and the pathogenesis of MME is debated.

Design: A retrospective observational case series.

Participants: Patients with nonarteritic ischemic optic neuropathy.

Methods: A retrospective observational case series was performed at the University Hospital of Liège, Belgium. The medical records of patients who were referred to our Neuro-ophthalmology department with a diagnosis of nonarteritic anterior ischemic optic neuropathy (NA-AION), between 2014 and 2021, were reviewed.

Main Outcome Measures: Ganglion cell complex thickness, acute and chronic inner nuclear change.

Results: In a cohort of 34 patients (mean age: 60 ± 12.5 years; 65.6% men) with NA-AION, we identified a transient microcystic change in the inner nuclear layer (INL) associated with optic disc swelling in 19 eyes at presentation. This early change was associated with a transudate of intraretinal and subretinal fluid originating from the optic disc. Among patients who had shown this transient change 3 subsequently developed MME, which remained fixed during the period of observation (range, 12–34 months). No MME was observed in patients without an early INL transient change. Microcystic macular edema was observed in patients with severe ganglion cell complex thinning at 6 months: mean (± SD) loss in superior hemimacula (−28.2 ± 5.2 μm [−33.3%, range, −22.3 to −30.3 μm]) and in inferior hemimacula (−30.7 ± 5.6 μm [−31.0%, range, −24.3 to 34.8 μm]).

Conclusions: Our study has revealed 2 causes of INL cystic change in the same patients experiencing NA-AION, 1 reversible and the other likely permanent. This finding highlights the distinction between genuine edema related to transudation of fluid (in this case secondary to ischemic optic disc swelling) and the phenomenon observed in RM that is related to the degree of retinal nerve fiber layer/ganglion cell complex thinning. Cystic change in the INL is associated with severe optic atrophy (MME). However, similar changes have been described in *retinal* pathology and the pathogenesis of MME is debated. *Ophthalmology Science 2023;3:100230 © 2022 by the American Academy of Ophthalmology. This is an open access article under the CC BY license (http://creativecommons.org/licenses/by/4.0/).*

Microcystic macular edema (MME) was first described in the context of OCT findings in multiple sclerosis by Gelfand et al.[1] The abnormality was more likely to be seen in patients who had had a previous episode of optic neuritis and in cases with more marked thinning of the retinal nerve fiber and ganglion cell layers. Inner nuclear layer (INL) cell loss and thinning had previously been reported in a histopathologic study of the retina in multiple sclerosis, which also correlated with the severity of axonal loss, without mention of the presence of cystic change.[2] The microcysts are located in the INL and show a perifoveal distribution.[1,3] Microcystic macular edema is associated with severe optic atrophy found in the following: optic neuritis[1,4]; neuromyelitis optica[5,6]; hereditary optic neuropathies[7,8]; toxic and nutritional deficiency neuropathy[9,10]; glaucomatous neuropathy[11,12]; compressive optic neuropathy[13]; and infiltrative optic neuropathy, such as glioma.[14,15] Abegg[14] has suggested the term *retrograde maculopathy* (RM) for INL cystic change in this context.[16] However, similar changes have also been described in *retinal* pathology, for example in the following: epiretinal membrane,[17] age-related macular degeneration, diabetic retinopathy, and central serous retinopathy.[18] Indeed, the earliest use of the term MME known to the authors (although in Romanian as *edemul macular microchistic*) was published in a description of an *isolated case* of suspected microcystic macular dystrophy in 1988.[19]

We consider the following case series concerning 3 patients with nonarteritic anterior ischemic optic neuropathy (NA-AION) to be of particular interest in this context. These

https://doi.org/10.1016/j.xops.2022.100230
ISSN 2666-9145/22

patients showed early acute *transient* microcystic changes in the INL associated with disc swelling in parallel with other evidence of retinal edema. Longstanding, perhaps permanent, MME was developed subsequently. The pathophysiologic basis for these 2 manifestations of INL cystic change following NA-AION will be discussed.

Methods

A retrospective observational case series was performed at the University Hospital of Liège, Belgium. Twenty-three patients who experienced sudden painless monocular loss of vision were referred to our neuro-ophthalmology department or to the emergency department (9 cases). Recruitment took place between 2014 and 2021. The diagnosis of NA-AION was based on the anamnesis (painless sudden loss of vision involving 1 eye) and fundus examination. The latter showed a swollen disc in the affected eye and, in the fellow eye, either a crowded disc (typical of the *disc at risk* associated with NA-AION[20–22]) or sectoral atrophy indicating a previous episode of NA-AION. Spontaneous resolution of the optic disc swelling was noted within 8 weeks and the outcome was sectoral infarction. Giant cell arteritis was excluded by appropriate investigations. The clinical features were not compatible with a diagnosis of optic neuritis. Two patients were excluded because optic nerve head drusen were identified on OCT. Patients were White European, representing the typical local population of the clinic, except 1 who was Turkish. The mean age of the subjects was 60 ± 12.5 years (range, 22–88 years, median: 60.5) and 65.6% were men. A favorable opinion from the ethics committee of the University of Liège for the study had been received. The study adhered to the tenets of the declaration of Helsinki and a written informed consent was obtained for the 3 patients described in this case series.

The patients were all followed up at baseline and at 1, 3, and 6 months postepisode. Fundus fluorescein angiography and a macular spectral-domain OCT (Heidelberg Engineering) were performed in 27 patients at baseline: 6-line radial scans and 25-line raster scans centered on the fovea were obtained. Subsequently, patients were seen annually. Clinical examination included best-corrected visual acuity (BCVA, Snellen scale), slit-lamp examination, and fundus biomicroscopy. At follow-up, patients underwent automated perimetry (VF, Humphrey 24-2), with appropriate refractive correction and OCT (high-definition OCT Cirrus, Carl Zeiss Meditec), for which manual correction of segmentation was not possible. The thickness of the peripapillary retinal nerve fiber layer (pRNFL) and of the ganglion cell complex (GCC) (inner plexiform layer + ganglion cell layer) were evaluated at each visit along with en face OCT B-scan. Studies demonstrating poor image quality, not allowing adequate visualization of all retinal layers, were excluded. Scans were analyzed for the presence of intraretinal fluid and subretinal fluid by 3 skilled observers who were masked as to the aim of the study. For the 3 patients described in this series, INL thickness was also evaluated initially and at the latest follow-up visit. For INL thickness assessment, adequate segmentation was assessed and adjusted manually in 1 case with macular spectral domain OCT.

Grading of the acute optic disc swelling was conducted as a function of the mean RNFL thickness and the numbers of quadrant sectors involved (temporal, superior, inferior, nasal). For example, optic disc swelling showing pRNFL thickening in at least 1 sector to be < 120 μm was considered moderate. In the 3 cases described below, the swelling of the disc was considered severe because all sectors were involved (pRNFL thickness of all sectors > 120 μm) and the mean pRNFL thickness was high (mean [± SD], 257.7 ± 81 μm; range, 189–347 μm).

Results

Summary of Findings

In a cohort of 34 patients (45 affected eyes and 23 healthy fellow eyes), we identified a transient microcystic change in the INL associated with optic disc swelling in 19 eyes at presentation. In these cases, the vacuoles were localized to the INL and were associated with transudation of intraretinal and subretinal fluid originating from the optic disc (see Fig 1 for 1 example). The microcystic change in these cases was transient and had resolved in all cases at 1 month (Fig 1). In cases with moderate optic disc swelling assessed in the global cohort, cystic changes were visible only in the peripapillary region (e.g., Fig 1). Four patients, who had shown this transient change subsequently developed MME that remained fixed during the period of observation (range, 12–34 months). The other cases (n = 30) did not show MME during the follow-up period.

At baseline, mean INL thickness in these 3 cases was 48.9 ± 17.03 μm in the affected eyes compared with 45.3 ± 1.7 μm in the unaffected eyes ($P = 0.77$). Inner nuclear layer thickening was greatest in case 2 associated with the greatest microcystic change (mean INL thickness: 68.4 and maximal INL thickness 137 μm). At the final follow-up visit (range, 2–3 years postepisode), no significant INL thinning was observed between the affected and unaffected eyes (40.7 ± 5.3 μm and 39.4 ± 2.0 μm, respectively). However, we observed an upward trend in affected eyes, possibly related to the continuing presence of microcystic change. Significant GCC thinning was observed at 6 months in all patients compared with the unaffected eye in the superior hemimaculae (mean loss of GCC thickness, −28.2 ± 5.2 μm [−33.3%, range, −22.3 to 30.3 μm]) and in the inferior hemimaculae (mean loss of GCC thickness, −30.7 ± 5.6 μm [−31.0%, range, −24.3 to 34.8 μm]) (Fig 2). We observed a significant GCC thinning in both hemimaculae in patients with MME compared with the entire cohort, in which greater involvement of the superior hemimacula is shown (mean superior hemimacula thinning: −23.01 ± 9.33, −27.9%, range, 1–40.7 μm, mean inferior hemimacula thinning: −19.14 ± 12.1 μm, −28.51%, range 5 to −39 μm; Fig 2). In 2 patients with similar lesion of GCC, only 1 had also MME (Fig 2). This additional patient of the cohort who had significant thinning of both the superior and inferior hemimaculae at 6 months had also significant MME observed (yellow dot in Fig 2). The other case without MME had a better fovea threshold (25 dB), suggesting a better residual function than the other (mean ± SD: 16 ± 2.6). Finally, in these 3 patients, we observed significant thinning of the RNFL at 6 months (mean pRNFL, 57.7 ± 2.5 μm; temporal RNFL, 48.7 ± 1.5; nasal pRNFL, 56 ± 6.2; inferior pRNFL, 62 ± 2.6 μm; and superior pRNFL, 63.7 ± 3.5). Mean pRNFL was especially thin compared with the overall cohort (mean pRNFL, 62.3 ± 9.7 μm; median, 61 μm; temporal pRNFL, 51.7 ± 15.5 μm; median, 49.5 μm, nasal pRNFL, 60.1 ± 11.8 μm;

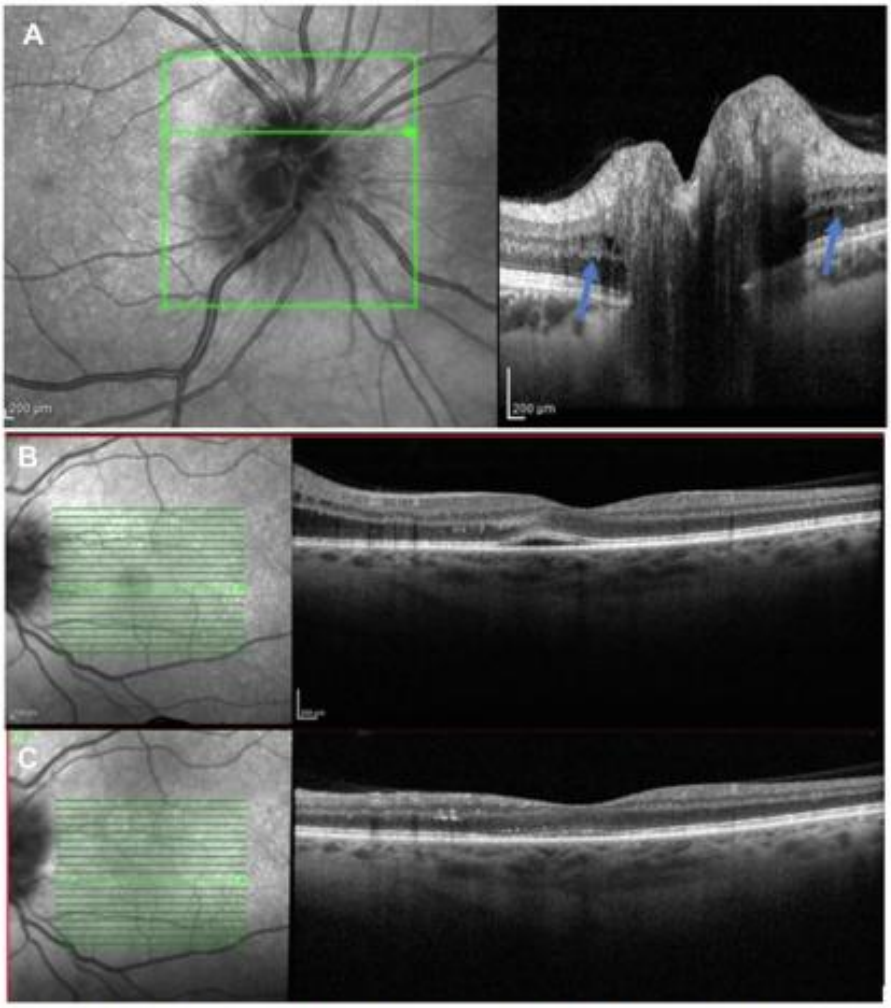

Figure 1. Spectral-domain OCT (Heidelberg Engineering) imaging. **A**, Microcystic change visible in the peripapillary region in moderate swelling of the disc (cohort case; blue arrows). **B**, Transudation of fluid through the retina at presentation. **C**, Twenty-three days later in 1 case selected from the 19 out 34 cases showing disc change without subsequent retrograde maculopathy (cohort case).

median: 49.5 µm; inferior pRNFL, 74.9 ± 24.4 µm; median, 66 µm; and superior pRNFL, 62.78 ± 13 µm; median, 62 µm).

Case Histories

Case 1. A 42-year-old man was referred because of sudden painless loss of vision in his right eye, which developed 4 days previously. At presentation, the BCVA was 1/20 in the right eye and 10/10 in the left eye. Funduscopy showed an optic disc swelling and hemorrhages in the right eye. In the left eye, a crowded disc was noted. A diffuse visual field defect with a central involvement was observed in the affected eye (Fig 3). OCT showed significant thickening of the mean pRNFL (363 µm) and a normal thickness of GCC (85 µm). Peripapillary microcystic edema in the INL was also observed on the macular OCT. Fundus fluorescein angiography showed a superior hypoperfusion of the optic disc and a late leakage around it. No choroidal filling defect was observed.

Complete blood count and inflammatory biomarkers (erythrocyte sedimendation rate or C-reactive protein) were within normal limits. However, hypercholesterolemia (low-density lipoprotein [LDL], 121 mg/dL; reference range, < 100 mg/dL) was noted. Severe obstructive sleep apnea was diagnosed following polysomnography, and preexisting hypertension was shown to have been inadequately treated. Magnetic resonance imaging with and without gadolinium enhancement of the brain demonstrated evidence of small vessel disease. A diagnosis of NA-AION was made.

At follow-up visits, OCT showed a diffuse thinning of the GCC (55 µm at 3 and 6 months) and a significant thinning of the mean pRNFL (64 µm at 3 months and 55 µm at 6 months). Microcysts were observed in the INL in a perifoveal circular distribution. The cysts appeared similar

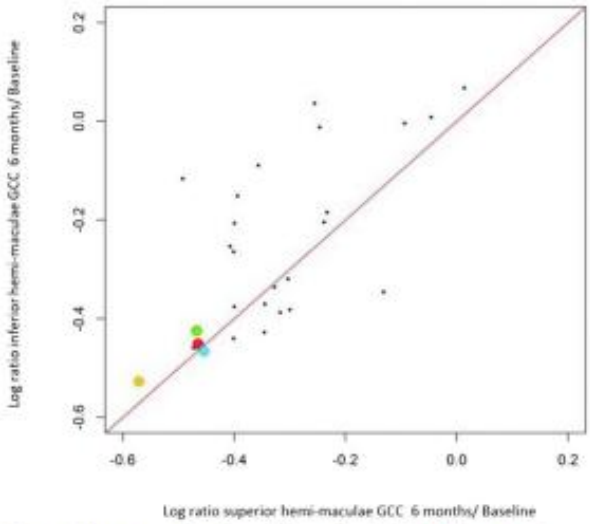

Figure 2. Log ratio of ganglion cell complex (GCC) thickness in the superior and inferior hemimaculae between 6 months and baseline. Patients with microcystic macular edema (MME) had significant thinning of both the superior and inferior hemimaculae (case 1: blue dot, case 2: green dot, and case 3: red dot). One additional patient of the cohort who had significant thinning of both the superior and inferior hemimaculae at 6 months had also significant MME observed (yellow dot).

to those seen at presentation apart from the location (Fig 4). The microcysts were first seen 4 months postepisode in the superior hemimacula, corresponding to the greater involvement of the inferior visual field. At 6 months cystic change in the inferior and central regions of the macula was observed and persisted unchanged at the most recent assessment (34 months; Fig 4).

Case 2. A 67-year-old man, seen for the first time in 2019, experienced sudden loss of vision associated with a superior visual field defect in his left eye (Fig 3). He had a medical history of treated hypertension and had had a pacemaker implanted. He was borderline overweight (body mass index, 24.3). Polysomnography was within normal limits.

At presentation, BCVA was 10/10 in the right eye and 1.5/10 in the left eye. Examination showed the left optic disc swelling. Perimetry revealed a superior visual field defect with a nasal step and central involvement. Early phases of fundus fluorescein angiography showed a superior sectoral delayed filling of the optic disc, confirming the diagnosis of NA-AION.[23] Late leakage at the macula was not observed, excluding local vasculopathy. Macular OCT showed subfoveal fluid and microcysts in the INL, which resolved within 1 month as did the pRNFL thickening. Ganglion cell complex analyses were difficult to interpret because of segmentation failure (mean GCC, 70 µm) and pRNFL was thickened (mean pRNFL, 189 µm).

Ophthalmic and neurologic examination were otherwise normal. Complete blood count, blood chemistry, and inflammatory biomarkers were within the respective reference ranges. Magnetic resonance imaging with and without gadolinium enhancement of the brain and orbits was normal.

Six months postepisode, pRNFL was reduced at 58 µm and GCC was thinned (mean GCC, 68 µm). At 1 year

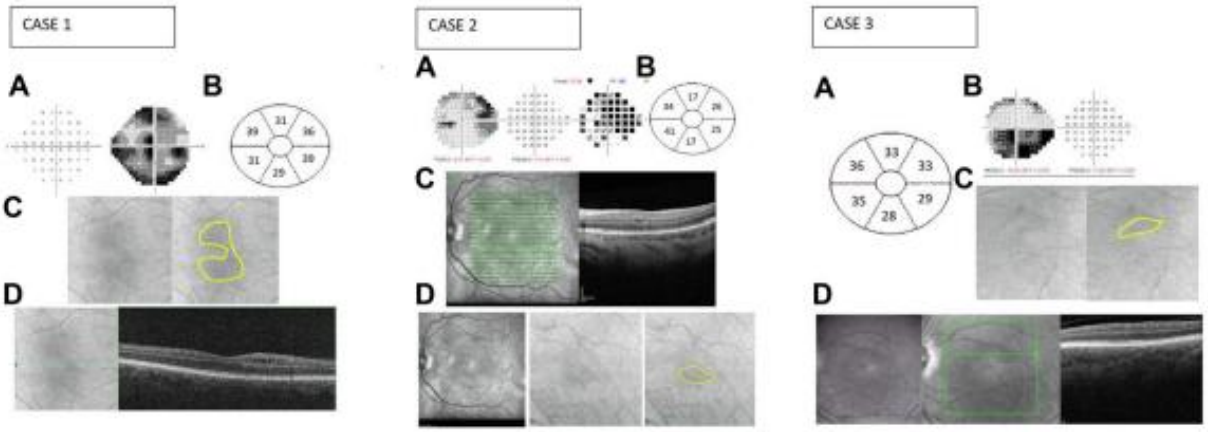

Figure 3. Case 1. **A**, Visual field showing central involvement. **B**, Illustration of Δ ganglion cell layer (GCL) thickness. **C**, Cirrhus high-definition OCT (HD-OCT) fundoscopic images showing a hypointense circular distribution of the inner nuclear layer cystic change. **D**, En face Cirrus OCT showing microcystic macular change (case 1). Case 2. **A**, Visual field showing a superior altitudinal defect. **B**, Illustration of corresponding ΔGCL (µm) thinning between the affected eye at 6 months and the unaffected eye. **C**, En face Heidelberg Retina Angiograph (HRA) OCT (Heidelberg Engineering) showing microcystic macular change located in the inferior hemimacula. **D**, HRA infrared imaging and Cirrhus HD-OCT funduscopic imaging showing an inferior hypointense distribution of the vacuoles. Case 3. **A**, Illustration of corresponding ΔGCL (µm) thinning between the eye before the event and 6 months postepisode. **B**, Visual field showing a superior altitudinal defect. **C**, HD-OCT funduscopy images showing hypointense lesion corresponding to location of microcyst. **D**, HRA en face OCT (Heidelberg Engineering) showing inner nuclear layer microcysts in the inferior hemimacula. This cystic change develops over time, is longstanding, may be permanent, and corresponds with the ganglion cell complex thinning and visual field loss. For each patient, the distribution of cystic change was confirmed by inspection of the horizontal scans.

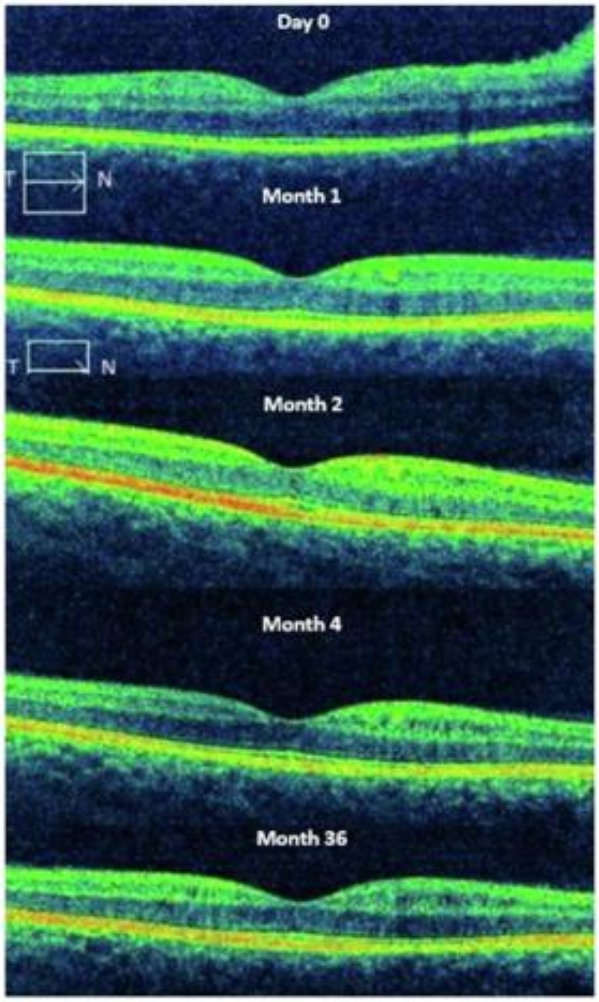

Figure 4. Evolution of the microcysts in the inner nuclear layer that persist over time (case 1) with spectral domian-OCT B-scans (high-definition-OCT Cirrus, Carl Zeiss Meditec).

follow-up, MME was observed to be limited to the inferior hemimacula (Fig 3) matching the area of greater GCC loss.

Case 3. A 52-year-old truck driver presented with blurred vision in his left eye. He had experienced previously blurred vision from an episode of NA-AION in the fellow eye. Best-corrected visual acuity was 1/20 in the right eye and 8/10 in the left eye. A swollen optic disc in the affected eye and diffuse pallor in the fellow eye were observed. The visual field showed an inferior altitudinal defect (Fig 3). Mean pRNFL and GCC were 237 and 67 µm, respectively. Macular OCT scans revealed the traction of the retina induced by the disc swelling associated with fluid between the retinal pigmentary epithelium and the outer nuclear layer together with cystic change in the INL. Fundus fluorescein angiography was not performed at presentation.

Hypercholesterolemia (total cholesterol: 220 mg/dL; reference range, < 190 mg/dL; LDL: 143 mg/dL; reference range < 100 mg/dL) and a slightly elevated glycosylated hemoglobin (43 mmol/mol; reference range, 20–42 mmol/mol) were noted although his complete blood count and inflammatory biomarkers (erythrocyte sedimentation rate or C reactive protein) were within the reference ranges. Polysomnography was performed because of a history of snoring and mild obstructive sleep apnea was diagnosed. Magnetic resonance imaging with and without gadolinium enhancement of the brain was within normal limits.

Thinning of the GCC was observed (55 µm at 3 months and 52 µm at 6 months) and the pRNFL (79 µm at 3 months and 60 µm at 6 months). Microcysts were observed in the superior hemimaculae 6 months postepisode and were persistent at the latest follow-up (24 months postepisode; Fig 4).

Discussion

A degenerative change in the INL following ganglion cell loss was first reported in 1963[24] in postmortem studies of primates following chiasmal transection and shown a few years later in postmortem studies of human cases of optic neuropathy.[25] In the primate study, the cystic degeneration was distributed in an annular perifoveal distribution from approximately 500 µm out, with the foveal margin extending over a further 1 mm, where the ratio of Müller cells to cone bipolar cells is low (1:4 rising to 1:1 at 3 mm eccentricity), although Müller cell to total bipolar cell ratio remains more constant.[26] Histologic examination in the primate study showed debris and tissue in the larger cysts[24]—confirming that is not edema—and some authors have suggested that degeneration of the Müller cells plays a key role because the MME is localized in the poorly perivascularized rim.[1,27,28] Müller cells are glial cells that provide metabolic and structural support to retinal neurons.[29] The microcystic appearance observed in the INL may correlate with the vertical orientation of Müller cells.[30]

Following the use of OCT, it has become possible to identify acute and chronic cystic change in the INL in daily practice and the clinical spectrum of appearances designated MME has widened in recent years.[18] Indeed, it has been described not only in retinal pathology but also in severe optic neuropathy with no known associated retinal pathology and this etiological diversity has led to some confusion among clinicians. There is no consensus regarding the pathogenesis of MME; some authors have suggested that it may be related to retrograde transsynaptic degeneration of bipolar cells[14,25] and others have suggested that it may be related to Müller cell dysfunction.[28,31]

Initially, the 3 patients described above had transient reversible microcystic changes affecting the INL. We propose that this is related to the transudation of fluid from the ischemic optic nerve head sectors extending within and under the retina. This finding recovered spontaneously after 1 month. These microcystic changes were observed in the peripapillary region and were associated with fluid localized between the ellipsoid zone and the outer plexiform layer in the parafoveal region (Fig 1). Because we are describing this microcystic change in the peripapillary region, and as it is likely to be genuine interstitial edema, a better term could be *microcystic peripapillary edema* within the INL

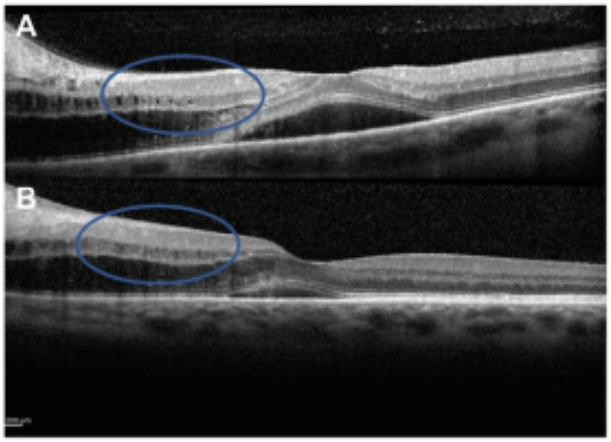

Figure 5. Spectral domain-OCT (Heidelberg Engineering) imaging. Extension of microcystic change in the inner nuclear layer close to the fovea in (**A**) one case from the cohort (cohort case) and (B) case 3. These changes correspond to the degree of optic disc swelling and are reversible with resolution of the retinal edema.

although it can extend into the macula (Fig 5). Subsequently, these 3 patients developed the now *classical* MME in the perifoveal region, which we have shown may be very longstanding, perhaps permanent.

Acute microcytic change associated with disc swelling is probably caused by a disruption of the blood–retinal barrier, as proposed by Gelfand et al,[5] leading to an overwhelming of Müller cell function. Over the past 5 years, various authors have described the presence of a paravascular transport system in the retina and around the optic nerve similar to the glymphatic system existing in the brain.[31–33] In a human postmortem study assessing a cross-section of the optic nerve, Wostyn et al[33] found an accumulation of India ink in paravascular spaces around the central retina vein and artery, which could correspond to an optic nerve glymphatic system. It has also been suggested that a hyporeflective area around the vessel walls observed on OCT provide evidence for such a system.[32] In NA-AION, the glymphatic system could be compromised along with the venous drainage by some common mechanisms observed in ischemia of the optic nerve. Müller cells and the superficial and deep vascular plexuses under normal conditions play a role in the reabsorption of fluid[28,31]; however, following arterial hypoperfusion and extensive extravasation of fluid from capillaries and venules, Müller cells and other mechanisms of tissue homeostasis are saturated. This explains why we observe the OCT microcysts in the INL, similar to what has been observed in MME,[1] although the retinal distribution differs. Another factor may be that the transudate forming subretinal fluid might induce traction on the Müller footplates, explaining the cystic appearance observed.[7,15] Once the disc swelling had resolved, we observed a complete resolution of the cystic change.

In contrast, MME appeared a few months post episode—after 4 months in the first case—and persisted over time (at least 34 months). Burggraaff et al[18] have described that MME was transient in 84% of their series, but most of the cases were age-related macular degeneration and epiretinal membrane traction, in which the pathogenesis may be quite different. In our cases, we observed the persistence of MME, indicating a likely permanent change as also observed by Abegg et al.[14] Therefore, retinal ganglion cell loss inducing vitreoretinal traction on the Müller cells is a less likely pathogenesis than a metabolic change related to retrograde transsynaptic degeneration,[8,16] either dysfunction of existing Müller cells[3] or empty space following Müller cell degeneration that filled with fluid.[13] Indeed, the stationary nature of the cysts over a long follow-up period (3 years), suggesting a fixed change is very unlikely to be interstitial edema (Fig 4).

In NA-AION, patients present with an altitudinal defect corresponding to the loss of ganglion cells induced by hypoperfusion (infarction) of $\geq$ 1 optic disc sectors. We observed a strong relationship between the location of MME and the thinning of ganglion cells, corresponding to the visual field defect. Indeed, MME seems to respect the horizontal meridian in cases 2 and 3, compatible with an effect of retrograde degeneration. Moreover, greater RNFL and GCC thinning were observed in these patients compared with the entire cohort (Fig 2). Contrary to the conclusions of Lee DH et al,[17] in NA-AION, a poorer overall visual outcome is not necessary to observe MME, but rather a significant localized loss of retinal ganglion cells is key. Microcystic macular edema was indeed observed by the authors (A.C.C., G.T.P.) in 2 patients who had poor vision (cases 1 and 2) but also in a patient with good overall vision because central vision was spared (case 3). The question arises as to the impact of the INL change on visual function. Clearly, it signifies greater retinal ganglion cell loss but whether any additional impairment of function occurs is unknown. To investigate this question in NA-AION would require detailed visual function analysis and possibly electroretinography concentrating on the macula, comparing cases with comparable visual field loss with and without MME.

In conclusion, our study indicates 2 causes of MME in the same patients suffering from NA-AION, 1 reversible and the other likely permanent. Müller cell dysfunction seems to play a key role in this finding and offers a potential explanation for both conditions. This finding highlights the distinction between genuine edema related to transudation of fluid (here associated with optic disc swelling) and the phenomenon observed in RM related to the degree of RNFL loss. We consider that MME might be considered a misnomer if there is no tissue edema and, until the exact pathology is identified, would recommend the use of the term *RM*.[13,16] The distribution of the change corresponded in our cases to both the more significant visual field loss and the greater GCC thinning. It appeared after a time interval of some weeks and may persist for many months or years. These are not the characteristics that would be expected if tissue edema were the underlying mechanism giving rise to the INL cystic change. Nonarteritic anterior ischemic optic neuropathy is also a useful model because of the localized retinal change corresponding to localized axonal loss, as has also been found in the nasal hemimacula in chiasmal compression.[34]

Footnotes and Disclosures

Originally received: July 12, 2022.
Final revision: September 13, 2022.
Accepted: September 13, 2022.
Available online: October 4, 2022. Manuscript no. XOPS-D-22-00166R2.

[1] Department of Ophthalmology, Central University Hospital of Liège, University of Liège, Liège, Belgium.

[2] Department of Neurodegeneration and Rehabilitation, UCL Institute of Neurology, Faculty of Brain Sciences, University College London, London, United Kingdom.

Disclosure(s):

All authors have completed and submitted the ICMJE disclosures form.

The authors have no proprietary or commercial interest in any materials discussed in this article.

HUMAN SUBJECTS: Human subjects were included in this study. A favorable opinion from the ethics committee at the University of Liège for the study had been received. The study adhered to the tenets of the Declaration of Helsinki and a written informed consent was obtained for the 3 patients described in this case series.

No animal subjects were used in this study.

Author Contributions:

Conception and design: Chapelle.

Data collection: Chapelle, Plant.

Analysis and interpretation: Chapelle, Plant.

Obtained funding: N/A

Overall responsibility: Chapelle, Rakic, Plant.

Abbreviations and Acronyms:
BCVA = best-corrected visual acuity; **GCC** = ganglion cell complex; **INL** = inner nuclear layer; **LDL** = low-density lipoprotein; **MME** = microcystic macular edema; **NA-AION** = nonarteritic anterior ischemic optic neuropathy; **pRNFL** = peripapillary retinal nerve fiber layer; **RM** = retrograde maculopathy; **VF** = automated perimetry.

Keywords:
Ischemic optic neuropathy, Microcystic macular edema, Neuro-ophthalmology, Retrograde maculopathy, Swollen disc.

Correspondence:
Anne Catherine Chapelle, MD, Department of Ophthalmology, Central University Hospital of Liege, University of Liege, Liège, Belgium. E-mail: ac.chapelle@chuliege.be.

References

1. Gelfand JM, Nolan R, Schwartz DM, et al. Microcystic macular oedema in multiple sclerosis is associated with disease severity. *Brain*. 2012;135:1786–1793.
2. Green AJ, McQuaid S, Hauser SL, et al. Ocular pathology in multiple sclerosis: retinal atrophy and inflammation irrespective of disease duration. *Brain*. 2010;133:1591–1601.
3. Dysli M, Rückert R, Munk MR. Differentiation of underlying pathologies of macular edema using spectral domain optical coherence tomography (SD-OCT). *Ocul Immunol Inflamm*. 2019;27:474–483.
4. Kaufhold F, Zimmermann H, Schneider E, et al. Optic neuritis is associated with inner nuclear layer thickening and microcystic macular edema independently of multiple sclerosis. *PLoS One*. 2013;8:e71145.
5. Gelfand JM, Cree BA, Nolan R, et al. Microcystic inner nuclear layer abnormalities and neuromyelitis optica. *JAMA Neurol*. 2013;70:629–633.
6. Sotirchos ES, Saidha S, Byraiah G, et al. In vivo identification of morphologic retinal abnormalities in neuromyelitis optica. *Neurology*. 2013;80:1406–1414.
7. Barboni P, Carelli V, Savini G, et al. Microcystic macular degeneration from optic neuropathy: not inflammatory, not trans-synaptic degeneration. *Brain*. 2013;136:e239.
8. Lujan BJ, Horton JC. Microcysts in the inner nuclear layer from optic atrophy are caused by retrograde trans-synaptic degeneration combined with vitreous traction on the retinal surface. *Brain*. 2013;136:e260.
9. Kisimbi J, Shalchi Z, Mahroo OA, et al. Macular spectral domain optical coherence tomography findings in Tanzanian endemic optic neuropathy. *Brain*. 2013;136:3418–3426.
10. Haldar S, Mukherjee R, Elston J. Microcystic macular edema in a case of tobacco-alcohol optic neuropathy. *Can J Ophthalmol*. 2017;52:e19–e22.
11. Murata N, Togano T, Miyamoto D, et al. Clinical evaluation of microcystic macular edema in patients with glaucoma. *Eye (Lond)*. 2016;30:1502–1508.
12. Brazerol J, Iliev ME, Höhn R, et al. Retrograde maculopathy in patients with glaucoma. *J Glaucoma*. 2017;26:423–429.
13. Abegg M, Dysli M, Wolf S, et al. Microcystic macular edema: retrograde maculopathy caused by optic neuropathy. *Ophthalmology*. 2014;121:142–149.
14. Abegg M, Zinkernagel M, Wolf S. Microcystic macular degeneration from optic neuropathy. *Brain*. 2012;135:e225.
15. Bhatti MT, Mansukhani SA, Chen JJ. Microcystic macular edema in optic nerve glioma. *Ophthalmology*. 2020;127:930.
16. Mahroo OA, Shalchi Z, Williamson TH, Plant GT. Re: Bhatti et al.: Microcystic macular edema in optic nerve glioma (*Ophthalmology*. 2020;127:930). *Ophthalmology*. 2021;128:e9.
17. Lee DH, Park SE, Lee CS. Microcystic macular edema and cystoid macular edema before and after epiretinal membrane surgery. *Retina*. 2021;41:1652–1659.
18. Burggraaff MC, Trieu J, de Vries-Knoppert WAEJ, et al. The clinical spectrum of microcystic macular edema. *Invest Ophthalmol Vis Sci*. 2014;55:952–961.
19. Munteanu G, Săräcăceanu L. [Idiopathic microcystic macular edema]. *Rev Chir Oncol Radiol O R L Oftalmol Stomatol Ser Oftalmol*. 1988;32:131–135.
20. Beck RW, Servais GE, Hayreh SS. Anterior ischemic optic neuropathy. IX. Cup-to-disc ratio and its role in pathogenesis. *Ophthalmology*. 1987;94:1503–1508.
21. Arnold AC. Pathogenesis of nonarteritic anterior ischemic optic neuropathy. *J Neuroophthalmol*. 2003;23:157–163.
22. Buono LM, Foroozan R, Sergott RC, Savino PJ. Nonarteritic anterior ischemic optic neuropathy. *Curr Opin Ophthalmol*. 2002;13:357–361.

23. Hayreh SS. Anterior ischaemic optic neuropathy. II. Fundus on ophthalmoscopy and fluorescein angiography. *Br J Ophthalmol*. 1974;58:964–980.
24. Van Buren JM. Trans-synaptic retrograde degeneration in the visual system of primates. *J Neurol Neurosurg Psychiatry*. 1963;26:402–409.
25. Gills JP, Wadsworth JA. Degeneration of the inner nuclear layer of the retina following lesions of the optic nerve. *Trans Am Ophthalmol Soc*. 1966;64:66–88.
26. Masri RA, Weltzien F, Purushothuman S, et al. Composition of the inner nuclear layer in human retina. *Invest Ophthalmol Vis Sci*. 2021;62:22.
27. Bringmann A, Reichenbach A, Wiedemann P. Pathomechanisms of cystoid macular edema. *Ophthalmic Res*. 2004;36:241–249.
28. Balk LJ, Killestein J, Polman CH, et al. Microcystic macular oedema confirmed, but not specific for multiple sclerosis. *Brain*. 2012;135:e226.
29. Bringmann A, Pannicke T, Grosche J, et al. Müller cells in the healthy and diseased retina. *Prog Retin Eye Res*. 2006;25:397–424.
30. Matet A, Savastano MC, Rispoli M, et al. En face optical coherence tomography of foveal microstructure in full-thickness macular hole: a model to study perifoveal Müller cells. *Am J Ophthalmol*. 2015;159:1142–1151.e3.
31. Petzold A. Retinal glymphatic system: an explanation for transient retinal layer volume changes? *Brain*. 2016;139:2816–2819.
32. Denniston AK, Keane PA, Aojula A, et al. The ocular glymphatic system and idiopathic intracranial hypertension: author response to "hypodense holes and the ocular glymphatic system". *Invest Ophthalmol Vis Sci*. 2017;58:1134–1136.
33. Wostyn P, De Groot V, Van Dam D, et al. The glymphatic system: a new player in ocular diseases? *Invest Ophthalmol Vis Sci*. 2016;57:5426–5427.
34. Monteiro MLR, Sousa RM, Araújo RB, et al. Diagnostic ability of confocal near-infrared reflectance fundus imaging to detect retrograde microcystic maculopathy from chiasm compression. A comparative study with OCT findings. *PLoS One*. 2021;16:e0253323.

Chapelle AC, Rakic JM, Plant GT. The Occurrence of Intra- and Sub-Retinal Fluid in Anterior Ischemic Optic Neuropathy: Pathogenesis, Prognosis and Treatment. Ophthalmology 2023.

AMERICAN ACADEMY
OF OPHTHALMOLOGY®

The Occurrence of Intraretinal and Subretinal Fluid in Anterior Ischemic Optic Neuropathy

Pathogenesis, Prognosis, and Treatment

Anne-Catherine Chapelle, MD,[1,*] *Jean-Marie Rakic, MD, PhD,*[1] *Gordon T. Plant, MD, FRCOphth*[2,*]

Purpose: To describe the frequency and characteristics of intraretinal and subretinal fluid in nonarteritic anterior ischemic optic neuropathy (NAAION) and to assess the influence on the visual deficit and optic nerve fiber/ganglion cell loss.

Design: A retrospective, single-center study.

Participants: Thirty-two patients with NAAION referred to our Neuro-ophthalmology Department between 2014 and 2021.

Methods: The study was carried out at the University Hospital of Liège, Belgium. For participants in whom subretinal fluid was identified on standard OCT (Carl Zeiss Meditec) an additional macular OCT (Spectralis Heidelberg) had been performed. The pattern and the maximal height of the retinal fluid were determined manually, and thicknesses of retinal layers were obtained using the OCT protocol analysis.

Results: The mean age of the cohort was 60 years (standard deviation, ±12.5; range, 22–88 years), and 65.6% were male. In the 21 eyes (46.7%) in which retinal fluid was observed, macular OCT findings were categorized according to fluid localization: 19 cases had parafoveal fluid (of whom 9 also had subfoveal fluid). One patient had subfoveal fluid alone, and 1 patient had peripapillary subretinal fluid alone. Specific patterns of optic disc (OD) swelling were associated with the occurrence and distribution of retinal edema. Visual acuity, visual field loss, and foveal thresholds were stable over the period of observation ($P = 0.74$, $P = 0.42$, and $P = 0.36$, respectively). No difference was found in visual function at 6 months between patients with retinal fluid treated (n = 10) or not treated (n = 11) with corticosteroids (visual acuity, $P = 0.13$; foveal threshold, $P = 0.59$; mean deviation, $P = 0.66$).

Conclusions: Subretinal fluid is found in a high proportion of cases of NAAION. Visual function remained largely stable from presentation in this cohort. Corticosteroid intake at presentation did not influence visual recovery or timing of the resorption of tissue edema. Our findings do not support treatment of NAAION with corticosteroids with or without evidence of subretinal fluid acutely. With regard to pathogenesis, we propose that the volume of transudate generated at the OD is the critical factor rather than dysfunction of retinal mechanisms subserving reabsorption.

Financial Disclosure(s): Proprietary or commercial disclosure may be found in the Footnotes and Disclosures at the end of this article. *Ophthalmology 2023;■:1–10 © 2023 by the American Academy of Ophthalmology*

After glaucoma, nonarteritic anterior ischemic optic neuropathy (NAAION) is the most common optic neuropathy affecting people aged more than 50 years.[1] The condition was first clearly defined as a clinical syndrome by Hayreh in 1974.[2] Patients present with painless unilateral acute loss of vision associated, by definition, with a swollen optic disc (OD).[1] Subacute loss (progression over days or weeks) may occur.[3] The fellow eye may be involved sequentially. The disc swelling results from ischemia secondary to sectoral hypoperfusion of the prelaminar optic nerve head due to failure of the posterior ciliary arteriolar supply. The ultimate cause of the failure of arterial supply is unknown, but a major risk factor is a "crowded" OD, which is a common variant of OD morphology (absence of a cup).[4,5]

Many important questions regarding the disorder remain unanswered. A significant pathological feature in the acute setting is the finding of subretinal fluid.[6,7] Our aim in this study has been to characterize the occurrence and significance of associated retinal edema. The use of corticosteroids to decrease the capillary leakage presumed to underly the formation of fluid has been proposed to decrease OD swelling and potentially improve visual outcome.[8] In the reported study, a higher probability of visual improvement was found in patients treated with oral prednisone 80 mg daily from presentation. However, Rebolleda et al[9] found no change with this intervention. Others have proposed the use of intravenous or oral prednisone specifically in patients with subretinal fluid.[10,11]

https://doi.org/10.1016/j.ophtha.2023.07.015
ISSN 0161-6420/23

OCT has revolutionized the analysis of optic nerve and retinal disorders. In addition to the demonstration of pathological changes in the thickness of the retinal layers, certain changes in their intrinsic architecture, in particular the presence of fluid, can be demonstrated. In studies of NAAION, OCT shows an increased peripapillary retinal nerve fiber layer (pRNFL) thickness[12] (confirming the clinical observation of OD swelling) followed by progressive thinning over a few months of the affected sectors as atrophy ensues.[6]

Therefore, subretinal fluid is now detected more easily in clinical practice.[13] Clinicians refer to serous retinal detachment when the source of subretinal fluid is the retinal vessels, choroidal vessels, or both, as in central serous retinopathy (CSR), central retinal venous occlusion (CRVO), or Vogt-Koyanagi-Harada syndrome.[14] However, subretinal fluid also can be seen in other pathological processes associated with a swollen disc (NAAION, myelin oligodendrocyte glycoprotein optic neuritis, papilledema due to raised intracranial pressure, and prelaminar optic neuritis such as neuroretinitis).[15] Subretinal fluid is observed between the retinal pigment epithelium (RPE) and the neurosensory retina in the subretinal space, the remnant of the embryonic optic vesicle.[16] The subretinal region concerned is composed of the interphotoreceptor matrix that surrounds the photoreceptors and their outer segments.[17] Anatomically this constitutes a *potential* space where fluid can accumulate in certain conditions.

The aim of the study reported has been to assess the incidence and severity of subretinal fluid at presentation using the precision of OCT measurement. We wanted to investigate the influence on visual outcome and to further elucidate the pathogenesis. We also wanted to highlight the frequency of this finding because its presence acutely or a subsequent "macular star" (formed by so-called hard exudates around the macula) may lead to a misdiagnosis of neuroretinitis (personal observations of the authors). We also considered that the study of anterior ischemic optic neuropathy may increase our understanding of edema dynamics in ischemic neural tissue.

Methods

This retrospective observational study aimed to assess the evolution of patients with NAAION after changes in both visual function and fundus imaging. The diagnosis of NAAION was made on clinical history and the funduscopic findings. Patients presented with unilateral painless loss of vision. There were no systemic signs or symptoms of giant cell arteritis, and inflammatory biomarkers (erythrocyte sedimentation rate or C-reactive protein) were within the respective reference ranges.

We reviewed the records of 34 patients (45 affected eyes and 23 healthy fellow eyes) who presented with NAAION between 2014 and 2021 in the Ophthalmology Department of the University Hospital of Liège, Belgium. Two patients (3 affected eyes and 1 healthy fellow eye) with NAAION associated with optic nerve drusen were excluded from the study. Seven patients had a subsequent episode and 4 patients had a previous episode of NAAION in the fellow eye (Graph 1). Risk factors such as obstructive sleep apnea (OSA), hypertension diabetes, and obesity were recorded for each patient. All patients, except those who had had a previous episode of NAAION, demonstrated OD crowding in the fellow eye. Prior medication including antihypertensive treatment was also noted. After the diagnosis of NAAION, blood pressure measurement and a polysomnography study were performed routinely for all patients. When blood pressure was found to be elevated at presentation, 24-hour ambulatory blood pressure monitoring was performed, whether or not there was a history of treated hypertension.

The following ophthalmic examinations were carried out: visual field (Humphrey 30-2), best-corrected visual acuity (Snellen scale), and OCT (HD-OCT Cirrhus, Carl Zeiss Meditec). The latter was performed at baseline and after 1, 3, and 6 months. Peripapillary retinal nerve fiber layer (pRNFL) and the inner plexiform layer + ganglion cell layer (ganglion cell complex [GCC]) thickness were evaluated at each visit. Fundus fluorescein angiography was performed at baseline in 27 affected eyes (64.3%).

Thirty-one eyes had an examination within a median of 5 days of symptom onset (range, 1−30 days). When subretinal fluid was identified on Cirrus OCT, a macular OCT (Spectralis) was performed. The maximal extent of both subfoveal and parafoveal fluid height was measured manually by one of the authors and by 2 technicians and 1 ophthalmologist, who were blinded as to the aim of the project. The maximal height was defined as the maximal distance between the RPE and the photoreceptor layer on the OCT images within the foveal area (in the case of subfoveal fluid) and the peripapillary region (peripapillary fluid). The maximal parafoveal fluid height was defined as the maximum vertical distance between the outer plexiform layer and ellipsoid zone in the peripapillary region on the macula OCT images. Interobserver reproducibility was evaluated by the intraclass correlation coefficient (ICC).

Results were expressed as mean and standard deviation (SD) for quantitative variables and as frequency tables (numbers, percentages) for qualitative findings. Spaghetti plots were used to display the evolution of vision over time among patients. The association between 2 quantitative variables was assessed by Spearman rank correlation coefficient. To compare mean values, 1-way analysis of variance was used, and the chi-square and Fisher exact tests were applied to compare proportions. Results were considered significant at the 5% critical level ($P < 0.05$). All statistical calculations were performed with SAS version 9.4 (SAS Institute Inc).

A post hoc analysis was performed to analyze the impact of corticosteroids on visual recovery in patients with subretinal fluid. When reviewing the charts, decision to treat was based on the clinician assessment and the severity of the swollen disc. Patients were also routinely treated if there had been a previous episode in the fellow eye. Within the subgroup found to have subretinal fluid (n = 21), the cases treated (n = 10) and not treated (n = 11) with corticosteroids were compared with respect to age, sex, initial visual acuity, intraocular pressure, identified risk factors, pRNFL and GCC thickness, visual field, and refractive error.

Informed consent was obtained from all patients. A favorable opinion of the ethics committee at the University of Liège for the study had been received. The study adhered to the tenets of the Declaration of Helsinki.

Data Availability

All data underlying the results are available within the article, and no additional source data are required.

Results

Summary of Findings

A total of 32 patients were included in the analysis, with a mean age of 60 years (SD, ±12.5; range, 22−88 years, median, 60.5). A

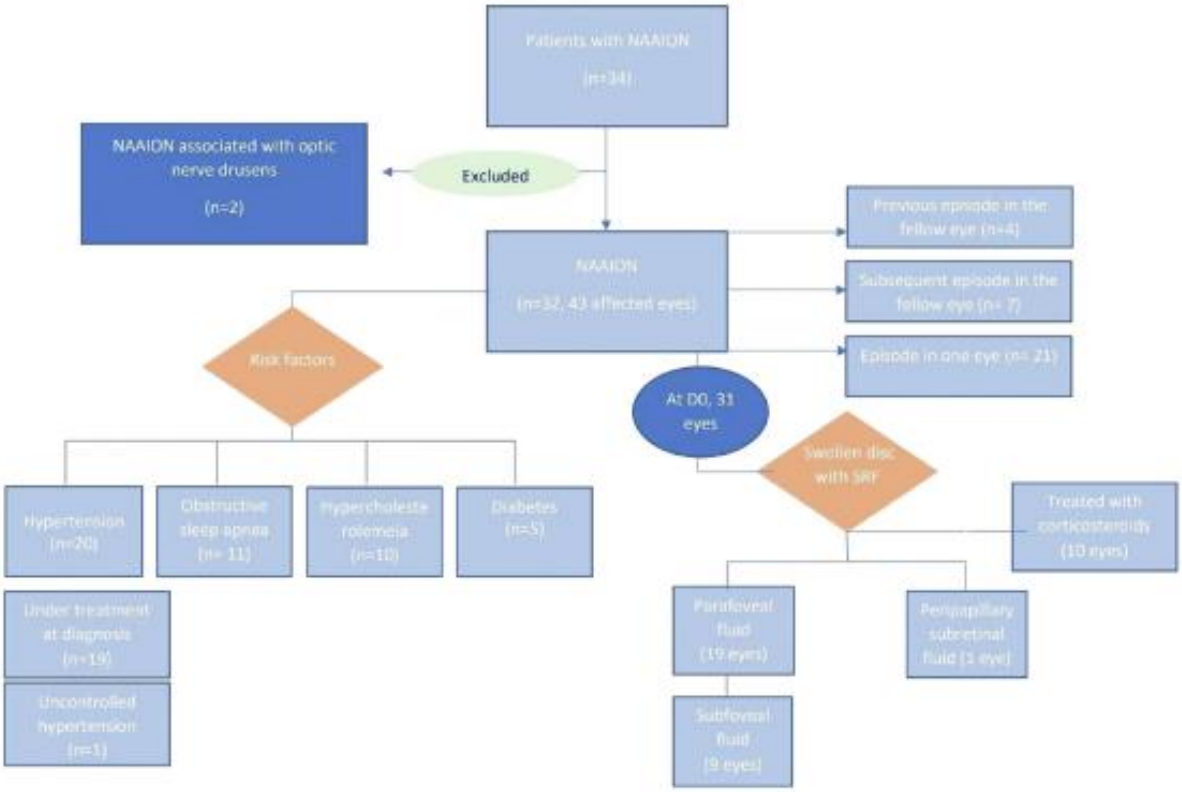

Figure 1. Flowchart of patients in the cohort study. NAAION = Non-Arteritic Anterior Ischemic Optic Neuropathy; SRF = subretinal fluid.

total of 65.6% were male (Fig 1). Four patients (12.5%) included in the study had a history of NAAION in the fellow eye. At presentation, mean (± SD) pRNFL thickness in patients with NAAION was 227.1 µm (±70.1) and 92.3 µm (±8.5) in the unaffected eyes ($P < 0.05$). At 6 months, a significant decrease was observed in the affected eyes (62.4 [±10.0] µm, $P < 0.0001$). Ganglion cell layer thickness at presentation and at 6 months in the NAAION eyes were 67.2 ± 18.7 µm and 61.1

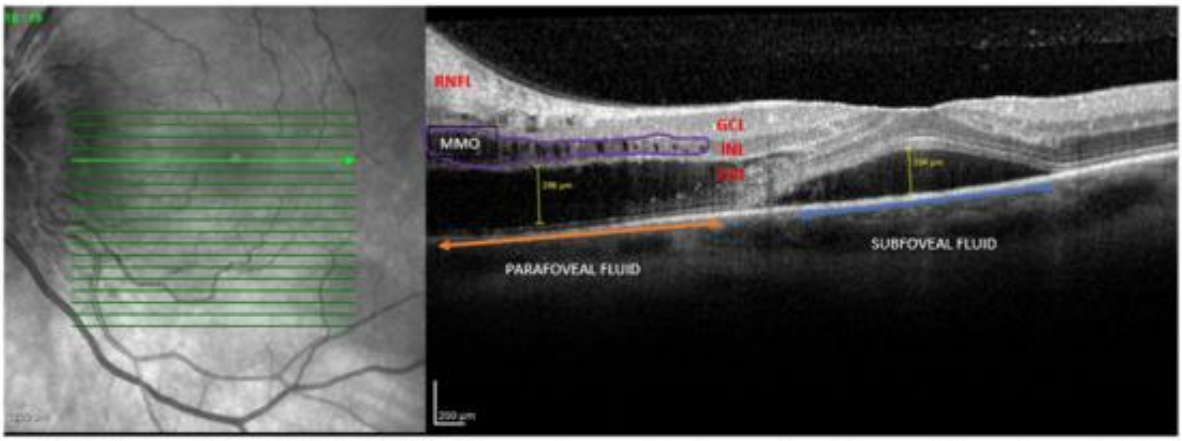

Figure 2. Macular spectral-domain (SD)-OCT (Heidelberg Engineering) imaging. Vertical section through the retina (right image) as indicated by the green arrow in the en face image (left). Thickening of the ganglion cell layer and retinal nerve fiber layer, microcystic macular edema (MME) in the inner nuclear layer, and fluid infiltration of the outer nuclear layer visible in the macular region in moderate disc swelling (cohort case in the subfoveal group). Arrows labeling subfoveal (blue) and parafoveal fluid (orange) and outline (purple) labeling MME. Measurements of fluid height are shown (see text). GCL = ganglion cell layer; RNFL = retinal nerver fiber layer; INL=inner nuclear layer; OPL= outer plexiform layer.

± 9.4 μm, respectively, a nonsignificant difference. However, when compared with the unaffected fellow eyes (80.9 ± 6.5 μm), we observed a significant reduction of the GCC thickness corresponding to a mean loss of 24.8% (median, 27.6%; range, 2.5%–42.6%; $P < 0.0001$) at 6 months. A slight increase of the GCC thickness was observed between baseline and 1 month, likely related to segmentation artefacts induced by the swollen disc and the presence of subretinal fluid. After excluding segmentation artefacts relating to subretinal fluid, the mean GCC at presentation was 72.8 ± 8.5 μm (n = 11), and a positive correlation ($r = 0.727$, $P < 0.005$) was observed between Δfoveal thickness and Δmean GCC thickness at 1 month, confirming a likely causative association. Finally, an inferior altitudinal defect, either complete or sectoral, was observed in the majority of patients (24 eyes, 75%).

Retinal Fluid Associated with NAAION

Macular OCT performed at presentation showed retinal fluid in 21 eyes (46.7%). The appearance was divided into 3 categories according to the localization of the fluid: peripapillary subretinal fluid (n = 1), that is, subretinal fluid localized to the peripapillary region; subfoveal fluid (n = 9), that is, subretinal fluid localized to the foveal region; and parafoveal fluid (n = 19), that is, fluid localized between the ellipsoid zone and the outer plexiform layer in the parafoveal region. Both subfoveal fluid and parafoveal fluid were found in 9 of 21 cases. One patient had subfoveal fluid alone (n = 1) in the context of NAAION associated with severe systemic hypertension. The maximal subfoveal fluid height ranged from 66 μm to 204 μm (mean ± SD, 136.8 ± 71.8 μm; median, 148 μm, ICC [95% confidence interval] and between the 4 observers was 0.90 μm (0.85–0.98 μm). The parafoveal height ranged from 59 μm to 310 μm (mean ± SD, 162.8 ± 68.9 μm; median, 165 μm; ICC (95% confidence interval) among the 4 observers was 0.70 (0.60–0.84). The maximal height of peripapillary subretinal fluid was 100 μm. OCT showed thickening of the ganglion cell layer and pRNFL layers and microcystic edema in the inner nuclear layer, similar to what has been termed "microcystic macular edema" (MME),[18] although unlike that finding was associated with fluid infiltration of the outer nuclear layer (Fig 2) and was a transient phenomenon.[19]

Macular thickness map analysis showed that extensive OD swelling involving the superior and inferior temporal sectors of the optic nerve head is associated with subretinal fluid. A "V" pattern (Fig 3) is seen in patients with subfoveal fluid and diffuse OD swelling. Patients with either superior or inferior swelling of the

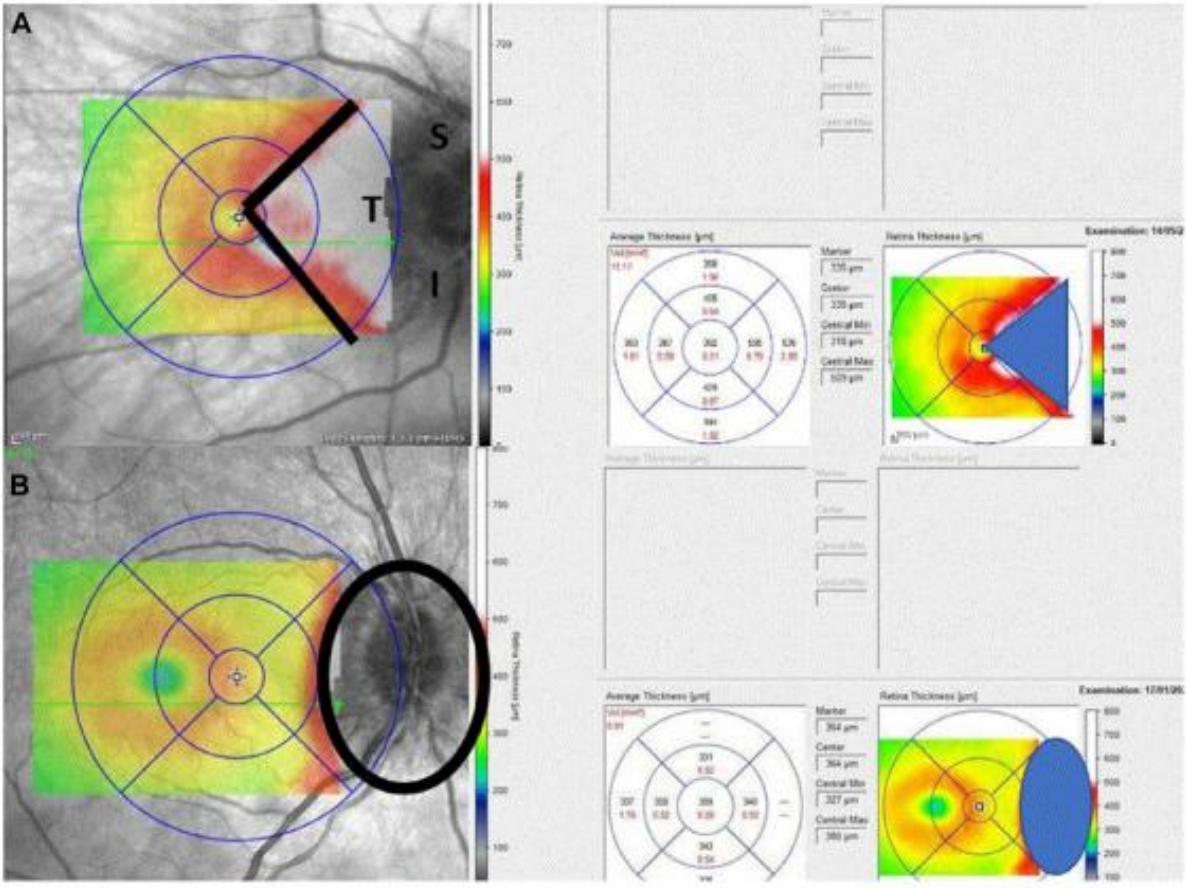

Figure 3. Retinal thickness map in the HRA(Heidelberg Research Architecture)/Spectralis viewing module (Heidelberg Engineering). **A,** Example of subfoveal fluid (blue triangle) observed in a patient with a "V" (black line) pattern of swelling localized to the inferior (I) and superior (S) temporal (T) sectors of the optic nerve. **B,** Example of parafoveal subretinal fluid limited (filled blue oval, right image) to the peripapillary region associated with an "O" pattern (black outline, left image) of optic disc (OD) swelling.

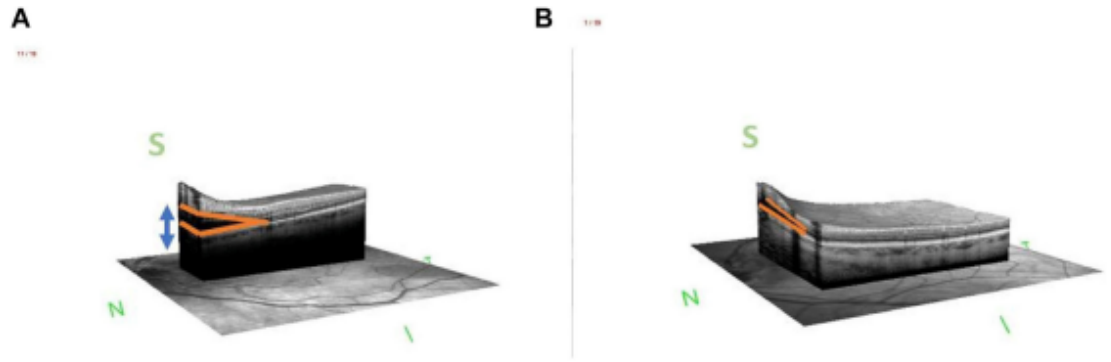

Figure 4. Three-dimensional images in the HRA/Spectralis viewing module (Heidelberg Engineering). **A,** Vitreoretinal traction associated with extensive swelling pushes inward the retinal nerve fiber layer (labeled by the orange outline) (cohort case). **B,** Moderate vitreoretinal traction in patient with optic disc (OD) swelling limited to the superior (S) sector (labeled by the orange line) (cohort case).

OD, but not both, were found to have subretinal fluid, whereas parafoveal subretinal fluid was associated with an "O" pattern (Fig 4). Patients showing the "V" pattern were found to have more marked traction on the retina, as can be observed on the 3-dimensional representation (Fig 5). Although the traction may contribute to the presence of subretinal fluid, it seems that the quantity of fluid generated is also an important factor. Indeed, parafoveal (intraretinal) fluid localized less than 1 mm from the fovea is strongly associated with the presence of subfoveal fluid ($P = 0.0021$) compared with fluid localized within 1 and 2 mm or within 2 and 3 mm from the fovea. One explanation might be that a greater volume of transudate led to traction of the retina and consequent overwhelming of reabsorption mechanisms. However, it is important to note that subfoveal fluid tended to resolve before peripapillary fluid. In some cases, subfoveal fluid may have been missed because it had already resolved. Fluorescein angiography, which was performed in 90% of patients with subretinal fluid (19/21 eyes), did not show any leakage in the macular region, excluding the presence of choroidal neovascularization or other factors local to the fovea.

At long-term follow-up, 4 patients were found to have MME (also known as "retrograde maculopathy" because of its association with ganglion cell loss).[20] These cases are described in detail by Chapelle et al.[19]

Evolution of Visual Acuity in Patients with NAAION Associated with Retinal Fluid

Overall, visual acuity, mean deviation (MD) (visual field), and foveal thresholds were stable over time after the initial assessment ($P = 0.74$, $P = 0.42$, and $P = 0.36$, respectively) (Fig 6). An upward trend observed between presentation and 1 month after the episode in patients with subfoveal fluid perhaps was related to the resorption of fluid ($P = 0.97$). However, it is also seen in the subgroup without subretinal fluid (Fig 7). Regarding visual acuity, no significant difference was seen between eyes with or without subretinal fluid ($P = 0.91$) or between the different subtypes of retinal fluid ($P = 0.42$) (Fig 7). There was not a correlation between the visual acuity and the thickness of subretinal fluid or between the foveal threshold and the thickness of subretinal fluid at presentation and at 6 months. Moreover, subjective refraction remained the same at presentation and after resorption of fluid in the subfoveal group (0.53 ± 1.3 and 0.48 ± 1.2), and evidence of acquired hyperopia was not found.

Effect of Corticosteroid Therapy on Visual Prognosis

Among eyes with a swollen disc associated with retinal fluid, 10 were treated with oral methylprednisolone (MP) 64 mg daily tapered down over 1 month and 11 eyes were not treated. Although there was no randomization, characteristics of both groups were similar for age (55.7 ± 13.1 in the MP group and 61.5 ± 7.8.; $P = 0.44$), gender (90% of men in the MP group and 72.7% in the control group; $P = 0.31$), degree of disc swelling at presentation (pRNFL: 242.6 µm in the MP group and 231.8 µm in the control group; $P = 0.7$), initial MD (−12.37 in the MP group and −10.69 in the control group, $P = 0.61$), refractive error (0.35 ± 1.1 in the MP group and 0.75 ± 1.5 diopters in the control group, $P = 0.51$), intraocular pressure (MP group: 17.9 ± 3.3.8 mmHg, control group: 16.18 ± 3.4; $P = 0.28$), and risk factors (arterial hypertension: 60% in the MP group and 72.7% in the control group, $P = 0.54$; OSA: 50% in the MP group and 45.5% in the control group, $P = 0.83$; hypercholesterolemia: 30% in the MP group and 54.5% in the control group, $P = 0.26$; diabetes: 20% in the MP group and 18.2% in the control group, $P = 0.92$). We did not observe any difference in visual function at 6 months (visual acuity, $P = 0.13$; fovea threshold, $P = 0.59$; MD, $P = 0.66$) between these 2 subgroups. Hayreh[8] postulated that corticosteroids accelerate the subretinal fluid resorption. In our study, all patients except 1 did not show subretinal fluid after the first month. To more precisely answer this question, measurements during the first 15 days would need to be performed.

Risk Factors Associated with NAAION

Hypertension was noted in 62.5% of patients (n = 20) and OSA was noted in 34.4% of patients (n = 11) in the entire cohort. Among patients with hypertension, 95% (n = 19) were receiving antihypertensive treatment before the attack. Only 1 patient in the entire cohort had uncontrolled hypertension confirmed by 24-hour blood pressure monitoring. This patient was found to have subretinal fluid. The hypertension rate in our study is not consistent with the previous studies that showed a lower rate, ranging from 34% to 57%.[5,21] A possible consideration is that it may be the hypotensive treatment

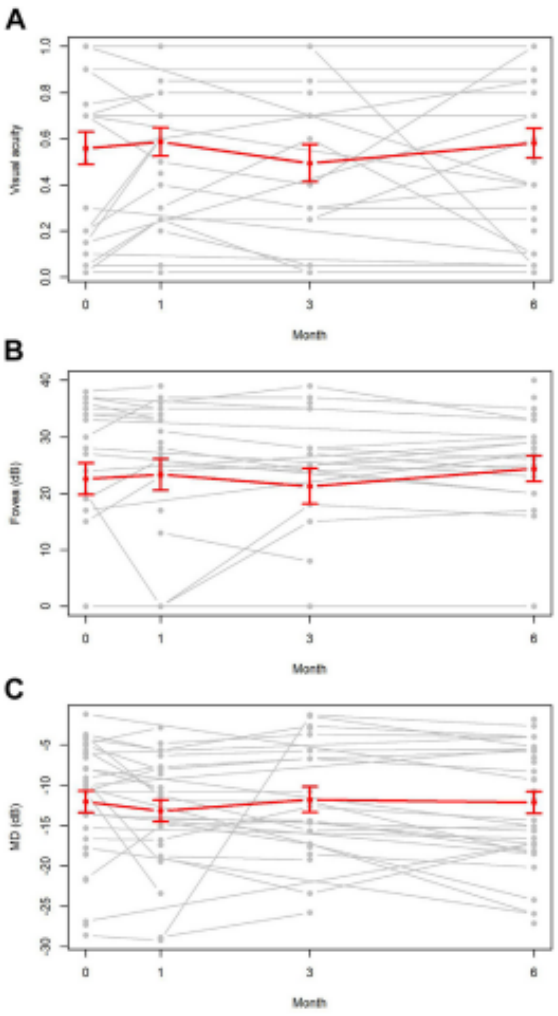

Figure 5. Spaghetti plot graph. **A,** Evolution of mean visual acuity (Snellen scale) over 6 months. **B,** Evolution of mean foveal threshold (decibels [dB]) over 6 months. **C,** Evolution of MD (dB) over 6 months. Overall, these measures remain stable from acute presentation to 6-month follow-up. MD = mean deviation.

(resulting in nocturnal hypotension) that is a risk factor for NAAION rather than hypertension (as has been suggested by Hayreh[22,23]), although in the authors' experience, NAAION occurring in the context of a documented episode of systemic hypotension tends to occur bilaterally. Five patients (15.6%) in the entire cohort had diabetes, but none of these patients demonstrated subfoveal fluid associated with the OD swelling.

Discussion

Influence of Retinal Fluid on Visual Outcome

In a study including 76 patients with NAAION, subretinal fluid was observed in 50% of patients but was subfoveal in only 10%,[7] a lower rate than found in the present study. This discrepancy likely is to be due to the first examination of the patients being undertaken with a median of 5 days after the onset of the symptoms, whereas patients in the cited study were examined up to 4 weeks after onset. It is important to recognize the association of NAAION with retinal fluid to avoid confusion with neuroretinitis[24] and some case of optic neuritis.[15] The question also arises as to whether the presence or absence of subretinal fluid influences outcome and thus, potentially, management.

A significant deterioration of visual acuity has been reported in idiopathic intracranial hypertension where subfoveal and parafoveal fluid due to papilledema[25] are observed and in patients with CRVO and serous retinal detachment.[26] However, we did not observe any effect of the presence of retinal fluid on visual acuity, MD, or foveal threshold at 6 months. In contrast to these other conditions, the rapid resolution of the subfoveal fluid in NAAION does not lead to photoreceptors or RPE dysfunction. In acute CSR, for example, impairment of RPE function generates fluid.[27] In NAAION, the transudate is passively transferred from the ischemic OD in the absence of local cellular dysfunction. However, it has also been demonstrated in CSR that subretinal fluid height itself may be negatively correlated with foveal retinal sensitivity and the foveal retinal defect even with preserved visual acuity.[28] In our study, there was no correlation between the presence or absence of subretinal fluid and the foveal retinal threshold. We assume that the volume of fluid was insufficient to impair contrast sensitivity. Some authors have suggested treatment with corticosteroids to accelerate recovery, perhaps by avoiding permanent macular damage[10] or by earlier resolution of OD swelling and subretinal fluid.[29] In our cohort, we found no significant difference in visual outcome between patients with retinal fluid (subfoveal or parafoveal fluid) who were treated with steroids and those who were not on recovery at 1, 3, and 6 months (Fig 7).

To conclude, we have addressed the following: "Does subfoveal fluid affect our management in NAAION?" One issue is that erroneous measurements using ganglion cell OCT analysis may occur in patients with subretinal fluid. Second, Hedges[7] and Hoye[25] found a correlation between visual acuity deficit and subretinal fluid. However, no statistical analysis was carried out and the cohort studied was small in number. Our findings confirm only a nonsignificant upward trend in visual acuity recovery in the subgroup of patients with subfoveal fluid. The detection of subretinal fluid in the acute assessment of NAAION may have little or no influence on prognosis. Furthermore, corticosteroid intake at presentation did not affect visual recovery in our cohort. Our findings do not support a change in management in cases of NAAION found to have subretinal fluid.

Pathogenesis of Intraretinal and Subretinal Fluid in NAAION Compared with Other Disorders

In NAAION, it is hypothesized that hypoperfusion of the optic nerve induces axoplasmic flow stasis and leads to

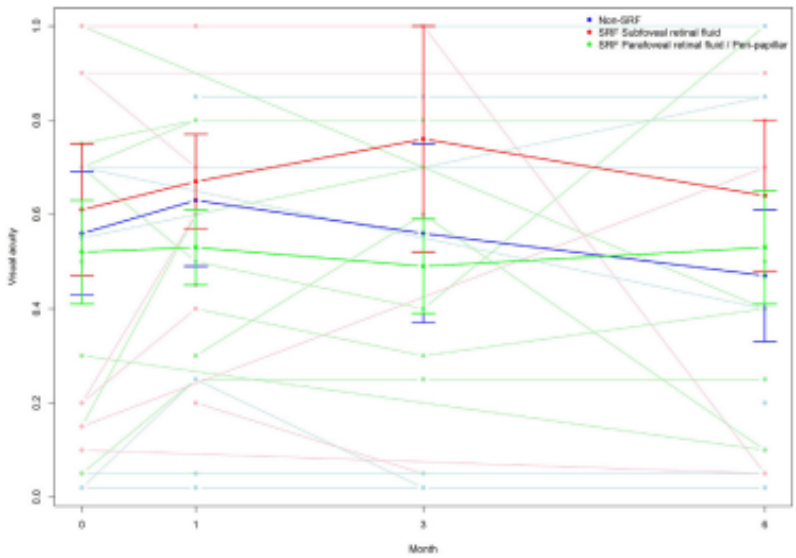

Figure 6. Spaghetti plot graph. **A,** Comparison of mean visual acuity over 6 months in patients with subretinal fluid and patients without retinal fluid (subgroup without subretinal fluid: blue line, subgroup with subfoveal fluid: red line, subgroup with parafoveal or peripapillary fluid: green line). Overall, visual acuity was roughly stable after a NAAION episode with time. A slight nonsignificant improvement between presentation and 3 months was observed in the subfoveal fluid group. SRF = Subretinal fluid.

axonal swelling and further vascular compromise.[30] This leads to an ischemic cascade, including leakage of the peripapillary vessels.[30] The fluid extravasates through the retina and accumulates as the result of hyperosmolarity.[31] A significant volume of fluid is generated and compensatory mechanisms are rapidly overwhelmed, which explain why subretinal fluid is seen in this condition.

In OD disorders where subretinal and parafoveal fluid occur, a transudate, an exudate, or a combination of the 2 may be present, as already confirmed by histopathologic studies in papilloedema.[32] A transudate results from the alteration of mechanical factors influencing the formation or resorption of fluid,[33,34] whereas an exudate occurs in the presence of diseases engendering inflammation (e.g., malignancy, tuberculosis, systemic lupus erythematosus).[33] For example, in pleural effusion, exudate has been distinguished from transudate in pleural effusion by having a protein concentration > 3.0 g/100 ml[35] and a cholesterol level > 40 mg/dl.[36]

In the case of subretinal fluid associated with NAAION, a transudate is likely because there is no evidence of inflammation and the so-called hard exudates are not commonly seen. A complete macular star results from the deposition of lipoproteins in the outer plexiform layer taking up the radiating pattern of fibers in Henle's layer.[37] Although such exudates located only in the nasal hemifovea and thus a hemi-star (or "fan") can occasionally occur in NAAION (Plant GT, Chapelle A-C, personal observation, 2017), no instance was observed in the present cohort. A macular star or hemi-star has been described in neuroretinitis, papilledema due to severe or long-standing intracranial hypertension[38] and myelin oligodendrocyte glycoprotein optic neuropathies.[39] In these cases, exudates form from a proteinaceous fluid composed of serum proteins and lipids, resulting from a breakdown of the blood retinal barrier.[40] The lipid component tracks in the outer plexiform layer and the liquid component accumulates in the subretinal space because liquid can percolate through the external limiting membrane.[31,41] In our series, no exudates were observed on OCT or indirect ophthalmoscopy, which is in favor of transudation. We propose that venous hypertension caused by the swollen disc is likely to induce transudation. Indeed, authors have hypothesized that OD swelling in general leads to compression of the superficial retinal veins or an increase in retrolaminar retinal venous pressure induced by an augmentation of the optic nerve tissue volume.[42,43] This hypothesis provides an explanation for the absence of spontaneous venous pulsation in patients with OD swelling, regardless of the cause.[42,43] It is also the case that in chronic papilledema, such as inidiopathic intracranial hypertension, exudates are observed only in long-standing and severe cases.[38]

It has been suggested that propagation of fluid within the retina can be promoted by vitreoretinal traction secondary to the optic nerve swelling in NAAION and other disorders.[6] Extensive swelling pushes forward the retinal nerve fiber layer, thus potentially allowing fluid to progress along the potential space. Our results show that patients who had subretinal fluid tend to have more extensive swelling in the temporal disc sector. The swelling is likely to represent a combination of optic nerve fiber swelling and tissue edema. In these cases, a "V" pattern was observed on the thickness map and subfoveal fluid was always present, which favors a role of vitreoretinal traction from the OD. However, we

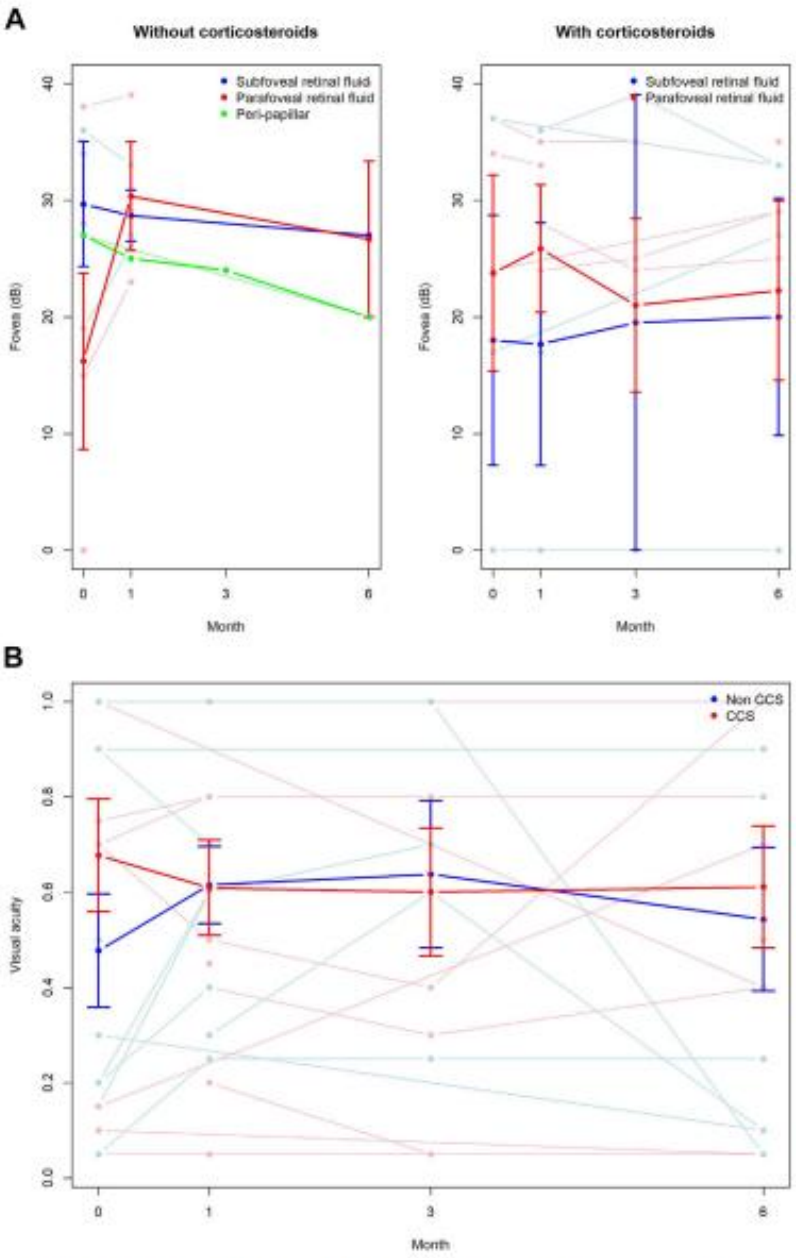

Figure 7. Spaghetti plot graph. **A,** Comparison of mean foveal threshold (dB) over 6 months in patients with subretinal fluid treated **(a)** and untreated with corticosteroids **(b)** (subgroup without subfoveal fluid: blue line, subgroup with parafoveal fluid: red line, subgroup with peripapillary fluid: green line). **B,** Comparison of mean visual acuity (Snellen scale) over 6 months in patients with subretinal fluid treated and not treated with corticosteroids (subgroup with subretinal fluid treated with corticosteroids: blue line, subgroup with subretinal fluid not treated with steroids: red line). No difference in visual function at 6 months (visual acuity and fovea threshold) was observed in subretinal fluid between patients treated and untreated with corticosteroids. CCS = corticosteroid.

consider the volume of transudate to be the more likely determining factor, which is also likely to be related to the degree of OD swelling. The mean retinal nerve fiber layer thickness was 242.42 ± 52.24 µm in patients with subretinal fluid compared with 201.45 ± 80.76 µm in patients without subretinal fluid ($P = 0.05$).

Similarities with subretinal fluid in macular pathologies, such as CSR, Vogt-Koyanagi-Harada, and CRVO, suggest a similar underlying mechanism. Many hypotheses have been proposed, such as overwhelming of the draining vascular system or the RPE mechanism.[26] In NAAION, however, the volume of fluid emanating from the optic nerve head is

likely to exceed the pump capacities of the RPE, leading to the accumulation of retinal fluid[10] without the need to hypothesize impaired intrinsic function.

Over the past 5 years, there has been increasing recognition of a paravascular transport system in the retina and around the optic nerve similar to the glymphatic system existing in the brain.[44,45] Moreover, this glymphatic system has the potential to communicate with the vascular system and could be involved in the generation of tissue edema after ischemia of the optic nerve. Müller cells and the superficial and deep vascular plexus under normal condition can reabsorb fluid.[45,46] We propose that in NAAION, after the generation of a vascular transudate, Müller cells are saturated. This is compatible with the observation on OCT of thickening and cystic change of the inner nuclear layer, where the Müller cells are located, similar to what has been observed in MME,[18] although rarely extending to the macula.[19] The fact that Müller cell density decreases with eccentricity might explain why we do not observe this change at the fovea.[47] Moreover, our study showed that parafoveal fluid localized less than 1 mm from the fovea is strongly associated with subretinal fluid. We propose that the critical factor determining the appearance of subretinal fluid is the *volume of fluid* generated acutely by the ischemic process at the optic nerve head resulting in overwhelming of the glymphatic system and other reabsorption mechanisms.[3]

Study Limitations

The main limitation of our study is that we do not have the OCT scans of patients at the onset of symptoms, which may give further insight into the pathogenesis and prevalence of subretinal fluid in patients with NAAION. Furthermore, follow-up studies during the first 15 days may better permit evaluation of the time course of fluid resorption and allow us to estimate the delay for the resorption of fluid. A randomized, masked prospective study would be required to evaluate definitively the efficacy of steroids in NAAION associated with subretinal fluid.

Acknowledgments

The authors thank Professor Anthony Arnold for his comments on our earlier draft.

Footnotes and Disclosures

Originally received: March 3, 2023.
Final revision: July 4, 2023.
Accepted: July 13, 2023.
Available online: ■■■. Manuscript no. OPHTHA-D-23-00383.

[1] Department of Ophthalmology, Central University Hospital of Liège, University of Liège, Liège, Belgium.

[2] Department of Neurodegeneration and Rehabilitation, UCL Institute of Neurology, Faculty of Brain Sciences, University College London, London, United Kingdom.

*Dr. Chapelle and Dr Plant contributed equally to this work.

Disclosure(s):

All authors have completed and submitted the ICMJE disclosures form.

The author(s) have made the following disclosure(s):

J.M.R.: Data safety monitoring board or advisory board for Novartis — BayerEye; Leadership or fiduciary role — EyeD Pharma.

HUMAN SUBJECTS: Human subjects were included in this study. The human ethics committees at the University of Liège approved the study. All research adhered to the tenets of the Declaration of Helsinki. All participants provided informed consent.

No animal subjects were used in this study.

Author Contributions

Conception and design: Chapelle, Rakic, Plant

Data collection: Chapelle

Analysis and interpretation: Chapelle, Plant

Obtained funding: N/A; Study was performed as part of regular employment duties at CHU Liège. No additional funding was provided.

Overall responsibility: Chapelle, Plant

Abbreviations and Acronyms:
CRVO = central retinal venous occlusion; **CSR** = central serous retinopathy; **GCC** = ganglion cell complex; **GCL** = ganglion cell layer; **HRA** = Heidelberg Research Architecture; **ICC** = intraclass correlation coefficient; **INL** = inner nuclear layer; **MD** = mean deviation; **MME** = microcystic macular edema; **MP** = methylprednisolone; **NAAION** = nonarteritic anterior ischemic optic neuropathy; **OD** = optic disc; **OPL** = outer plexiform layer; **OSA** = obstructive sleep apnea; **pRNFL** = peripapillary retinal nerve fiber layer; **RPE** = retinal pigment epithelium; **SD** = standard deviation; **SRF** = subretinal fluid.

Keywords:
Corticosteroids, Ischemic optic neuropathy, Microcystic macular edema, Subretinal fluid, Swollen disc.

Correspondence:
Anne Catherine Chapelle, MD, Central University Hospital of Liège, Avenue de l'hôpital, 4000, Liège, Belgium. E-mail: ac.chapelle@chuliege.be.

References

1. Miller NR, Arnold AC. Current concepts in the diagnosis, pathogenesis and management of nonarteritic anterior ischaemic optic neuropathy. *Eye*. 2015;29:65–79.
2. Hayreh SS. Anterior ischaemic optic neuropathy. II. Fundus on ophthalmoscopy and fluorescein angiography. *Br J Ophthalmol*. 1974;58:964–980.
3. Dickersin K. Optic nerve decompression surgery for nonarteritic anterior ischemic optic neuropathy (NAION) is not effective and may be harmful. *JAMA*. 1995;273:625.
4. Beck RW, Servais GE, Hayreh SS. Anterior ischemic optic neuropathy. IX. Cup-to-disc ratio and its role in pathogenesis. *Ophthalmology*. 1987;94:1503–1508.

5. Arnold AC. Pathogenesis of nonarteritic anterior ischemic optic neuropathy. *J Neuroophthalmol*. 2003;23:157–163.
6. Savini G. Detection and quantification of retinal nerve fiber layer thickness in optic disc edema using Stratus OCT. *Arch Ophthalmol*. 2006;124:1111.
7. Hedges TR. Subretinal fluid from anterior ischemic optic neuropathy demonstrated by optical coherence tomography. *Arch Ophthalmol*. 2008;126:812.
8. Hayreh SS. Treatment of non-arteritic anterior ischemic optic neuropathy with high-dose systemic corticosteroid therapy. *Graefes Arch Clin Exp Ophthalmol*. 2013;251: 1029–1030.
9. Rebolleda G, Pérez-López M, Casas-LLera P, et al. Visual and anatomical outcomes of non-arteritic anterior ischemic optic neuropathy with high-dose systemic corticosteroids. *Graefes Arch Clin Exp Ophthalmol*. 2013;251:255–260.
10. Demirel S, Batıoğlu F, Oguz YG, Özmert E. Macular involvement and response to steroid therapy demonstrated by optical coherence tomography in non-arteritic anterior ischaemic optic neuropathy. *Neuroophthalmology*. 2013;37: 161–164.
11. Takayama K, Kaneko H, Kachi S, et al. High-dose intravenous pulse steroid therapy for optic disc swelling and subretinal fluid in non-arteritic anterior ischemic optic neuropathy. *Nagoya J Med Sci*. 2017;79:103–108.
12. Carta A, Mora P, Aldigeri R, et al. Optical coherence tomography is a useful tool in the differentiation between true edema and pseudoedema of the optic disc. *PLoS One*. 2018;13:e0208145.
13. Kang Li, Xiaodong Wu, Chen DZ, Sonka M. Optimal surface segmentation in volumetric images-a graph-theoretic approach. *IEEE Trans Pattern Anal Mach Intell*. 2006;28: 119–134.
14. Ghazi NG, Green WR. Pathology and pathogenesis of retinal detachment. *Eye*. 2002;16:411–421.
15. Petzold A, Fraser CL, Abegg M, et al. Diagnosis and classification of optic neuritis. *Lancet Neurol*. 2022;21: 1120–1134.
16. Amer R, Nalcı H, Yalçındağ N. Exudative retinal detachment. *Surv Ophthalmol*. 2017;62:723–769.
17. Ishikawa M, Sawada Y, Yoshitomi T. Structure and function of the interphotoreceptor matrix surrounding retinal photoreceptor cells. *Exp Eye Res*. 2015;133:3–18.
18. Gelfand JM, Nolan R, Schwartz DM, et al. Microcystic macular oedema in multiple sclerosis is associated with disease severity. *Brain*. 2012;135(Pt 6):1786–1793.
19. Chapelle AC, Rakic JM, Plant GT. Nonarteritic anterior ischemic optic neuropathy. *Ophthalmol Sci*. 2023;3: 100230.
20. Abegg M, Dysli M, Wolf S, et al. Microcystic macular edema: retrograde maculopathy caused by optic neuropathy. *Ophthalmology*. 2014;121:142–149.
21. Kim DH, Shin GR, Choi YJ. Risk factors for non-arteritic anterior ischaemic optic neuropathy in a Korean population. *Neuro-Ophthalmology*. 2017;41:68–75.
22. Hayreh S, Podhajsky P, Zimmerman MB. Role of nocturnal arterial hypotension in optic nerve head ischemic disorders. *Ophthalmologica*. 1999;213:76–96.
23. Hayreh SS. Role of nocturnal arterial hypotension in the development of ocular manifestations of systemic arterial hypertension. *Curr Opin Opthalmol*. 1999;10:474–482.
24. Finger ML, Borruat FX. Dynamics of intraretinal fluid accumulation evidenced by SD-OCT in a case of cat scratch neuroretinitis. *Eye*. 2014;28:770–771.
25. Hoye VJ. Optical coherence tomography demonstrates subretinal macular edema from papilledema. *Arch Ophthalmol*. 2001;119:1287.
26. Ozdemir H, Karacorlu M, Karacorlu S. Serous macular detachment in central retinal vein occlusion. *Retina*. 2005;25: 561–563.
27. Pizzimenti JJ, Daniel KP. Central serous chorioretinopathy after epidural steroid injection. *Pharmacotherapy*. 2005;25: 1141–1146.
28. Dinc UA, Yenerel M, Tatlipinar S, et al. Correlation of retinal sensitivity and retinal thickness in central serous chorioretinopathy. *Ophthalmologica*. 2010;224:2–9.
29. Hayreh SS, Zimmerman MB. Non-arteritic anterior ischemic optic neuropathy: role of systemic corticosteroid therapy. *Graefes Arch Clin Exp Ophthalmol*. 2008;246:1029–1046.
30. Hayreh SS. Ischemic optic neuropathy. *Prog Retin Eye Res*. 2009;28:34–62.
31. Marmor MF. Mechanisms of fluid accumulation in retinal edema. *Doc Ophthalmol*. 1999;97:239–249.
32. Reese AB. Peri-papillary detachment of the retina accompanying papilledema. *Trans Am Ophthalmol Soc*. 1930;28: 341–351.
33. Light RW. Pleural effusions: the diagnostic separation of transudates and exudates. *Ann Intern Med*. 1972;77:507.
34. Agostoni A, Marasini B. Orosomucoid contents of pleural and peritoneal effusions of various etiologies. *Am J Clin Pathol*. 1977;67:146–148.
35. Carr DT, Power MH. Clinical value of measurements of concentration of protein in pleural fluid. *N Engl J Med*. 1958;259:926–927.
36. Hamm H, Brohan U, Bohmer R, Missmahl HP. Cholesterol in pleural effusions. *Chest*. 1987;92:296–302.
37. El-Dairi M. Neuroretinitis. In: *Handbook of Pediatric Retinal OCT and the Eye-Brain Connection*. Elsevier; 2020:308-309.
38. Morris AT, Sanders MD. Macular changes resulting from papilloedema. *Br J Ophthalmol*. 1980;64:211–216.
39. Moura FC, Sato DK, Rimkus CM, et al. Anti-MOG (myelin oligodendrocyte glycoprotein)–positive severe optic neuritis with optic disc ischaemia and macular star. *Neuro-Ophthalmology*. 2015;39:285–288.
40. Otani T, Kishi S. Tomographic findings of foveal hard exudates in diabetic macular edema. *Am J Ophthalmol*. 2001;131: 50–54.
41. Kitamei H, Kitaichi N, Namba K, et al. Clinical features of intraocular inflammation in Hokkaido, Japan. *Acta Ophthalmologica*. 2009;87:424–428.
42. McCulley TJ, Lam BL, Feuer WJ. Nonarteritic anterior ischemic optic neuropathy and surgery of the anterior segment: temporal relationship analysis. *Am J Ophthalmol*. 2003;136: 1171–1172.
43. Jacks AS. Spontaneous retinal venous pulsation: aetiology and significance. *J Neurol Neurosurg Psychiatry*. 2003;74:7–9.
44. Wostyn P, De Groot V, Van Dam D, et al. The glymphatic system: a new player in ocular diseases? *Investig Ophthalmol Vis Sci*. 2016;57:5426–5427.
45. Petzold A. Retinal glymphatic system: an explanation for transient retinal layer volume changes? *Brain*. 2016;139: 2816–2819.
46. Balk LJ, Killestein J, Polman CH, et al. Microcystic macular oedema confirmed, but not specific for multiple sclerosis. author reply e227 *Brain*. 2012;135(Pt 12):e226.
47. Masri RA, Weltzien F, Purushothuman S, et al. Composition of the inner nuclear layer in human retina. *Invest Ophthalmol Vis Sci*. 2021;62:22.